RANDOM RESPONSE OF ARTICULATED ROAD VEHICLES

by

MOHAMED MOHAMED ELMADANY, M.Eng.

A Thesis

Submitted to the School of Graduate Studies

in Partial Fulfilment of the Requirements

for the Degree

Doctor of Philosophy

McMaster University

May 1979

RANDOM RESPONSE OF ARTICULATED ROAD VEHICLES

DOCTOR OF PHILOSOPHY (1979)
(Mechanical Engineering)

McMASTER UNIVERSITY
Hamilton, Ontario

TITLE: Random Response of Articulated Road Vehicles

AUTHOR: Mohamed Mohamed ElMadany, B.Sc. (Alexandria University)
M.Eng. (McMaster University)

SUPERVISOR: Professor M.A. Dokainish

NUMBER OF PAGES: xxi, 230

ABSTRACT

A method for determining and analyzing the linear dynamic response of the complex articulated vehicle structures to road surface undulations, represented as stationary Gaussian random excitations, is formulated. The procedure is used to estimate the influence of various parameters on the dynamic behaviour of the articulated vehicle. In particular, the influence of vehicle suspension systems, load patterns, speed, and road characteristics on the ride comfort and ride safety is evaluated.

An analytical method based on the equivalent linearization technique is developed in order to study the effect of the system nonlinearities on the ride behaviour of the articulated vehicle. The nonlinearities include dry friction, bump stops and wheel hop. The vehicle is treated as a discrete, nonlinear, time-invariant, multi-degree-of-freedom dynamic system subjected to random road irregularities.

An extensive review of the available literature is presented as background to the present work. The review provides details of various proposed methods of modelling the road surface undulations, and vehicle components as well as methods of performing the analysis necessary to obtain the vehicle vibrational response and assessing the ride quality.

ACKNOWLEDGEMENTS

The author wishes to express his sincere appreciation to his research advisor Dr. M.A. Dokainish for his guidance and encouragement during the preparation of this thesis. Thanks are due to Professor J.N. Siddall, Dr. B. Latto and Dr. W.K. Tso for their assistance and support throughout the period of this research.

Sincere thanks are due to Professor A.B. Allan for his revising and criticising this thesis.

Thanks are owed to Dr. S.T. Ariaratnam, Dr. L.D. Lutes, Dr. M.A. Samaha and fellow researcher M.S. Gadala for many interesting discussions and valuable suggestions.

The financial assistance of McMaster University and of the National Research Council of Canada in the form of scholarships is appreciated.

Appreciation and thanks are expressed to Nancy Sine of the Word Processing Centre for her patient and very skillful typing of this manuscript.

Gratitude is expressed to my beloved wife Samia, who has been to me the most lovely, encouraging, and understanding person involved in the generation of this thesis.

To my wife, my parents and my parents-in-law I dedicate this thesis.

TABLE OF CONTENTS

TABLE OF CONTENTS (continued)

TABLE OF CONTENTS (continued)

LIST OF SYMBOLS

Superscripts ' and * will denote, respectively, the transpose and the conjugate of a matrix or a vector. Subscript j which denotes suspension system locations may take on values from 1 to 6 as follows:

1. tractor front suspension
2. tractor rear suspension
3. semitrailer suspension
4. tractor front tire
5. tractor rear tire
6. semitrailer tire

The following is a list of frequently used symbols. Others will be defined when they are used.

a_d	vertical position of the driver
a_i	vehicle dimensions
A	transformation matrix
b_d	horizontal position of the driver
b_i	vehicle dimensions
B_{ij}	bump-stop forces
c_j	suspension damping rates (j = 1, 2, 3)
c_{tj}	tire damping rates (j = 4, 5, 6)
c^e_{ij}	elements of equivalent damping matrix
C, C_f	damping and forced damping matrices, respectively

LIST OF SYMBOLS (continued)

C_e	equivalent damping matrix
$\bar{e}$	error vector
erf	error function
erfc	complementary error function
exp	exponential
E[ ]	expectation operator
f	frequency in Hz
f_j	suspension dry friction forces (j = 1, 2, 3)
$\bar{f}(t)$	vector of excitation force
F_{ij}	dry friction forces in equation i due to friction element j
$\bar{g}(\dot{\bar{y}},\bar{y})$	vector of nonlinear functions
h(t)	impulse response function matrix
H(f)	frequency response function matrix
i	$\sqrt{-1}$
I_s, I_t	sprung mass moment of inertias for the semitrailer and tractor about their centre of gravities, respectively
k_j	suspension spring rates (j = 1, 2, 3)
k_{oj}	suspension series spring rates (j = 1, 2, 3)
k_{tj}	tire spring rates (j = 4, 5, 6)
k^e_{ij}	elements of equivalent stiffness matrix
K, K_f	stiffness and forced stiffness matrices, respectively
K_e	equivalent stiffness matrix
ℓ_{jk}	distance between jth and kth wheels

LIST OF SYMBOLS (continued)

L_j	tire deflections ($j = 4, 5, 6$)
M	mass matrix
M_j	unsprung axle masses ($j = 1, 2, 3$)
M_s, M_t	sprung masses of the semitrailer and tractor,, respectively
M_4	total mass of the tractor ($M_t + M_1 + M_2$)
M_5	total mass of the semitrailer ($M_s + M_3$)
n	spatial frequency of road roughness
n_o	$1/2\pi$ c/m
p	probability density function
p_j	axle static loads ($j = 1, 2, 3$)
Pr	probability distribution function
q_{ij}	nonlinear functions
Q_{ij}	nonlinear functions
r_1, r_2	waviness
$R_{\bar{f}}(\tau)$	force correlation function matrix
$R_{\bar{w}}(\tau)$	temporal correlation function matrix
$R_{\bar{x}}(\tau)$	response correlation function matrix
$R_{\bar{x}}(0)$	instantaneous correlation function matrix
$R_{\bar{w}}(\delta)$	spatial correlation function matrix
$\delta(n)$	spatial spectral density of the road roughness
$\delta(n_o)$	roughness coefficient
sgn	sign
$S_{\bar{f}}(f)$	force spectral density function matrix

LIST OF SYMBOLS (continued)

$S_{\bar{w}}(f)$	temporal spectral density function matrix
$S_{\bar{x}}(f)$	response spectral density function matrix
$S_{\bar{w}}(n)$	spatial spectral density function matirx
t	time
T	transformation matrix
T_{ij}	tire spring forces
$\bar{u}$	vector of displacement excitations
v	vehicle speed
$\bar{w}$	vector of temporal displacement excitations
$\overline{w}(x)$	road profile
$\{\overline{w}(x)\}$	random process
$\bar{x}$	vector of generalized coordinates
X_s, X_t	horizontal motions coordinates of the centre of gravities of the semitrailer and tractor, respectively
$\bar{y}$	relative displacement vector across the nonlinear elements
$\bar{y}_c$	constant offset vector
Y_j	vertical motion coordinates of vehicle axles ($j = 1, 2, 3$)
Y_s, Y_t	vertical motion coordinates of the centre of gravities of the semitrailer and tractor, respectively.
$\bar{z}$	random vector with zero mean value
α_{ij}^e	equivalent linear damping
$\bar{\beta}$	vector of nonlinear functions
γ_{ij}^e	equivalent linear stiffness

δ	distance lag
δ_{oj}	bump-stop clearance (j = 1, 2, 3)
ξ	critical damping ratio
θ_s, θ_t	rotational coordinates about the centre of gravities of the semitrailer and tractor, respectively.
λ_j	yield level (j = 1, 2, 3)
ψ_{jk}	phase angles
ν	complex eigenvalue
σ	decay rate
τ	time lag
τ_{jk}	time delay between the jth and kth wheels
X	steady state amplitude
ω	damped natural frequency
ω_n	undamped natural frequency
ω_{aj}	average frequency across nonlinear elements (j = 1, 2, 3)

LIST OF FIGURES

LIST OF FIGURES (continued)

LIST OF FIGURES (continued)

LIST OF FIGURES (continued)

LIST OF FIGURES (continued)

LIST OF FIGURES (continued)

LIST OF FIGURES (continued)

LIST OF FIGURES (continued)

LIST OF TABLES

CHAPTER 1

INTRODUCTION

1.1 Preliminary Remarks

The dynamic response of articulated vehicles to random road surface undulations has been of major design concern to automotive engineers for many years. This concern arises from the fact that excessive levels of vibration can lead to ride discomfort, ride safety problems, dynamic stressing in vehicle frame and suspension components as well as to cargo damage or destruction.

Changes in vehicle configuration, coupled with changes in road conditions, speed limits, and vehicle loadings, plus the necessary greater operator awareness have made a knowledge of the dynamic behaviour of such vehicles more critical. Prediction and analysis of the dynamic characteristics of articulated vehicles, with particular reference to the ride comfort and road safety, are required as a first step toward a solution to these operating problems.

The ultimate objective of ride dynamicists is to provide background by which automotive engineers may produce vehicle structures that are functional and economical and yet provide ride characteristics that are acceptable. In achieving this goal, the results of both theoretical and experimental investigations must be integrated in providing design parameters. Ideally the final result should be such that the vehicle structures may be designed to accommodate all road

irregularities while maintaining operator comfort and acceptable cargo ride plus assuring ride safety through continuous tire contact with the road.

Experimental tests on heavy vehicle structures, both in the laboratory or on the road, are very expensive. Also it is difficult to isolate the effect of a particular parameter, and to determine its effect on vehicle riding quality, without extensive and tedious experimentation. In these circumstances, theoretical studies of vehicle riding behaviour become practical provided that the vehicle model can be shown to be representative of the actual structure and that the unevenness of the road surface is accurately reproduced in the representation by a random process. Using particular mathematical techniques, the significant parameters affecting vehicle ride motion may be isolated and studied. The theoretical analysis thus provides a means by which engineering designers may introduce and test ride improvements during the vehicle design process, and then may incorporate new features in the resulting vehicles with adequate indications of their probable effect on ride characteristics.

Both linear and nonlinear mathematical models have been developed to predict the ride motion of the vehicle in response to road surface irregularities. The motion of the vehicle can be obtained using either simulation techniques or analytical techniques. Recent studies have employed simulation techniques [40,48,60,86,108,129,140,141]. While such techniques are very useful for providing detailed information on the riding behaviour of the vehicle, they tend to be expensive due to

the necessity of applying numerical methods to integrate the equations of motion of the system, and to the time consumed in processing the obtained results into statistical characteristics.

The analytical techniques for determining the dynamic characteristics of the vehicle have received much less attention due to the complexities involved [125]. When the analytical techniques are applied, such techniques are far more useful for design and theoretical studies. They contribute to the general understanding of the behaviour of vehicle systems by providing direct relationships between the observed response characteristics and the system properties which cause them. These analytical techniques can be used in performing design trade-off studies of vehicle system components, highlighting new concepts, and comparing alternate approaches.

The work to be presented here provides a study of the analytical techniques used in assessing ride quality of articulated vehicles. The analytical work is undertaken with the objective of describing qualitatively and quantitatively the ride behaviour of such vehicles, determination of the significant design parameters and an evaluation of the effect of these design parameters on the vehicle ride characteristics.

It has been observed, in carrying out the literature survey [56], that there is a need for a detailed investigation of the linear vibratory motions of the complex heavy highway vehicles caused by random road irregularities, such that the interaction between the vehicle and the road surface can be assessed. It also becomes apparent that the

dynamic effects of system nonlinearities, such as Coulomb friction in the suspension systems, bump stops, and wheel hop, on the behaviour of the articulated vehicle have not received the attention they deserve.

1.2 Object and Scope

The objective of this present investigation is three-fold:

(i) to provide a review of the available literature dealing with the dynamic response of articulated vehicles to road surface undulations. In the review the techniques that have been put forward for describing road input characteristics, modelling the vehicle components, and performing the analysis necessary to obtain the vibrational response are presented and discussed. Finally, the indices that have been proposed for ride comfort and ride safety are provided and the manners in which various researchers relate these to the vibrational characteristics of the vehicles are described.

(ii) to provide a method for determining and analyzing the linear dynamic response of the complex articulated vehicle structures to road surface undulations which are represented as stationary Gaussian random excitations. The procedure is used to estimate the influences of various parameters on the articulated vehicle dynamic behaviour. In particular, the influences of suspension

springing and damping, tire springing and road characteristics as well as vehicle speed and load pattern on the ride comfort and ride safety are evaluated.

(iii) to develop an analytical method based on the equivalent linearization technique to study the effect of the system nonlinearities on the ride behaviour of the articulated vehicle. The nonlinearities considered include dry friction damping, bump stops and wheel hop. The vehicle is treated as a discrete, nonlinear, time invariant, multi-degree-of-freedom dynamic system subjected to random road irregularities.

CHAPTER 2

RIDE DYNAMICS OF ARTICULATED VEHICLES

A LITERATURE SURVEY

The available literature dealing with the dynamic response of articulated vehicles to road surface undulations has been reviewed. The techniques that have been put forward for describing road input characteristics, for modelling the vehicles in a range of degrees of freedom, and for performing the analysis necessary to obtain the vibrational response have been stated and discussed. Finally the indices that have been proposed for ride comfort and ride safety are given and the manners in which various researchers relate these to the vibrational characteristics of the vehicles are described.

2.1 Introduction

Over the past two decades, there has been an increased interest in the betterment of ride quality in the large articulated vehicles presently in use on our roads. The study of ride quality requires an assessment of the response of the vehicle to the inputs at the road surface. This mathematical assessment is normally termed the study of "ride dynamics" which is defined as the response in terms of mechanical vibration in the various components of the vehicle, to the random roughness that may be found in any given section of road. The mechanical vibration induced in the vehicle may lead to driver

discomfort, wear and damage to vehicle components, damage or destruction of the cargo, and possibly to traction loss, and it is for these reasons that the betterment of ride quality is sought.

Two factors have contributed to the widening of interest and discussion of the ride quality in the particular form of vehicle. First, the advent of computer systems capable of dealing with complex mathematical problems has simplified the solution of the equations describing the vehicle motions. Secondly, a large body of relevant work is available describing the ride characteristics of simpler vehicles, such as automobiles and light trucks which can provide a ready background to an understanding of the more complex motion of the articulated vehicles.

Articulated vehicles are very complicated dynamic systems, whose various components interact, in a variety of ways, with input from the road surface. In order to assess, mathematically, the ride quality of such a system, it is necessary to describe the road inputs, the vehicle, and the methods of evaluating the vehicle ride performance.

A given section of road represents a specific input to a vibrating system. It is, however, impractical to attempt to determine the input waveform. Equally it becomes impossible to assess the profile of all roads likely to be traversed by a particular vehicle. Also, considering that seasonal changes in profile and surface degeneration might change the character of the road, it becomes logical to treat the road input to the vehicle system as a random phenomenon.

Articulated vehicles have a substantially different ride performance when compared to passenger cars. The differences are due to many factors, but the prime difference is the result of the vast increase in mass and inertia. In general, suspension systems are simpler, and the power unit is designed for the heavy vehicle, with operation at much reduced power to weight ratios. Finally the ride is affected by the vehicle weight difference that will be encountered in laden and unladen condition.

Many studies on ride dynamics of articulated vehicles have been conducted. Mathematical models have been developed by various researchers, including Ellis, Noon, Walther et al., Helling, and others. However, the most comprehensive model has been put forward by Van Deusen.

The models proposed in the past for the study of ride dynamics relied mainly on simplified linear dynamic models, operating on a road profile simulated by a sinusoidal input. Recent studies, however, have based the analysis on complex multi-degree-of-freedom linear and nonlinear models subjected to road inputs of a random nature, approaching "real world" conditions.

Two major factors must be considered in evaluating the ride performance of a vehicle; first, the ride comfort, both of the driver and any passenger, as well as cargo, and second, the ride safety. Ride comfort is normally interpreted as the capability of the vehicle suspension, in the particular vehicle configuration, to maintain the motion within the range of human comfort and, as well, within the range

necessary to assure that there is no damage to the cargo. Ride safety is defined as the ability of the suspension to assure wheel-to- road surface contact under rough road conditions.

It is possible to obtain good ride quality while making the vehicle difficult to control, or, conversely, to obtain excellent vehicle control while destroying the driver comfort. It is clear that the design of the vehicle suspension must be a practical compromise between ride comfort and ride safety. Both performance criteria have to be considered in assessing the ride quality of any vehicle.

The present tendency is toward changes in vehicle configuration along with increases in vehicle speeds and payloads. Operator awareness must increase, and thus requires improvements in ride comfort and safety. Coupled to these is the requirement that road construction and maintenance costs be minimized, which tends to make ride quality requirements even more difficult to achieve.

The objectives, therefore, of the studies of ride dynamics are to assess the response of the vehicle system to road surface inputs and to provide the best possible ride quality through proper design of the suspension systems.

It is the purpose of this chapter to draw together, in summary form, the technical literature bearing on articulated vehicle analysis and ride comfort and safety. Thus, all phases of the problem, as described in the various papers, are included, with emphasis being placed on the means of describing the road surface, the dynamics of

articulated vehicles, and the methods of solution to obtain the vibrational characteristics of the vehicles. Finally, the literature presenting the indices of ride comfort and safety is reviewed and the relation of these indices to the results of the analysis is presented.

2.2 Road Description

Roadways traversed by vehicles are much more rigid than the supporting tires. Therefore, it can be assumed, for the purpose of investigating vehicle dynamics and ride qualities, that such roadways are perfectly rigid and that the profiles, measured under no-load conditions, in fact represent the dynamic tire disturbances.

An n-wheeled articulated vehicle traversing a road is subjected to n road input displacements, one at each wheel. Consequently, to describe adequately the displacement imposed at each wheel and any correlation between the n displacements, it is necessary to provide a complete description of the road surface. This can be done, deterministically, by providing a digital survey of the several road tracks which the vehicle might traverse. However, obvious practical difficulties arise in obtaining and handling the requisite information. Therefore, analytical techniques which are more economical both in description and analysis are sought [119].

The road roughness is frequently so irregular that it is most accurately described as a random process. A few transient shocks due to occasional large irregularities such as potholes, crash stops, etc., may be present but these can often be isolated and treated separately. If

this is the case, the road surface can be represented as a stationary Gaussian random process, and the stochastic process theory developed into the theory of random vibration can be applied [10, 34, 35, 38, 96, 118].

Various techniques are used to measure and classify road profiles [5, 91, 100, 133, 147, 150, 152]. Most of these techniques yield a continuous signal which provides a recording proportional to the instantaneous height of the road profile. The spectral density of the profile is obtained by means of a frequency analyzer. This spectral density is presented in terms of mean square amplitude per unit bandwidth plotted against spatial frequency.

Three analytical models of increasing complexity have been used to describe statistically the road surface undulations [43, 44, 45, 85, 105, 120]. The first model describes the road as consisting of a cylindrical surface which can be defined by means of a single longitudinal track, i.e., the model takes no account of the differing excitations imposed on off-side and near-side wheels of the vehicle. The track profile forms part of a stationary Gaussian process with a zero mean value. In this case, the road excitation may be described by the power spectral density of a single track.

The second model considers the surface consisting of random fluctuations in the longitudinal direction with a constant lateral slope which varies randomly for each longitudinal increment. A complete description of this surface is provided by the two uncorrelated spectra of the mean track and lateral slope variations, or by the spectral

density of any longitudinal track and the coherency function which describes the related properties of any two parallel tracks [85, 43].

In the third model, the road surface is considered as part of a two-dimensional completely homogeneous and isotropic random process. Dodds and Robson [45] have demonstrated that the hypothesis of isotropy leads to an estimate of cross-spectra for the profiles of parallel tracks on typical roads. Kamash and Robson [83, 84, 120] have considered the analytical properties of isotropic random surfaces and the restrictions to which descriptions of such surfaces are subject. They have shown that most good approximations to actual road descriptions satisfy the hypothesis of isotropy. They have also shown that coherency functions derived from the proposed model are validated by comparison with coherencies based on measurement. Then, this model provides a practical and plausible description of the actual surface, and allows for its complete description by a single autocorrelation function. Therefore, the spectral density of any longitudinal track provides the exhaustive probability characteristics necessary to describe the surface.

2.3 Articulated Vehicle Characteristics

An articulated vehicle is a very complex structure. It has many components and variable parameters which affect its vibration and response characteristics and thus its ride behaviour. The tractor and semitrailer are coupled dynamic vibrating systems and the interplay between the two units cannot be ignored. Frame beaming, cab mounting,

suspension, and tires play a major role in influencing vehicle ride.

Ride improvement for the cargo should not be overlooked, as it is as important as the ride improvement of the tractor. Both the tractor and the semitrailer are judged by their riding quality. The knowledge of the interaction of tractor and semitrailer is important. Results based on investigations of either tractor or semitrailer, separately, can easily lead to wrong conclusions. For example, as the semitrailer has four or five times the sprung weight of the tractor in the laden case, the semitrailer dictates the tractor ride.

There are some geometric peculiarities of the articulated vehicle which cause certain vibrations. One such peculiarity is the articulation at the fifth wheel which allows the two units to pitch and to yaw relative to each other. Another peculiarity is the vertical offset of the fifth wheel kingpin from a line connecting the centres of gravity of the tractor and semitrailer. This offset causes pitching motions of the tractor and semitrailer to induce fore and aft motions in both components.

As the driver sits forward and well above the centre of gravity of the tractor, he is subjected to vertical and fore and aft motions resulting from the bouncing and pitching modes of vibration. The vertical motion produces bouncing in the seat, while the fore and aft motion, if severe enough, may cause back slapping against the seat and driver head-snapping [30, 131].

The backbone of the vehicle is the frame and it has a definite influence on the vibratory motion of the vehicle. The beam vibration in

the main chassis frame may result in an unpleasant motion of the cab, known as "cab-nod". The basic factors affecting frame beaming are the imposed static and dynamic loads, resulting bending moments, and the side rail moment of inertia at the point of maximum stress [131].

The cab is subjected to induced vibration from the beaming and pitching. It is necessary, therefore, to isolate the cab from frame vibrations while avoiding amplification of the lower frequency pitch motion of the chassis on its suspension. To accomplish these requirements it is necessary that the isolator should have low spring rates and optimum damping elements.

There are basically two types of cabs; cab-over-engine and conventional cab. The ride characteristics may be influenced by the way the cab is mounted to the chassis.

Articulated vehicle suspension systems may vary considerably in detail, but normally comprise a spring, damper, links and rubber bushes. The main functions of the suspension are:

i) to provide vehicle support and directional control. In order to provide the proper directional control, the adequate wheel-road contact must be maintained, otherwise considerable lateral motion may occur during turning maneuvers.

ii) to provide effective vibration isolation from road disturbances.

Also, the suspension must be insensitive to externally applied loads. For example, cross winds and cargo weight variations should result in a minimum of vehicle vibratory motion.

The requirements necessary to fulfill these various functions

have always conflicted to various degrees. Guidance requires a suspension that is neither very stiff nor very soft in order to maintain good road holding. Insensitivity to external loads requires a stiff suspension, whereas vibration isolation demands a soft suspension.

The appreciable increases in vehicle speeds and also in the laden weights have led to increase in the energy to be dissipated by vehicle suspension systems, and consequently further damping is required. This damping is essential to control vehicle motion on the suspension.

The unsprung mass (each axle with its wheels and tires) constitutes an independent vibrating system in which the unsprung mass bounces between the tires and suspension springs with these spring elements acting in parallel. The vertical oscillation of the tire and wheel assembly is referred to as wheel hop. This oscillation is effectively damped by the relatively high interleaf friction of the laminated springs. Axle frequencies fall in the range of frame bending frequencies and therefore axle motions produce exciting forces at or near resonance with the frame vibration.

The effect of unsprung mass on the ride quality has been studied by Ryba [122, 123]. His work has shown that the unsprung mass has a minor positive influence on the comfort of the sitting passenger but it causes greater acceleration of the body of the vehicle, which means greater material stress. However, the problem of dynamic tire load becomes more serious when the unsprung mass is relatively high.

The tires act as vertical suspension units. They provide the primary means of support and guidance for the vehicle, and determine the

vibration level transmitted to the vehicle body from the road and the force level to the road. The tire should have a low vertical stiffness to be most effective as a cushion but a simple toroidal envelope that is very flexible in the vertical direction is also very flexible in the lateral direction. The latter produces poor vehicle handling and tire wear.

The major problems that are derived from variabilities in manufacturing the tires are as follows [2, 12]:

i) Excessive weight increases unsprung weight on the vehicle and reduces the effectiveness of vibration damping.

ii) Imbalance due to non-symmetrical distribution of mass of materials around the tire.

iii) Variable vertical and lateral stiffnesses around the periphery of the tire.

The nonuniformity in the tire produces a periodic impulsive force on a moving vehicle. If any of the resulting frequencies of vibration is not adequately damped, the ride qualities of the vehicle will suffer.

2.4 Articulated Vehicle Dynamics

2.4.1 Modelling

Modelling is one of the major tasks in the study of the ride quality of the articulated vehicle. Modelling involves distribution of vehicle physical characteristics, road excitation, and environmental influences. Decisions pertinent to the modelling task may enhance or constrain the results of the mathematical analyses.

The investigators have used mathematical models with varying degrees of complexity depending on the objectives of the individual investigations. The objectives of the investigations are to obtain an understanding of the ride dynamics of the vehicle, to improve the existing vehicles, and to meet the increased demands on vehicle performance.

Most investigators of articulated vehicle dynamics have considered the cab, engines and tractor chassis as one rigid body. The semitrailer with its chassis has been treated similarly. Both units are allowed to translate in the forward and vertical directions and to pitch except as constrained by the fifth wheel.

Due to the constraints imposed by the fifth wheel on the motion of the tractor and semitrailer, the two units together have three-degree-of-freedom; pitching and bouncing motions of the tractor centre of gravity, and pitching motion of the semitrailer centre of gravity. Ellis [50] has used this model to study the ride motion of the vehicle. He has found that fore and aft shake which occurs due to the relative heights of the centres of gravity of the two units and the fifth wheel may be a significant factor in determining driver and load ride conditions.

Noon [104] has considered the motion of the cab on the tractor chassis, but neglected the axle bounce and fore-aft motions of the tractor and semitrailer.

Walther et al. [148] included in their model the bounce motion of the unsprung mass of each wheel and axle assembly. The fore-aft motions

of the tractor and semitrailer were ignored and a stiff spring was substituted for the fifth wheel kingpin.

In articles published by Helling [68, 69], the derivation of the equations of motion for a tractor-semitrailer vehicle was shown, and analogue computer program for the solution of these equations was described. The vehicle model including heave and pitch motions and the vertical motions of the three axles, had six degrees of freedom. The theoretical results were compared with the experimental results obtained from actual vehicle experiments.

Van Deusen [140, 141] has developed linear and nonlinear two-dimensional mathematical models of both the tractor and semitrailer for a large military tractor-semitrailer combination. The linear model consists of a total of thirty eight degrees of freedom. A brief description of the pertinent elements of the linear model follows.

The tractor frame flexibility which has been considered to be an important parameter in influencing the ride behaviour, has been modeled as a lumped parameter system consisting of twelve concentrated mass elements interconnected by beam equations to reflect the varying sectional properties. Each beam element represents two degrees of freedom, those of vertical translational motion and pitch rotational motion. The tractor has front and rear bogies. Each bogie is modeled in three degrees of freedom. The rotational motion of the bogie action is represented by a rigid beam element which has the proper inertial characteristics to represent the rotation of the entire bogie assembly on a frictionless pivot point. The unsprung mass of the wheel and axle

assembly is then represented by two point masses having vertical translational freedom only. The cab is modeled as a rigid assembly having two degrees of freedom on flexible cab mounts and the driver and seat assembly is modeled as a single degree of freedom system attached to the cab frame.

The semitrailer is modeled in five degrees of freedom. These are the vertical and rotational motion of the rigid semitrailer body and payload, the rotational motion of the walking beam assembly of its two front axles, and the vertical motions of the unsprung masses of its two rear axles.

ElMadany and Dokainish [54] have developed a mathematical model of a tractor-semitrailer to evaluate vehicle response to sinusoidal inputs. The model describes the longitudinal, vertical, lateral, pitching, rolling and yawing motions of the vehicle as it is affected by the road profile. In the three dimensional study of the mathematical model, the entire vehicle is considered as a vibrating system, and the problem is analyzed as a multiple input-output system.

2.4.2. Linear Analyses

The linear equations of motion can be written for a variety of articulated vehicle models ranging from a simple, three degrees of freedom model of the tractor and semitrailer units (ignoring the unsprung masses) to the complex model of a complete vehicle with thirty eight degrees of freedom developed by Van Deusen [140, 141]. The simpler models have been useful in studying the fundamental behaviour of

the vehicle, such as, system eigenvalues and eigenvectors which condenses the dynamic behaviour and is suited to comparing overall behaviour. However, more complex models are needed to provide realistic results for predicting actual vehicle behaviour.

The linear equations of motion of the articulated vehicle, in general, are used to evaluate vehicle ride quality and to conduct sensitivity studies of the influence of various design parameters on the vehicle dynamic response.

The following assumptions are made in deriving the linear equations of motion in most dynamic analyses of articulated vehicles:

i) The cab, engine, and tractor chassis are considered as one rigid body; similarly, the semitrailer with its chassis and each axle with its wheels.

ii) All displacements are small.

iii) The springs, dampers, and springing and damping characteristics of the tires may be described by linear functions of displacement and velocity, respectively.

iv) The wheels remain in contact with the road surface at all times.

v) The tractor and semitrailer units are symmetrical about the vertical plane.

vi) Equal road profiles are applied to the right and left vehicle tracks.

vii) The road input displacement function is applied to a point at the centre of the tire contact patch.

viii) Nonlinearities resulting from suspension stops and dry friction

in suspension elements are neglected.

The symmetries (v,vi) result in a set of equations of motion in which the vertical motions (vertical, longitudinal and pitch) are uncoupled from the lateral motions (lateral, roll and yaw).

Beam vibration in the tractor or semitrailer chassis can also be handled in simulating vehicle ride, [20, 70 140]. For example, it may be assumed that the total motion response of the vehicle is given by a linear superposition of the beam bending modes and rigid body modes. The frame flexibility can also be modeled as lumped parameter elements interconnected by beam equations.

The parameters required to analyze the bending modes in the vehicle chassis may be obtained from an experimental setup wherein the unit is suspended by soft springs and subjected to sinusoidal forces at various points along the frame. The parameters can also be obtained from a detailed finite element numerical analysis (see for example, references [41, 94, 103, 117]).

To determine vehicle response, there are two approaches that have found favour with authors in the past, deterministic frequency response approach, and a power spectral density approach.

In the deterministic approach, the frequency response function is determined using a sinusoidal input profile. This approach has been used initially for two reasons; (a) no data was available on random spectra of road profile, (b) available experimental data relating to human vibration tolerances was expressed in terms of the objectionable amplitude at a discrete sinusoidal frequency [77, 142].

ElMadany, Dokainish, and Siddall [55, 56] have utilized a frequency response analysis to obtain the optimum suspension of the articulated vehicle. By minimization of peak acceleration values of the cab, Walther et al. [148] compared the theoretical frequency response analysis to an experimental investigation. The experimental results showed only marginal verification of the theoretical results. Walker and Potts [146] presented a linear analysis solution for the deterministic vibration of a tractor-semitrailer. Le Fevre [93], using the deterministic approach, discussed the qualitative aspects of the articulated vehicle ride.

Several factors have allowed the complete detailed analysis of vehicle random vibrations to be determined. The recent advent of high speed digital computers and the modern profilometer techniques have made it relatively easy to measure and describe statistically the roughness of road surface in terms of amplitude and wave length distribution [5, 100, 133]. It has also become practical to obtain the frequency response function of large and sophisticated system models. Specifications of ride quality in terms of the vertical, lateral, and fore and aft acceleration power spectral densities have been available [4, 6].

In the power spectral density approach, the road surface is described by its power spectral density spectrum, and the vehicle by its complex frequency response. This response can be used as a transfer function operating on the road spectrum to derive the spectrum of vibration of the vehicle when it is moving along the road at any given

speed [44, 45, 46].

2.4.2.1 Random Response of Nonarticulated Vehicles

A search of the available literature reveals that vast numbers of articles have been published on investigations into the dynamic behaviour of nonarticulated vehicles. In a series of four articles by Cotes, Kozin, and Bogdanoff [15, 31, 32, 89] the methods of obtaining ground spectra were described. The equations of motion for a simple idealized mathematical vehicle model were formulated, the power spectral densities of various aspects of the vibrational environment were obtained, and the assessment of the severity of the power spectra of the vibrational environments was examined. Hanamoto [65] and Tidbury [134] have described a more detailed investigation of the theoretical statistical analysis. Whitehead [151] used a statistical approach to evaluate the physiological effects of the vehicle vibrations. An evaluation of vehicle ride using a statistical analysis and experimental results was given by Bobbert [14], and Parkhilovskiy and Zeitseva [106]. Mitschke [102] has considered the general factors that influence ride comfort and ride safety of an automobile using Fourier analysis. He concludes that to improve ride comfort, the acceleration should be small and to improve ride safety, the ratio of the axle dynamic load to its static load should be small. Also he indicates that it is necessary to limit changes of wheel load and the extreme case in which a wheel leaves the road must be avoided. Lins [95] used frequency domain techniques to determine and evaluate vehicle vibration. By comparing frequency domain

technique with the time-domain technique, he found that the former was somewhat more efficient for linear systems having stationary random input than was the latter. Van Deusen [137, 138, 139], Rossini [121], Bieniek [13] and Craggs [33] have studied the vehicle ride problems related to road irregularities. Dodds and Robson [44] have shown that successful analytical prediction of vehicle component response can be carried out using simple analytical models and a statistical description of the road surface.

2.4.2.2 Random Response of Articulated Vehicles

It was possible to find only a small number of papers which dealt with the vibrational characteristics of an articulated vehicle subjected to random inputs.

Van Deusen [140, 141] analyzed a linear model of thirty eight degrees of freedom in the frequency domain using transfer function concepts. The theoretical results were compared with the experimental data. The comparison showed relatively good correlation between the theoretical and experimental results.

Dokainish and ElMadany [46] have investigated the ride quality of a tractor-semitrailer vehicle travelling over a random road surface. Applying a stationary random input to the vehicle and using the frequency domain technique has demonstrated the manner in which the ride quality and ride safety are affected by suspension springing and damping characteristics, tire springing characteristics and vehicle speed. In a recent article [47], the same authors describe an analytical study of

the dynamic behaviour of a tractor-semitrailer vehicle. A digital computer simulation was used to describe the longitudinal, vertical, and pitching motions of the vehicle travelling over a stationary random road surface. A man-seat model was incorporated into the simulation. Solution of the linear equations of motion provides power spectra, and root mean square values for component displacements and accelerations.

A brief discussion of the dynamic response of the articulated vehicle to random surface undulations will be given in the following paragraphs, from materials drawn from references [1, 46, 47, 58, 63, 64, 78, 79, 80, 81, 113, 115, 144]. The discussion of the results of these publications will help clarify the ride motion of the articulated vehicle.

The tractor-semitrailer vehicle possesses many natural modes due to its individual components and their interaction with the vehicle as a whole. Some of the important modes and their typical vibrational frequencies are given in Table 2.1.

Table 2.1

Vehicle Vibrational Frequencies

Mode Description	Frequency Range (Hz)
Driver-seat Bounce	1.7 - 2.5
Vehicle Bounce	1.6 - 3.6
Vehicle Pitch	2.0 - 5.8
Vehicle Frame Bending	6 - 10
Single Axle Bounce	9 - 14
Tandem suspension Bounce	10 - 15

These modes of oscillations are frequently encountered in the normal mode of operation of an articulated vehicle. Vehicle pitch, bounce and frame bending frequencies are in the range of human body resonance indicating an uncomfortable ride for the operator. Frame beaming and wheel hop frequencies contribute significantly to vehicle ride safety. Therefore, careful consideration must be given to damping the unsprung mass on tire resonance and thus ensure good tire-road contact.

The fore and aft motions which occur due to the relative heights of the centre of gravity of the tractor and semitrailer units and the fifth wheel kingpin are functions of the combined tractor and semitrailer pitching motions. As human beings are much more sensitive to fore and aft vibrations, complaints about head snapping action are

more prevalent than those about seat bounce. This indicates that the pitching mode motions of both the tractor and semitrailer have a significant contribution to operator discomfort and much attention should be given to reduce their effect.

The response of such a complex system to road surface undulations is very complicated. Due to the application of the road inputs at several tire contact points of the vehicle, displaced by a certain time delay, depending on vehicle speed and the distance between the various axles, and due to the effects of coupling in a multiple degree-of-freedom system where one vibration is likely to influence others, the shape of the response curves may be remarkably varied: peaks may be attenuated, shifted to a different frequency or may even almost completely disappear.

The analysis of the vibration of the articulated vehicle suspension shows that high spring rates are a deterent to ride quality and the operator comfort can be greatly improved by a suspension with low spring rates. Therefore low values of the springing parameters are recommended, but the minimum values are limited by other consideratons, such as suspension static deflection, stroke deflection, and roll stiffness. However, lowering the spring rates below certain values results in an increase in the dynamic tire loads.

The analysis shows that care should be given to the choice of the ratio of front static deflection to rear static deflection of the springs on the tractor. Neither should the deflections be equal nor should the deflection ratio be large because either one of these is

detrimental to both pitch frequency and pitch centre of location and consequently to ride quality.

Maximum forced oscillation amplitudes are likely to occur when the excitation frequency is close to the low natural frequencies of the vehicle; (bounce and pitch frequencies). In the vicinity of these natural frequencies, the higher the damping factor, the lower the resulting oscillation amplitude. Consequently, a high damping factor is beneficial. However, at frequencies well in excess of the low natural frequencies, high damping factors are detrimental. A compromise is therefore necessary to ensure satisfactory response to random excitation in the vicinity of the natural frequencies of the vehicle on the suspension, while at the same time avoiding an unfavourable response to higher frequency excitation.

For vehicle ride safety, increasing the damping in the suspension, in general, decreases the tire dynamic force. However, with high damping the dynamic force increases again, because high damping stiffens the suspension and transmits more force to the road. Therefore, adequate damping is essential to control resonance and reduce average dynamic tire movements and hence the probability of wheel hop.

Suspension systems for the driver's seat can provide a degree of isolation from vertical vibration, and in some designs, from fore and aft vibration. Seat with passive isolation system is generally used due to its low cost and simplicity. The resonant frequency should be adjusted as low as possible for maximum isolation. The degree of isolation is limited by the fact that large static deflections are

undesirable for operator controllability. The amount of damping present in the isolator determines the resonant transmissibility. Selection of isolator design parameters, generally, requires compromise between resonant vibration control and high frequency vibration isolation.

The cab mounting system provides a means to improve ride comfort. There are two types of cab suspension systems. In the first type, the suspension systems are provided at the rear of the cab while the other end of the cab pivots about a fixed point. Some improvement in longitudinal ride quality can be obtained in this case at the expense of losing vertical ride quality. This occurs due to the fact that generally more vibrations are present at the cab hinge than at the rear cab mount.

In the second type, the suspension systems are provided at all four corners of the cab for better isolation from the chassis. Cab isolation requires low-rate front and rear springs to achieve the desired ride improvement. However, as the cab natural frequency is lowered, the cost increases and the space required for cab travel relative to the chassis increases.

2.4.3 Nonlinear Analyses

In situations where a more complete understanding of the qualitative and the quantitative behaviour of the tractor-semitrailer vehicle is required, it is often necessary to include nonlinear effects. These nonlinearities refer mainly to:

i) the characteristics of shock absorbers, suspension springs, tires, jounce stops, etc.

ii) Coulomb friction in the suspension.

iii) the separation of the tires from the road surface.

The damping characteristics of the vehicle suspension may be proportional to some power of the stroking velocity, with the damping in compression being different from that in the recoil. Torsion bars, coil springs, and rubber springs may have variable rate characteristics to account for the variation in loading [28]. Tire characteristics may be nonlinear functions of loading. Suspension stops, which cause bottoming, i.e., solid contact between the unsprung mass and the sprung mass, may permit large force impulses to be transmitted to the frame, the driver, and the cargo.

The normal articulated vehicle suspension system is made up of conventional leaf springs. Leaf springs suffer from two basic disadvantages that are especially important in terms of determining the level of ride quality of the vehicle. One is that the interleaf friction is usually high and unpredictable. The other one is that forces equal to the friction forces are transmitted through the suspension elements by the friction, so that there is a tendency for high frequency vibrations to reach the vehicle body.

The degree of dry friction depends on the frictional surfaces, their material and quality. The friction force is as much as 7-20% of the static load on the front axles, and 15-30% of the static load on the rear axles for the semi-elliptical laminated springs [78]. This static

frictional force will cause the vehicle to vibrate on the tires, since there is no deflection of the springs until the tire deflection produces sufficient force to overcome the breakaway friction. As such the static friction is not desirable due to its often irrational action as well as the reduction of its effect near a resonant frequency. Consequently, the frictional force generated in laminated springs has a large influence on the ride comfort and road safety of the vehicle.

This series of nonlinearities can be expected to influence the ride dynamics of the vehicle to an appreciable degree. Consequently, there is a need to evaluate the effects of nonlinearities on the general behaviour of the vehicle.

Typically, the response of a discrete nonlinear dynamical vehicle system is described by a set of second order nonlinear differential equations. There are two principal methods of analysis that can be employed to determine the response of nonlinear systems subjected to deterministic or to random excitation, a deterministic analysis and a statistical analysis.

In the deterministic analysis the solution of the differential equations in the time domain is accomplished through a series of integrations. This type of analysis is particularly well suited to high speed digital computers where the integrations are performed using numerical techniques, as well as analogue computers where the integrations are performed electronically. The effect of nonlinearities in various components can be accommodated in a step by step manner as the solution of the differential equations progresses. The solution

results are obtained in the form of time traces requiring further analysis to reduce the data.

The analysis allows the transient and steady-state motion of the vehicle to be investigated in the time domain. Transient motion studies have been quite valuable in determining the response of the vehicle system to a given excitation and thereby play an important role in design and analysis of real vehicle. Moreover, the steady-state motion studies give a clear overall view of the manner in which various system parameters affect the response.

In simulating vehicle response to actual deterministic road input, it is necessary to have the surface profile as a funotion of time. This requires that a record of the actual profile as a digitally sampled function be available for digital simulation, or a continuous time record of the profile on magnetic tape be available for an analogue simulation. If an artificial random input is used the excitation may be generated by a random white noise generator. It would be necessary that the signal output of this generator be properly filtered to give the correct frequency content.

There are several drawbacks to the deterministic analysis used in the simulation. First it is difficult to achieve a good approximation of the expected value for displacement, velocity and acceleration variances in the time domain. Secondly, a relatively large amount of computer time is required for good statistical accuracy. Finally, the simulation is costly. These facts suggest the need for development of techniques for approximate statistical analysis.

Usually, the response of a discrete nonlinear dynamical system subjected to random excitation is modeled by a set of second order stochastic differential equations. It is clear that in this case the response of the nonlinear system can no longer be considered as a single deterministic function, but should more properly be regarded as a family of functions characterized by some suitable statistics.

Several approximate techniques for solving nonlinear systems subjected to random excitation have been developed. One such is the classical perturbation technique which may be used to solve weakly nonlinear systems. The expansion of the response in a series for the coefficient of the nonlinear terms, yields a chain of linear systems which may be solved to obtain an approximate response. This approach has been applied to stationary random vibration of nonlinear systems by Crandall [37]. Tung [136] extended this technique to more general multi-degree-of-freedom systems.

Another method which is used in the study of nonlinear random systems is the equivalent linearization technique [25, 26]. In this technique, an auxiliary set of linear differential equations for the original nonlinear system is defined. Some coefficients of the auxiliary set may still be unknown. The solution of the original nonlinear system is approximated by the solution of the auxiliary and the unknown coefficients are chosen in such a way that some measure of the difference between the two sets of equations is minimum.

To date, however, there has been little work carried out on the application of these techniques to study the nonlinear behavior of the

vehicle (see, for example, references [125, 136]).

2.4.3.1 Nonlinear Vibration of Nonarticulated Vehicles

The behaviour of a single degree of freedom vehicle model moving with a constant velocity over an uneven pavement was studied by de Pater [42]. The road profile was presented as a sinusoidal input and both analogue computer and experimental methods were used. Ellis and Goldwyn [52] made use of an analogue computer and investigated the more general case of a pavement with a periodical profile. Ellis [49] simulated vehicle vibration deterministically using an analogue computer. Comparison between the theoretical and experimental displacement histories of the vehicle coordinates was made. In all these investigations of vehicle vibratory motion the possiblity that a wheel could lose contact with the road was taken into account in the analysis, so that the problem was nonlinear. The results showed that it was possible to simulate this type of nonlinearity with a fair degree of success.

Clark [29] investigated the road loading forces imparted to the pavement surfaces by using an analogue computer. The single case of sinusoidal pavement profile was studied. The results demonstrated that a given amount of Coulomb friction on a given road profile would be decreasingly effective in suspension damping even for a constant peak to peak road input amplitude as vehicle speed was increased.

Unsymmetrical damping and dry friction in the shock absorber gland were studied by Burns and Sachs [18]. The base excitation was

a sine wave. In comparing the symmetric to the unsymmetric systems, the response curve decay for the unsymmetric system was delayed from that of the symmetric case such that more time was required for the oscillation to reach a steady state response. The addition of Coulomb damping resulted in a more rapid decay of the response.

Thompson [132] used an analogue computer to study the effect of unsymmetrical damping on the ride quality of two degrees of freedom vehicles. Simulated step-function inputs and random road inputs were used in the analysis. He concluded that unsymmetrical damping provided better isolation from large bumps and obstacles at the expense of only very moderate increases in the mean square values for random inputs.

Ilosvai and Szucs [71] discussed the effect of the value of frictional forces generated in laminated springs on the vibration comfort and stability of two degrees of freedom vehicle. Several stochastic road profiles were used to excite the computer model. The results showed that due to dry friction in the suspension, the frequency of dominant vibrations would increase and would get into a range less bearable by human beings. The results showed also that increasing the frictional force would increase the probability of the wheel departure from the road.

2.4.3.2 Nonlinear Vibration of Articulated Vehicles

Using an analogue computer, Metcalf [101] studied the ride behavior of a three-element articulated vehicle with nonlinear suspension. The nonlinearities considered were limited displacement

suspension, tire spring effects, and wheel hop. The ride behaviour of the vehicle was evaluated on the basis of the probability distribution of the vertical and pitching accelerations of the sprung mass, and the percentage of time each wheel assembly lost contact with the ground, in response to random terrain input. His results indicated that the forward speed of the vehicle could be increased by increasing the suspension bump-stop clearance or by "tuning" the vehicle suspension to the specific terrain encountered. He also indicated that using extreme low-pressure tires with a small vertical spring rate might allow the tire to bottom on the rim and cause vehicle ride to deteriorate.

As mentioned previously Van Deusen [140, 141] developed a nonlinear articulated vehicle model. Using a digital computer and numerical integration techniques, the set of nonlinear equations of motion were solved in the time domain. The nonlinearities consisted of (1) separation of the tires from the surface, (2) jounce stops, (3) Coulomb friction in the suspension, and (4) angular nonlinearities to account for the shock absorber damping changes with geometry. The results showed that a small amount of suspension friction is beneficial in the absence of shock absorbers. The results showed also that tire surface separation did not significantly affect the optimum values of shock absorber obtained from linear vehicle model.

Potts and Walker [108] have developed a nonlinear deterministic computer program which may be used to determine the displacement, velocity and acceleration of each coordinate of the vehicle system. The nonlinearities considered are Coulomb friction damping, wheel hop, the

nonlinear force-deflection characteristics of the springs and tires, and the force-velocity characteristics of the dampers. They have checked the deterministic program by comparing their output by the experimental measured motions of a model truck constructed in the laboratory. The general characters of the theoretical and experimental results are in close agreement. By comparing the linear and nonlinear deterministic analyses with the experimental results, the nonlinear theory comes closer to predicting the measured vibratory motions than does the linear theory, especially at a resonant condition.

2.5 Ride Comfort

The combination of the factors which must be considered in achieving passenger ride smoothness, increased vehicle speed and reduced shock and vibration for sensitive cargo makes the evaluation of vehicle riding comfort extremely complex.

An extensive amount of research dealing with human sensitivity to vibration has been reported in the literature over the past few decades. Reviews of the literature on this subject are available in works by Goldman [61], Goldman and Von Gierke [62], Van Eldik Thieme [142], Carstens and Kresge [21], Hanes [66], Bekker [9], Janeway [82], and Healey [67]. The research in this area revealed that the subjective response of an individual to an imposed vibration depends not only on the physiological and bio-mechanical response of his body but also on a number of psychological and environmental factors. It has revealed also that human reaction to vibration is not only a function of the

amplitudes, accelerations, and frequencies applied to the body, but also of the direction (vertical, fore and aft, lateral) and character of motion (linear, rotational). The time during which the human body is exposed to vibration is also important.

Three major concepts have been proposed for describing comfort criteria; ride index concept [77, 142], absorbed power concept [92, 109, 110, 111, 112], and power spectral density and transfer function concept [4, 6, 19].

Ride indices are numerical evaluations of the human response to combinations of acceleration amplitudes and frequencies. A given ride index represents a particular response or sensation, and may originate from any of an infinite number of acceleration and corresponding frequency values. Several sets of tolerance curves have been developed to define limits on vibrational intensity. These curves were obtained by exposing test subjects to rides during which they were subjected to various vibrational frequencies and amplitudes and then asking them to form an opinion of the ride sensation. Several objectives have been used by various investigators to describe the limit of acceptable vibration, such as uncomfortable, disturbing, annoying, unpleasant, fatiguing, objectionable and intolerable.

There are two drawbacks to the means of obtaining the ride index. The first is the imprecise definitions used to describe the limit of acceptable vibration. This cannot be avoided in such type of testing, which requires a definition of discomfort to be used for the individual subjective assessments. The second is that the investigators have used

sinusoidal inputs generated in the laboratory. Since road surface irregularities are random, the actual motions felt by vehicle passengers are random vibrations with frequency content spread over all frequencies. Consequently, it is difficult to make a meaningful comparison between the comfort criteria expressed in terms of sinusoidal vibrations, and the actual random vibration of the vehicle.

In the 1960's, Pradko, Lee, Orr and Kaluza [92, 109, 110, 111, 112], introduced a new comfort parameter called "absorbed power". Absorbed power is an energy flow rate which depends on the complex damped elastic properties of the human anatomy, and is related to passenger subjective responses.

While the elastic body is subjected to vibration, the vibrational energy distorts it, changes its dimension and this in turn produces reactions that tend to restore the body to its original position. The work performed in the process balances the applied load. Consequently, the body's elasticity produces restoring forces which are related to displacement. The body's vibratory motion continues until the energy imparted to it is dissipated or removed. The time rate at which this energy is used is called absorbed power. Low levels of absorbed power correspond to good ride quality.

Absorbed power can be described in the frequency domain and/or in the time domain. In the frequency domain the absorbed power is computed as the product of the mean squared acceleration and a conversion constant. In the time domain, the absorbed power is calculated using the impedence description of the human body.

In the power spectral density and transfer function concept, the acceleration spectrum is broken into different frequency bands. A correlation of the square acceleration in each band with subjective response to the vibration gives a meaningful and useful ride criterion.

In a recent document concerning the Urban Tracked Air Cushion Vehicle [4], specifications of ride quality in terms of the vertical, lateral and longitudinal acceleration power spectral densities were given. These spectral density specifications were based on experimental measurements.

The International Standard Organization (ISO) "Guide for the Evaluation of Human Exposure to Whole-Body Vibration", ISO 2630 [6, 127, 145], has incorporated most of the experimental data regarding human exposure to vibration available from all countries and has recently gained acceptance for many applications.

The International Standard Organization (ISO) defines and gives numerical values for limits of exposure to vibrations transmitted from solid surfaces to the human body in the frequency range 1 to 80 Hz. These limits cover human sensitivity to vertical, lateral, and fore and aft vibrations of a periodic, nonperiodic or random nature. The exposure times are ranging from 1 minute to 24 hours. Periodic excitation is evaluated by the rms acceleration amplitude, while broad band excitation by the rms acceleration levels measured through one third octave band filter. In the ISO guide, the human passengers are more sensitive to vibration frequencies in the 4 - 8 Hz range for vertical motion and 1 - 2 Hz range for lateral and fore and aft motion,

and the human tolerance of vibration decreases in a characteristic way with increasing exposure time.

The tendency toward a higher vehicle speed to travel over most roadways has made ride requirements increasingly difficult to achieve. Increasing vehicle speed for a given vehicle and roadway combination generally intensifies vehicle vibration which usually downgrades ride quality.

There are numerous publications dealing with the tolerance of cargo to specific levels of vibrations (see, for example, reference [17]). The cargo safety criteria is given in rms acceleration or in boundaries between acceleration and frequency.

2.6 Ride Safety

Longitudinal and lateral forces, developed through friction are necessary for accelerating, braking and steering a moving vehicle. These forces depend on the wheel-road friction, wheel construction, surface condition, and the normal load at the wheel/road interface as well as the vehicle dynamic characteristics and suspension geometry parameters. Friction forces are relatively large on a smooth, dry, plane pavement, but may be reduced due to the dynamic wheel forces exerted through the wheel of a moving vehicle, on an uneven and undulating pavement.

In a report by Wambold et al. [149], the loss of tire braking friction due to road roughness was simulated and measured experimentally in a test machine designed to produce simultaneous wheel slip and

vertical vibration of the contact surface. Their results showed that simulated roughness amplitudes and frequency had strong influence on the average force available for braking.

From the viewpoint of directional control of vehicles, it is necessary to minimize the loss of road-to-wheel contact, that is, to maximize the force available at the road, to resist lateral skidding and transmit deceleration and acceleration forces from the tires to the road. Consequently, knowledge of the dynamic wheel forces may be of considerable importance in studies of vehicle safety.

Since most road surface profiles are random, the resulting dynamic wheel forces are also random and statistical representation of these forces is required. One statistical method most commonly used to estimate the dynamic wheel forces is to determine the road surface roughness power spectral density function, and the vehicle response characteristics, to obtain the dynamic wheel force power spectrum. The power spectrum may be used to compute the rms values or the probability of exceeding a particular level or range of a given value of wheel dynamic load.

Mitschke [102] used this method to investigate the influence of road roughness on the dynamic wheel loads. He concluded that, in general, the dynamic loads should be kept small for vehicle safety. Quinn and Hildebrand [114] have studied the effect of pavement roughness on the steering behaviour of a vehicle. They have shown that the variation in the normal forces between the tires and the pavement influences the steering capability that in turn affects the lateral

forces needed to control the vehicle. Sattaripour [124] has shown that the statistical distribution of the lateral tire forces appears to provide a valuable criterion of pavement roughness that is directly related to safe vehicle handling conditions. Dokainish and ElMadany [46] used the power spectral density approach to study the effect of vehicle parameters on the dynamic wheel loads for a tractor-semitrailer vehicle. They found that decreasing suspension spring stiffness produced slightly larger peak dynamic load in the vicinity of axle hop frequencies. They also found that, with damping in the suspension, the dynamic loads are affected appreciably near body and axle resonances.

The mean square dynamic load is used generally as a measure of control of direction stability [11, 102]. The percentage of time the wheels are off the ground may also be used [101].

2.7 Summary and Conclusions

As suggested in the statement of the purpose of this chapter, a better ride is sought by more vehicle operators than any single improvement of truck operation. The desired improvement includes both reduced bounce and pitch, but primarily the latter. Ride is a very subjective matter, but it is, however, possible to define ride indices.

The preceeding review of the available technical literature dealing with articulated vehicle ride dynamics has shown that it is possible to model the vibrational response of the units mathematically. The means of describing the road surface inputs at the tire contact points is present, and although the articulated truck units are an

extremely complex dynamic system, the mathematical model can be of sufficient complexity that the interaction of the various internal forces with the inputs at the wheels may be determined. Finally, the means of obtaining solutions to the describing equations of the vehicle models are discussed and the form of the output results from the mathematical analysis is given for the various situations proposed by the individual researcher.

Thus, this chapter describes the various means by which it is possible to determine the dynamic response of an articulated vehicle where dimensions and mass distribution are known. The results obtained from such an analysis tend to approach 'real world' conditions and results relate well to the measured vibrational response of operating vehicles. Such mathematical modelling provides a strong tool for engineering designers to vehicle structures, suspension, etc. Using the analytical techniques to determine the effect of changes, coupled with the ride indices for comfort and safety, provides a means of testing prior to making physical changes on an actual vehicle.

The state-of-the-art survey in articulated vehicle ride shows that significant advances have been made on the analysis of articulated vehicle response to road surface undulations through the use of linear and nonlinear models and advanced computational techniques. However, there are a number of areas in which further research would be fruitful. These areas include the following: Road surface description by statistical methods is of primary importance in determining vehicle dynamic response. Available spectra for typical types of road-surface,

generally, are in the form of spectral density of a single profile. However, the implication that road inputs to nearside and offside wheels do not interact is contrary to any realistic conception. Therefore, it has been suggested that certain types of road roughness can be described as homogeneous, isotropic, Gaussian distributed process. The hypothesis of homogeneity causes the road input to be stationary for a vehicle traveling at constant speed. The hypothesis of isotropy means identical spectral properties in all directions. These hypotheses of homogeneity and isotropy lead to a very considerable simplification of road surface description. That is, complete probabilistic description of the road surface may be inferred from the probabilistic description of a single profile. However, further work is needed to examine, in depth, these hypotheses.

Although the models of articulated vehicles are sufficiently comprehensive for the prediction of vehicle response to road surface undulations, more effort should be expended to examine the sensitivity of the vehicle response to modelling assumptions.

Further experimental validation of the predictive articulated vehicle models is required. The use of these models to assess the ride quality over a wide range of vehicle parameters and operating conditions is one area where additional research is needed.

Analytical techniques and computer modelling techniques are used to obtain the dynamic response of vehicles to random road inputs. The analytical techniques using stochastic process theory have been primarily applied to linear response analysis of vehicle models. The

extension of these techniques to nonlinear vehicle models would be beneficial. This area of endeavor is open for further study. The computer modelling techniques to analyze nonlinear systems require numerical techniques for computer solution and these have not been fully developed for random inputs.

CHAPTER 3

RIDE ANALYSIS OF ARTICULATED VEHICLES MOVING ON RANDOM ROAD SURFACE UNDULATIONS

3.1 Introduction

There has been, over the past years, an increasing effort to improve the ride quality in articulated vehicles used for transport on our intercity highways. For these improvements to be realized, there must be not only a means of assessing ride quality, but as well a means by which engineering designers may incorporate and test ride improvements at the earliest possible moment in the design process.

In the work presented here, the motions of the various components of the vehicle structure are described by linear equations, and the entire analysis is carried out using a sufficient number of degrees of freedom that the results present a realistic assessment of the interaction of the various components. The input to the vehicle structure at the road-tire interface is the roughness of the road surface over which the vehicle would operate. The random road surface is described by its power spectral density, presenting averaged measure of the amplitude of its frequency components. The combination of the characteristic of the road surface and the dynamic description of the vehicle structure will permit the vibration response of the vehicle systems to be obtained in a manner that will allow the interaction of the vehicle systems components to be assessed, as well as the quality of

the vehicle ride to be determined.

The objective of the present work is to provide a method for determining and analyzing the response of articulated vehicles to road-surface undulations which are represented as stationary random excitations. The method utilizes the power spectral density approach to solve the linear equations of motion.

3.2 Articulated Vehicle Model

The articulated vehicle model adopted in this study is illustrated in Figure 3.1. It is seen to be two-dimensional in the longitudinal and vertical plane. The cab, engine, and tractor chassis are considered as one rigid body; similarly, the semitrailer with its chassis. Both units are allowed to translate in the forward and vertical directions, and to pitch except as constrained by the fifth wheel. The unsprung mass of each wheel and axle assembly is represented by a mass having vertical translational freedom only. The tractor-semitrailer suspension is represented by linear springs and linear viscous dampers. Each of the tires on the tractor and semitrailer is assumed to be a linear spring and damper having point contact with the road surface.

By considering the constraints imposed by the fifth wheel on the motion of the tractor and the semitrailer, the model includes six degrees of freedom: pitching and bouncing motions of the tractor centre of gravity, pitching motion of the semitrailer centre of gravity, and vertical motion of each wheel and axle assembly.

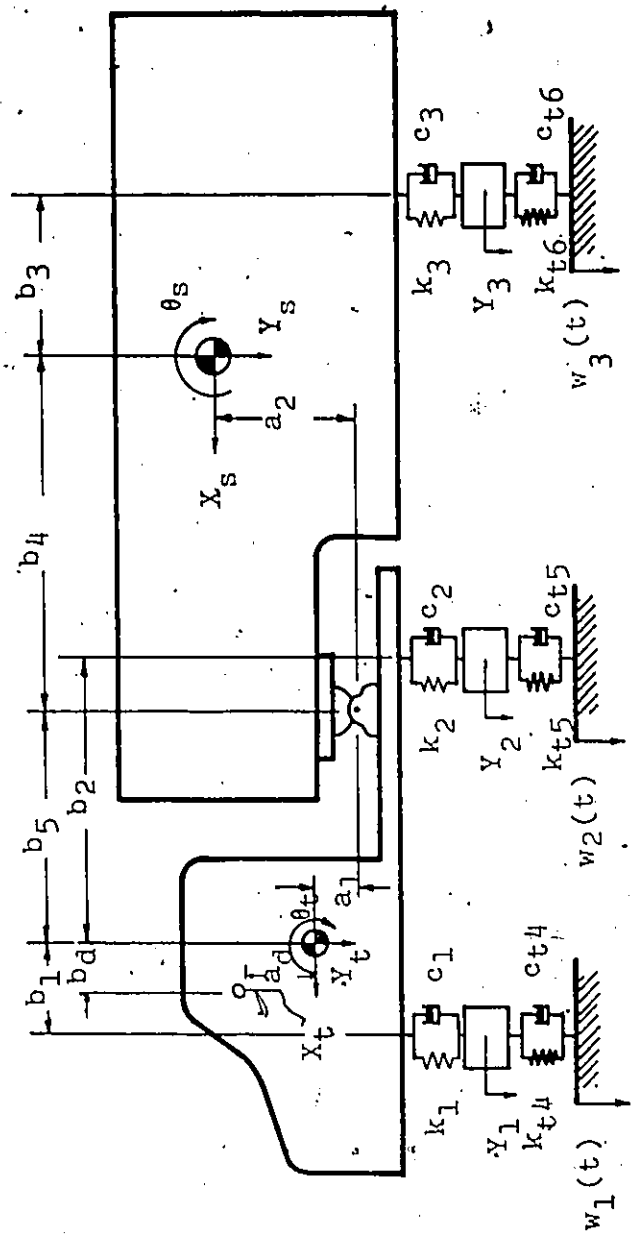

Figure 3.1 Articulated vehicle-linear model.

Although the linear vehicle model is used in this study, many of the fundamental effects of vehicle-road dynamic interactions may be realistically studied, and considerable insight into the behaviour of the system may be gained. The linearized analysis allows computation of the results in the frequency domain using transfer function which provides the engineer with a clear and concise description of the system behaviour. This technique is particularly useful to conduct sensitivity studies of the influence of various design parameters on the vehicle dynamic response.

3.3 Equations of Motion

By assuming small perturbations relative to the overall dimensions of the tractor-semitrailer, the linearized equations of motion of the vehicle are given in Appendix I, and they may be put in the following form:

$$M\ddot{\bar{x}} + C\dot{\bar{x}} + K\bar{x} = C_f \dot{\bar{w}} + K_f \bar{w} = \bar{f}(t) \qquad (3.1)$$

where M,C,K are the mass, damping and stiffness matrices, respectively.

C_f, K_f are the forced damping and stiffness matrices, respectively.

$\bar{x}, \bar{w}, \bar{f}$ are column vectors of the generalized coordinates, excitation displacements and excitation forces, respectively.

If $\bar{f}(t)$ is a random vector process, equation (3.1) is a stochastic differential equation and $\bar{x}$ is also a random vector process.

To compute the transfer function matrix, H(f), let

$$\bar{f} = \bar{f}_o \exp(i2\pi ft), \tag{3.2.a}$$

$$\bar{x} = H(f)\ \bar{f}_o \exp(i2\pi ft) \tag{3.2.b}$$

The transfer function matrix, H(f), is then given by

$$H(f) = [-(2\pi f)^2 M + i2\pi fC + K]^{-1} \tag{3.3}$$

3.4 Road Description

It has been recognized from a number of measurements on roadways that their roughness is normally distributed and can be accurately represented as a stationary random process [119]. As the power spectral density of the input process is a quantity suitable for the analysis of the dynamic behaviour of the vehicle on which a random process is acting, the road random disturbances are represented by their power spectral densities. The power spectrum of the road profile characterizes the essential aspects of the profile and gives at a glance the manner in which the roughness is distributed to the various frequency components. References 5, 44 and 91 discuss the spectral densities that closely approximate available experimental data and propose that road roughness can be described by

$$\begin{aligned} \delta(n) &= \delta(n_o)\left(\frac{n}{n_o}\right)^{-r_1}, \quad n \le n_o \\ &= \delta(n_o)\left(\frac{n}{n_o}\right)^{-r_2}, \quad n \ge n_o \end{aligned} \tag{3.4}$$

where

$\delta(n)$ is the spatial spectral density of the road roughness, $(m^2/c/m)$.

$\delta(n_o)$ is the roughness coefficient (the value of the spectral density at the discontinuity frequency, n_o).

n is the spatial frequency of road roughness

n_o is $1/2\pi$ c/m

r_1, r_2 are waviness.

3.5 Power Spectral Density Approach

Consider an n-degree-of-freedom linear system excited by a stationary random vector process, $\bar{f}(t)$, having a spectral density function matrix, $S_{\bar{f}}(f)$, and a correlation function matrix, $R_{\bar{f}}(\tau) = E[\bar{f}^*(t_1)\, \bar{f}'(t_2)]$, where * and ' denote matrix conjugation and transposition, respectively, E [ ] is the expectation operator and $\tau = t_1 - t_2$.

The matrices $R_{\bar{f}}(\tau)$ and $S_{\bar{f}}(f)$ form a Fourier-transform pair. They are related as follows:

$$S_{\bar{f}}(f) = \int_{-\infty}^{\infty} 2\, R_{\bar{f}}(\tau)\, \exp(-i2\pi f\tau)\, d\tau \qquad (3.5.a)$$

$$R_{\bar{f}}(\tau) = \int_{-\infty}^{\infty} \frac{1}{2}\, S_{\bar{f}}(f)\, \exp(i2\pi f\tau)\, df \qquad (3.5.b)$$

The impulse response function matrix, h(t), and the corresponding frequency response function matrix, H(f), also form a Fourier Transform pair.

$$h(t) = \int_{-\infty}^{\infty} H(f) \exp(i2\pi ft)df \tag{3.6.a}$$

$$H(f) = \int_{-\infty}^{\infty} h(t) \exp(-i2\pi ft)dt \tag{3.6.b}$$

If the impulse response function matrix, $h(t)$, is known, the random response, $\bar{x}(t)$, due to the random excitation, $\bar{f}(t)$, is given by the convolution integral

$$\bar{x}(t) = \int_{-\infty}^{\infty} h(t-\tau)\bar{f}(\tau)d\tau \tag{3.7}$$

The correlation function matrix, $R_{\bar{x}}(\tau)$, of the response is given by

$$R_{\bar{x}}(\tau) = R_{\bar{x}}(t_1-t_2) = E[\bar{x}^*(t_1)\bar{x}'(t_2)]$$

$$= \int\int_{-\infty}^{\infty} h^*(t_1-\tau_1)E[\bar{f}^*(\tau_1)\bar{f}'(\tau_2)]h'(t_2-\tau_2)d\tau_1 d\tau_2$$

$$= \int\int_{-\infty}^{\infty} h^*(t_1-\tau_1)R_{\bar{f}}(\tau_1-\tau_2)h'(t_2-\tau_2)d\tau_1 d\tau_2$$

$$= \frac{1}{2} \int\int\int_{-\infty}^{\infty} h^*(t_1-\tau_1)S_{\bar{f}}(f)h'(t_2-\tau_2)\exp[i2\pi f(\tau_1-\tau_2)]d\tau_1 d\tau_2 df$$

$$= \frac{1}{2} \int_{-\infty}^{\infty} H^*(f)S_{\bar{f}}(f)H'(f) \exp(i2\pi f\tau)df \tag{3.8}$$

where $H^*(f)$ and $H'(f)$ are the conjugate and transpose of $H(f)$, respectively.

From the relation between $R_{\bar{x}}(\tau)$ and the spectral density function matrix of the response, $S_{\bar{x}}(f)$, which is of the same form as that given

in equation (3.5), is given by

$$S_{\bar{x}}(f) = H^*(f)\, S_{\bar{I}}(f) H'(f) \tag{3.9}$$

In equation (3.9) the diagonal elements of $S_{\bar{x}}(f)$ are the spectral densities of the generalized displacements. The off-diagonal elements are the cross spectral densities of the generalized displacements. The power spectral densities for the corresponding accelerations can be determined from the relationship

$$S_{\bar{x}}^{\cdot\cdot}(f) = (2\pi f)^4 S_{\bar{x}}(f) \tag{3.10}$$

The response spectral densities, $S_{\bar{z}}(f)$, at coordinates other than the generalized coordinates can be obtained by using a transformation matrix, T, and is given by

$$S_{\bar{z}}(f) = T^*\, S_{\bar{x}}(f)\, T' \tag{3.11}$$

The relationship between the instantaneous correlation matrix, $R_{\bar{x}}(0)$, of the random response and its spectral density function matrix, $S_{\bar{x}}(f)$, can be determined by putting $\tau=0$ in equation (3.8) which reduces to

$$R_{\bar{x}}(0) = E[\bar{x}^*(t)\ \bar{x}'(t)] = \int_{-\infty}^{\infty} \frac{1}{2} S_{\bar{x}}(f)\, df$$

$$= \int_{0}^{\infty} S_{\bar{x}}(f)\, df \tag{3.12}$$

The probability that the tire leaves the road can be calculated from the following equation:

$$Pr = (1/2)\ \{1 - erf(p_s/\sqrt{2E[p_d^2]}\ )\}, \tag{3.13}$$

where p_s and p_d are the static and dynamic wheel loads, respectively.

In the above equation, erf is the error function, and $E[p_d^2]$ is the mean square of the dynamic wheel load.

3.6 Input Spectral Density Matrix

Suppose that the articulated vehicle moves with a constant forward velocity, v, along a road profile given by, $\bar{w}(x)$, which can be considered to be a member function of a stationary Gaussian random process, $\{\bar{w}(x)\}$, and the argument of which is the instantaneous location on the track, x. Let the mean value $E[\bar{w}(x)] = 0$.

As the vehicle is moving along a rough road, it is subjected to three vertically imposed spatial displacement functions, $\bar{w}_j(x)$, (j = 1, 2, 3), one at each wheel set. Let the imposed spatial displacement inputs to the mathematical model, $w_j(x)$, have correlation function matrix, $R_{\bar{w}}(\delta) = E[\bar{w}^*(x_1)\bar{w}'(x_2)]$, (where $\delta = x_2 - x_1$), and a spatial spectral density function matrix $S_{\bar{w}}(n)$. Conversion of the spatial inputs, $w_j(x)$, to temporal inputs, $w_j(t)$, is accomplished through a simple transformation whereby the spatial coordinate x is replaced by vt. Therefore, the relation between $w_j(x)$ and $w_j(t)$ is given by

$$w_j(vt) = w_j(t), \qquad j = 1, 2, 3 \tag{3.14}$$

Suppose that the corresponding input temporal correlation function matrix and temporal spectral density matrix are given by $R_{\bar{w}}(\tau) = E[\bar{w}^*(t_1)\bar{w}'(t_2)]$ and $S_{\bar{w}}(f)$, respectively.

The relationship between the spatial and temporal correlation functions and their corresponding spectral density functions can be derived as follows.

By considering that $f = n\nu$ and $\delta = v\tau$, the correlation function, $R_{\bar{w}}(\tau)$, is given by

$$\begin{aligned} R_{\bar{w}}(\tau) &= E[\bar{w}^*(t)\ \bar{w}'(t+\tau)] \\ &= E[\bar{w}^*(vt)\ \bar{\bar{w}}'(vt+v\tau)] \\ &= E[\bar{w}^*(x)\ \bar{w}'(x+\delta)] \\ &= R_{\bar{w}}(\delta) \end{aligned} \tag{3.15}$$

The spectral density function, $S_{\bar{w}}(f)$, is given by

$$\begin{aligned} S_{\bar{w}}(f) &= \int_{-\infty}^{\infty} 2R_{\bar{w}}(\tau)\ \exp(-i2\pi f\tau)d\tau \\ &= \frac{1}{v} \int_{-\infty}^{\infty} 2R_{\bar{w}}(\delta)\ \exp(-i2\pi n\delta)d\delta \\ &= \frac{1}{v}\ S_{\bar{w}}(n) \end{aligned} \tag{3.16}$$

In the matrix $S_{\bar{w}}(f)$, $S_{jk}(f)$ is the input displacement spectral density to the vehicle at the tire contact point. When $j=k$, $S_{jk}(f)$ represents the direct power spectral density of $w_j(t)$ and in this case $S_{jj}(f) = 1/v\ \ S_{jj}(n)$. When $j \neq k$, $S_{jk}(f)$ represents the cross spectral density of $w_j(t)$ and $w_k(t)$.

To compute the cross spectral density, $S_{jk}(f)$, assume that the vehicle rear wheels follow the same profile as the front wheel, but are separated by a constant time delay, $\tau_{jk} = \ell_{jk}/v$, where ℓ_{jk} is the spacing between jth and kth wheel. The cross-correlation function of any two wheels, j and k, is given by

$$R_{jk}(\tau) = E[w_j^*(t)w_k(t+\tau)]$$

$$= E[w_j^*(t)w_j(t+\tau - \ell_{jk}/v)]$$

$$= R_{jj}(\tau - \ell_{jk}/v) \qquad (3.17)$$

and hence the cross-spectrum

$$S_{jk}(f) = \int_{-\infty}^{\infty} 2\, R_{jk}(\tau - \ell_{jk}/v)\, \exp(-i2\pi f\tau)\, dt$$

$$= \int_{-\infty}^{\infty} 2\, R_{jk}(\tau - \ell_{jk}/v)\, \exp[-i2\pi f(\tau - \ell_{jk}/v)]\, d(\tau - \ell_{jk}/v) \cdot \exp(-i2\pi f\, \ell_{jk}/v)$$

$$= S_{jj}(f)\, \exp(-i2\pi f\, \ell_{jk}/v) \qquad (3.18)$$

Combining equations (3.16) and (3.18) and considering the property of cross-spectra:

$$S_{jk}(f) = S_{kj}^*(f) \quad , \qquad (3.19)$$

the temporal input displacement spectral density matrix, $S_{\underline{w}}(f)$, may be written in terms of the surface profile as follows:

$$S_{\underline{w}}(f) = \frac{\delta(n)}{v} \begin{bmatrix} 1 & e^{-i\mu_{12}} & e^{-i\mu_{13}} \\ e^{i\mu_{12}} & 1 & e^{-i\mu_{23}} \\ e^{i\mu_{13}} & e^{i\mu_{23}} & 1 \end{bmatrix} \qquad (3.20)$$

where $\mu_{jk} = 2\pi f\, \ell_{jk}/v$

To compute the excitation power spectral density function matrix, $S_{\underline{f}}(f)$, the damping and elastic properties of the tires are used. In

this case the excitation correlation function is given by $R_{\bar{f}}(\tau) = E[K_f^* \bar{w}^*(t)\bar{w}'(t+\tau)\ K_f' + C_f^* \bar{w}^*(t)\ \bar{w}'(t+\tau) C_f']$ and by taking the Fourier transformation of $R_{\bar{f}}(\tau)$, the excitation spectral density matrix, $S_{\bar{f}}(f)$, is given by

$$S_{\bar{f}}(f) = (K_f + i2\pi f C_f)^* S_{\bar{w}}(f) (K_f + i2\pi f C_f)' \qquad (3.21)$$

Figure 3.2 describes the analysis of the vehicle system excited by road irregularities. The spatial spectrum of the road roughness, $\delta(n)$, is converted into the temporal spectrum, $S_{jj}(f)$. Taking into account the time delay caused by the wheelbase, the excitation displacement matrix of all wheelsets, $S_{\bar{w}}(f)$, is obtained. This excitation displacement matrix can be calculated in terms of the exciting force matrix, $S_{\bar{f}}(f)$, using the forced stiffness and damping matrices.

To obtain the response (displacements, velocities, accelerations, loads, etc. ...) in coordinates other than the generalized coordinates, a transformation matrix, T, is used.

The dynamic behaviour of the vehicle is then evaluated according to ride comfort and ride safety criteria. Ride comfort evaluation could, for example, be carried out according to ISO 2631 [6] or UTACV [4] standards, while ride safety evaluation could be carried out according to rms dynamic load, or percentage of time the wheels are off the road.

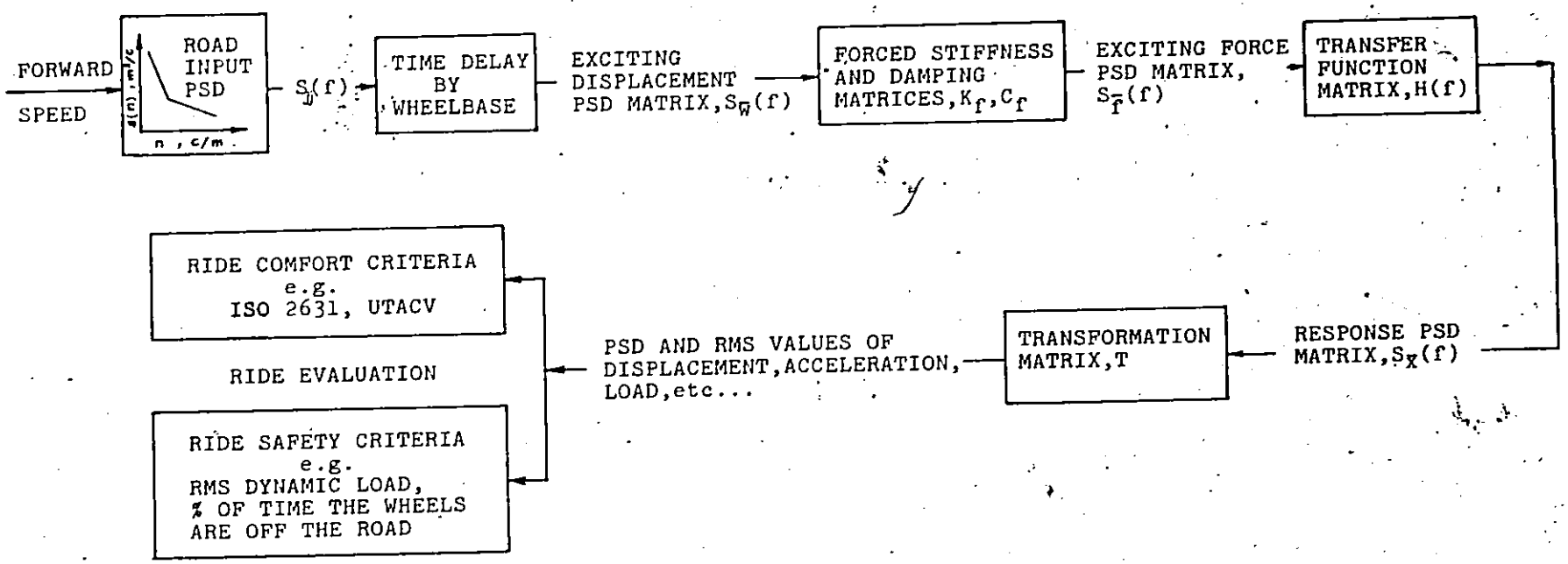

Figure 3.2 Vehicle ride analysis.

3.7 Summary

The method of vehicle analysis described here makes it possible to determine the dynamic response of articulated vehicle systems. The road roughness description used in the analysis tends to let the results obtained approach the "real world" conditions and provide an opportunity to check the vibrational responses obtained against measured values for operating vehicles. These mathematical modelling techniques are a further strong tool for engineering designers working on vehicle structures, suspension, etc.

CHAPTER 4

RANDOM RESPONSE OF ARTICULATED VEHICLES

LINEAR ANALYSES

4.1 Introduction

The method for determining and analyzing the dynamic response of articulated vehicle structures to road surface undulations presented in Chapter 3 will be applied in this chapter for the examination of the interaction between the road and the articulated vehicle and for the evaluation of the vehicle ride performance. The conflicting objectives for articulated vehicle suspension designed to accommodate the road irregularities while maintaining driver comfort, an acceptable cargo ride and reducing the fluctuation of the wheel dynamic loads will be investigated using the theory of stochastic processes.

The tractor-semitrailer vehicle is treated as a discrete, linear, time-invariant dynamic system subjected to a stationary random input from the road surface. The vehicle is assumed to be travelling over a roadbed for which the roughness is specified in terms of the power spectral density of the variation of the height of the track from a nominal reference. The vehicle model describes the longitudinal, vertical and pitching motions of the vehicle as it is affected by the road profile; Figure 3.1.

The theoretical investigation described here represents an attempt to obtain a better understanding of the influence of various

parameters on articulated vehicle dynamic response. In particular, the influences of vehicle speed, vehicle suspension elements, load pattern, and road characteristics on (a) the vibrations transmitted from the roadbed to the tractor-semitrailer vehicle, and (b) the dynamic forces at the tire-road interface, are evaluated.

The results of the computer analyses of vehicle and road are presented in three forms; system eigenvalues, the amplitude spectra and the root mean square amplitudes which are used to predict vehicle ride quality and evaluate the design concepts.

4.2 Results and Discussions

To describe the dynamic behaviour of this complex road-tractor-semitrailer, the eigenvalues of the model are evaluated, and the power spectra and rms values of the vehicle response are calculated and plotted.

The natural frequencies and damping ratios of the vehicle are determined by vehicle structural characteristics, suspension characteristics (suspension stiffness and damping), and load pattern. The excitation which the vehicle suspension receives depends on the number of axles, axle spacing, and road harmonic content. Vehicle speed determines when the road harmonic excitation frequencies match the vehicle natural vibration frequencies leading to vehicle resonance.

Two variations of the basic model are investigated. These are the unloaded vehicle and the loaded vehicle. A typical set of parameters, Table 4.1, is selected as the reference design to represent

Table 4.1
Baseline Values for Articulated Vehicle Model

I. Tractor

a. General

sprung mass (M_t)	6440 kg
front unsprung mass (M_1)	360 kg
rear unsprung mass (M_2)	1450 kg
pitch moment of inertia (I_t)	3390 kgm^2

b. Dimensions

b_1	1.27 m	b_5	1.4 m
b_2	2.03 m	a_1	-0.3 m
b_d	0.51 m	a_d	0.95 m

II. Semitrailer

a. General	Laden	Unladen
sprung mass (M_s)	15180 kg	3660 kg
unsprung mass (M_3)	1450 kg	1450 kg
pitch moment of inertia (I_s)	152000 kgm^2	48140 kgm^2
b. Dimensions		
b_3	3.96 m	3.11 m
b_4	4.57 m	5.42 m
a_2	1.02 m	-0.23 m

III. Suspension Characteristics

k_1	357 kN/m	c_1	11.5 kNs/m
k_2	630 kN/m	c_2	29 kNs/m
k_3	630 kN/m	c_3	29 kNs/m

IV. Tire Characteristics

k_{t4}	1560 kN/m	c_{t4}	0.7 kNs/m
k_{t5}	5250 kN/m	c_{t5}	1.2 kNs/m
k_{t6}	5250 kN/m	c_{t6}	1.2 kNs/m

V. Vehicle Speed 80 km/h

the vehicle. Two different road surfaces are considered. The parameters of these two road surfaces are given in Table 4.2. The first road is a smooth one and will be referred to as route A. The second road is a rough one and will be referred to as route B.

Table 4.2
Road Surface Characteristics

Route	$\delta(n_o)$ (m^3/c)	r_1	r_2
A, Motorway	13.0×10^{-6}	2.1	1.42
B, Minor Road	28.4×10^{-6}	3.3	1.48

The computer results are presented in five sections. The first section gives the eigenvalues of the vehicle system, the second section shows the effect of load pattern and road characteristics on vehicle accelerations, the third section indicates the effect of speed on vehicle motion, the fourth section shows the effect of vehicle suspension systems on vehicle accelerations, and the fifth section shows the effect of vehicle suspension systems on the dynamic wheel loads.

4.2.1 Eigenvalue Analysis

An eigenvalue analysis of the system is important to both designers and development engineers of vehicles in that it indicates the relative stability, damping ratios, and natural frequencies of the system. The eigenvalues are calculated for both the loaded and unloaded vehicle. In these particular cases the modes are all complex so they

occur in conjugate pairs. The results are tabulated in Table 4.3 where only one of each pair is listed.

A complex eigenvalue is denoted by

$$\nu = \sigma + i\omega$$

The imaginary part ω defines the damped natural frequency while σ defines an associated decay rate related to the amount of modal damping. In terms of an undamped frequency ω_n and a critical damping ratio ζ, σ and ω become, for $\omega_n \neq 0$

$$\sigma = -\zeta\omega_n, \qquad \omega = \omega_n\sqrt{1-\zeta^2}$$

The tractor bounce and pitch and semitrailer pitch natural frequencies are 1.28, 2.59 and 1.54 Hz respectively for the loaded vehicles, but they rise to 1.52, 3.67 and 2.65 Hz respectively for the unloaded vehicle by virtue of the large change in mass and pitch moment of inertia of the semitrailer. These frequencies for the unloaded case are in the range of human body resonances.

4.2.2 Effect of Load Pattern and Road Characteristics on Vehicle Accelerations

The road surface is described by its power density spectrum, equation (3.4), and the vehicle by its complex frequency response, H(f), equation (3.3). This frequency response is used as a transfer function operating on the road spectrum to derive the spectrum of vibration of the vehicle when it is moving along the road at a specified speed.

Table 4.3

Eigenvalues for the Articulated Vehicle

Case	Decay Rate (σ), 1/s	Damped Frequency (ω), 1/s	Undamped Frequency (ω_n), Hz	Mode Description
a-Loaded Vehicle	- 1.13	8.00	1.28	Tractor bouncing mode
	- 1.77	9.53	1.54	Semitrailer pitching mode
	-4.69	15.55	2.59	Tractor pitching mode
	-11.41	61.36	9.93	Axle wheel hop modes
	-10.88	62.26	10.06	
	-17.96	69.70	11.46	
b-Unloaded Vehicle	- 1.30	9.43	1.52	Tractor bouncing mode
	- 5.62	15.71	2.66	Semitrailer pitching mode
	- 9.96	20.78	3.67	Tractor pitching mode
	-12.06	59.00	9.58	Axle wheel hop modes
	-11.63	60.72	9.84	
	-17.90	69.56	11.43	

Figure 4.1 gives lines of constant comfort levels of acceleration for both the vertical and fore and aft motions for various exposure times. These are boundaries of reduced comfort. The ISO guide [6] has been converted into equivalent spectral values [127]. It is apparent from the figure that the most sensitive frequency is 4-8 Hz for vertical motion and 1-2 Hz for fore and aft motion; and that human tolerance of

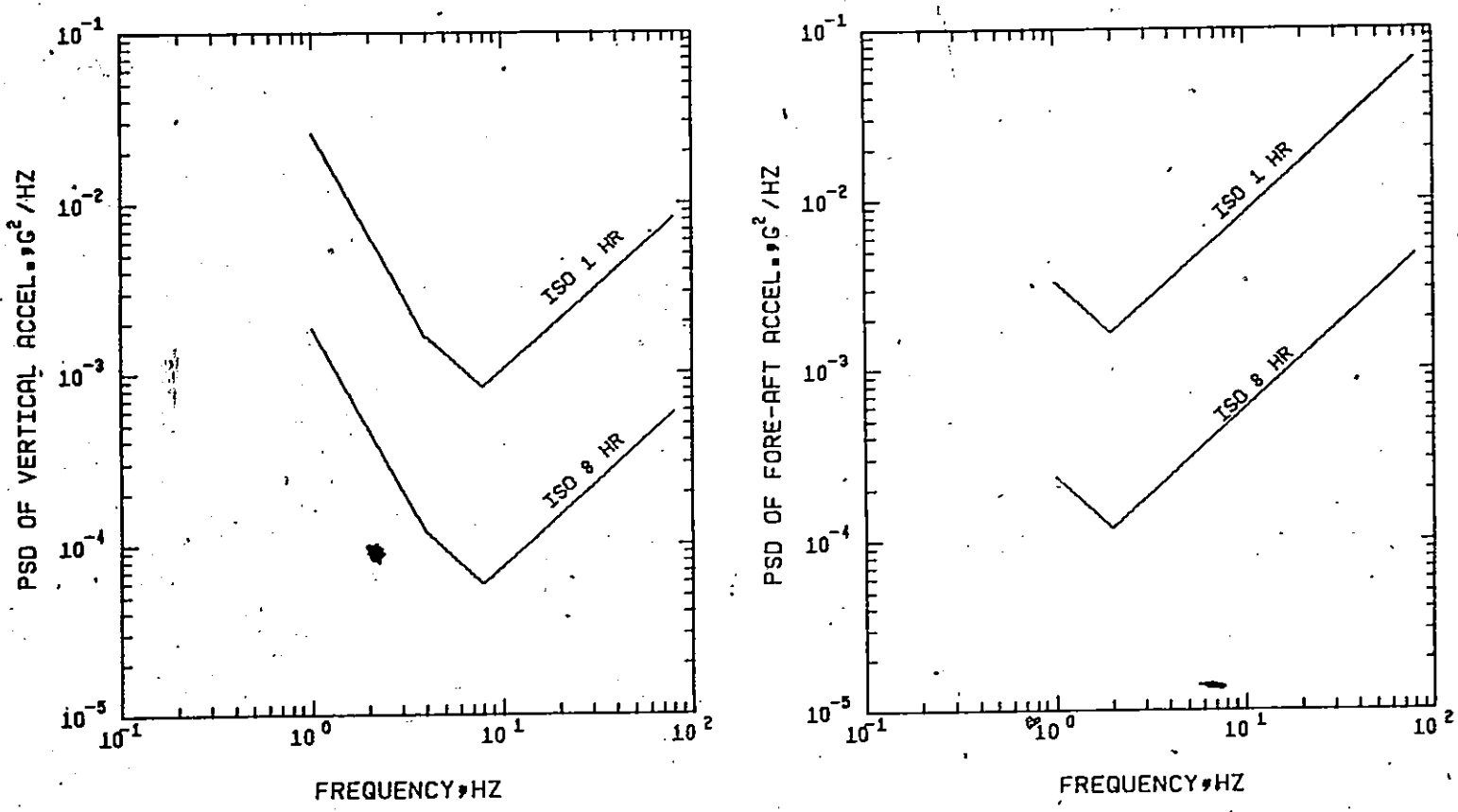

Figure 4.1 Reduced comfort boundaries for 1-hour and 8-hour exposure from ISO 2631 - vertical and fore and aft directions.

vibration decreases in a characteristic way with increasing exposure time.

The tractor-semitrailer vehicle possesses six natural modes due to its individual components, Table 4.3. It is expected to have six peaks in the frequency spectrum corresponding to its natural frequencies. However, due to the application of the road input at three wheel contact points of the vehicle, displaced by a certain time delay, depending on vehicle speed and the distance between the three axles, and due to the effects of coupling in a multiple degree-of-freedom system where one vibration is likely to influence others, the shape of the response curves may be remarkably changed: peaks may be attenuated, shifted to a different frequency or may even almost completely disappear.

Figure 4.2 gives the road spectra in g^2/Hz for different vehicle speed. These spectra are for route A and route B. From the figure it can be seen that increasing the forward speed will increase the road excitations received at the tire contact points.

Figures 4.3-4.6 show the vertical and fore and aft acceleration spectra of the tractor centre of gravity and the driver for both smooth and rough roads, respectively, compared to the ISO guide for one hour and eight hours reduced comfort boundaries. Both the loaded and unloaded vehicle model results are given.

For vertical motions, in a loaded vehicle case, the peaks around 1.3 Hz and 2.7 Hz correspond primarily to tractor bounce mode and

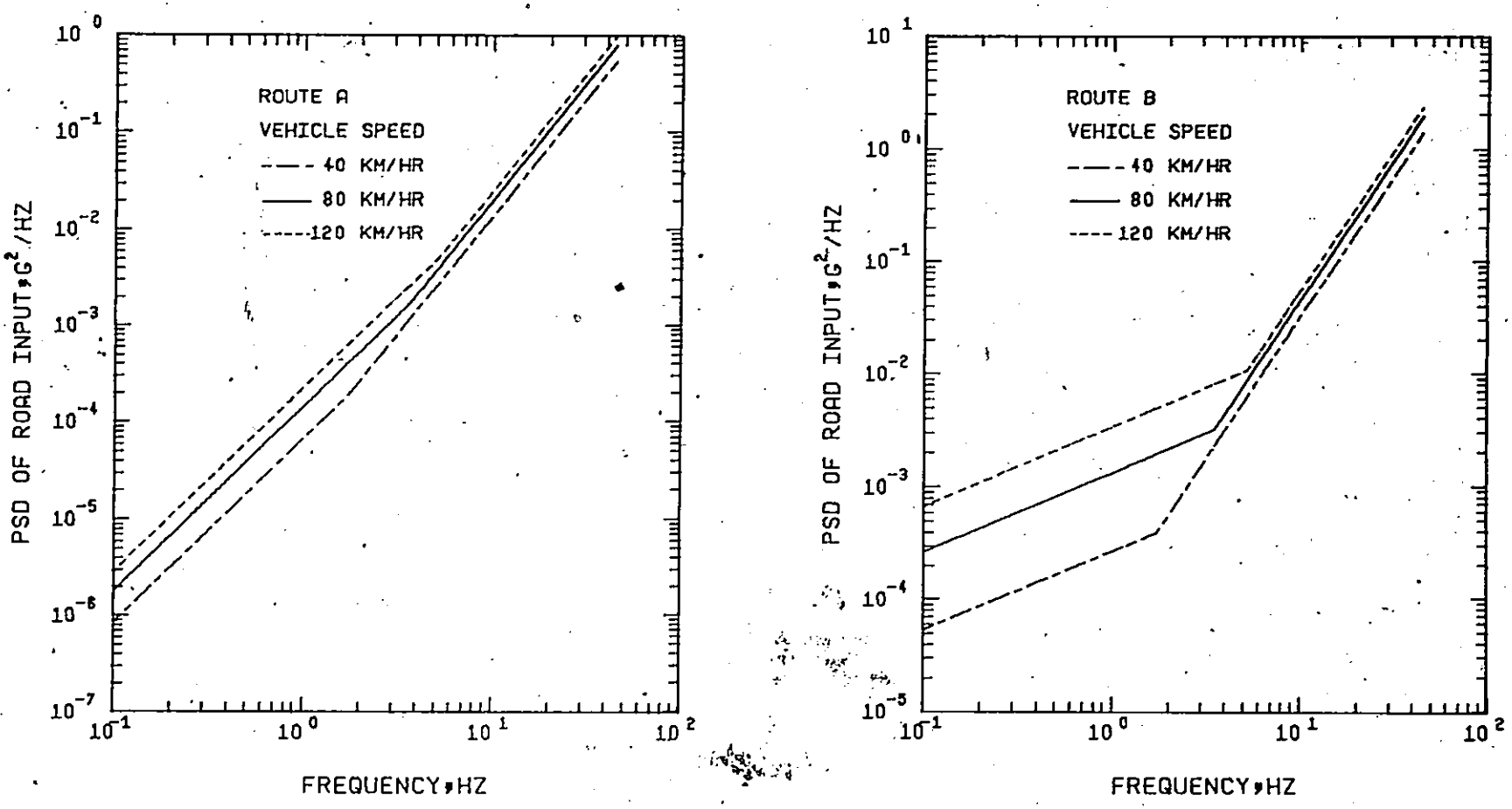

Figure 4.2 Road input spectra - smooth and rough roads.

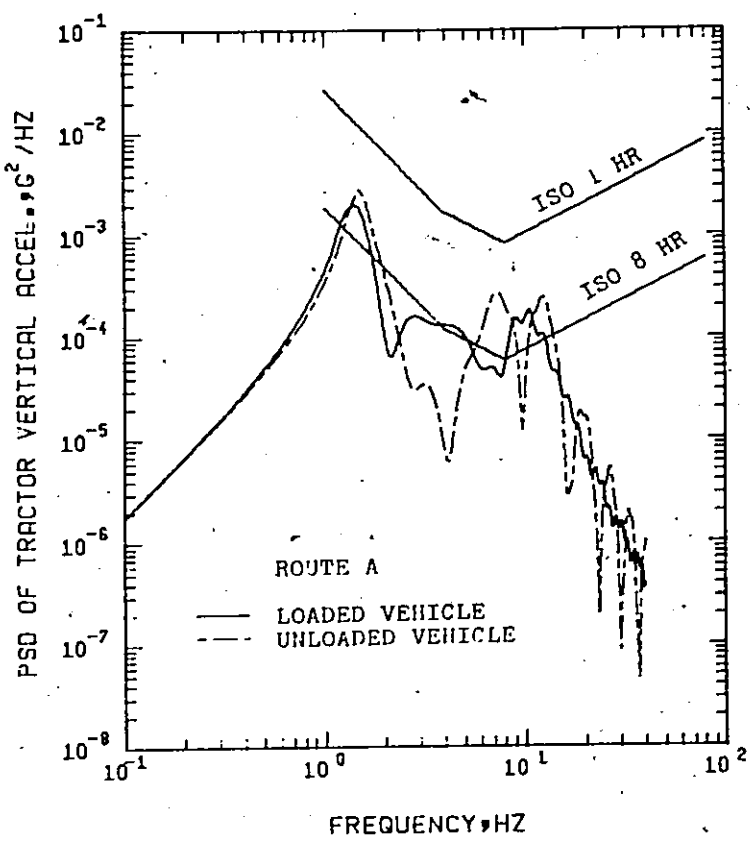

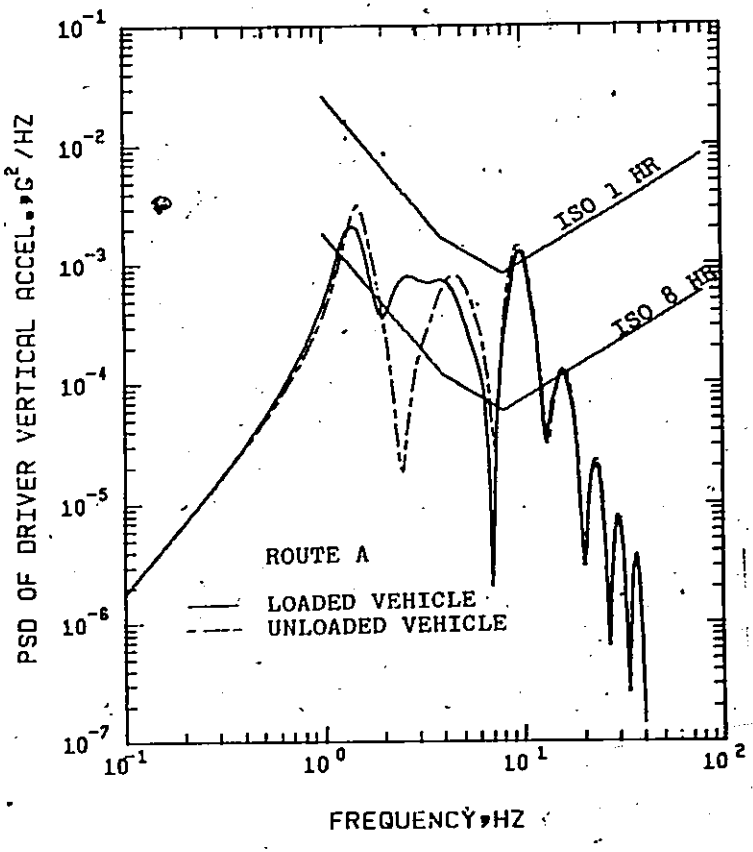

Figure 4.3 Tractor and driver vertical acceleration spectra - smooth road.

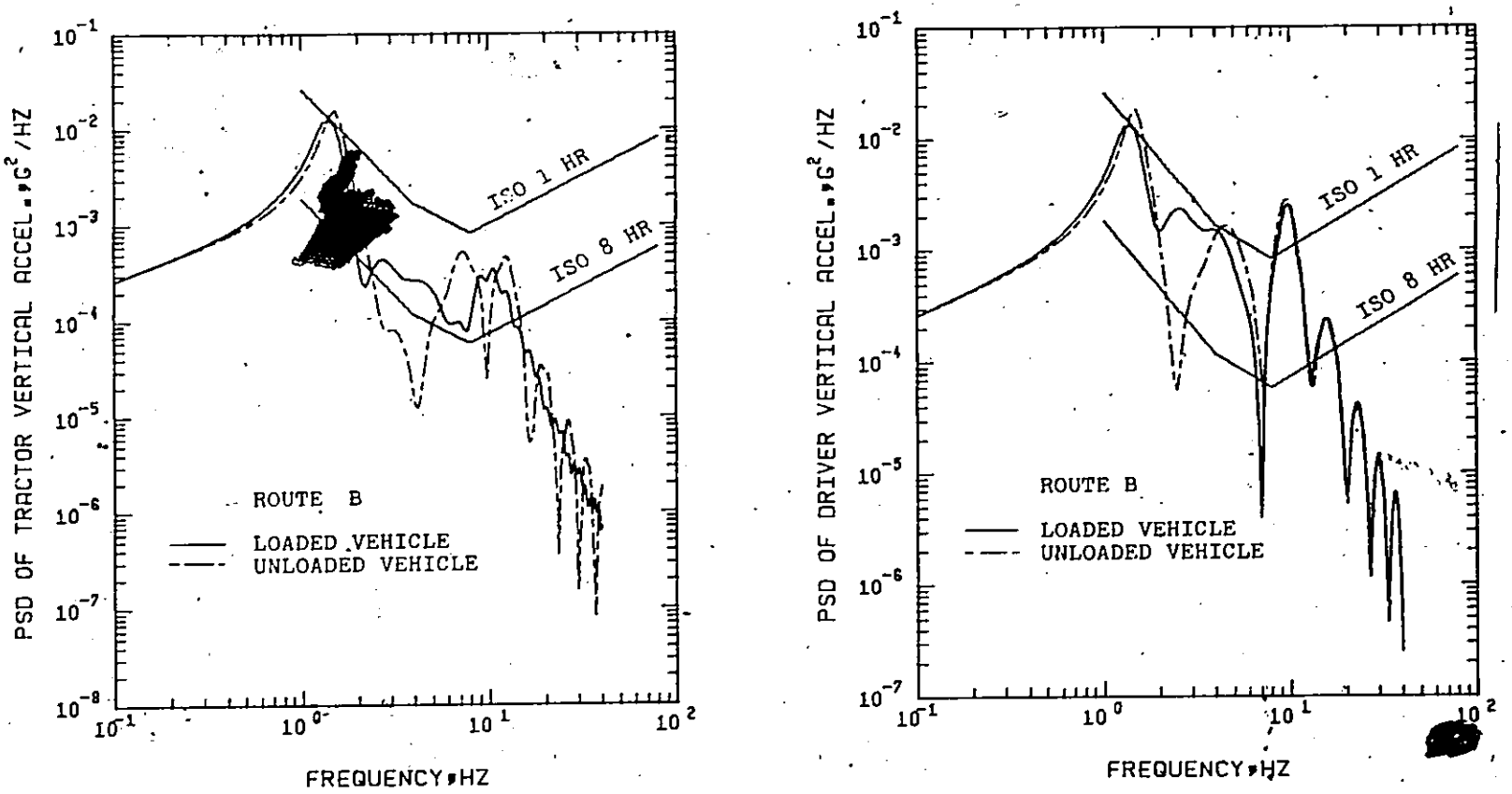

Figure 4.4 Tractor and driver vertical acceleration spectra - rough road.

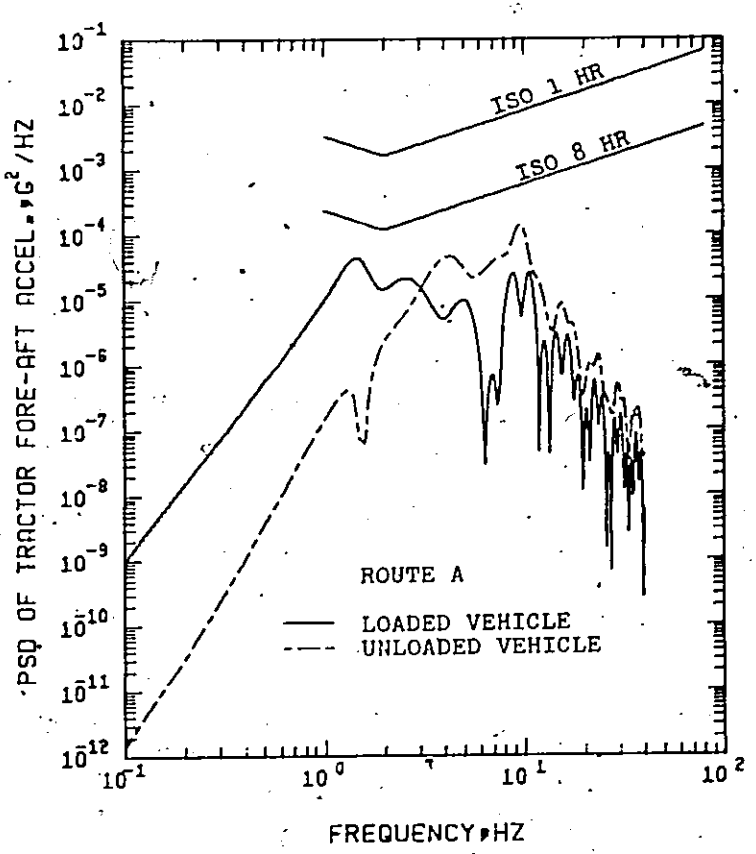

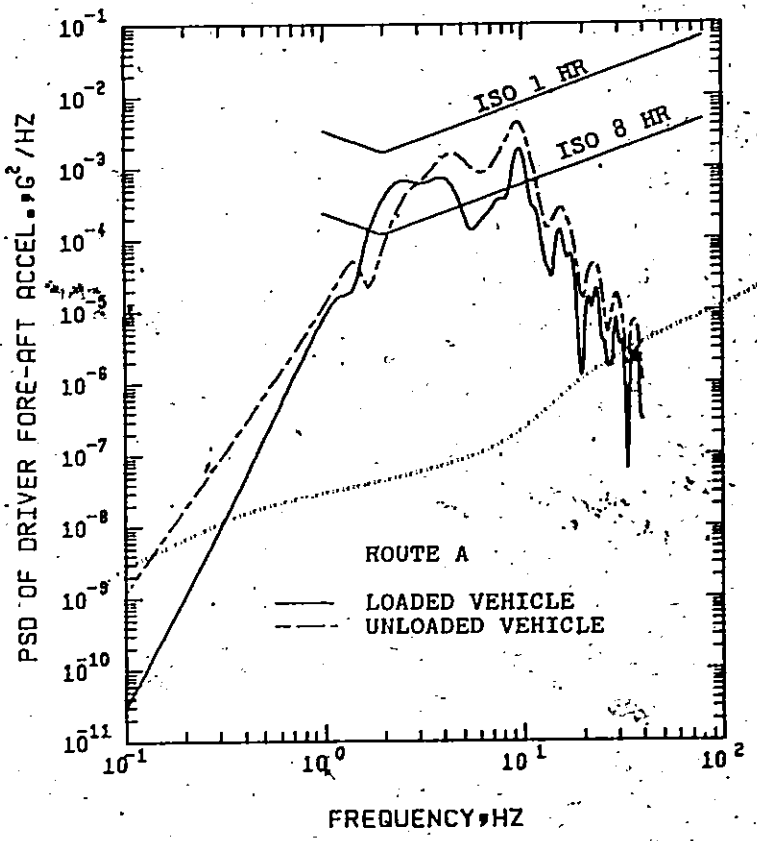

Figure 4.5 Tractor and driver fore and aft acceleration spectra - smooth road.

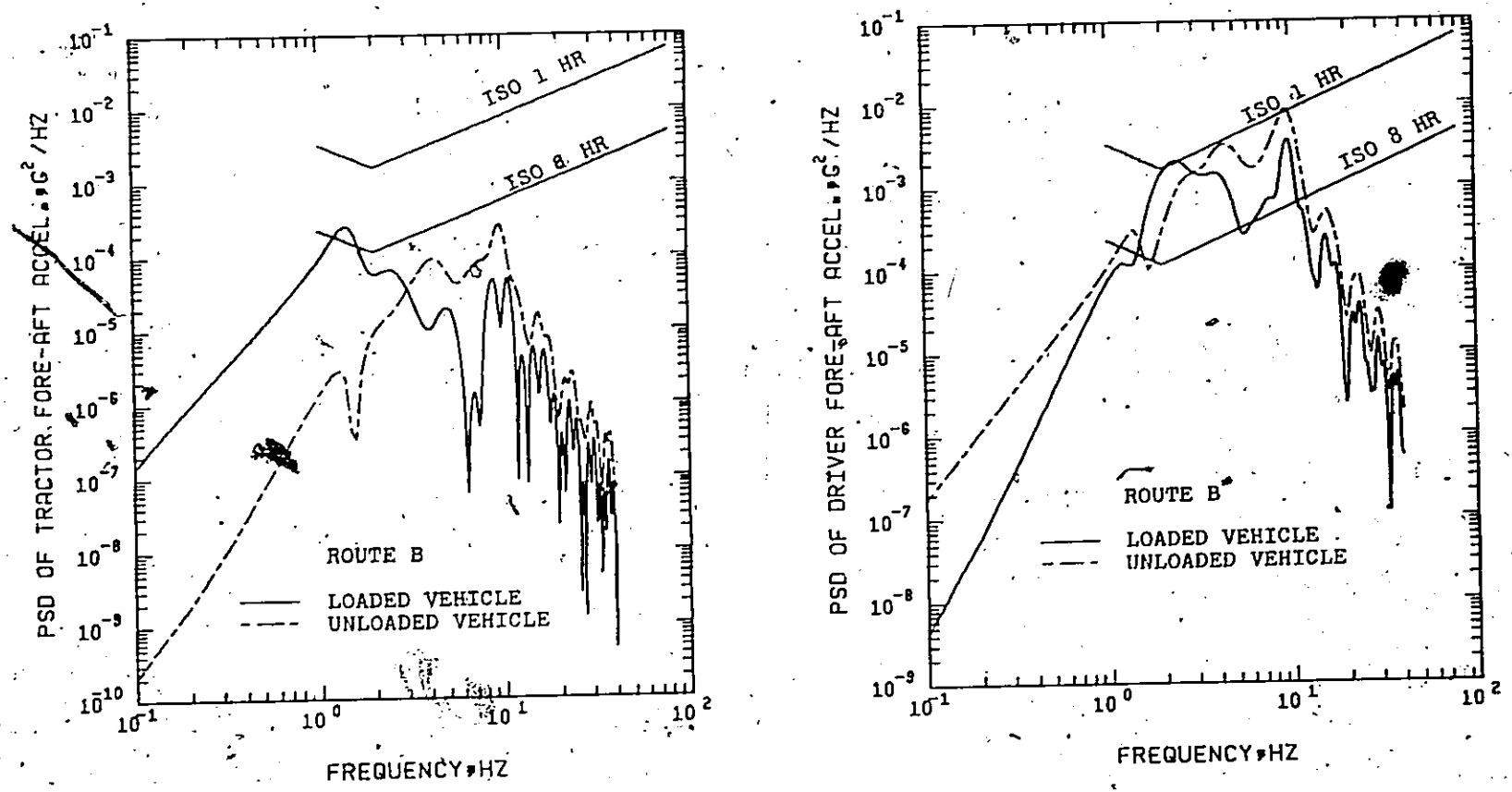

Figure 4.6 Tractor and driver fore and aft acceleration spectra - rough road.

tractor pitch modes respectively, while the peaks around 9-12 Hz are associated with wheel axle bounce modes. The remainder of peaks shown in the figure relate to joint frequencies.

For an unloaded vehicle there is one dominant peak around 1.5 Hz corresponding to tractor bounce mode and two peaks in the ranges of 5-7 and 9-12 Hz. The reason for the absence, or attenuations of some of the expected peaks corresponding to system natural frequencies can be explained as follows. Since the three road inputs to the vehicle are spatially distributed, restrictions are imposed which, at an eigenvalue frequency, do not allow the mode shape predicted by that eigenvalue to be developed.

Comparing the results for smooth and rough roads indicates that the general shape of the response spectra is preserved. However, in the low frequency range, 0.1 to 1 Hz the rate of increasing the acceleration level for the smooth road is much higher than the acceleration level rate for the rough road.

As seen in these figures, the acceleration spectra for the smooth and rough roads exceed the 8 hour ISO guide by a considerable margin. Then according to ISO criteria the ride vibration levels for the tractor-semitrailer model used are excessive in the vertical motion.

For consideration of fore and aft acceleration at the driver neck level, several features of these spectra may be noted. First, there is a strong wide peak in loaded vehicle response in the range of the tractor pitching frequency which exceeds the ride comfort limits. In general, the fore and aft acceleration levels do not exceed the 1 hour

ISO guide while they exceed the 8-hour ISO guide in both low and high frequency range. This result occurs because the fore and aft motion is a function of the combined tractor and semitrailer pitching random motions. The tractor and semitrailer pitch frequencies for both loaded and unloaded vehicle are in the range of 1.5 to 3.7 Hz which are in the range of human body resonance. The result of beating of the different modes of vibration within the system is new dominant modes and consequently, extra peaks. Therefore, the fore and aft acceleration levels are very high for high frequencies. This indicates that the pitching mode motions of both the tractor and the semitrailer contribute significantly to driver discomfort and much attention should be given to reducing their effect. For the rough road, there is an increase in the whole frequency range content of fore and aft vibrations.

Spectral densities of tractor and semitrailer pitch accelerations are given in Figures 4.7 and 4.8 for both loaded and unloaded vehicles travelling at 80 km/h on a smooth road and a rough road, respectively. Pitch acceleration levels are, in general, higher in the high range of the spectrum for the unloaded vehicle. This result is due to the increase in the natural frequencies of the system for the unloaded vehicle. For the loaded vehicle, tractor pitch acceleration reaches an initial peak between 1.2 - 1.3 Hz. This level subsides significantly around 1.5 Hz, but quickly rises again and reaches a maximum value at about 2.4 Hz. For the unloaded vehicle, the same result occurs but at generally higher frequencies.

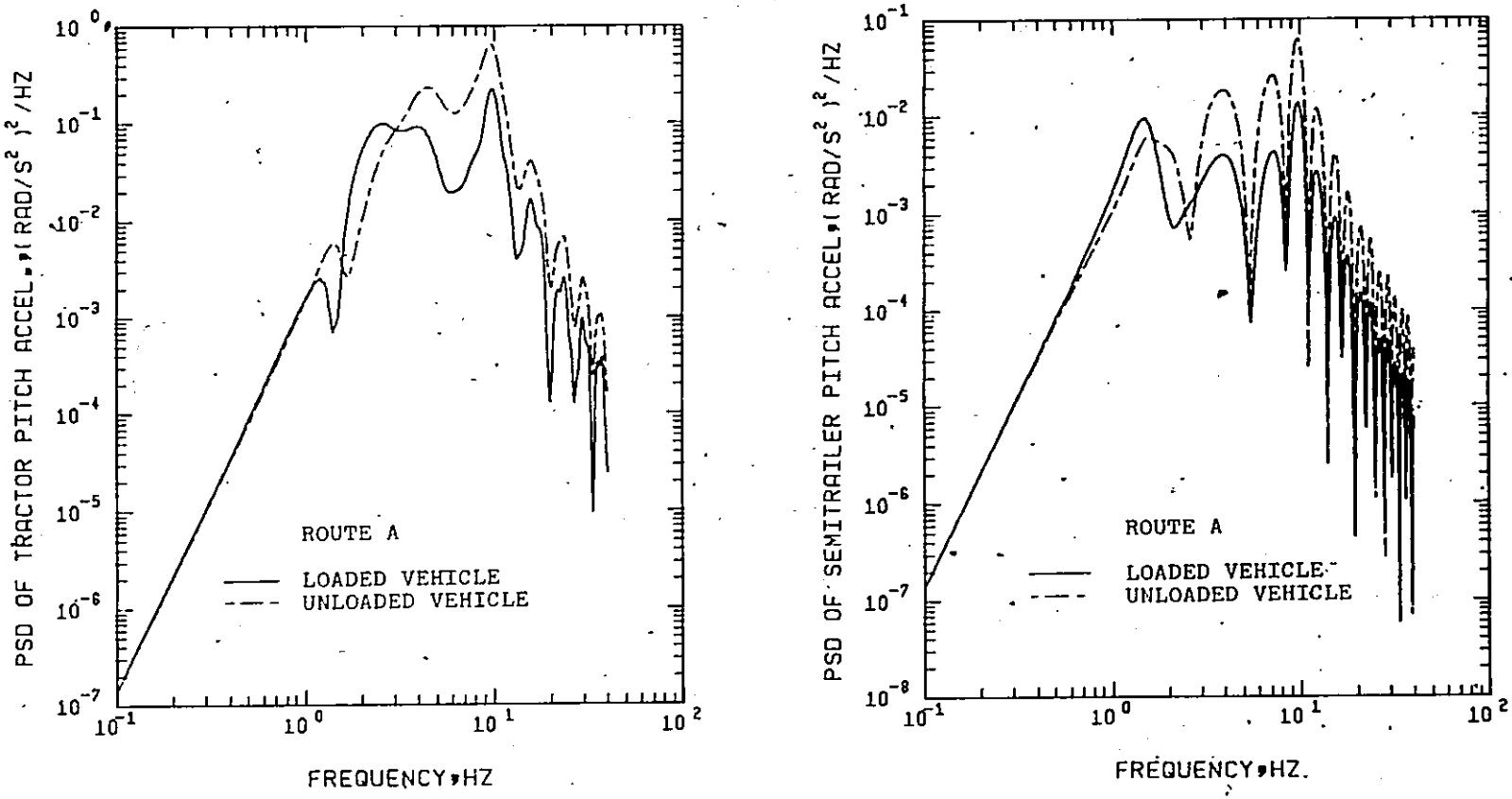

Figure 4.7 Tractor and semitrailer pitch acceleration spectra - smooth road.

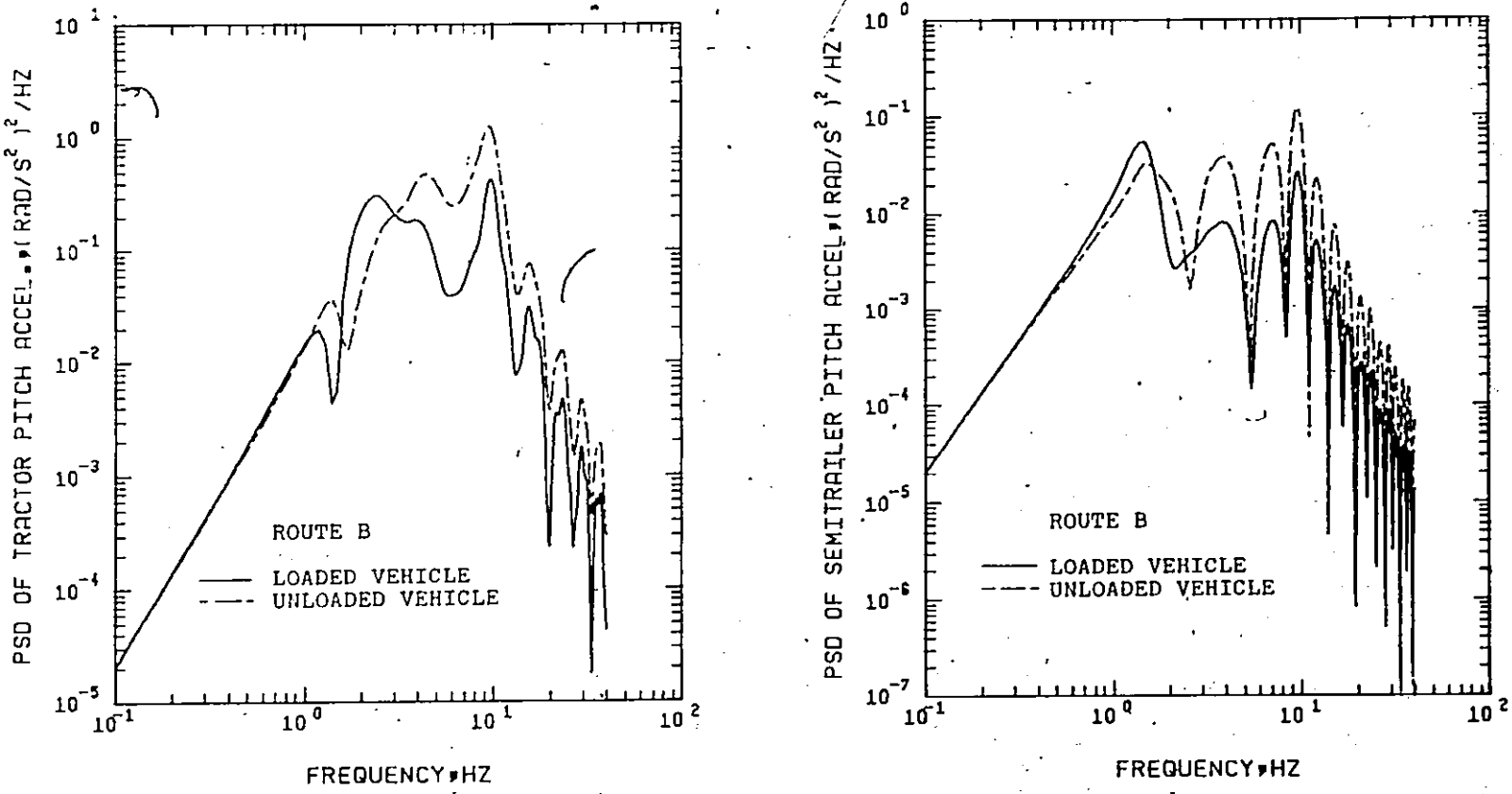

Figure 4.8 Tractor and semitrailer pitch acceleration spectra - rough road.

For semitrailer pitch acceleration, the figures illustrate that, except for the first peak around 1.6 Hz, acceleration peaks for the unloaded vehicle are higher than those for the loaded vehicle. The figures also illustrate that the resonant frequencies for the unloaded vehicle are higher than those for the loaded one.

Comparing the driver fore and aft acceleration with tractor pitch acceleration, we notice that they have almost the same shape. This is partly due to the large values of tractor pitch acceleration, and partly due to the height of the driver's neck above the centre of gravity of the tractor which increases the contribution of tractor pitch acceleration.

To explain the undulation that occurs in the pitch and fore and aft acceleration spectral densities, Figure 4.9 is plotted. This figure gives the power spectral density of tractor and semitrailer pitch accelerations when the three road inputs at the wheel contact points are in phase at vehicle speed 120 km/h, and when the time delay is taken into consideration for the two speeds 40 and 120 km/h. Several graphic characteristics may be observed. The shape of the curve for the three inputs in phase is relatively smooth. The amplitude of the acceleration is strongly influenced by vehicle speed. Several peaks on the 40 km/h curve do not have the same frequencies as peaks on the 120 km/h curve. This would appear to be due primarily to the more rapid change of the amplitude spectra at lower speeds. However, certain peaks at both 40 and 120 km/h do have identical frequencies.

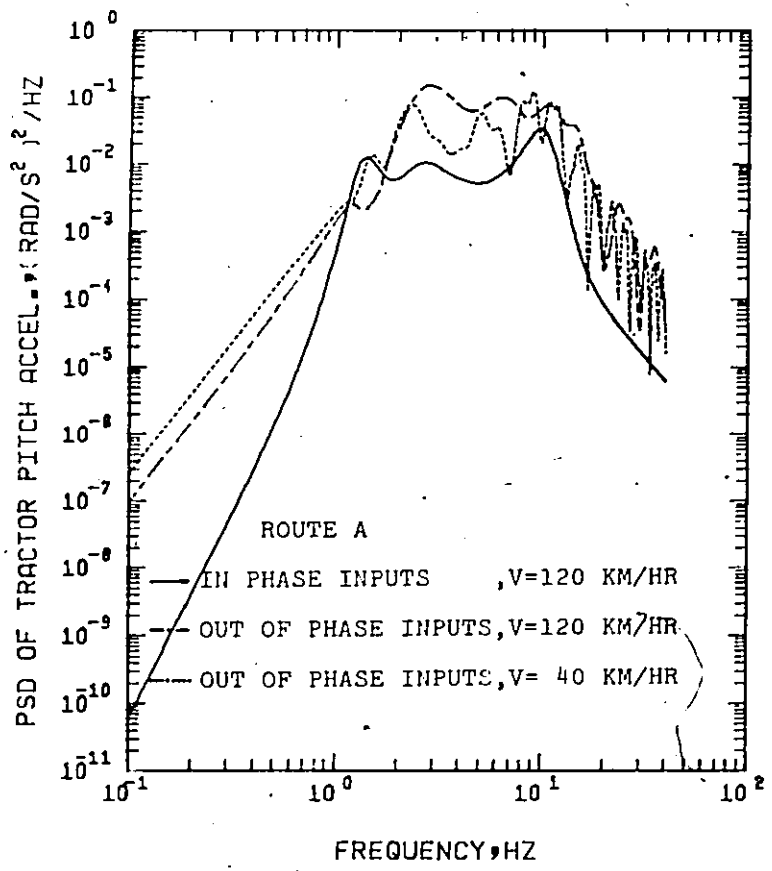

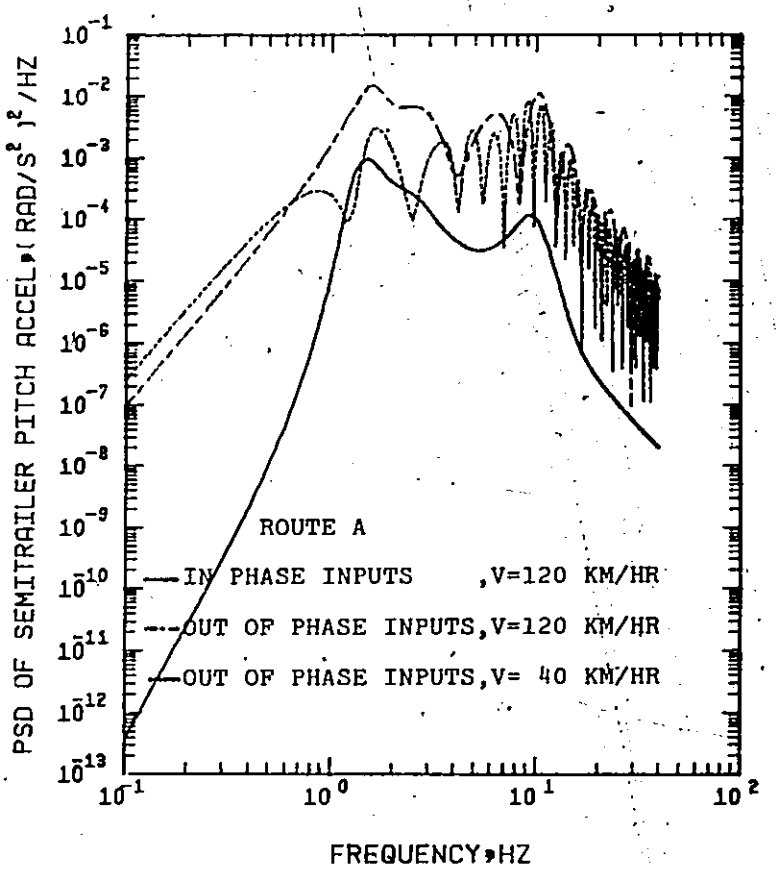

Figure 4.9 Effect of phase inputs on tractor and semitrailer pitch acceleration spectra.

4.2.3 Effect of Speed

Variations with vehicle speed of the rms accelerations are obtained to investigate the effect of vehicle speed on vehicle motion. Each spectrum is integrated in the frequency range of 0.1 to 40 Hz to obtain the rms value.

The rms tractor vertical and fore and aft accelerations versus vehicle speed are plotted in Figure 4.10 for smooth and rough roads, respectively. In the figure it can be seen that the rms vertical accelerations for loaded and unloaded vehicle decrease with vehicle speeds up to 30 km/h, while an increase is exhibited from 40 to 120 km/h. In the case of rms fore and aft accelerations, the figure shows that the curves for the loaded and unloaded vehicles, in general, increase uniformly with increasing the speed, with the values for the unloaded vehicle double the values for the loaded vehicle. For the rough road, Figure 4.10, the response curves take approximately the same shape as the smooth road, however, the values of the former are approximately 2.4 times the values of the latter at speeds above 50 km/h.

The rms vertical accelerations for both the loaded and unloaded vehicles show a high rate of increase above 50 km/h compared to the values of the smooth road. In the case of the rough road the curves for the rms vertical accelerations show that the response increases uniformly with vehicle speed. The rms driver vertical and fore and aft accelerations which are due to the combined heaving and pitching random motion are given in Figure 4.11 for smooth and rough roads,

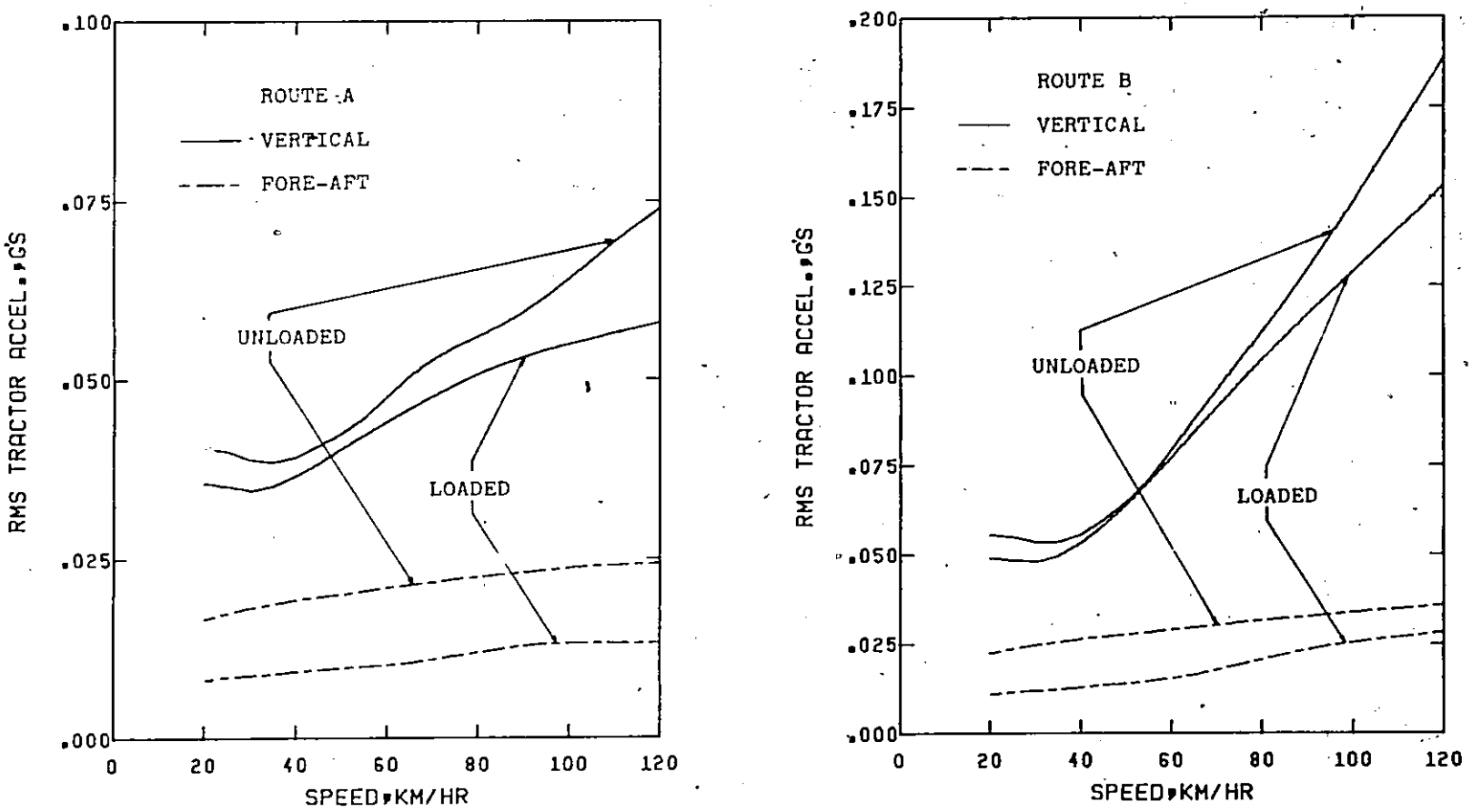

Figure 4.10 Effect of speed on rms tractor vertical and fore and aft accelerations.

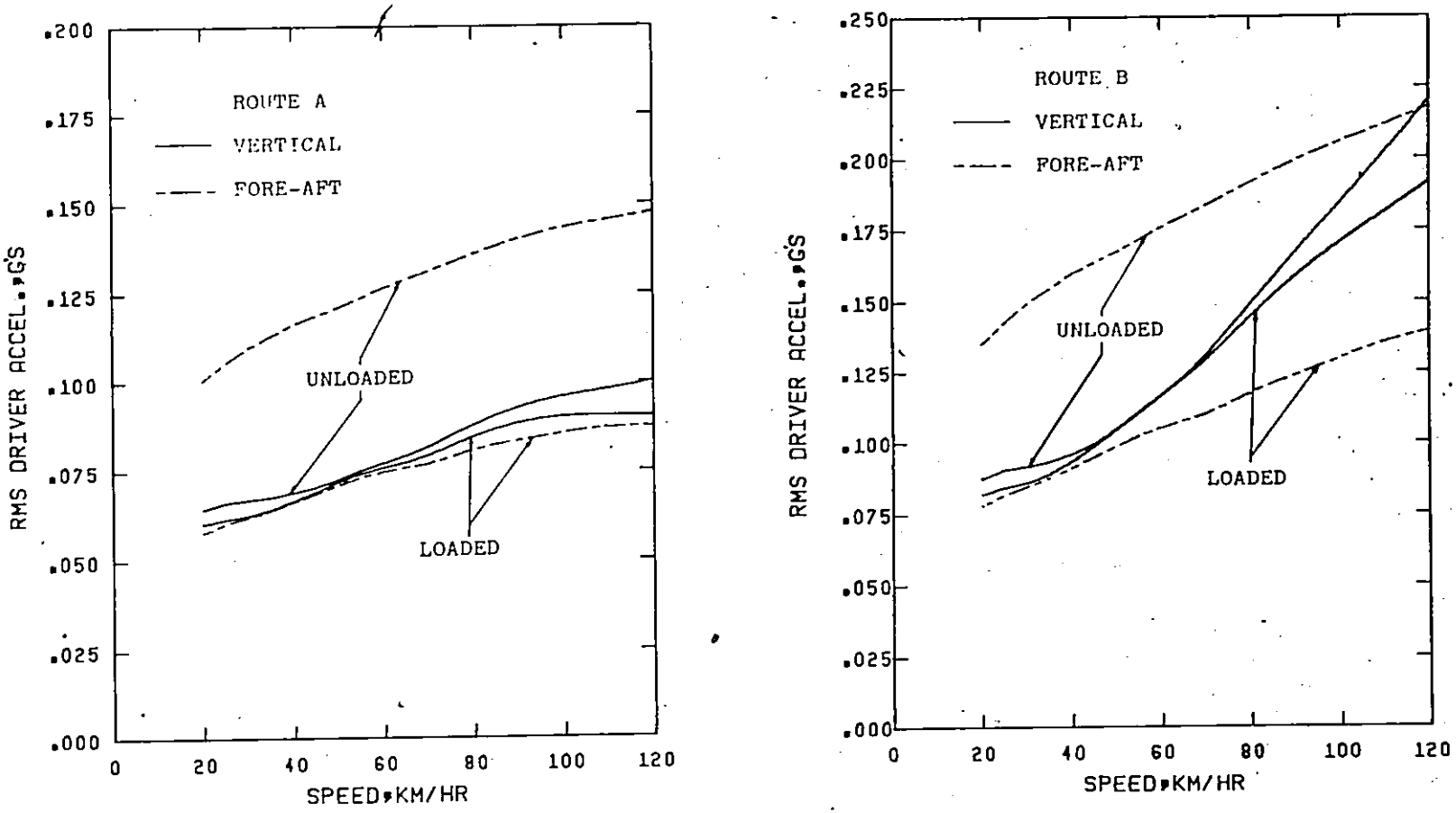

Figure 4.11 Effect of speed on rms driver vertical and fore and aft accelerations.

respectively. For the loaded and unloaded vehicles, the rms accelerations increase with increasing the speed. However, at high speeds the responses show a lower rate of increase for the vehicle operating on the smooth road.

4.2.4 Effect of Vehicle Suspension Systems on Vehicle Accelerations

Excursions in each of the vehicle suspension system parameters are examined, one by one, while all of the remaining system variables are held constant at the baseline values given in Table 4.1. The motions of the vehicle are obtained while it is operating on a smooth road.

Figures 4.12 and 4.13 show the effect of the tractor front and rear axle spring rates, k_1 and k_2, respectively on the tractor vertical acceleration response spectra. In each curve three peaks occur, one in the region of tractor body bounce natural frequency, the second in the region of pitching natural frequencies, and the third in the region of axles natural frequencies. As expected, it can be seen from these figures that the stiffer the suspension spring rates, the larger the resonant frequencies at which the spectral density peaks occur. In the case of the first and second resonance regions the effects of changing in k_1 and k_2 are pronounced, but they do not have this effect in the third resonance region.

A three dimensional plot of the rms tractor vertical acceleration versus parameters k_1 and k_2 is given in Figure 4.14. It may be noticed

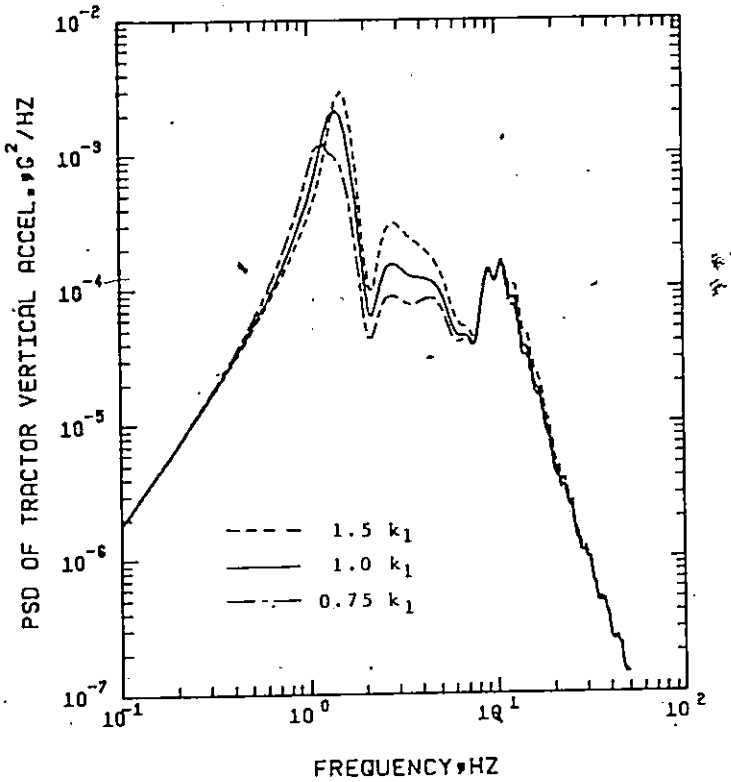

Figure 4.12 Effect of tractor front suspension spring rate on tractor vertical acceleration spectra.

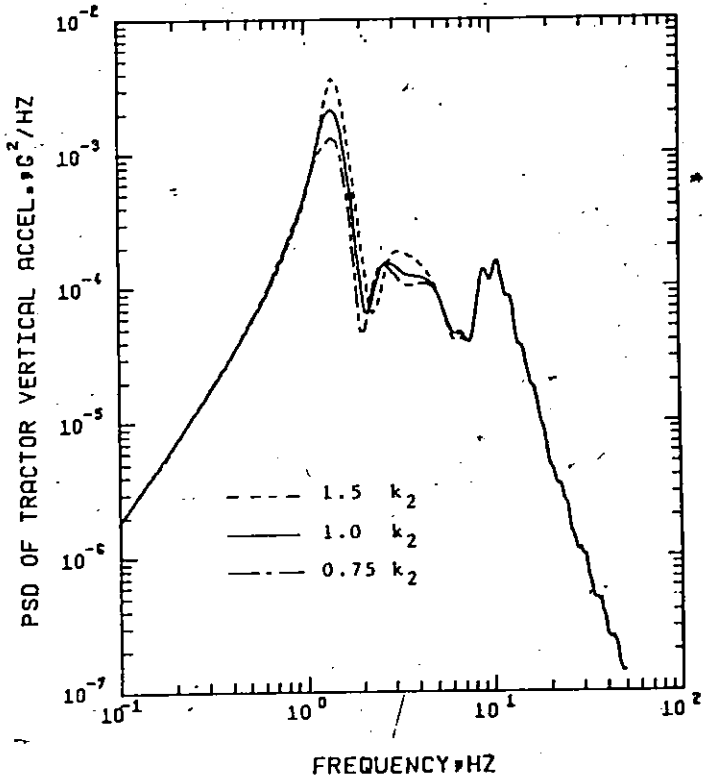

Figure 4.13 Effect of tractor rear suspension spring rate on tractor vertical acceleration spectra.

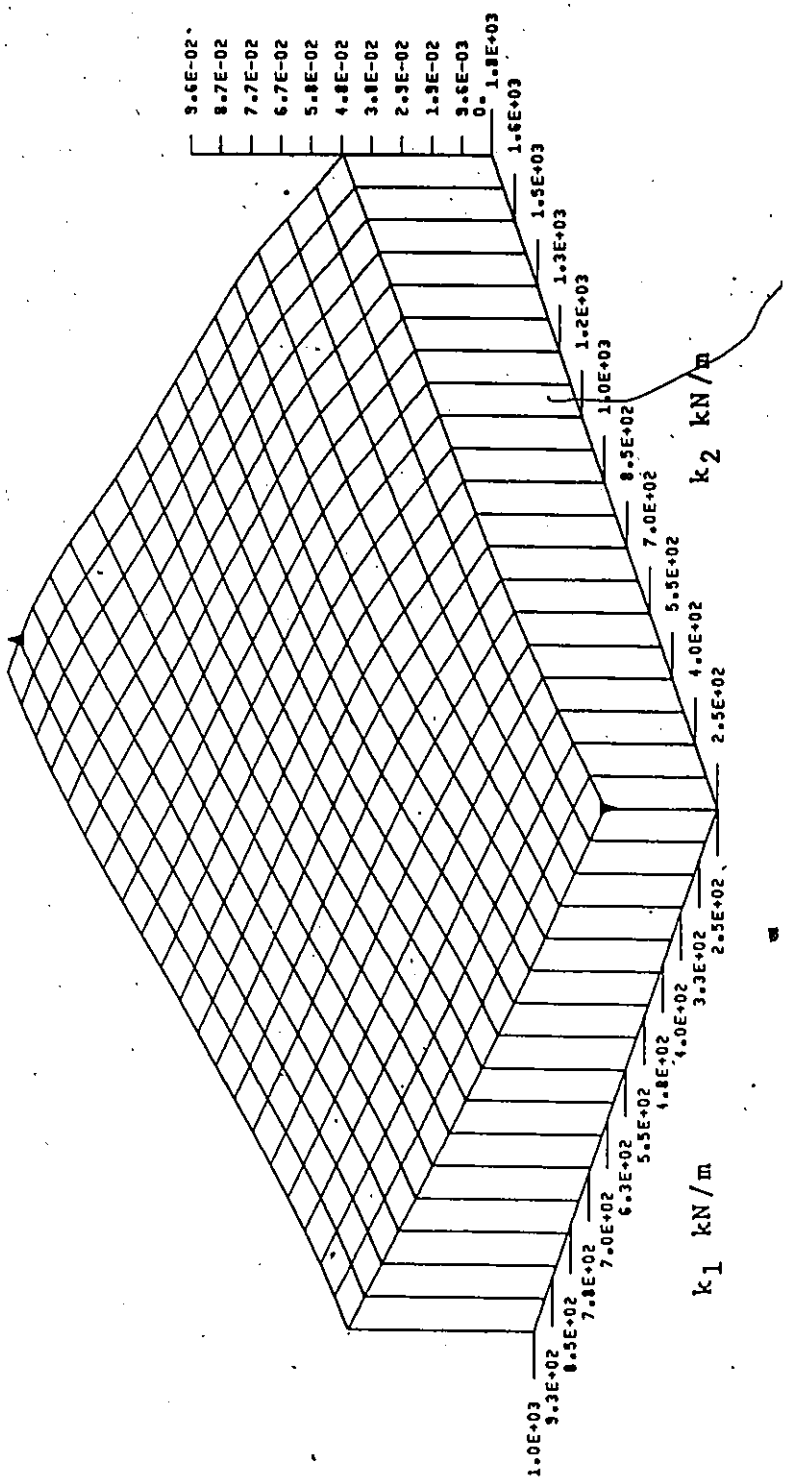

Figure 4.14 Effect of tractor front and rear suspension spring rates on rms tractor vertical acceleration.

that rms tractor vertical acceleration increases approximately linearly with increasing k_1 and k_2. These results indicate that decreased suspension spring rates of the tractor can produce improved ride quality based on rms index. Therefore, low values of the tractor axles springing parameters are desirable, but the minimum values are limited by other considerations, such as suspension static deflection, stroke deflection, and roll stiffness.

Figure 4.15 shows the behavior of rms semitrailer vertical acceleration resulting from variations in the suspension elements between the tractor body and axles, k_1 and k_2. The figure indicates that the increase in the rms values varies almost linearly with k_1. The rms values are waving with varying the values of k_2. It may inferred from Figure 4.15 that there are several minima and maxima occurring at different values of k_1 and k_2 in the design space.

Figure 4.16 gives the power spectral density of tractor longitudinal acceleration for different values of k_1. The figure illustrates that the amplitude density increases with stiffer suspension. The spectral density peak of tractor longitudinal acceleration is about 0.2 of tractor vertical peak acceleration. This longitudinal acceleration is more critical to driver comfort, probably because the human body is inherently not adapted to resist fore-and-aft forces. Similar results for k_2 may be obtained.

Figure 4.17 shows the effect of the semitrailer spring rate, k_3, on the amplitude spectra of the semitrailer vertical acceleration. From

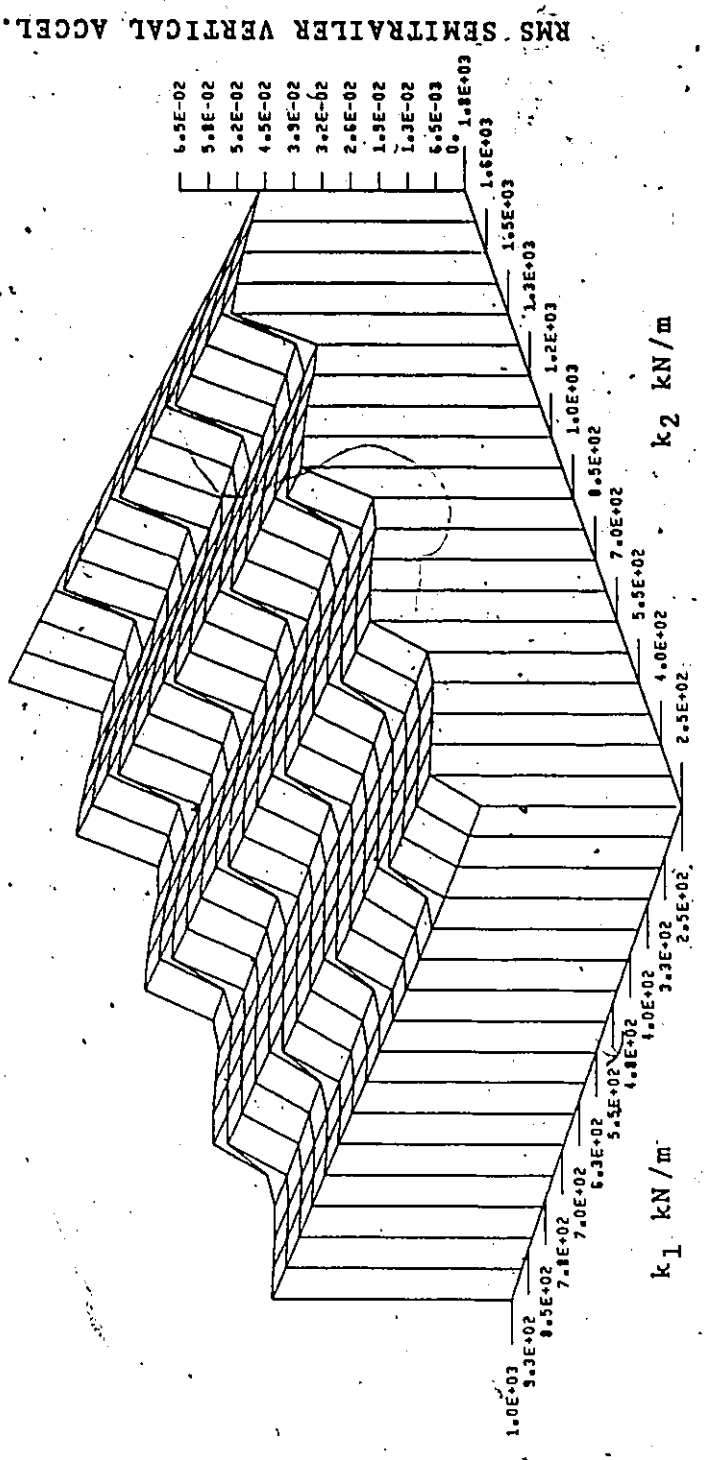

Figure 4.15 Effect of tractor front and rear suspension spring rates on rms semitrailer vertical acceleration.

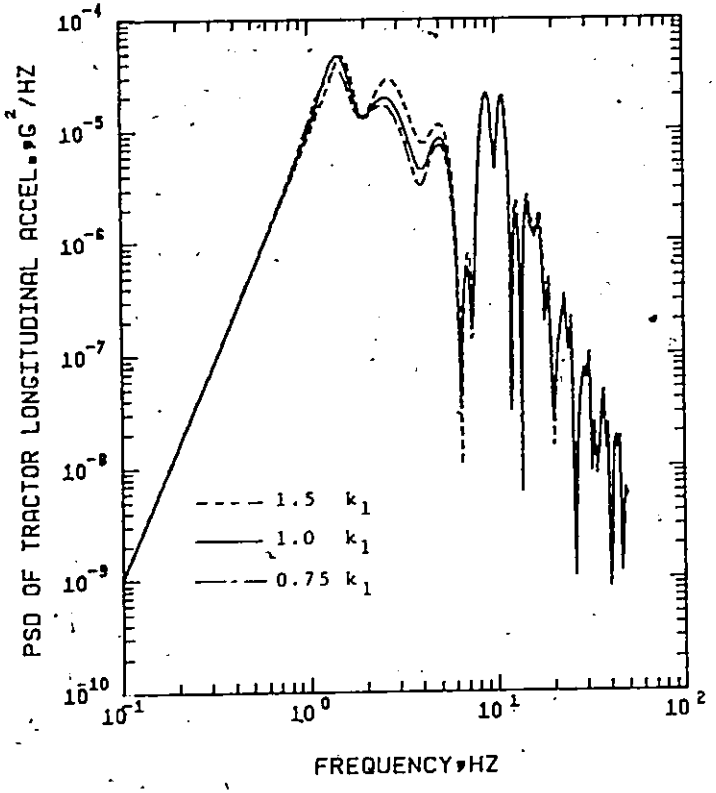

Figure 4.16 Effect of tractor front suspension spring rate on tractor fore and aft acceleration spectra.

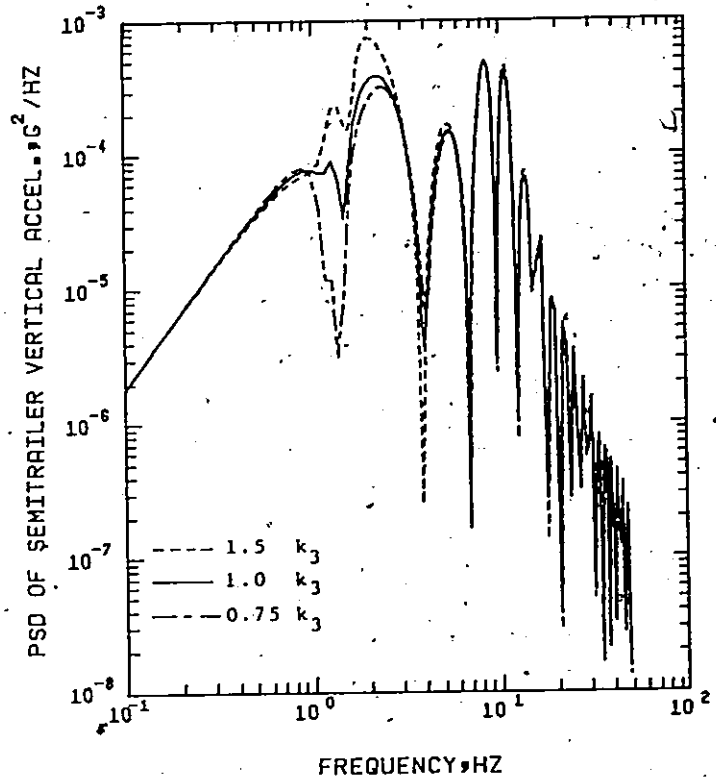

Figure 4.17 Effect of semitrailer suspension spring rate on semitrailer acceleration spectra.

the figure, it is concluded that the semitrailer vibration is particularly sensitive to variation in this parameter in the vicinity of the first resonant region.

Figures 4.18 and 4.19 show the effect of changing the damping parameter, c_1, in the suspension on the tractor vibration acceleration response. The figures indicate that, increasing the suspension damping diminishes the peak amplitude spectra at tractor body resonance and increases the high-frequency spectra. Consequently, a value of the viscous damping must be selected that results in a satisfactory compromise between resonant vibration control and high-frequency vibration isolation. The rms tractor vertical acceleration versus the tractor suspension dampings, c_1 and c_2 is plotted in Figure 4.20. It may be concluded from the figure that the ride quality measured in terms of rms tractor acceleration is sensitive to changes in c_1 and relatively less sensitive to changes in c_2. It may be also inferred that the rms values are high for small damping because it permits higher acceleration at tractor body resonance. The rms values increase again with high damping because it stiffens the suspension and transmits more of the exciting force to the tractor body.

Figure 4.21 presents the effect on the tractor vertical acceleration response of varying the tire springing characteristics. The figure shows that, while the tire spring rates have a negligible effect on the peak response at body resonance they significantly affect it in the region of axle resonance.

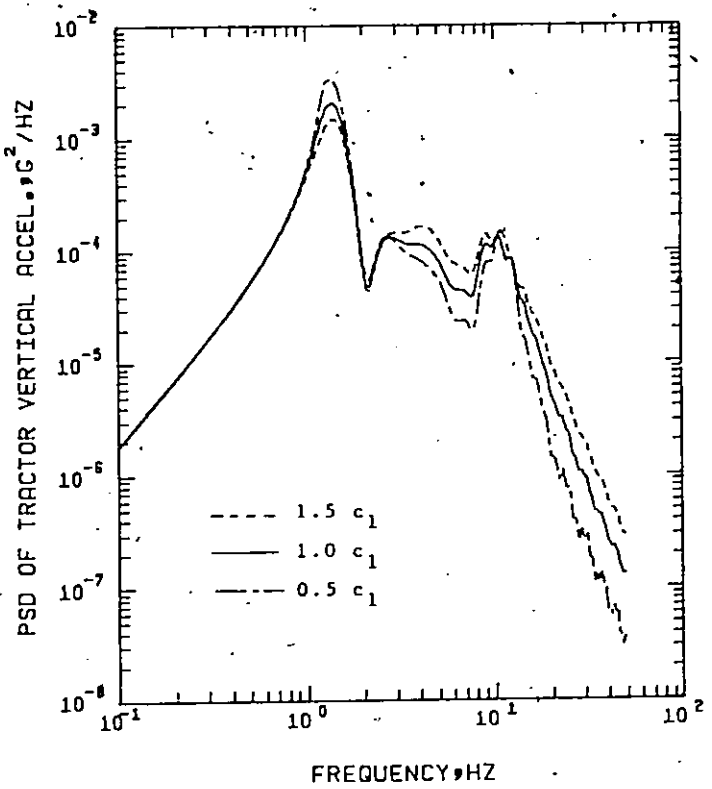

Figure 4.18 Effect of tractor front suspension damping rate on tractor vertical acceleration spectra.

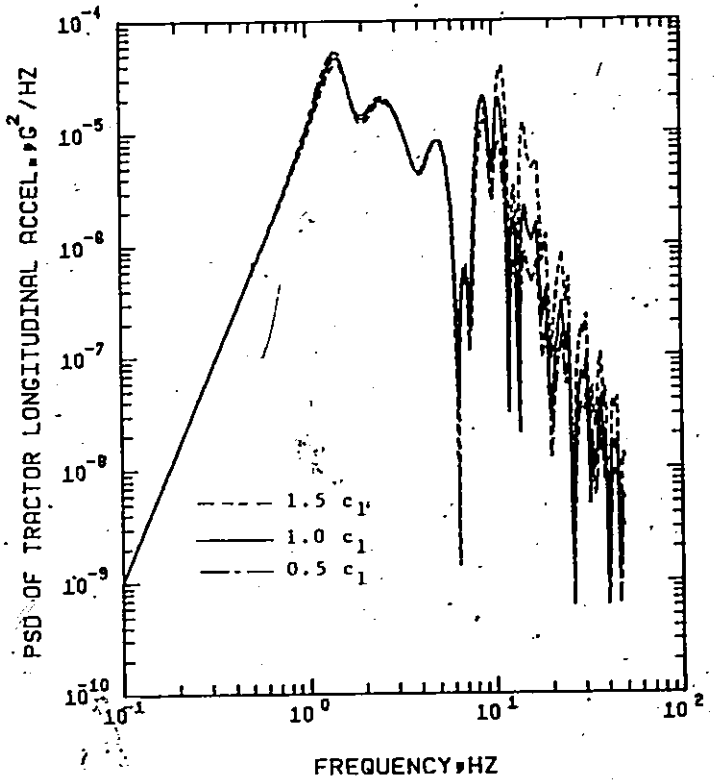

Figure-4.19 Effect of tractor front suspension damping rate on tractor fore and aft acceleration spectra.

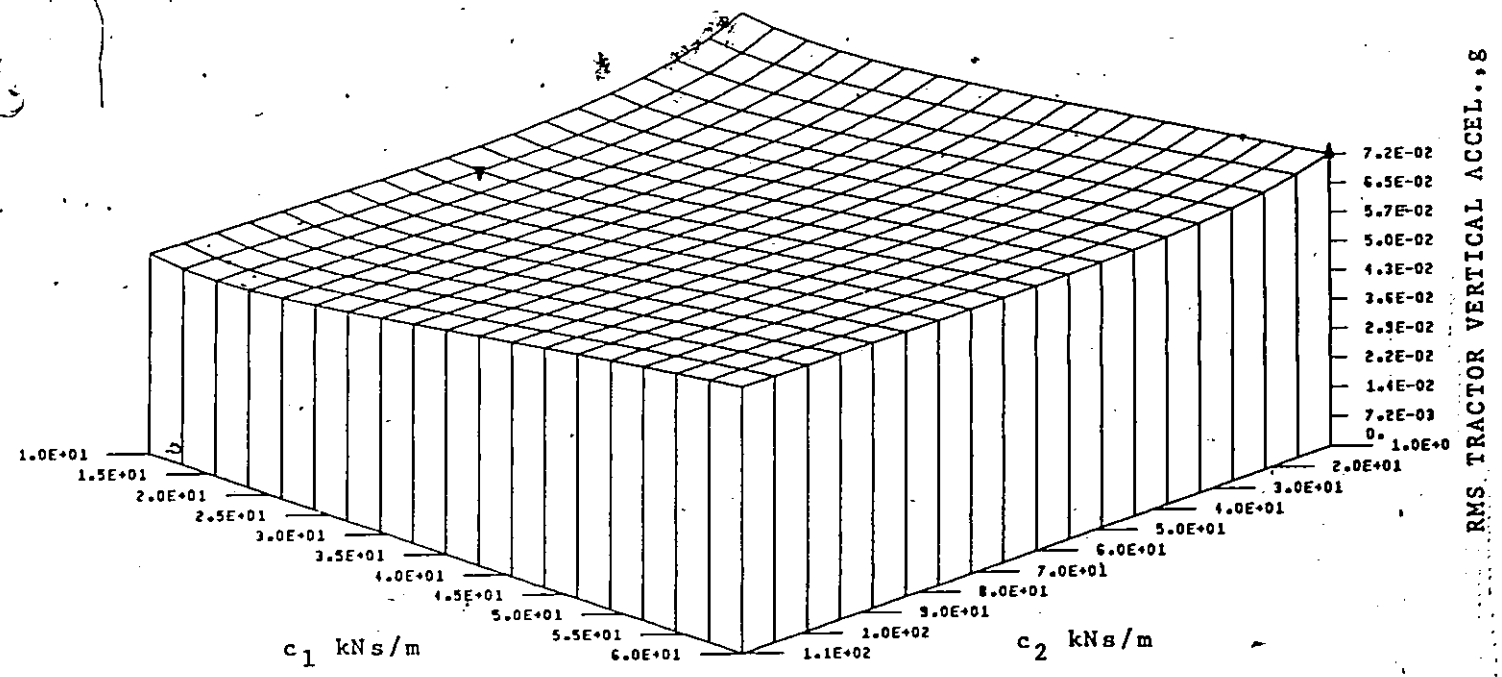

Figure 4.20 Effect of tractor front and rear suspension damping rates on rms tractor vertical acceleration.

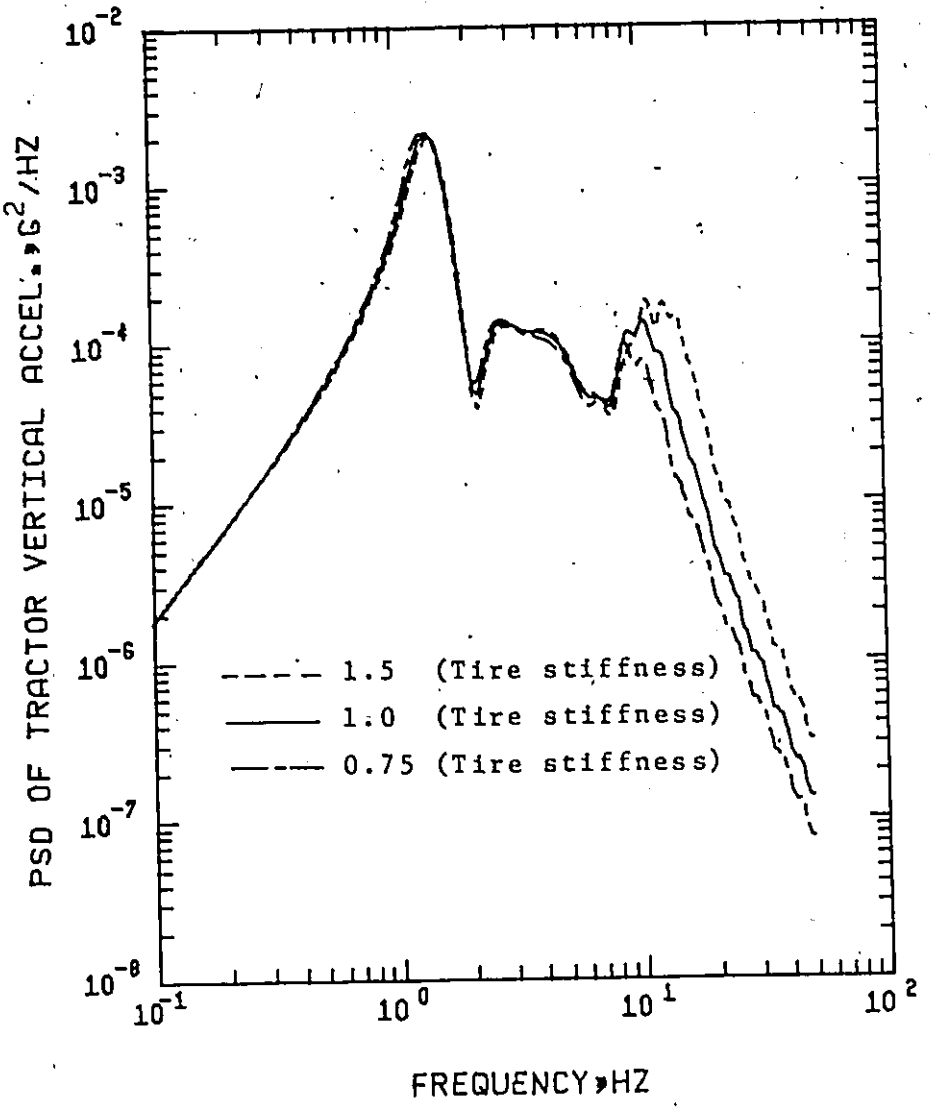

Figure 4.21 Effect of tire spring rates on tractor vertical acceleration spectra.

4.2.5 Effect of Vehicle Suspension Systems on the Dynamic Wheel Loads

To study the influence of vehicle parameters on the dynamic wheel loads which the vehicle imposes on the surfaces, several values of suspension springings and dampings and tire spring characteristics have been considered. The power spectral densities of the ratio of dynamic wheel load to static wheel load given in Figure 4.22 depict the influence of tractor rear axle suspension, k_2, on the wheel dynamic load. In the first and second resonance regions the wheel dynamic load becomes smaller as the suspension becomes softer. However, in the third resonance region, decreasing the suspension spring stiffness produces slightly larger peak dynamic load. The effect of k_1 on the tractor rear wheel dynamic load is given in Figure 4.23 and it can be seen that k_1 has no effect in the vicinity of the axle resonance region. The three-dimensional plot of the rms tractor front wheel dynamic load to static load versus k_1 and k_2 shown in Figure 4.24 is drawn to gain insight into the general dependence of wheel dynamic load on the vehicle parameters, k_1 and k_2. While the rms value of the tractor front wheel dynamic load increases approximately linearly with increasing k_1, there are several peaks and valleys with varying k_2, as shown in Figure 4.24.

The manner in which the dynamic wheel loads of the articulated vehicle vary with the damping parameters, c_2 and c_3, respectively, is described in Figures 4.25 and 4.26. The conclusion from the figures is that, with damping in the suspension the dynamic loads are affected appreciably near body and axle resonances. Shown in Figure 4.27 is the

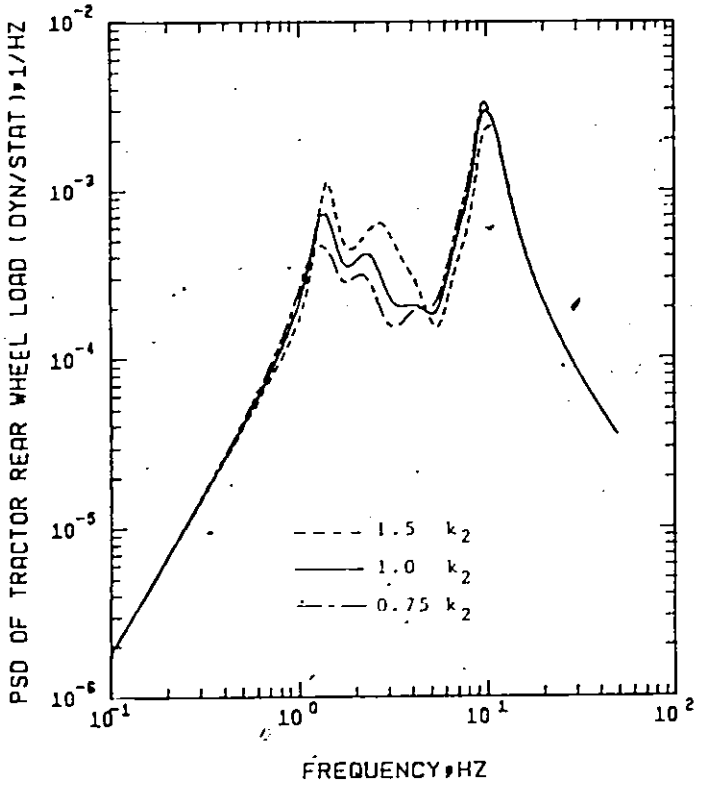

Figure 4.22 Effect of tractor rear suspension spring rate on tractor rear wheel load spectra.

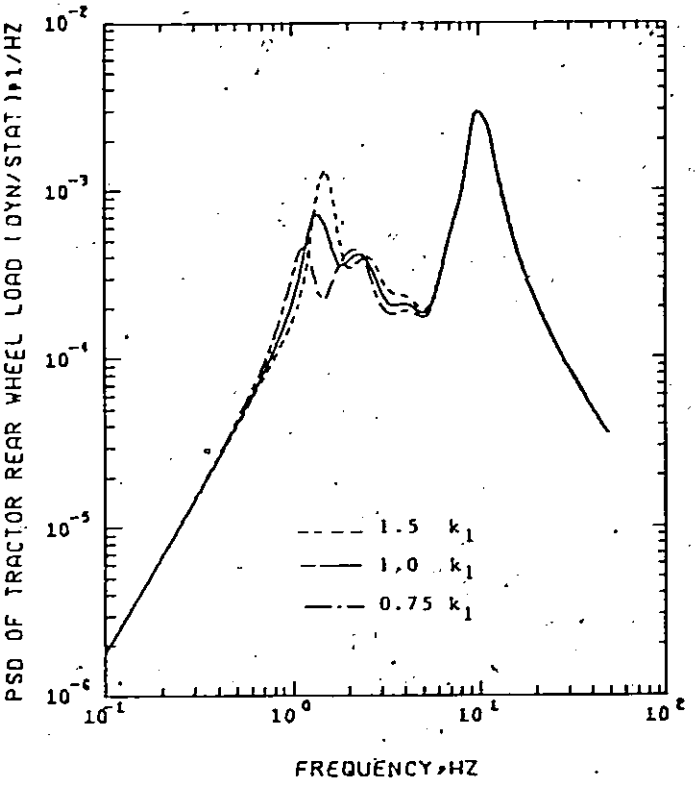

Figure 4.23 Effect of tractor front suspension spring rate on tractor rear wheel load spectra.

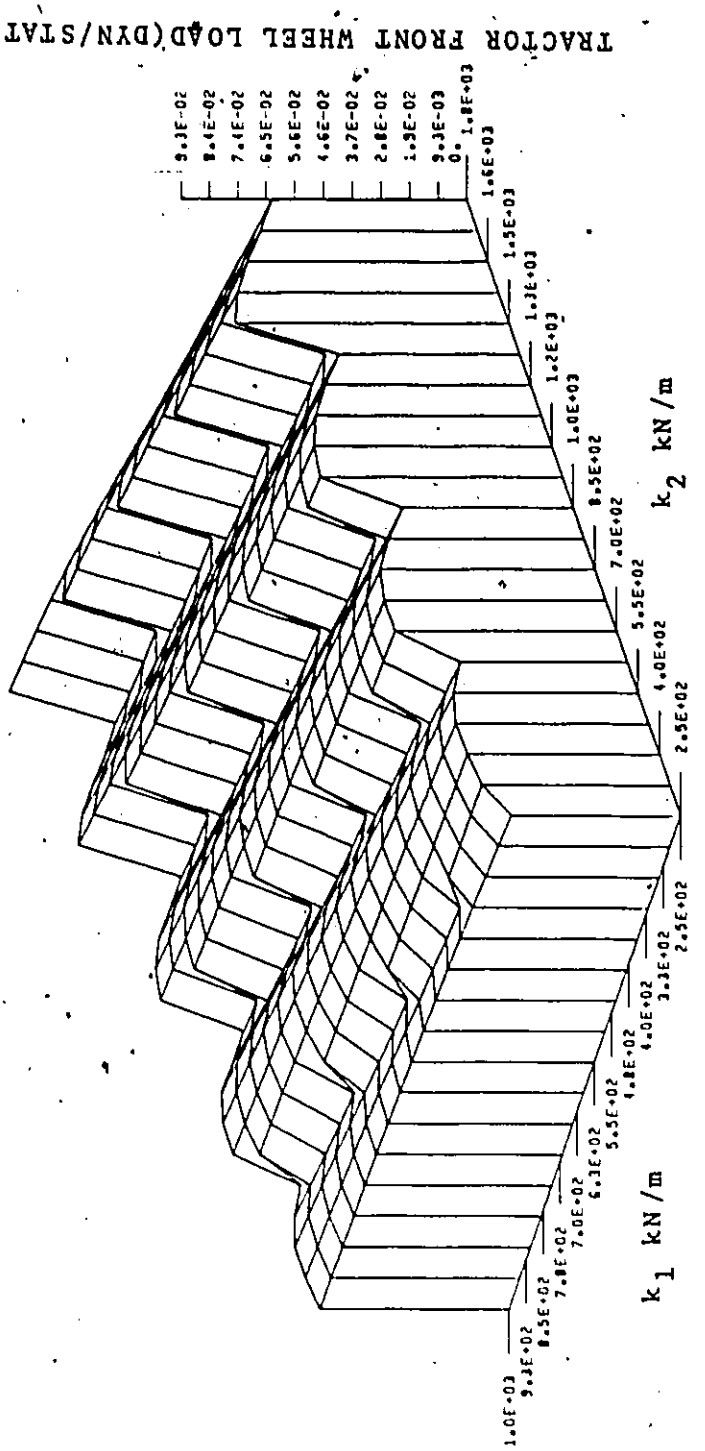

Figure 4.24 Effect of tractor front and rear suspension spring rates on rms tractor front wheel load.

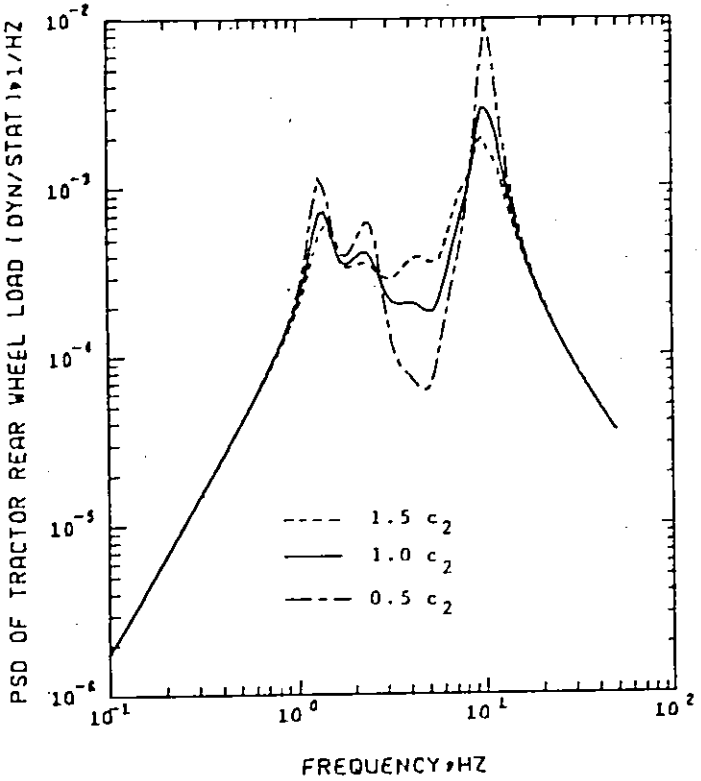

Figure 4.25 Effect of tractor rear suspension damping rate on tractor rear wheel load spectra.

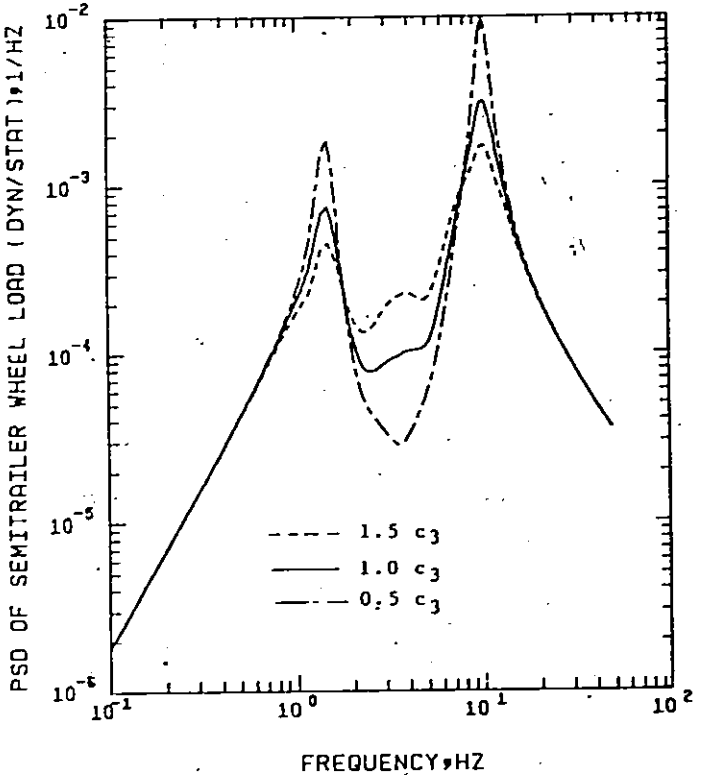

Figure 4.26 Effect of semitrailer suspension damping rate on semitrailer wheel load spectra.

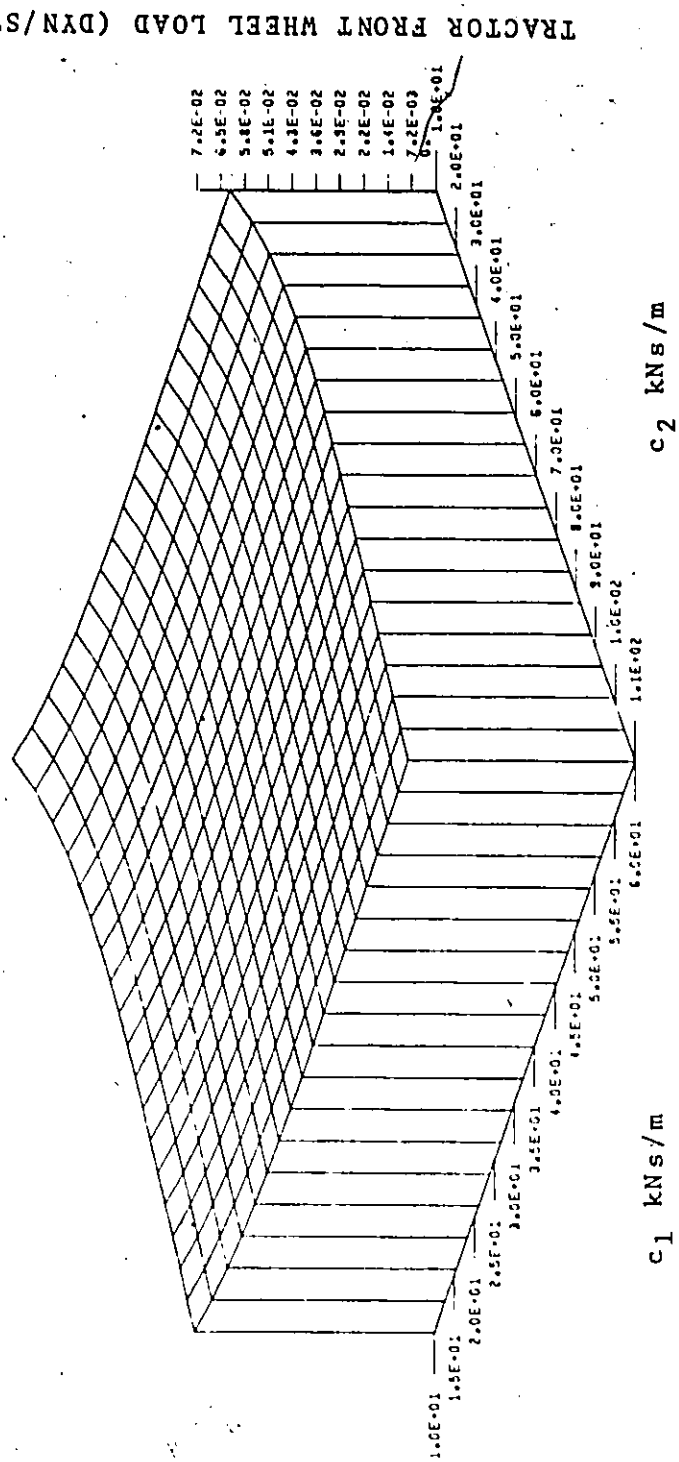

Figure 4.27 Effect of tractor front and rear suspension damping rates on rms tractor front wheel load.

effect of c_1 and c_2 on the rms value of the tractor front wheel dynamic load. The figure indicates that, increasing the damping, c_1 and c_2, decreases the rms wheel force first, but with high damping the rms value increases again, because high damping stiffens the suspension and transmits more force to the road.

Figures 4.28 and 4.29 show that changing the stiffness of the tires appreciably affects the amplitude spectra of the dynamic load between the wheel and road at axle resonance. The higher peak value at axle resonance for the small stiffness results in a higher rms wheel load.

4.3 Summary

It is necessary for the designers of articulated vehicles to aim at good vibrational characteristics and good riding qualities of the designed vehicles. For this purpose, the dynamic analysis of vehicle/road interaction using the theory of stochastic processes is carried out to clarify the effects of the many factors on the vibration of the articulated vehicle. Applying stationary random inputs to the vehicle and using the frequency domain analysis have demonstrated how the dynamic response of vehicle and vehicle/road interaction are affected by load pattern, road characteristics, suspension springing and damping characteristics, tire spring characteristics and vehicle speed.

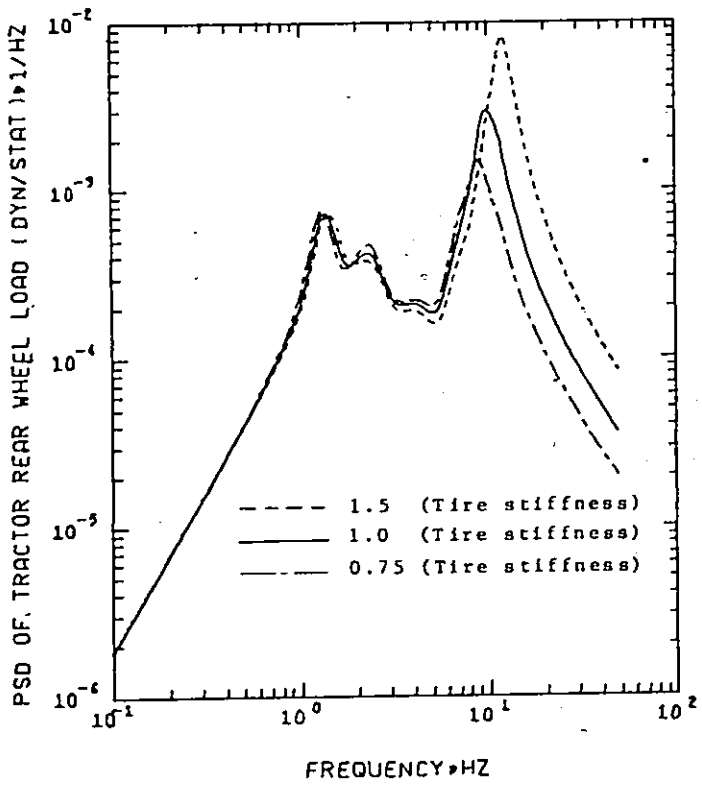

Figure 4.28 Effect of tire spring rates on tractor rear wheel load spectra.

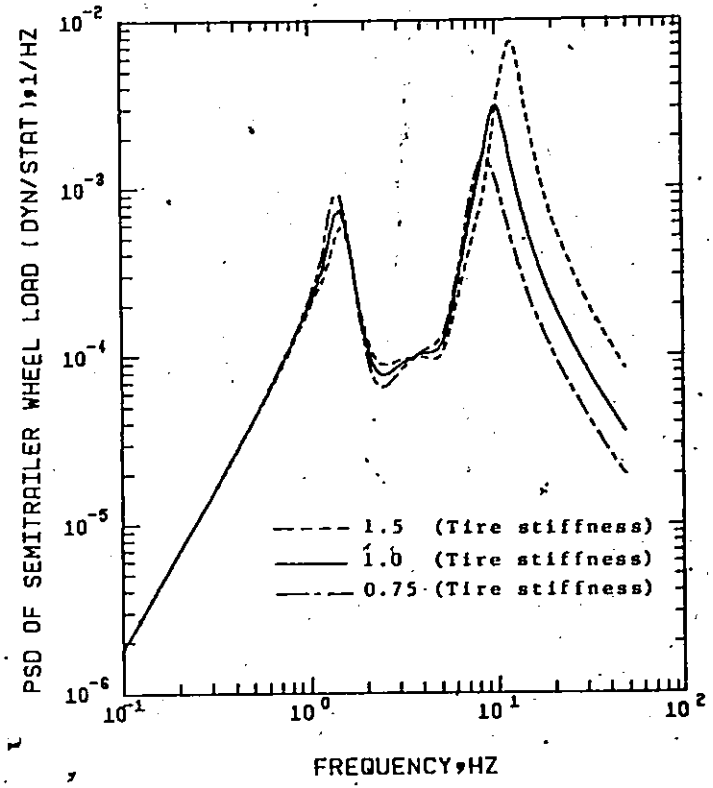

Figure 4.29 Effect of tire spring rates on semitrailer wheel load spectra.

The results of the computer analyses of vehicle and road are presented in two forms: the amplitude spectra and root mean square amplitudes which are used to predict ride quality and evaluate the design concept.

CHAPTER 5

RANDOM RESPONSE OF ARTICULATED VEHICLES

NONLINEAR ANALYSES

5.1 Introduction

In Chapters 3 and 4 the dynamic response of the articulated vehicle to random surface undulations was treated using a simplified vehicle model by assuming linear suspension systems. The linear analyses of articulated vehicle dynamics have provided an invaluable understanding of the effect of the various vehicle parameters on the riding behaviour of the vehicle [27, 39, 72, 88, 116]. The assumption of linearity is justifiable to simplify the consideration of basic features of vehicle ride motion, but system nonlinearities should be included in the practicality of suspension design. Nonlinear characteristics that are frequently present in articulated vehicles include dry friction (Coulomb friction), bump stops, and wheel hop. These nonlinearities may be expected to have a strong influence on the behaviour of the articulated vehicle.

The resulting nonlinear model can be analyzed using simulation techniques by utilizing analogue and digital computers to integrate the equations of motion. However, the practicality of such techniques is severely limited by the expense of computer time and the need to simulate the response to a wide variety of initial conditions to thoroughly examine the vehicle behaviour. Therefore, an analytical

technique, equivalent linearization, is sought for the analysis of the nonlinear dynamic motion response of the articulated vehicle.

The equivalent linearization technique is adapted and further developed to give a technique applicable to the articulated vehicle ride problem. The influence of dry friction, bump stops, and wheel hop on vehicle riding quality is reported, and the nature of the vibratory motions is described. It is the object of this chapter to examine these nonlinearities in order to gain a measure of their relative importance on the dynamic response of the articulated vehicle to the random road surface undulations. This will give a guide to the accuracy which must be attained in assessing their effects for a real vehicle so as to enable successful prediction of vehicle response to be carried out. The results have been obtained from an analysis of nonlinear equations of motion written for an articulated vehicle, modelled in heave and pitch modes.

5.2 Background

5.2.1 Stationary Random Vibrations of Multi-Degree-of-Freedom Nonlinear Systems

The response of nonlinear structural and mechanical systems to excitations which are stochastic in character has attracted considerable interest in recent years. One major reason for this interest is the fact that most real systems are nonlinear by their very nature. A further reason for this interest is that the excitation, (earthquake, wind, ocean wave forces, and road irregularities), is usually so complex

that it can only be described statistically. Therefore, the need for more precise study, qualitatively and quantitatively, of the behaviour of such systems requires that the nonlinear effects should be included and the statistical characteristics of both the excitation and the response should be considered.

Typically, the response of a discrete nonlinear dynamical system subjected to random excitation is described by a set of second order nonlinear stochastic differential equations and the response is regarded as a family of functions characterized by some suitable statistics.

The interest and research in the solution of the stochastic differential equations has led to several probabilistic techniques. An excellent state-of-the-art report of the application of probabilistic techniques to dynamical systems is given by Caughey [26].

Generally, there are three approaches which are used in the analysis of multi-degree-of-freedom nonlinear systems subjected to random excitations:

(i) The Fokker-Planck approach,

(ii) The perturbation approach, and

(iii) The equivalent linearization approach.

The Fokker-Planck approach [3, 7, 24, 128] provides an exact method of studying the stationary random response of a nonlinear system. If the excitation is a Gaussian white noise, then the transitional probability density of the response is governed by the Fokker-Planck equation. This transitional probability density can completely define the response process. Unfortunately, to date there is no systematic way

of solving the complete Fokker-Planck equation for the general second-order nonlinear system. However, the equation governing the first probability density for the stationary response process of a nonlinear system has been solved under three severe restrictions [26]; viscous damping, Gaussian white noise excitations, and proportionality of the spectral density matrix of excitation to the damping matrix of the system. These requirements are seldom met in physical systems. Under the foregoing restrictions, the exact solution may be found for a variety of systems [36, 87, 98, 99]. Unfortunately, these systems do not include the interesting hysteretic systems which are distinctly important in modelling vehicle suspension with dry friction.

In the case where the nonlinear terms of the dynamical system are small compared to the linear terms and the level of excitation is sufficiently low, the approximate random response may be obtained using the perturbation approach. In this approach, the expansion of the response process in a series of the coefficient of the nonlinear terms, yields a chain of linear systems which may be solved to obtain an approximate solution. Crandall [37] applied the classical perturbation method to random vibration analysis of single-degree-of-freedom oscillators, while Tung, et al. [135], and Tung [136] extended this method to more general multi-degree-of-freedom systems. However, major difficulties arise in the application of the perturbation approach in the absence of linear viscous damping, or when the nonlinear oscillator exhibits hysteretic behaviour.

In the equivalent linearization approach, the solution of the original nonlinear equations is approximated by solving an equivalent linear set of equations. The coefficients of the linear equations are determined in such a way that the error vector, which is usually chosen to be the difference between the nonlinear and linear equations with identical highest derivative terms is minimum. Since, in random vibration problems, statistical quantities play the important role, the minimization criterion selected is related to the mean square value of the error vector. By minimization of the mean square value of the error vector, some of the coefficients of the equivalent linear system will in turn depend on the moments of the response. Depending then on the complexity of the original nonlinear system, the approximate instantaneous correlation matrix of the response may be obtained by a cyclic iteration scheme or by solving the resulting nonlinear algebraic equations, if they can be explicitly found [76].

The equivalent linearization approach, which is basically the statistical extension of Krylov and Bogoliubov [90] linearization technique, was independently presented by Booton [16] and Caughey [22]. Later, Caughey [25], Foster [59], Iwan and Yang [76], Iwan [74], Atalic and Utku [8], and Spanos [130] generalized the method of the equivalent linearization technique and applied it to obtain approximate solutions of the random response of multi-degree-of-freedom nonlinear systems.

Among the methods mentioned above to solve nonlinear random vibration problems, equivalent linearization approach has the widest applicability [8]. In most cases the only restriction put on the system

is that the excitations are assumed to be stationary and Gaussian. Although the method is more effective, and the results more dependable, when the nonlinearities of the system are small, it has been shown [8] that even for some highly nonlinear systems the error is about 10%. The increased number of degrees of freedom does not impose any additional problems since the method is easy to implement on the computer. Basically, the equivalent linearization technique is an iterative method, but in certain problems, closed form solutions may be obtained.

5.2.2 Hysteretic Systems

The suspension elements with friction damping generally have hysteresis characteristics. In order to study the effect of hysteresis on system performance it is desirable to have a mathematically tractable model of the system in question. It must be emphasized that since the restoring force of a hysteretic system depends not only on the instantaneous displacement, but also on its past history, the analytical modelling of such a system under random excitation is not a straightforward matter. References [23, 73, 125] describe various hysteretic models.

Many studies have been carried out on the vibration systems with nonlinear hysteresis characteristics. Caughey [23] investigated the effects of input level on the response of single-degree-of-freedom systems subjected to random input by applying the equivalent linearization technique. Using analogue simulation, Iwan and Lutes [75] studied random vibration problems with nonlinear hysteresis

characteristics. They compared the analogue results with ones obtained by the equivalent linearization technique. Lutes [97] predicted the hysteretic system response by substituting the equivalent nonlinear system without hysteresis characteristics for the one with hysteresis properties, and then using Caughey's solution [24] of the corresponding Fokker-Planck equation. He compared these results with the ones obtained by the equivalent linearization technique and with experimental results. Shimogo [125], using equivalent linearization technique, discussed the isolation problem of random vibration by laminated spring with Coulomb friction damper.

5.3 Articulated Vehicle Model

In order to determine the ride performance of the articulated vehicle travelling over a random road surface, it is necessary first to develop a mathematical model that is a satisfactory representation of the actual physical system. Thus, the model is chosen to be a representation of actual vehicles without introducing unnecessary complications or irrelevant degrees of freedom.

The articulated vehicle system adopted for this study is similar to the simplified model described in Chapter 3, and is shown in Figure 5.1. The assumptions and the vibratory motions of the vehicle are restated here for convenience, and then followed by the description of the nonlinear suspension and tire forces. The vehicle is considered to

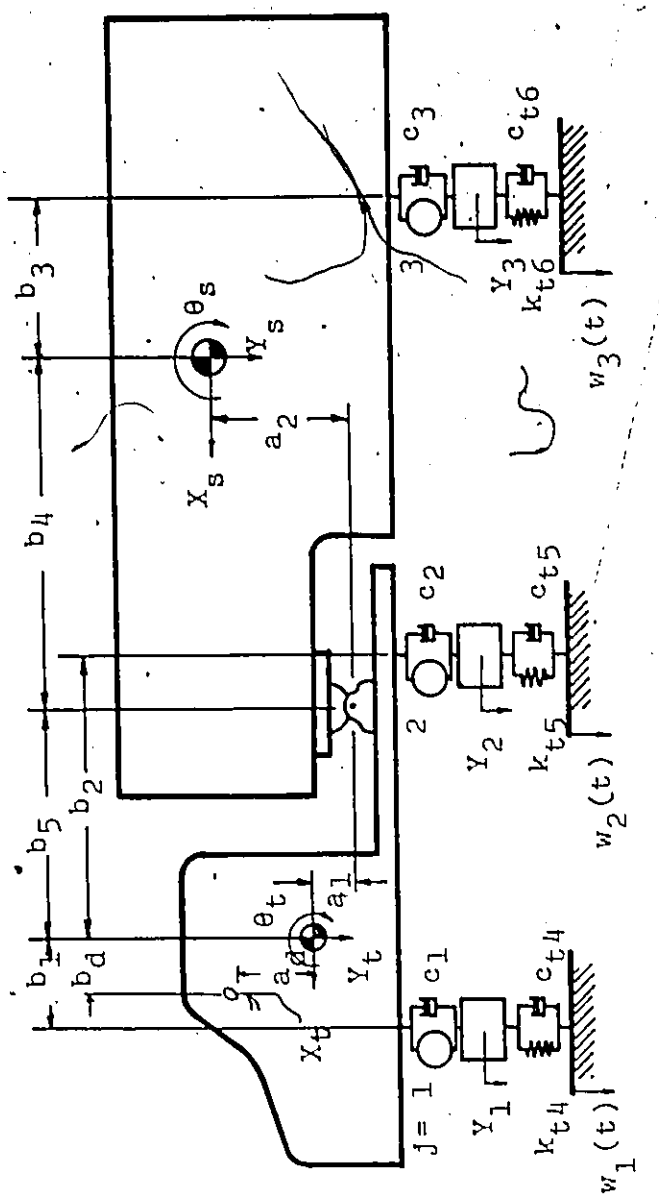

Figure 5.1 Articulated vehicle-nonlinear model.

be travelling over an uneven road at a constant forward velocity. The vehicle is subjected to disturbances from road irregularities. It is assumed that the roughness elements are equal in the left and right tracks. Vibration of the mathematical model is thus constrained to the longitudinal plane. It is also assumed that the vehicle components are perfectly rigid, and the suspension systems can adequately be represented by a point contact model. The tractor and semitrailer are allowed to translate in the forward and vertical directions, and to pitch except as constrained by the fifth wheel. The vehicle is supported by three axle suspension systems. The wheels and axles which are considered as dynamic systems, are supported through the tire springs and dampers by the road.

By considering the constraints imposed by the fifth wheel on the motion of the tractor and semitrailer, the model includes six degrees of freedom; pitching and heaving motions of the tractor centre of gravity, (Y_t, θ_t), pitching motion of the semitrailer centre of gravity, (θ_s), and the vertical motions of the three axle suspension systems, (Y_1, Y_2, Y_3). The suspension and tire forces are described below.

The general forms of the relationship between the main suspension spring force and the deflection are given in Figures 5.2 to 5.4 for a car [125], a tractor and a semitrailer [153] suspension, respectively. These curves were obtained for multileaf springs by gradually loading and unloading the suspension and measuring the deflections. The hysteresis loops are due to the effect of static friction in the suspension.

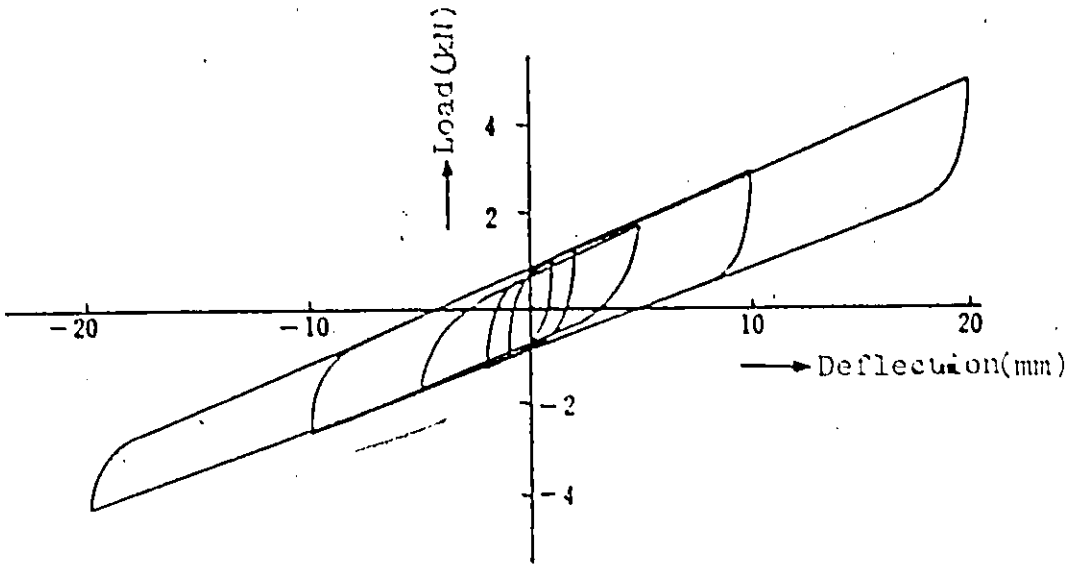

Figure 5.2 Car suspension characteristics [125].

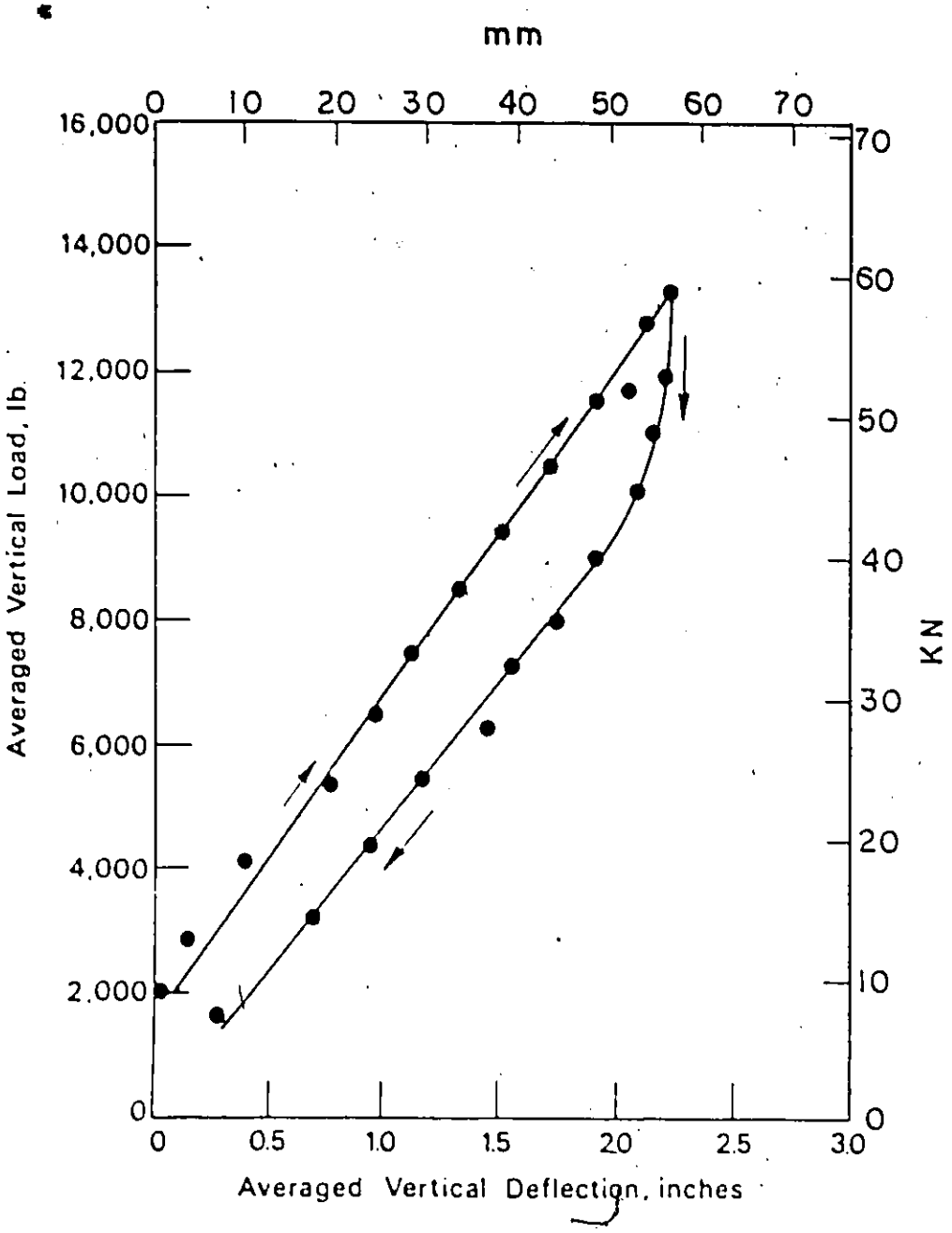

Figure 5.3 Tractor suspension characteristics [153].

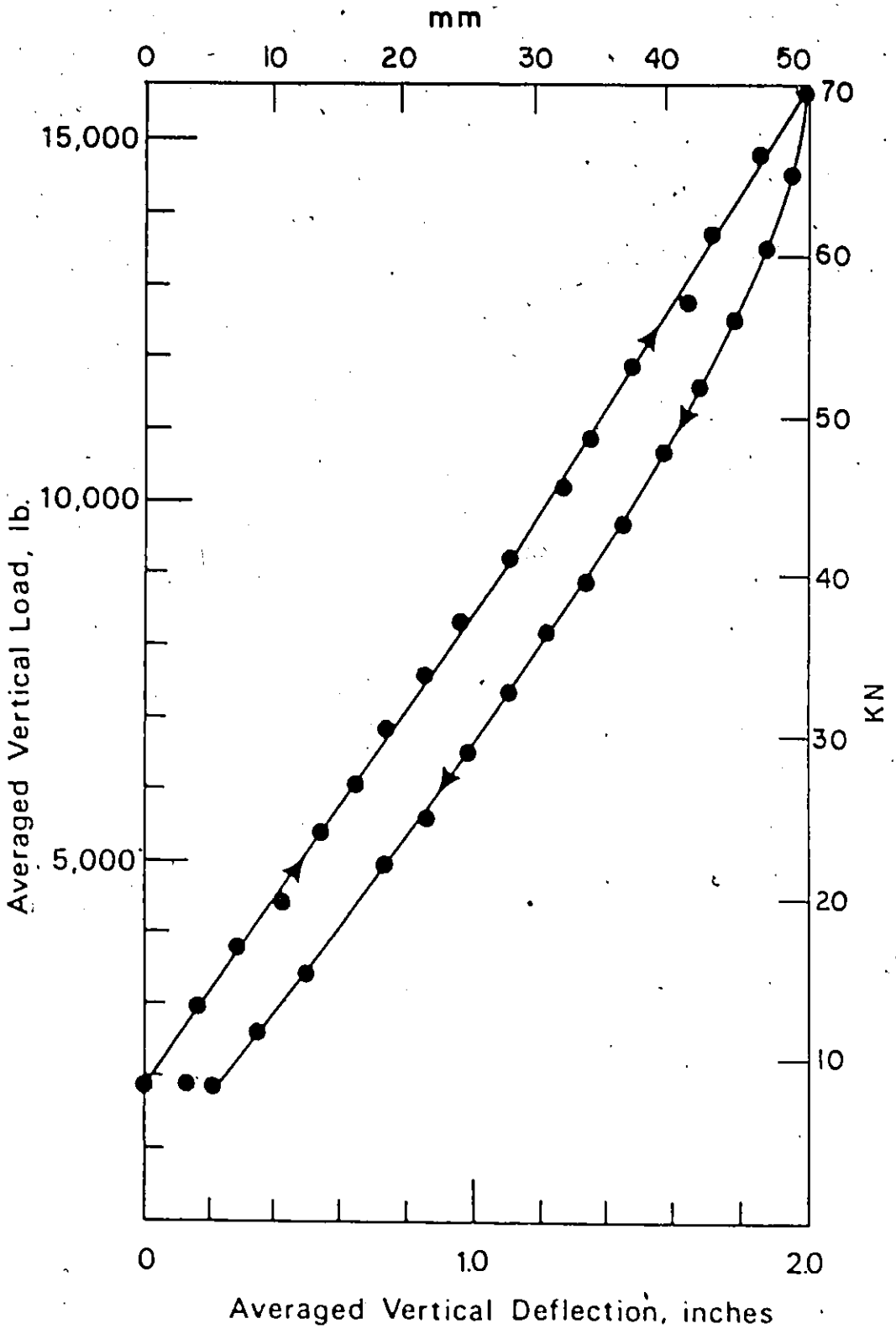

Figure 5.4 Semitrailer suspension characteristics [153].

For the purpose of the analytical work to be carried out here, the Coulomb friction present in the suspension associated with real articulated vehicles, is modeled in two forms:

(a) a linear spring and friction damper acting in parallel (directly coupled friction damping)

(b) a linear spring in parallel with an elastically friction damper (elastically coupled friction damping).

The force-deflection characteristics of these elements are shown in Figures 5.5 and 5.6, respectively. The damping in the suspension is assumed to be linear.

The model allows for the presence of bump stops by the inclusion of a spring with very high stiffness attached to the sprung mass, and which comes into contact with the unsprung mass only when the suspension deflection is greater than a preselected value. This characteristic is illustrated in Figure 5.7.

Each tire is represented by a spring-damper system having point contact with the road surface. The tire is allowed to leave the road. The phenomena of separation of the tire from the road is modeled through a bilinear spring with the corresponding properties given in Figure 5.8.

5.4 Analysis of Articulated Vehicle Motion Using Equivalent Linearization Technique

The vehicle system can be considered as an n-degree-of-freedom system connected by nonlinear elements. The mathematical equations

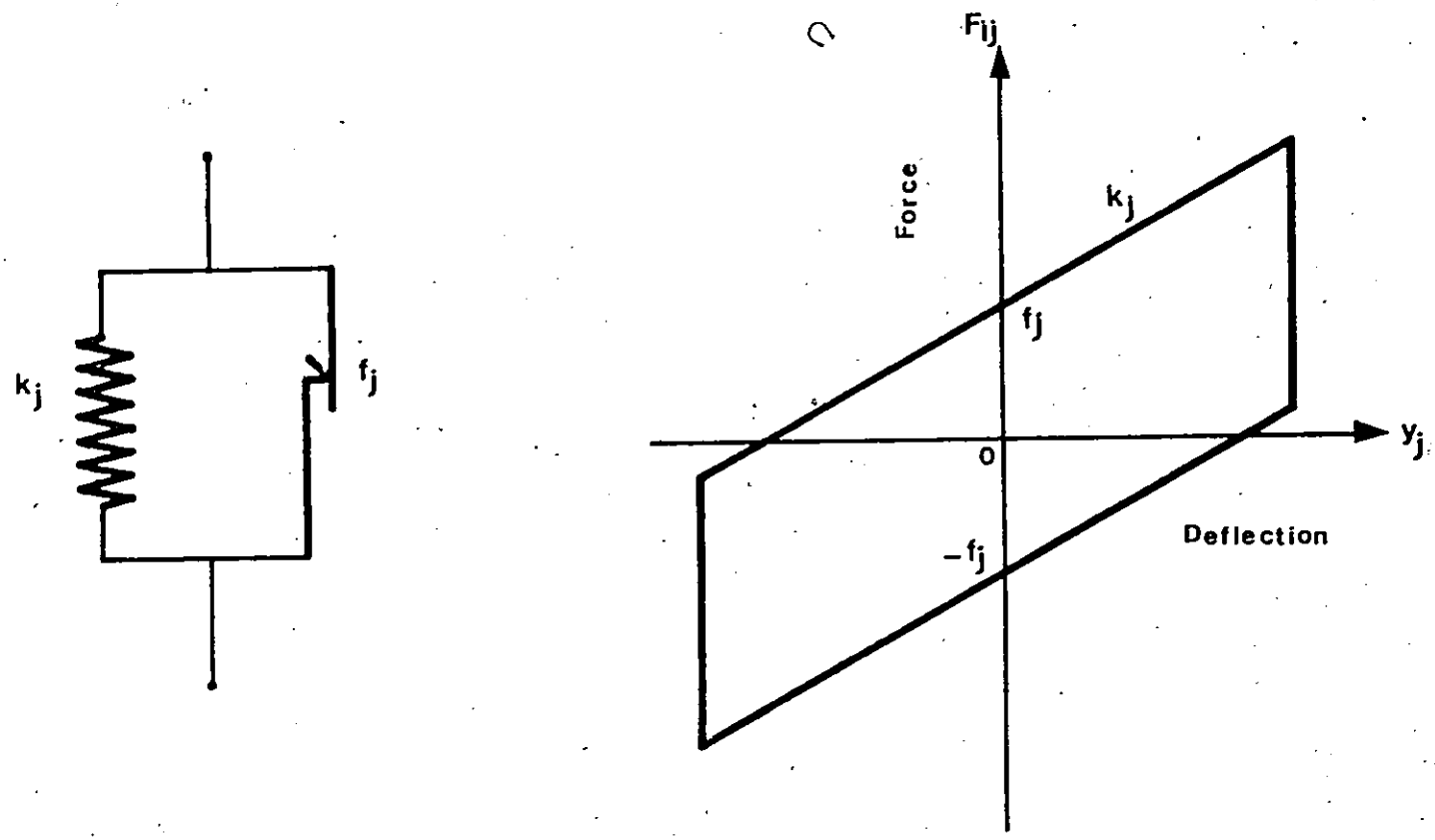

Figure 5.5 Directly coupled friction damping characteristics.

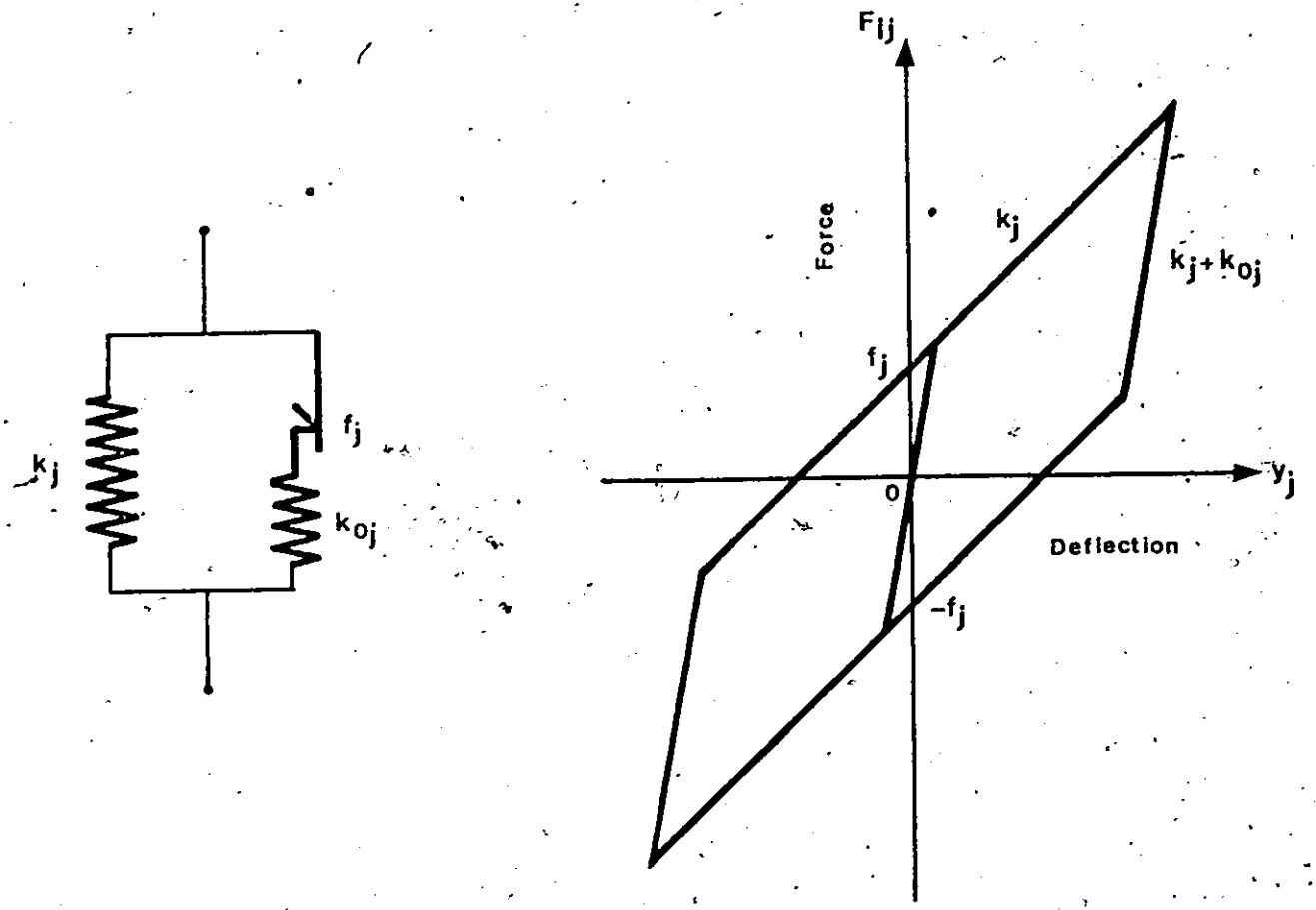

Figure 5.6 Elastically coupled friction damping characteristics.

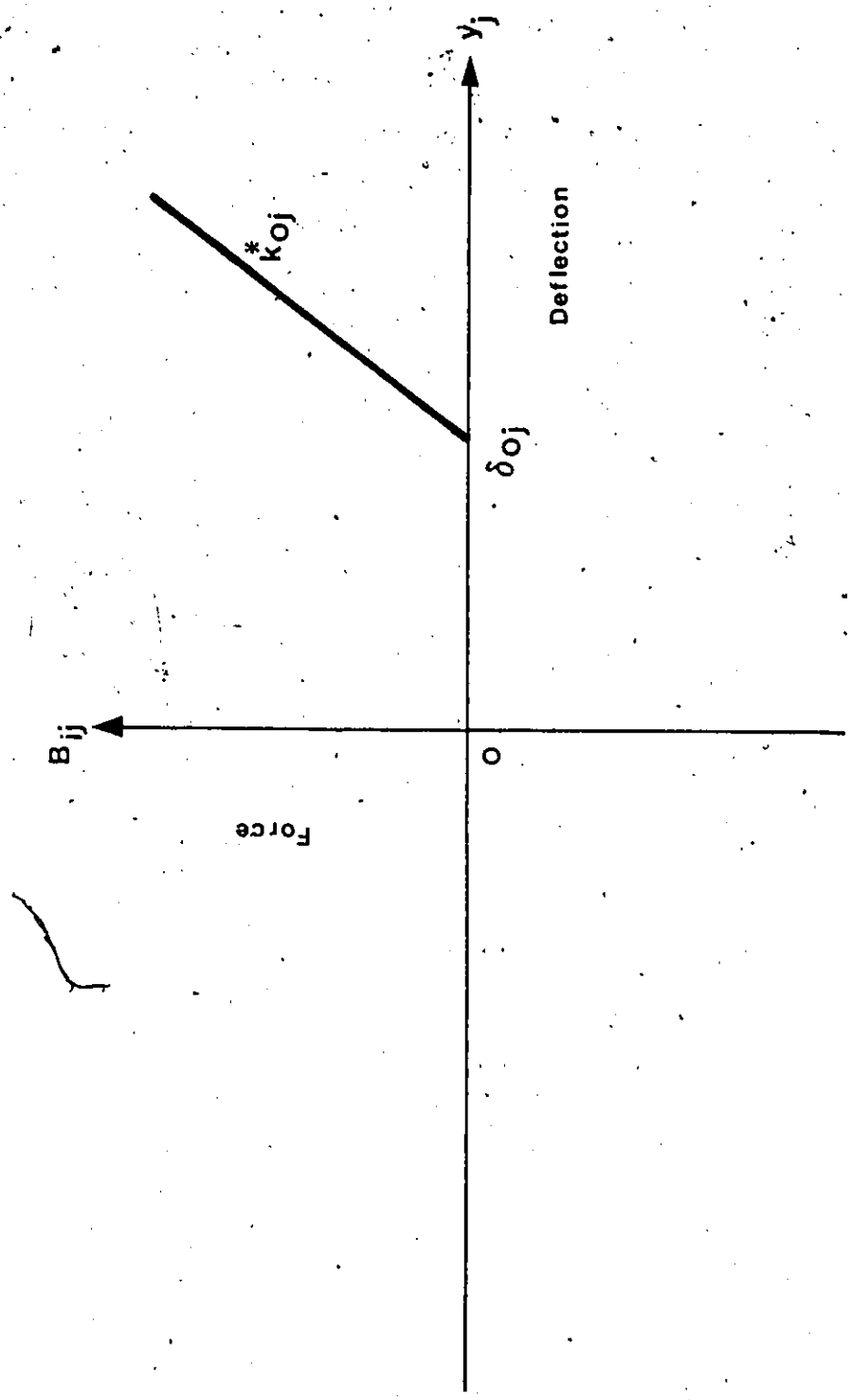

Figure 5.7 Bump stop characteristics.

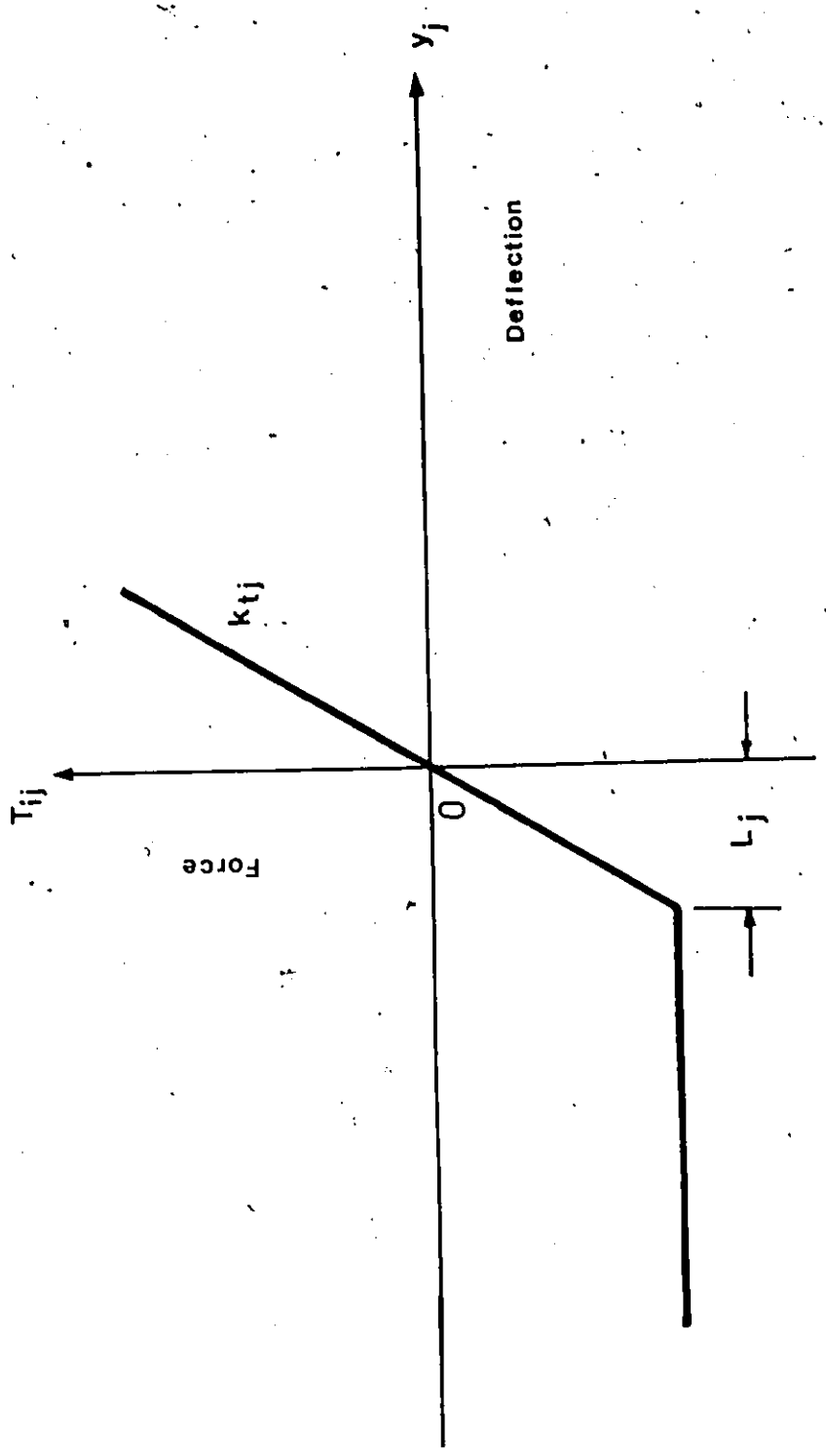

Figure 5.8 Tire spring characteristics.

which describe the response of the system are given in Appendix I. These equations may be written as:

$$M\ddot{\bar{y}} + C\dot{\bar{y}} + K\bar{y} + g(\dot{\bar{y}},\bar{y}) = \bar{f}(t), \tag{5.1}$$

$$\bar{y} = A\bar{x} + \bar{u} \tag{5.2}$$

where $\bar{x}' =$ $[Y_t, \theta_t, \theta_s, Y_1, Y_2, Y_3]$ is the generalized displacement vector

$\bar{y}$ is the relative displacement vector across the nonlinear elements

$\bar{u}$ is the excitation displacement vector

A is a transformation matrix given in Appendix I

M,C&K are the mass, damping and stiffness matrices, respectively

$\bar{g}(\dot{\bar{y}},\bar{y})$ is a nonlinear vector function of the dependent variable $\bar{y}$ and its derivative $\dot{\bar{y}}$

$\bar{f}(t)$ is the excitation force vector

Due to the nonsymmetric nonlinear function $\bar{g}(\dot{\bar{y}},\bar{y})$, the steady-state solution of such a system exhibits a constant offset.

Let

$$\bar{y}(t) = \bar{y}_c + \bar{z}(t), \tag{5.3}$$

where $\bar{y}_c$ is a constant vector, and $\bar{z}(t)$ is a stationary random vector with zero mean.

Substituting transformation (5.3) into equation (5.1) yields

$$M\ddot{\bar{z}} + C\dot{\bar{z}} + K\bar{z} + K\bar{y}_c + \bar{g}(\dot{\bar{z}}, \bar{y}_c + \bar{z}) = \bar{f}(t) \tag{5.4}$$

Taking the expectation of (5.1) gives

$$M\,E[\ddot{\bar{y}}] + C\,E[\dot{\bar{y}}] + K\,E[\bar{y}] + E[\bar{g}(\dot{\bar{y}},\bar{y})] = 0 \tag{5.5}$$

From the stationarity of $\bar{y}$ it follows that

$$E[\dot{\bar{y}}] = \frac{d}{dt} E[\bar{y}] = 0, \tag{5.6.a}$$

$$E[\ddot{\bar{y}}] = \frac{d^2}{dt^2} E[\bar{y}] = 0 \tag{5.6.b}$$

Hence, equation (5.5) reduces to

$$K\bar{y}_c + E[\bar{g}(\dot{\bar{y}},\bar{y})] = 0 \tag{5.7}$$

Define the function $\bar{\beta}$ as

$$\bar{\beta}(\dot{\bar{z}},\ \bar{y}_c + \bar{z}) = K\bar{y}_c + \bar{g}(\dot{\bar{z}},\ \bar{y}_c + \bar{z}) \tag{5.8}$$

Then, because of condition (5.7) it is seen that $\bar{\beta}$ is symmetric with respect to $\bar{z}$.

Equation (5.4) can be written as

$$M\ddot{\bar{z}} + C\dot{\bar{z}} + K\bar{z} + \bar{\beta}(\dot{\bar{z}},\ \bar{y}_c + \bar{z}) = \bar{f}(t) \tag{5.9}$$

Because of the scarcity of exact solutions of equation (5.9) when the function $\bar{\beta}(\dot{\bar{z}},\ \bar{y}_c + \bar{z})$ is nonlinear, attention has been directed toward equivalent linearization technique, which gives an approximate analysis. The principle of the technique is to replace the nonlinear dynamical system (5.9) by another auxiliary system for which the exact analytical formula for solution is known. The replacement is made so as to be optimum with respect to some measure of the difference between the

original and the auxiliary system. The auxiliary system is called the equivalent linear system. While this equivalent linear system is effectivley linear, the system response depends on signal amplitude, a basic characteristic of nonlinear behaviour.

The equivalent linear system is defined by the linear differential equation

$$M\ddot{\bar{z}} + (C + C_e)\dot{\bar{z}} + (K + K_e)\bar{z} = \bar{f}(t), \qquad (5.10)$$

where C_e and K_e are two arbitrary matrices. These matrices are to be determined so that the difference $\bar{e}$ between the original system and the equivalent linear system is minimized for every $\bar{z}$ belonging to a certain class of functions of the independent variable t. The difference $\bar{e}$ is defined by

$$\bar{e} = \bar{\beta}(\dot{\bar{z}}, \bar{y}_c, \bar{z}) - C_e\dot{\bar{z}} - K_e\bar{z} \qquad (5.11)$$

Since the excitation of the linear system is assumed Gaussian it is well known that the response will be Gaussian as well. Therefore, the matrices C_e and K_e must be such that the random vector $\bar{e}$ is minimized for every stationary Gaussian random vector $\bar{z}$. A criterion that might be handled effectively would be to require that the mean square value of $\bar{e}$ is minimum, that is

$$E[\bar{e}'\ \bar{e}] = \text{minimum} \qquad (5.12)$$

Then the necessary conditions for (5.12) to be true are

$$\frac{\partial}{\partial c^e_{ij}}(E[\bar{e}'\ \bar{e}]) = 2E[\bar{e}'\ \frac{\partial \bar{e}}{\partial c^e_{ij}}] = 2E[e_j\ \dot{z}_k] = 0, \qquad (5.13.a)$$

$$i,j = 1,2,\ldots,n$$

$$\frac{\partial}{\partial k^e_{ij}} (E[\bar{e}' \bar{e}]) = 2E[\bar{e}' \frac{\partial \bar{e}}{\partial k^e_{ij}}] = 2E[e_j z_k] = 0 \qquad (5.13.b)$$

Substituting equation (5.11) into equation (5.13), yields

$$E[\bar{\beta}(\dot{\bar{z}}, \bar{y}_c, \bar{z})\dot{\bar{z}}'] = C_e E[\dot{\bar{z}} \dot{\bar{z}}'] + K_e E[\bar{z} \dot{\bar{z}}'] \qquad (5.14.a)$$

$$E[\bar{\beta}(\hat{\bar{z}}, \bar{y}_c, \bar{z})\bar{z}'] = C_e E[\dot{\bar{z}} \bar{z}'] + K_e E[\bar{z} \bar{z}'] \qquad (5.14.b)$$

By defining a vector $\hat{\bar{z}}$ as

$$\hat{\bar{z}} = (\dot{\bar{z}}', \bar{z}') \qquad (5.15)$$

Equations (5.14) may be written as

$$[C_e, K_e] E [\hat{\bar{z}} \hat{\bar{z}}'] = E[\bar{\beta}(\dot{\bar{z}}, \bar{y}_c, \bar{z})\hat{\bar{z}}'] \qquad (5.16)$$

or

$$[C_e, K_e] = E[\bar{\beta}(\dot{\bar{z}}, \bar{y}_c, \bar{z})\hat{\bar{z}}'] E [\hat{\bar{z}} \hat{\bar{z}}']^{-1} \qquad (5.17)$$

The existence and uniqueness of the equivalent linear system, K_e and C_e, depends on the nature of the matrix $E[\hat{\bar{z}} \hat{\bar{z}}']$. If the matrix $E[\hat{\bar{z}}, \hat{\bar{z}}']$ is nonsingular, there exists a unique equivalent linear system. If this matrix is singular, an equivalent linear system, if it exists, is non-unique.

The coefficients of the matrices C_e and K_e may be determined analytically if the nonlinear function $\bar{\beta}(\hat{\bar{z}}, \bar{y}_c + \bar{z})$ can be decomposed into a sum of simpler nonlinear elements, each of these nonlinear elements depends solely on the relative displacement and velocity of the masses of the system. Let the nonlinear function $\bar{\beta}(\hat{\bar{z}}, \bar{y}_c + \bar{z})$ take the following form

$$\beta_i(\dot{\bar{z}},\ \bar{y}\ +\ \bar{z}) = \sum_{j=1}^{n} k_{ij}\, y_{cj} + g_i(\dot{\bar{z}},\ \bar{y}_c + \bar{z})$$

$$= \sum_{j=1}^{n} k_{ij}\, y_{cj} + \sum_{j=1}^{n} q_{ij}(\dot{y}_j,\ y_j) \qquad (5.18)$$

Multiplying expression (5.15) by $\dot{z}_r$ and averaging both sides and then repeating the same for z_r,

$$E[\beta_i(\dot{\bar{z}},\ \bar{y}_c,\ \bar{z})\dot{z}_r] = \sum_{j=1}^{n} E[q_{ij}(\dot{y}_j,\ y_j)\dot{z}_r] \qquad (5.19.a)$$

$$E[\beta_i(\dot{\bar{z}},\ \bar{y}_c,\ \bar{z})z_r] = \sum_{j=1}^{n} E[q_{ij}(\dot{y}_j,\ y_j)z_r] \qquad (5.19.b)$$

Using the mathematical properties of the multi-dimensional Gaussian distribution, it can be proved that (see reference [154]),

$$E[q_{ij}(\dot{y}_j,y_j)\dot{z}_r] = E[q_{ij}(\dot{y}_j,y_j)\dot{z}_j]E[\dot{z}_r\ \dot{z}_j]/E[\dot{z}_j^2]$$

$$+ E[q_{ij}(\dot{y}_j,y_j)z_j]E[\dot{z}_r\ z_j]/E[z_j^2] \qquad (5.20.a)$$

$$E[q_{ij}(\dot{y}_j,y_j)z_r] = E[q_{ij}(\dot{y}_j,y_j)\dot{z}_j]E[\dot{z}_r\ z_j]/E[\dot{z}_j^2]$$

$$+ E[q_{ij}(\dot{y}_j,y_j)z_j]E[z_r\ z_j]/E[z_j^2] \qquad (5.20.b)$$

Then the coefficients of the matrices C_e and K_e given in equations (5.14) can be defined as follows:

$$c_{ij}^e = E[q_{ij}\ (\dot{y}_j,\ y_j)\ \dot{z}_j]/E[\dot{z}_j^2] \qquad (5.21.a)$$

$$k_{ij}^e = E[q_{ij}\ (\dot{y}_j,\ y_j)\ z_j]/E[z_j^2] \qquad (5.21.b)$$

For the problem on hand, the nonlinear functions $q_{ij}(\dot{y}_j,y_j)$ are linear functions of the interconnecting nonlinear elements $Q_{ij}(\dot{y}_j,y_j)$.

Therefore, the preceding analysis can be stated as follows:

Given the dynamical system (5.1) with non-symmetric nonlinear function of the form (5.18), an equivalent linear system may be obtained by replacing each interconnecting element according to the rule

$$Q_{ij}(\dot{y}_j, y_j) \rightarrow \alpha_{ij} \dot{y}_j + \gamma_{ij} y_j, \tag{5.22}$$

where

$$\alpha^e_{ij} = E[Q_{ij}(\dot{y}_j, y_j)\dot{z}_j]/E[\dot{z}^2_j], \tag{5.23.a}$$

$$\gamma^e_{ij} = E[Q_{ij}(\dot{y}_j, y_j)z_j]/E[z^2_j], \tag{5.23.b}$$

and the elements c^e_{ij} and k^e_{ij} of the matrices C_e and K_e are linear combinations of α^e_{ij} and γ^e_{ij}, i, j = 1, ..., n.

5.5 Method of Solution

The lack of "symmetry" of any components g_i, i = 1, ..., n, of the nonlinear function $\bar{g}(\dot{\bar{y}}, \bar{y})$ necessitates the addition of a mean vector $\bar{y}_c$ to the stationary solution of the problem.

A cyclic procedure may be devised as follows:

(a) Assume initial vlaues for both the matrices C_e and K_e and the mean vector $\bar{y}_c$.

(b) Solve the equation of motion of the linearized system (5.10), and evaluate the mean square responses

(c) Construct the average of the nonlinear function

(d) Use (5.7) to evaluate the new $\bar{y}_c$ vector

(e) Use (5.23) to construct the new C_e and K_e matrices

(f) Repeat steps (b) to (e) until results from cycle to cycle are similar.

5.6 Applications on System Nonlinearities

Many nonlinearities, such as Coulomb friction, bump stops and wheel hop, play an important role in the behaviour of the vehicle. The best way to obtain an idea about the effects of these nonlinearities is to begin by studying them one by one. In the following subsections the analytical expressions for vehicle system nonlinearities are derived using the analysis given in section 5.4.

5.6.1 Directly Coupled Friction Damping

Let the friction force be given by the following expression

$$F_{ij}(\dot{y}_j, y_j) = f_j \, \mathrm{sgn}(\dot{y}_j) \tag{5.24}$$

Since the nonlinear force is symmetric, then

$$y_j(t) = z_j(t), \tag{5.25}$$

and equations (23) can be written as

$$\alpha^e_{ij} = E[f_j \, \mathrm{sgn}(\dot{y}_j) \, \dot{y}_j]/E[\dot{y}_j^2] \tag{2.26.a}$$

$$\gamma^e_{ij} = E[f_j \, \mathrm{sgn}(\dot{y}_j) \, y_j]/E[y_j^2] \tag{5.26.b}$$

The relative displacements and velocities, y_j and $\dot{y}_j$, will not be Gaussian because of nonlinearity; however, for the equivalent linearization technique they are taken to be Gaussian. Representing the probability density $p(y_j, \dot{y}_j)$ by two-dimensional Gaussian distribution with zero mean ($E[y_j \, \dot{y}_j] = 0$),

$$P(y_j,\dot{y}_j) = \frac{1}{2\pi\sqrt{E[y_j^2]E[\dot{y}_j^2]}} \exp[-\frac{1}{2}[\frac{y_j^2}{E[y_j^2]} + \frac{\dot{y}_j^2}{E[\dot{y}_j^2]}] \qquad (5.27)$$

Substituting equation (5.27) into equations (5.24), the following solution can be obtained since $p(y_j, \dot{y}_j)$ is symmetric

$$\alpha_{ij}^e = \frac{\sqrt{2}}{\sqrt{\pi}} f_j/\sqrt{E[\dot{y}_j^2]} \qquad (5.28.a)$$

$$\gamma_{ij}^e = 0 \qquad (5.28.b)$$

5.6.2 Elastically Coupled Friction Damping

The bilinear hysteretic system is the nonlinear system having the restoring force-deformation characteristics as shown in Figure 5.9. This figure represents steady state response with amplitude χ_j and yield level $\lambda_j = f_j/k_{oj}$.

Define the average frequency across each nonlinear element as the ratio of the rms velocity response $\sqrt{E[\dot{y}_j^2]}$ to the rms displacement response $\sqrt{E[y_j^2]}$, [143], i.e.,

$$\omega_{aj} = \sqrt{E[\dot{y}_j^2]}/\sqrt{E[y_j^2]} \qquad (5.29)$$

Assume the following:

(i) The response of the nonlinear element is contained within a narrow frequency band.

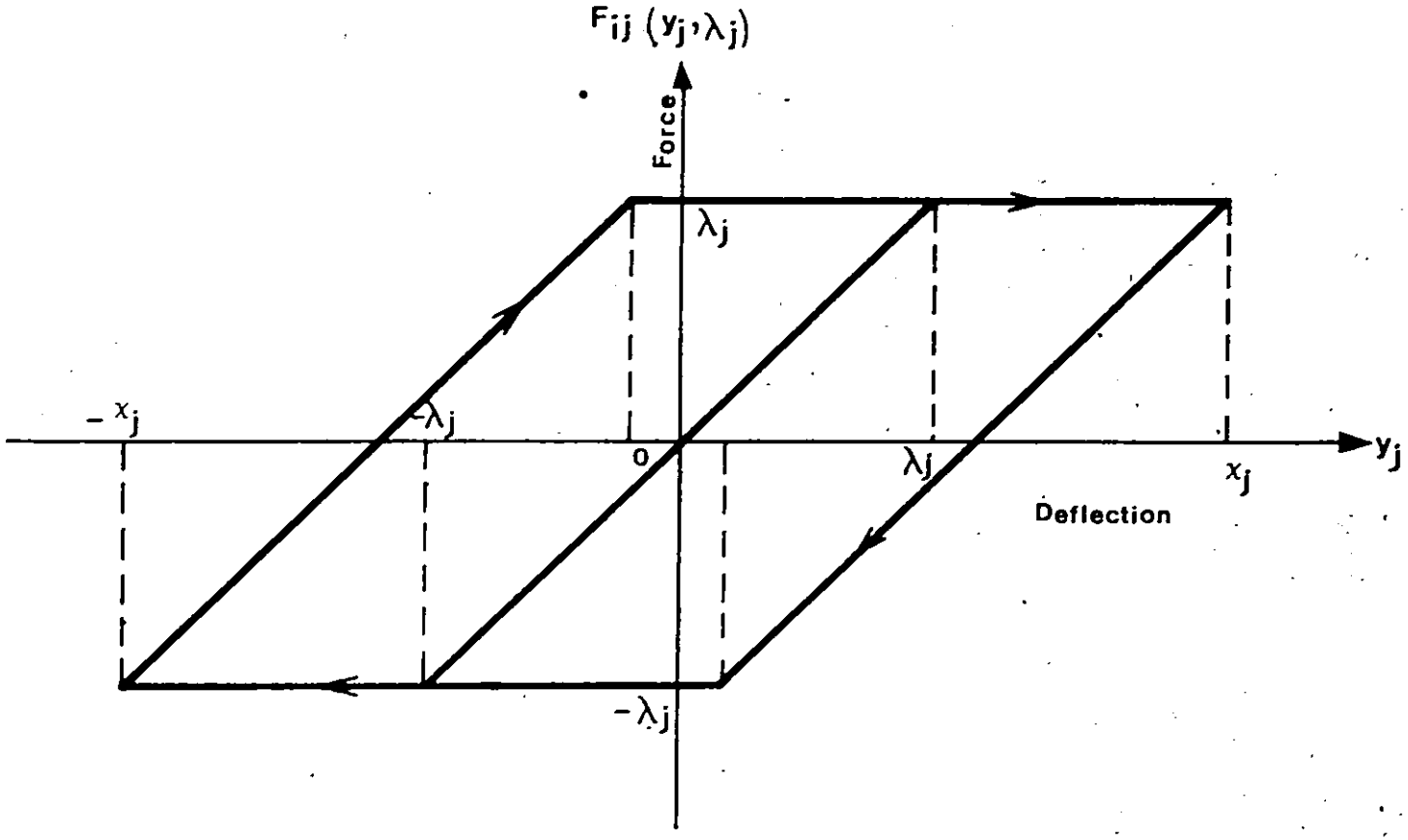

Figure 5.9 Force-deflection characteristics of elastically friction damping.

(ii) The probability density of the amplitude of this narrow band response is the Rayleigh distribution, i.e.,

$$p(\chi_j) = (\chi_j/E[y_j^2]) \exp(-\chi_j^2/2E[y_j^2]) \tag{5.30}$$

Using the above assumptions the response y_j is given by

$$y_j = \chi_j(t) \cos(\omega_{aj}t + \Omega_j(t)) \tag{5.31}$$

or

$$y_j = \chi_j(t) \cos \psi_j(t), \tag{5.32}$$

where χ_j, Ω_j, and ψ_j are slowly varying parameters of time.

Substituting equation (5.32) into equations (5.23), then

$$\alpha_{ij}^e = -\Big[\int_0^\infty \Big\{\frac{1}{2\pi}\int_0^{2\pi} F_{ij}(\chi_j \cos\psi_j, \lambda_j)\chi_j \omega_{aj}\sin\psi_j \, d\psi_j\Big\}$$

$$p(\chi_j)\, d\chi_j\Big]/(E[y_j^2]\omega_{aj}^2), \tag{5.33.a}$$

$$\gamma_{ij}^e = \Big[\int_0^\infty \Big\{\frac{1}{2\pi}\int_0^{2\pi} F_{ij}(\chi_j \cos\psi_j, \lambda_j)\chi_j\cos\psi_j \, d\psi_j\Big\}$$

$$p(\chi_j)d\chi_j\Big]/E[y_j^2] \tag{5.33.b}$$

Let

$$S(\chi_j) = \frac{1}{2\pi}\int_0^{2\pi} F_{ij}(\chi_j\cos\psi_j, \lambda_j)\sin\psi_j \, d\psi_j \tag{5.34.a}$$

and

$$C(\chi_j) = \frac{1}{2\pi}\int_0^{2\pi} F_{ij}(\chi_j\cos\psi_j, \lambda_j)\cos\psi_j \, d\psi_j \tag{5.34.b}$$

The mathematical expressions for $F_{ij}(y_j, \lambda_j)$ are as follows: For $\chi_j \leq \lambda_j$, the force is given by

$$F_{ij}(y_j, \lambda_j) = k_{oj}\, y_j = k_{oj}\, \chi_j \cos\psi_j \qquad (5.35)$$

For $\chi_j > \lambda_j$, the force may be expressed as

$$F_{ij}(y_j,\lambda_j) = \begin{cases} k_{oj}\{y_j - (\chi_j - \lambda_j)\}; & 0 \le \psi_j \le \phi_j \\ -k_{oj}\,\lambda_j \quad ; & \phi_j \le \psi_j \le \pi \\ k_{oj}\{y_j + (\chi_j - \lambda_j)\}; & \pi \le \psi_j \le \pi+\phi_j \\ k_{oj}\,\lambda_j \quad ; & \pi+\phi_j \le \psi_j \le 2\pi \end{cases} \qquad (5.36)$$

where $\phi_j = \cos^{-1}\dfrac{\chi_j - 2\lambda_j}{\chi_j}$

Using the mathematical expressions for $F_{ij}(y_j, \lambda_j)$ and equations (5.34), the expressions of $S(\chi_j)$ and $C(\chi_j)$ are given by

$$\begin{aligned} S(\chi_j) &= -k_{oj}(\chi_j/\pi)\sin^2\phi_j && (\chi_j > \lambda_j) \\ C(\chi_j) &= k_{oj}(\chi_j/\pi)\{\phi_j-(\sin\ 2\phi_j)/2\} && (\chi_j > \lambda_j) \\ S(\chi_j) &= 0 && (\chi_j \le \lambda_j) \\ C(\chi_j) &= k_{oj}\,\chi_j && (\chi_j \le \lambda_j) \end{aligned} \qquad (5.37)$$

Now the expressions of $E[\chi_j\, S(\chi_j)]$ and $E[\chi_j\, C(\chi_j)]$ are given by

$$E[\chi_j\, S(\chi_j)] = -\frac{k_{oj}}{\pi}\int_{\lambda_j}^{\infty} \chi_j^2 \sin^2\phi_j\, p(\chi_j)d\chi_j, \qquad (5.38.a)$$

$$E[\chi_j\, C(\chi_j)] = k_{oj}\int_0^{\lambda_j} \chi_j^2\, p(\chi_j)d\chi_j + \frac{k_{oj}}{\pi}\int_{\lambda_j}^{\infty} \chi_j^2(\phi_j - \frac{1}{2}\sin 2\phi_j)$$

$$p(\chi_j)d\chi_j \qquad (5.38.b)$$

Using the definition of the Rayleigh distribution $p(\chi_j)$, then

$$\int \chi_j^2\, p(\chi_j)d\chi_j = -(\chi_j^2 + 2E[y_j^2])\exp(-\chi_j^2/2E[y_j^2]) \qquad (5.39a)$$

and

$$\frac{d}{dx_j}\left(\phi_j - \frac{1}{2}\sin 2\phi_j\right) = -\frac{8\lambda_j^2}{x_j^3}\sqrt{x_j/\lambda_j - 1} \qquad (5.39.b)$$

Substituting equations (5.39) into equations (5.38), the following expressions for $E[x_j\, S(x_j)]$ and $E(x_j\, C(x_j)]$ are obtained,

$$E[x_j\, S(x_j)] = \frac{-4E[y_j^2]k_{oj}}{\sqrt{\pi}\ \eta_j}\ \mathrm{erfc}\left(\frac{1}{\eta_j}\right), \qquad (5.40.a)$$

$$E[x_j\, C(x_j)] = 2k_{oj}E[y_j^2]\left\{1 - \frac{8}{\pi}\int_1^\infty \frac{1}{\xi_j^3}\sqrt{\xi_j - 1}\right.$$

$$\left.\left(1 + \frac{\xi_j^2}{\eta_j^2}\right)\exp\left(\frac{-\xi_j^2}{\eta_j^2}\right) d\xi_j\right\}, \qquad (5.40.b)$$

where, $\eta_j = \sqrt{2E[y_j^2]}/\lambda_j$, $\xi_j = x_j/\lambda_j$,

and $\mathrm{erfc}\left(\frac{1}{\eta_j}\right) = \frac{2}{\sqrt{\pi}}\int_{1/\eta_j}^\infty e^{-u^2}\, du$

Substituting (5.40) into (5.33), then

$$\alpha_{ij}^e = \frac{2k_{oj}}{\omega_{aj}\sqrt{\pi}\eta_j}\ \mathrm{erfc}\left(\frac{1}{\eta_j}\right), \qquad (5.41.a)$$

and

$$\gamma_{ij}^e = k_{oj}\left[1 - \frac{8}{\pi}\int_1^\infty \frac{1}{\xi_j^3}\sqrt{\xi_j - 1}\left(1 + \frac{\xi_j^2}{\eta_j^2}\right)\exp\left(\frac{-\xi_j^2}{\eta_j^2}\right) d\xi_j\right] \qquad (5.41.b)$$

As $k_{oj} \to \infty$, $\xi_j \to \infty$

$$\text{and} \quad \alpha^e_{ij} = \frac{2k_{oj}\, f_j/k_{oj}}{\omega_{aj}\sqrt{\pi}\,\sqrt{2E[y^2]}} = \frac{\sqrt{2}}{\sqrt{\pi}}\, f_j/\sqrt{E[\dot{y}_j^2]}, \tag{5.42.a}$$

since $\omega_{aj} = \sqrt{E[\dot{y}_j^2]}/\sqrt{E[y_j^2]}$.

$$\gamma^e_{ij} = k_{oj}\left[1 - \frac{8}{\pi}\int_1^\infty \frac{1}{\xi_j^3}\sqrt{\xi_j - 1}\, d\xi_j\right] = 0 \tag{5.42.b}$$

5.6.3 Bump Stops

The bump stop characteristics are shown in Figure 5.7 with coordinates y_j and B_{ij}. The bump stop force may be expressed mathematically as

$$B_{ij}(y_j, \delta_{oj}) = \begin{cases} 0 & y_j \le \delta_{oj} \\ k^*_{oj}(y_j - \delta_{oj}) & y_j \ge \delta_{oj} \end{cases} \tag{5.43}$$

By assuming that

$$y_j(t) = z_j(t) + y_{cj}, \tag{5.44}$$

where y_{cj} is the mean value of the random process y_j, then the force can be written as

$$B_{ij}(z_j, y_{cj}, \delta_{oj}) = \begin{cases} 0 & z_j \le \delta_{oj} - y_{cj} \\ k^*_{oj}(z_j + y_{cj} - \delta_{oj}), & z_j > \delta_{oj} - y_{cj} \end{cases} \tag{5.45}$$

Since the response is assumed to be Gaussian, the amplitude probability density is given by

$$p(z_j) = \frac{1}{\sqrt{2\pi E[z_j^2]}} \exp(-z_j^2/2\sqrt{E[z_j^2]}), \tag{5.46}$$

and in this case the mean value for the nonlinear force is given by

$$\begin{aligned} E[B_{ij}(z_j,y_{cj},\delta_{oj})] &= \frac{k_{oj}^*}{\sqrt{2\pi E[z_j^2]}} \int_{\delta_{oj}-y_{cj}}^{\infty} (z_j+y_{cj}-\delta_{oj})\exp(-z_j^2/2E[z_j^2])dz_j \\ &= k_{oj}^* \{\sqrt{E[z_j^2]/2\pi}\ \exp(-(\delta_{oj}-y_{cj})^2/2E[z_j^2]) \\ &\quad - \frac{1}{2}(\delta_{oj}-y_{cj})(1-\mathrm{erf}((\delta_{oj}-y_{cj})/\sqrt{2E[z_j^2]}))\} \end{aligned} \tag{5.47}$$

Using equation (5.23.b), the equivalent linear stiffness is given by

$$\begin{aligned} \gamma_{ij}^e &= \frac{k_{oj}^*}{E[z_j^2]} \{ \int_{\delta_{oj}-y_{cj}}^{\infty} (z_j+y_{cj}-\delta_{oj})z_j p(z_j)dz_j \} \\ &= \frac{1}{2} k_{oj}^* \{1 - \mathrm{erf}((\delta_{oj}-y_{cj})/\sqrt{2E[z_j^2]})\} \end{aligned} \tag{5.48}$$

5.6.4 Wheel Hop

The tire characteristics are shown in Figure 5.8 with coordinates y_j and T_{ij}. The static deflection of each tire under the vehicle weight is L_j. The tire force may be expressed as

$$T_{ij}(y_j, L_j) = \begin{cases} k_{tj}\, y_j & -L_j \le y_j \le \infty \\ -k_{tj}\, L_j & -\infty \le y_j \le -L_j \end{cases} \tag{5.49}$$

by assuming that

$$y_j(t) = z_j(t) + y_{cj}, \tag{5.50}$$

then the tire force may be written as

$$T_{ij}(z_j, y_{cj}, L_j) = \begin{cases} k_{tj}(z_j+y_{cj}) & -L_j-y_{cj} \le z_j \le \infty \\ \\ -k_{tj}L_j & -\infty \le z_j \le -L_j - y_{cj} \end{cases} \tag{5.51}$$

The mean value of the nonlinear tire force is given by

$$E[T_{ij}(z_j,y_{cj},L_j)] = k_{tj}\{ \int_{-L_j-y_{cj}}^{\infty} (z_j+y_{cj})p(z_j)dz_j$$

$$- L_j \int_{-\infty}^{-L_j-y_{cj}} p(z_j)dz_j\} \tag{5.52}$$

Considering that the response is Gaussian, and carrying out the above integral, the following result is obtained:

$$E[T_{ij}(z_j,y_{cj},L_j)] = k_{tj}\{\sqrt{E[z_j^2]}/\sqrt{2\pi}\ \exp(-(L_j+y_{cj})^2/2E[z_j^2])$$

$$- L_j + \frac{1}{2}(y_{cj}+L_j)[1-\mathrm{erf}(-(L_j+y_{cj})/\sqrt{2E[z_j^2]})]\} \tag{5.53}$$

The equivalent linear tire stiffness can be calculated using equation (5.23.b) as follows,

$$\gamma_{ij}^e = \frac{1}{E[z_j^2]}\{ \int_{-L_j}^{\infty} k_{tj}(z_j+y_{cj})z_j p(z_j)dz_j - \int_{-\infty}^{-L_j-y_{cj}} L_j z_j p(z_j)dz_j\}$$

$$= \frac{1}{2} k_{tj}\{1 - \mathrm{erf}(-(L_j+y_{cj})/\sqrt{2E[z_j^2]})\} \tag{5.54}$$

5.7 Results and Discussions

In the course of the dynamic studies, two variations of the basic model have been investigated. These are the loaded vehicle and the unloaded vehicle. The vehicle parameters are given in Table 4.1. Two road characteristics are considered: smooth road, A, and rough road, B. The parameters of these two road surfaces are given in Table 4.2. In both cases, the model representing the vehicle travels with a constant forward velocity of 80 km/h.

The ride behaviour of the articulated vehicle has been evaluated according to the following ride comfort and ride safety indices:

1. The power spectral densities of the vertical and fore and aft accelerations at the driver's location and at the centre of gravity of the tractor. The acceleration spectra are compared with the ISO guide for one hour and eight hours.
2. The power spectral densities of tractor and semitrailer pitch accelerations, and axle dynamic excursion, that is, the displacement of the unsprung mass relative to the sprung mass.
3. The rms accelerations and displacements at different locations in the vehicle.
4. The power spectral densities of dynamic wheel loads.
5. The rms of dynamic wheel loads.
6. The percentage of time each wheel assembly loses contact with the road, indicating loss of "road holding" or controllability.

5.7.1 Effect of Dry Friction

5.7.1.1 Directly Coupled Friction Damping

Vehicle Accelerations: The power spectral density curves for the vertical accelerations at the centre of gravity of the tractor and at the driver position for the loaded and unloaded vehicle operating on route A are shown in Figures 5.10 and 5.11, respectively. The dry friction force in each suspension is considered to be a percentage of the corresponding axle static load. The curves are plotted for different values of the ratio of the friction force to the axle static load; 0% (linear model), 2%, 4% and 6%.

In each case the acceleration spectrum has three predominant frequencies. The first frequency corresponds primarily to tractor bounce mode, while the second frequency corresponds to tractor and semitrailer pitch modes, and the third is associated with the wheel axle bounce modes.

The results indicate that inclusion of the dry friction in the analysis affects the system response to an appreciable degree. Increasing the dry friction force diminishes the peak response in the low frequency region corresponding to the bounce frequency. However, the response increases considerably in the high frequency region by increasing the dry friction force. Specifically, the vibration comfort in the frequency range 3-4 Hz becomes poorer and reaches ISO 1 hour boundary. In other words, increasing the friction will cause the formation of a second resonance peak in the range of 3-4 Hz. These

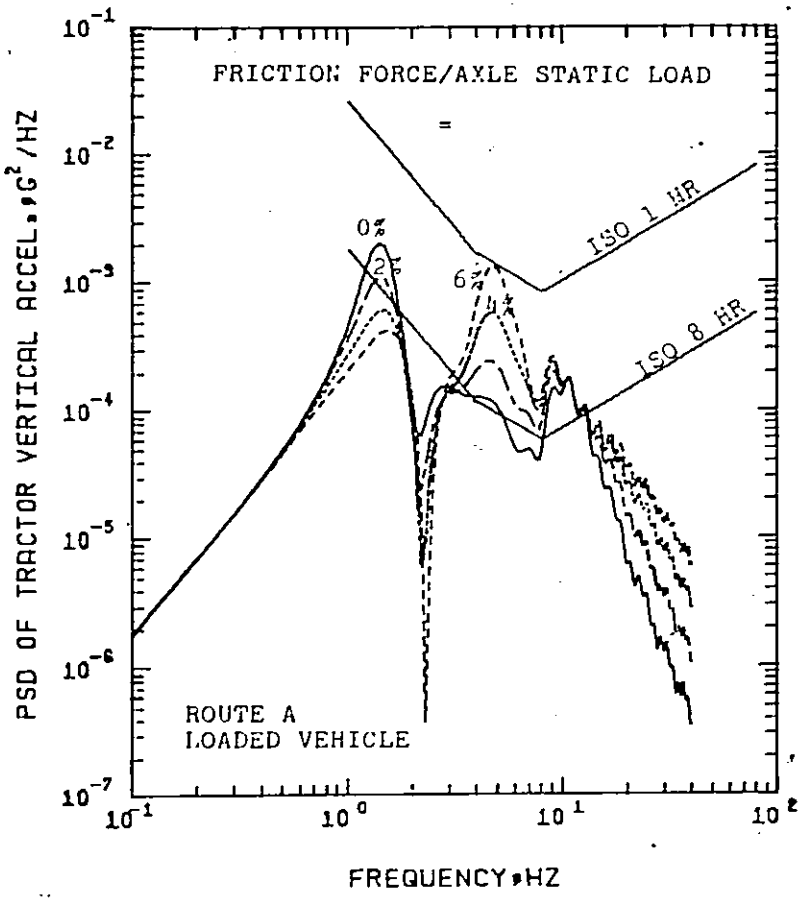

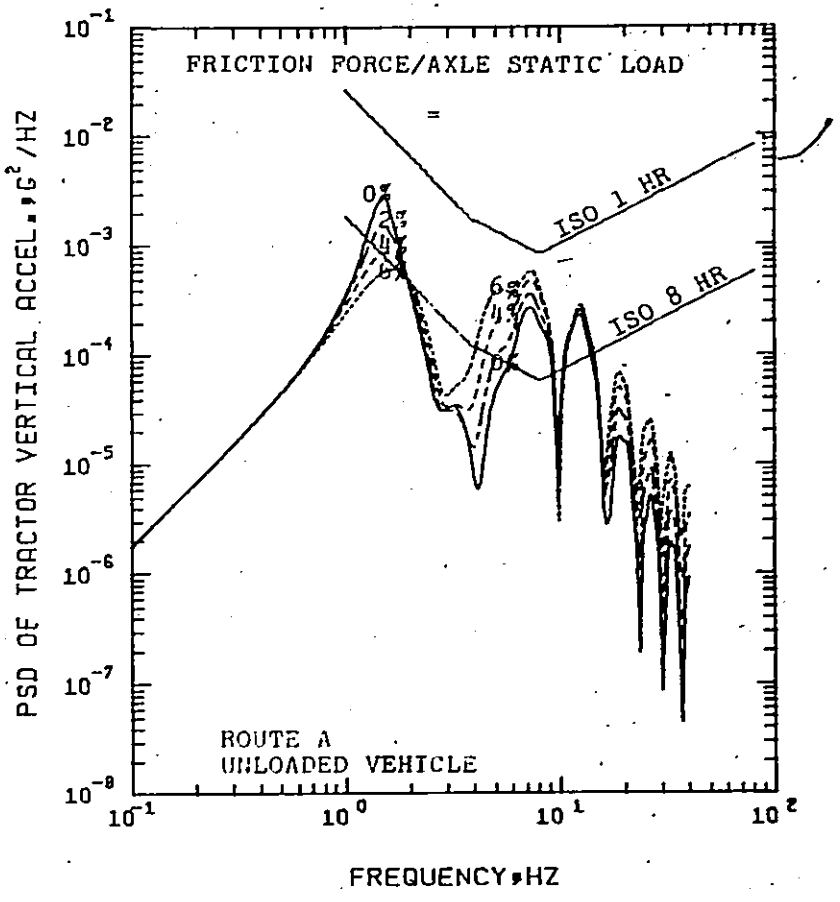

Figure 5.10 Effect of directly coupled friction damping on tractor vertical acceleration spectra - smooth road.

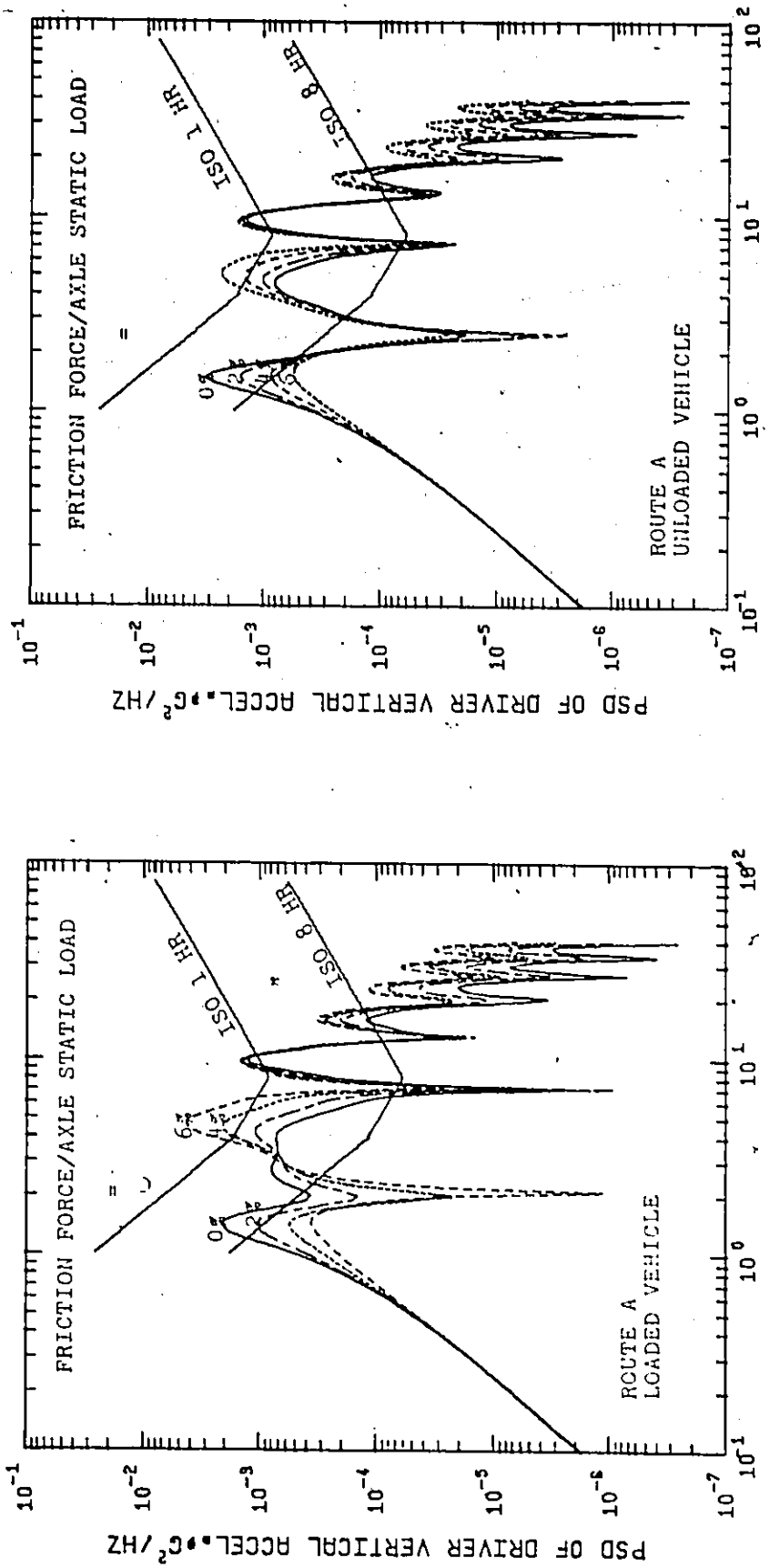

Figure 5.11 Effect of directly coupled friction damping on driver vertical acceleration spectra - smooth road.

frequencies are in the range of human body resonances and as can be seen from the figures, it is deleterious to the ride motion.

It should be noted that the amount of friction in the suspension for the loaded vehicle is larger than the corresponding values in the unloaded vehicle. As may be seen in the various figures, the acceleration spectra for the unloaded vehicle are primarily below the 1-hour ISO guideline. By considering the fact that the amount of friction in the unloaded vehicle is less than the corresponding value in the loaded vehicle in the cases studied, it can be observed that the comfort of an unloaded vehicle is considerably worsened due to the existing frictional force in the vehicle suspension.

It can be seen from Figure 5.11 that several peaks occur in the high frequency range with a wide band peak in the frequency range of 3-6 Hz. The effect of the dry friction is noticeable. Significant attenuation is obtained below 2 Hz. It is seen from the figure that increasing the dry friction will stiffen the suspension and more energy will be transmitted to the sprung masses. The spectrum exceeds the 8-hour ISO guide in both the low and high frequency range for the linear system. However, increasing the friction made the spectra exceed the 1-hour ISO guide in the high frequency range. This ride is definitely rough, corresponding to 80 km/h for a smooth road, and would be unacceptable for a 1-hour duration.

Figure 5.12 shows the effect of the dry friction on the loaded vehicle acceleration spectra for route B. It can be seen that there is

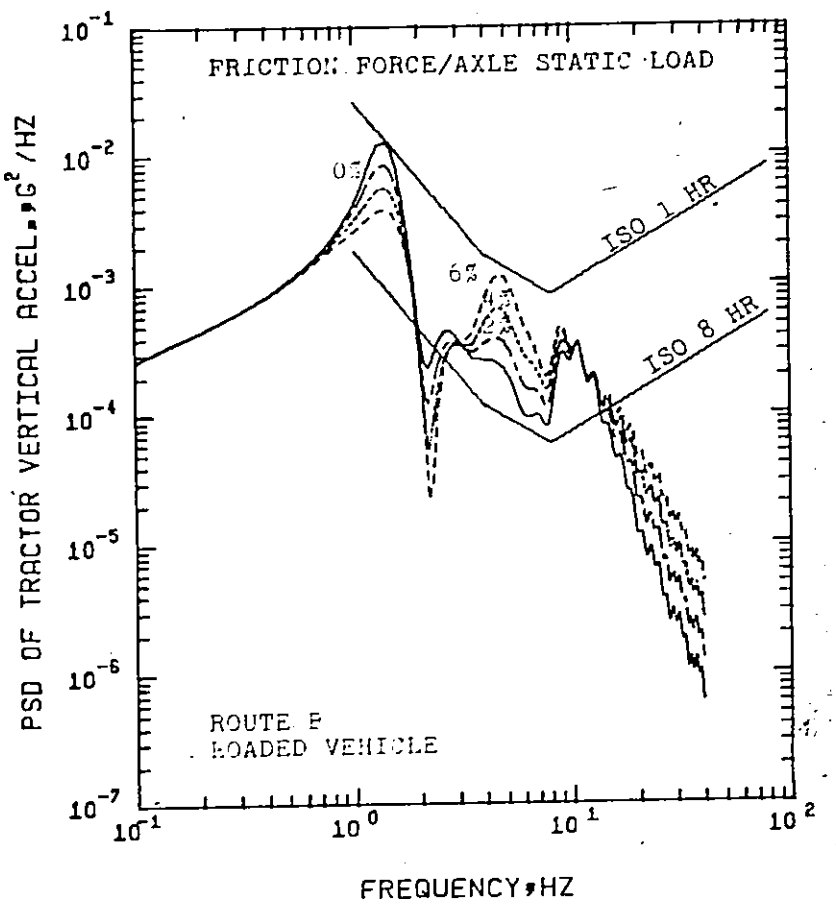

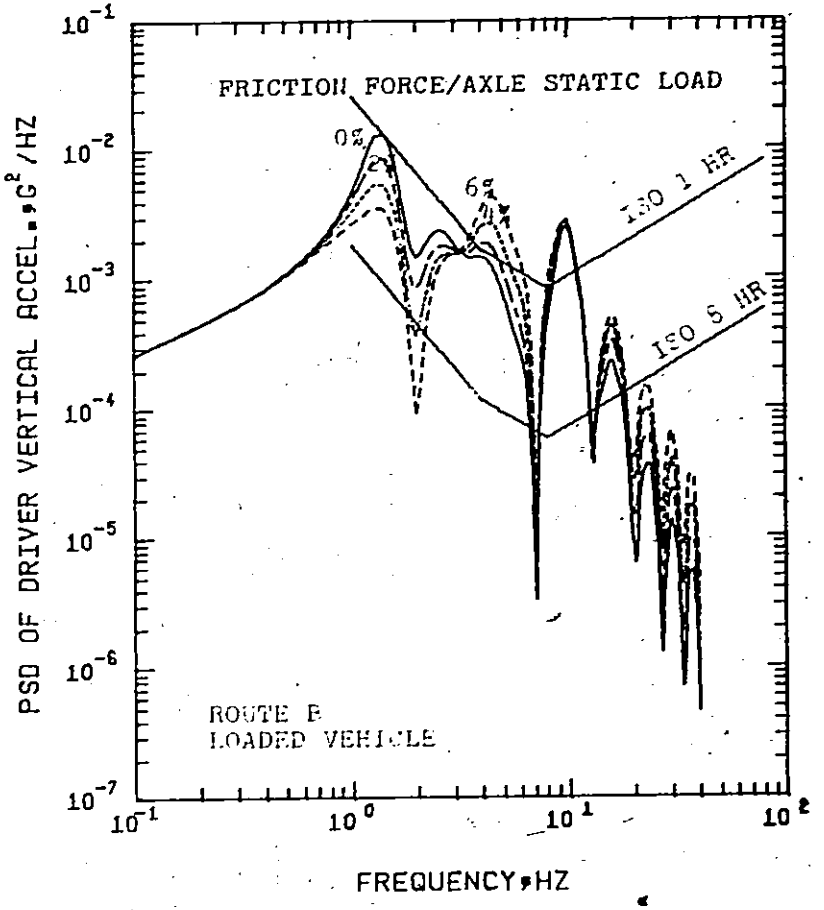

Figure 5.12 Effect of directly coupled friction damping on tractor and driver acceleration spectra - rough road.

a definite increase in 0.1 - 40 Hz range content of the vertical vibrations. The rate of increase of the amplitude spectra for route A is higher than that for route B in the low frequency range. The acceleration spectra does not meet the ISO guide for 1 hour at the high frequency range. The reduction of vibration amplitude in the 0.8 - 2 Hz range is accompanied by some increase in amplitude in the 3.5 - 6 Hz range.

By comparing the results for the smooth road and for the rough road, it can be observed that the rate of reduction of the amplitude spectra in the frequency range 0.8 - 2 Hz and the rate of increase of the amplitude spectra in the frequency range 3.5 - 6 Hz are higher for the smooth road than the corresponding values for the rough road.

Clearly illustrated in Figures 5.11 and 5.12 are the resonances occurring due to tractor and semitrailer pitch modes excitations. Pitch modes contributions are apparent here due to the fact that the driver location is not at the tractor's centre of gravity.

Figures 5.13 and 5.14 show the effect of the dry friction damping on the fore and aft acceleration spectra at the tractor's centre of gravity and at the driver's neck level, respectively. In each figure the acceleration spectra are given for the loaded and unloaded vehicle operating on route A. It may be seen from Figure 5.13 that increasing the frictional forces will decrease the magnitude of the first resonance peak for the loaded vehicle. However, almost the entire frequency content is increased with increasing the frictional forces for the

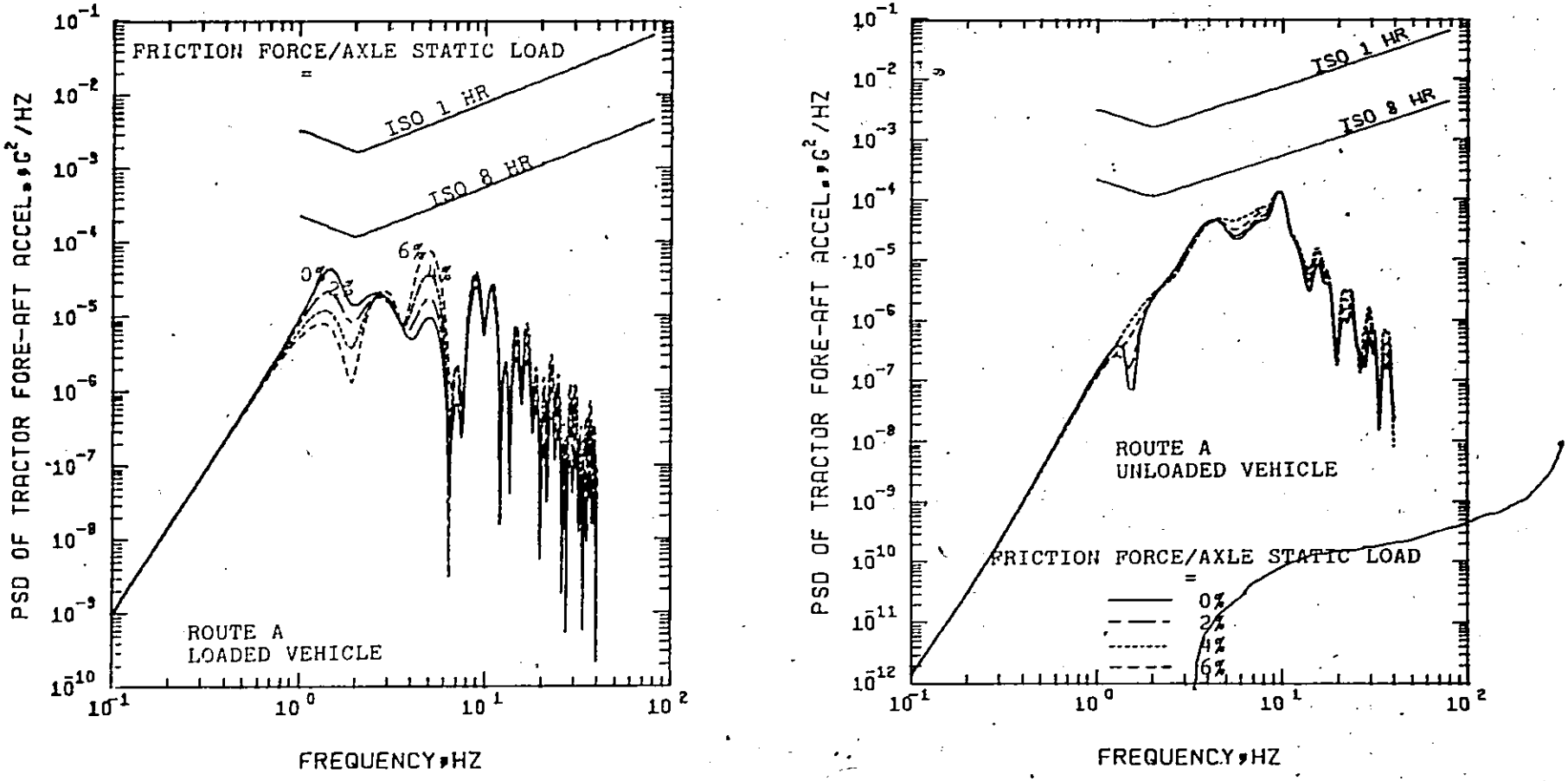

Figure 5.13 Effect of directly coupled friction damping on tractor fore and aft acceleration spectra - smooth road.

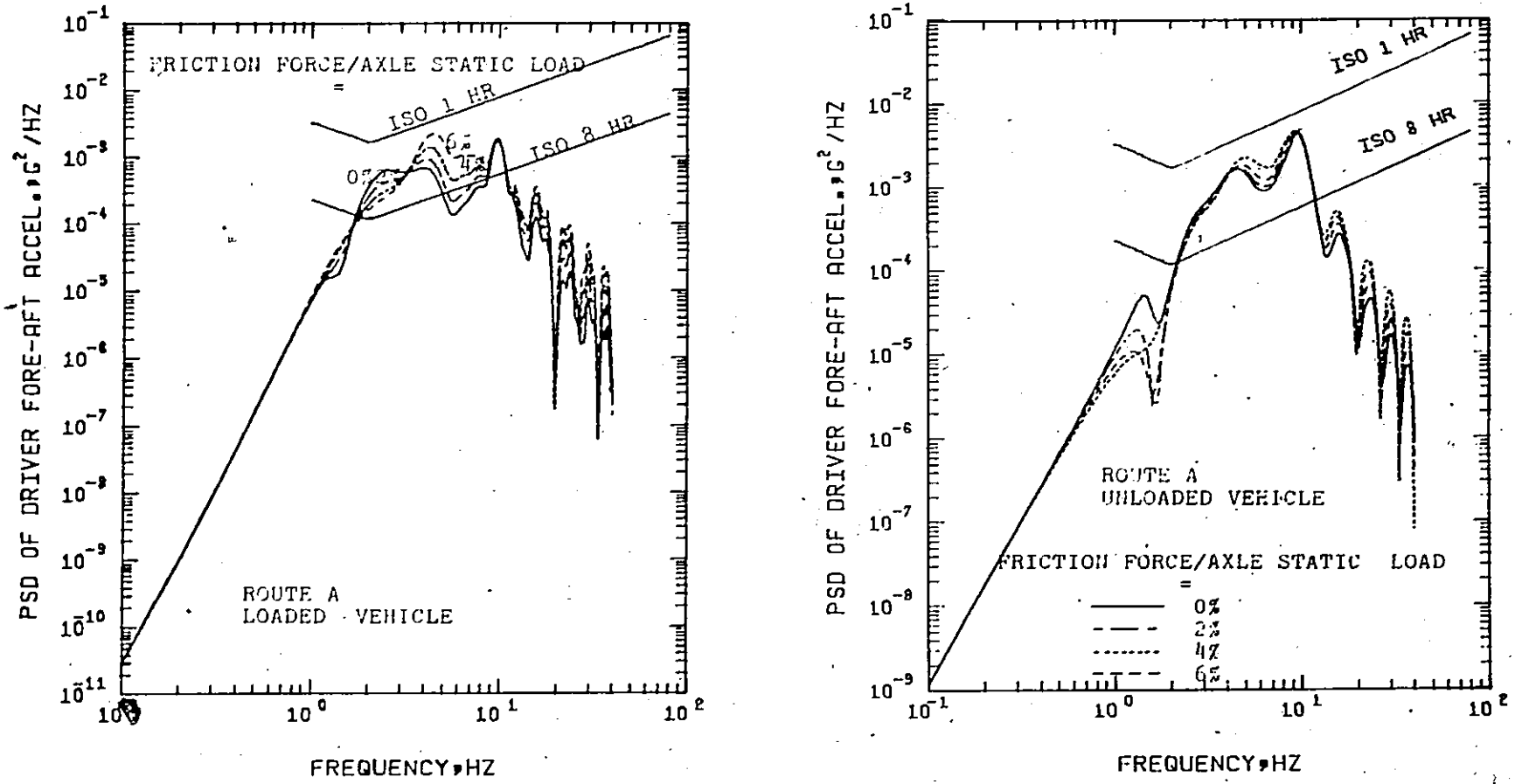

Figure 5.14 Effect of directly coupled friction damping on driver fore and aft acceleration spectra - smooth road.

unloaded vehicle. It may also be concluded, from studying Figure 5.14, that the frictional forces have a negative effect on the fore and aft acceleration spectra at the medium and high frequency range.

Through comparison of the fore and aft acceleration spectra at the driver's neck level with the tractor and semitrailer pitch acceleration spectra given in Figures 5.15 and 5.16, it may be concluded that the tractor pitch accelerations contribute significantly to the excessive level of acceleration at the driver location.

On the basis of the data exhibited in Figures 5.17 to 5.19, it is concluded that due to the presence of a high level of dry friction in the suspension, the ride dynamics of articulated vehicles are largely determined by the fact that the tires are the main suspension medium. This results in inadequate damped vibration with resonance at frequencies less bearable by human beings, that is, frequencies to which man is particularly sensitive.

To show the effect of tractor front and rear suspenson friction dampings on the vehicle vibrational responses, the level of dry frictional forces are varied while all other vehicle parameters are held constant at the baseline values. Figures 5.20 and 5.21 are three-dimensional plots of the rms accelerations at the tractor's centre of gravity, while Figures 5.22 and 5.23 are three-dimensional plots of the rms vertical accelerations at the driver's location. These plots are obtained for the loaded vehicle operating on route A and route B, respectively, at 80 km/h. The rms accelerations are plotted in terms of

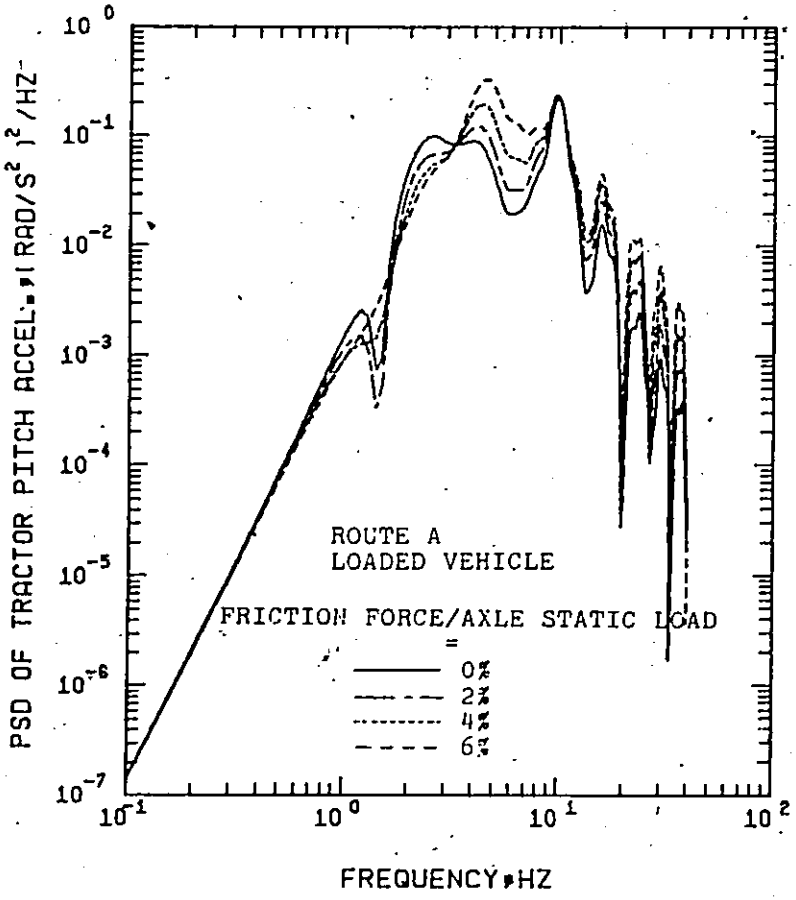

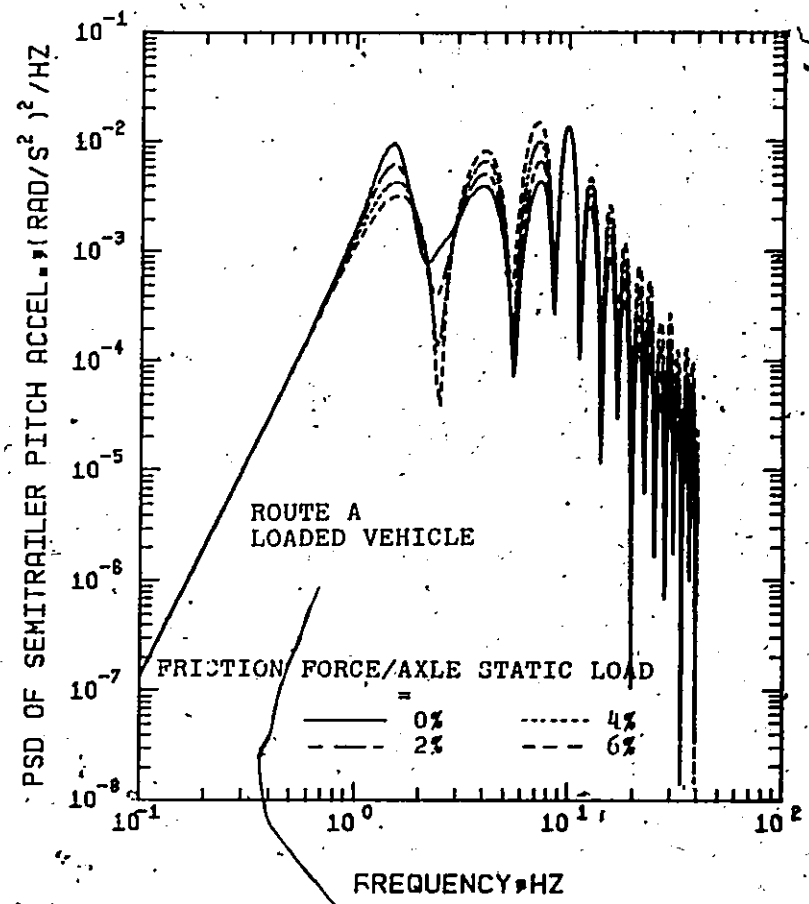

Figure 5.15 Effect of directly coupled friction damping on tractor and semitrailer pitch acceleration spectra - loaded vehicle, smooth road.

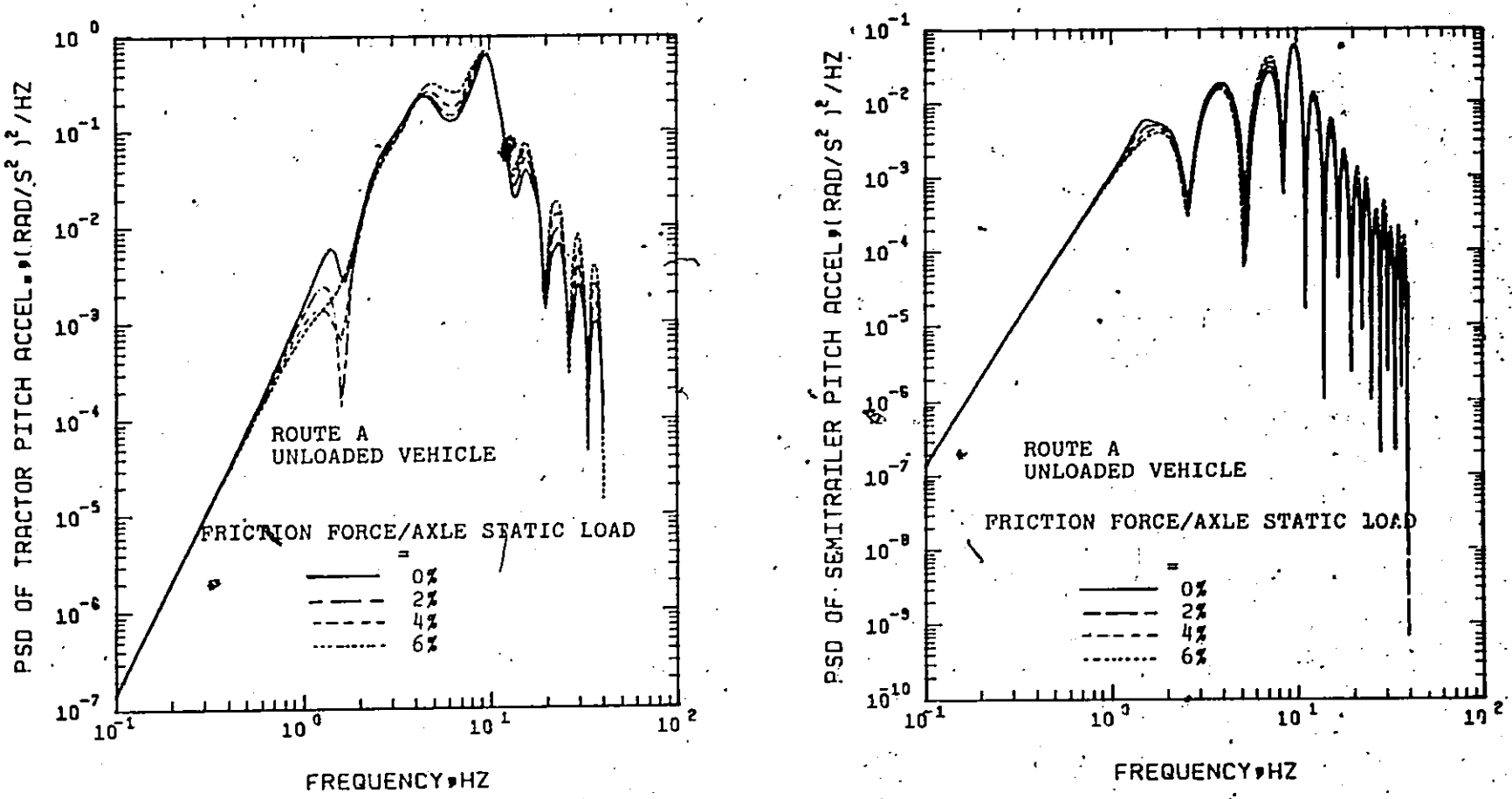

Figure 5.16 Effect of directly coupled friction damping on tractor and semitrailer pitch acceleration spectra - unloaded vehicle, smooth road.

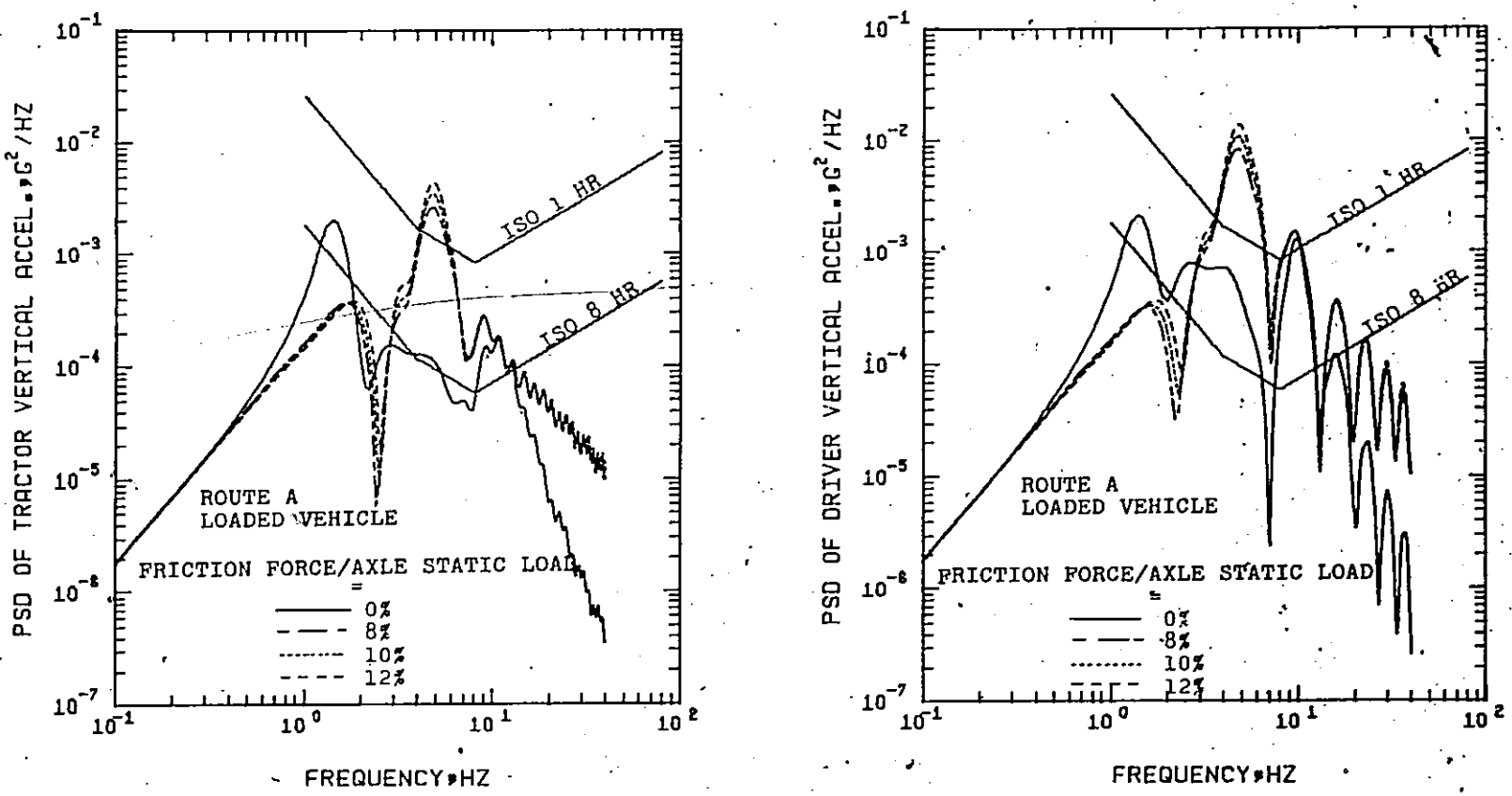

Figure 5.17 Effect of high values of directly coupled friction damping on tractor and driver acceleration spectra - smooth road.

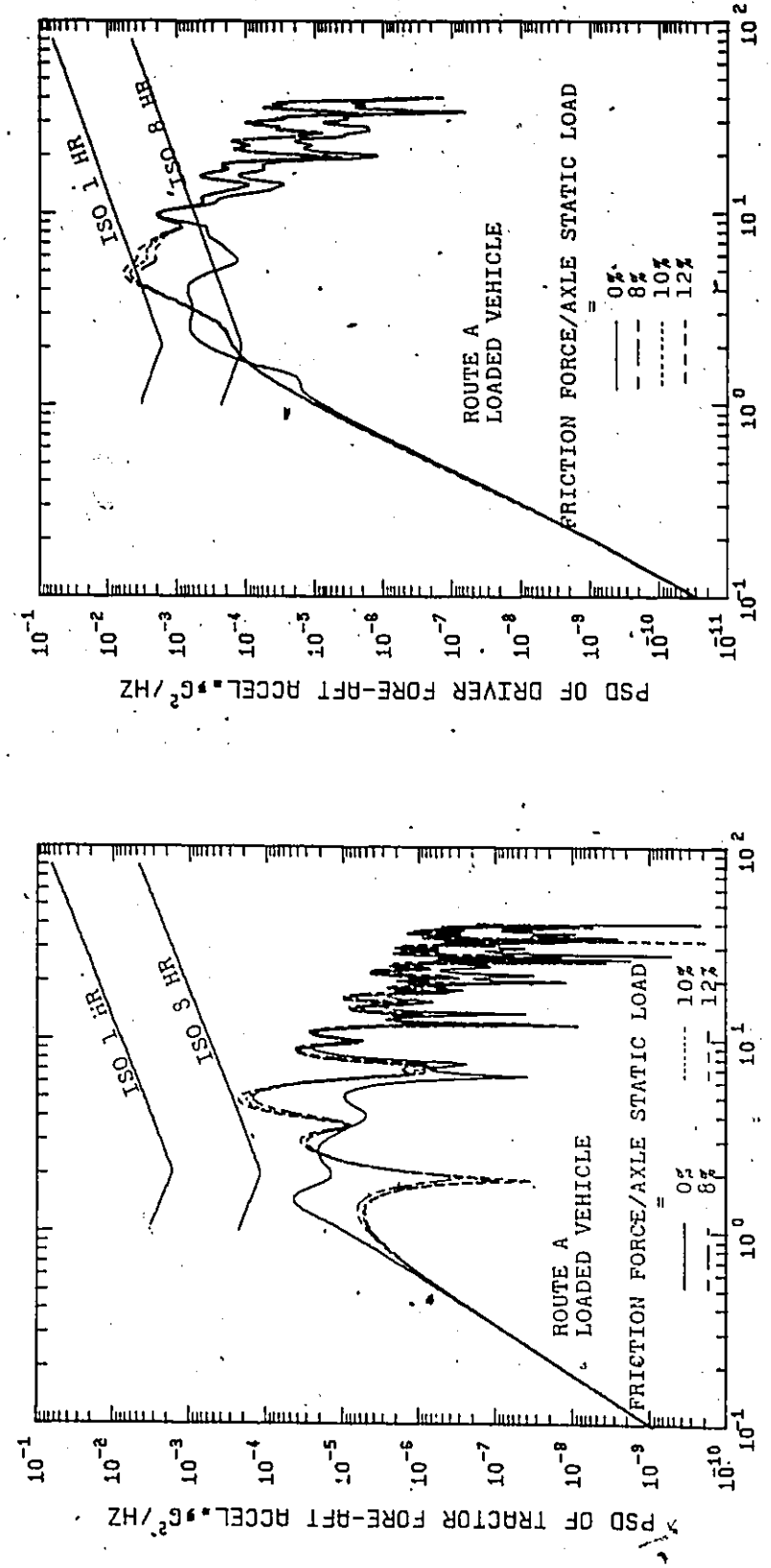

Figure 5.18 Effect of high values of directly coupled friction damping on tractor and driver fore and aft acceleration spectra - smooth road.

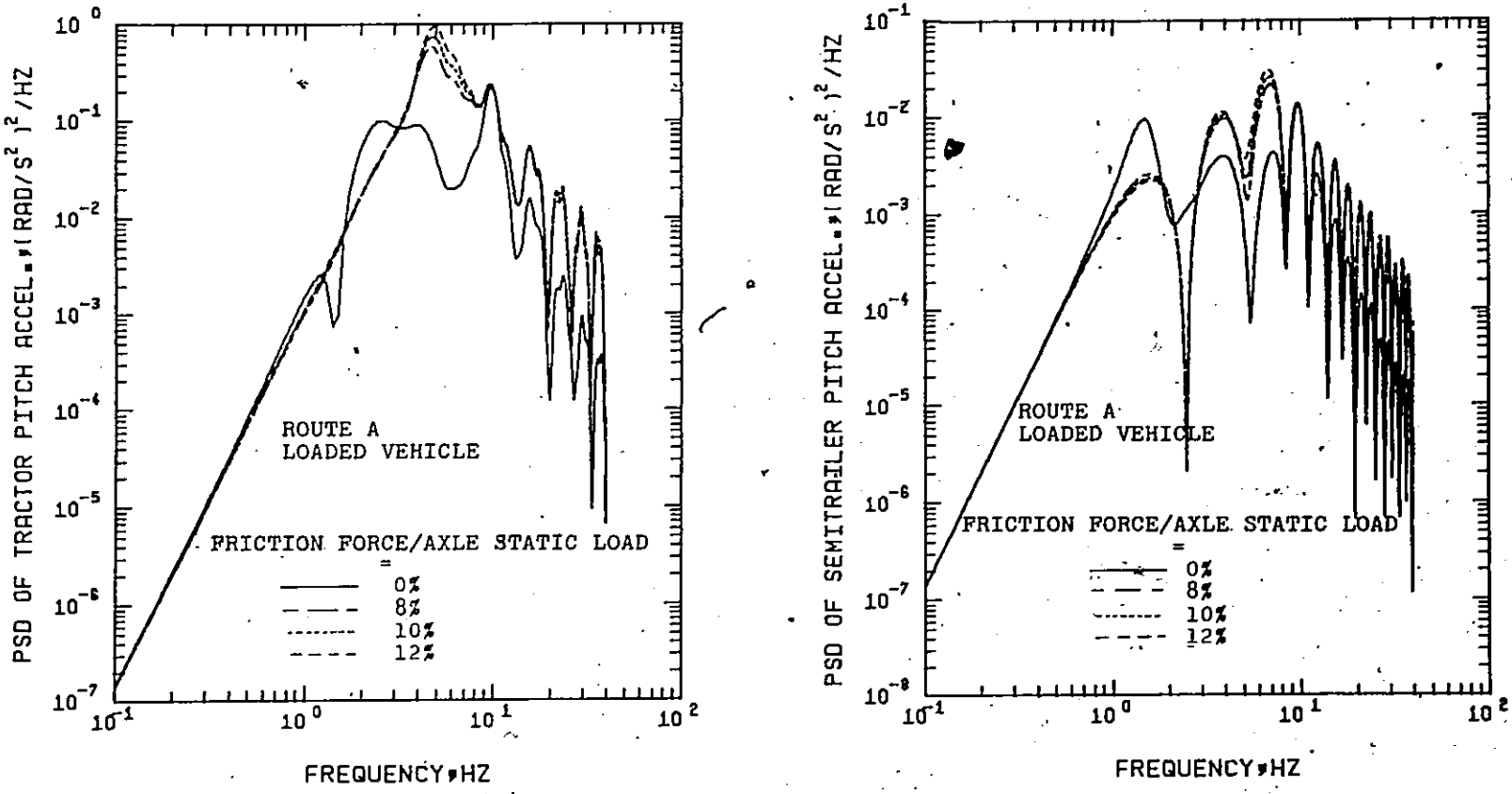

Figure 5.19 Effect of high values of directly coupled friction damping on tractor and semitrailer pitch acceleration spectra - smooth road.

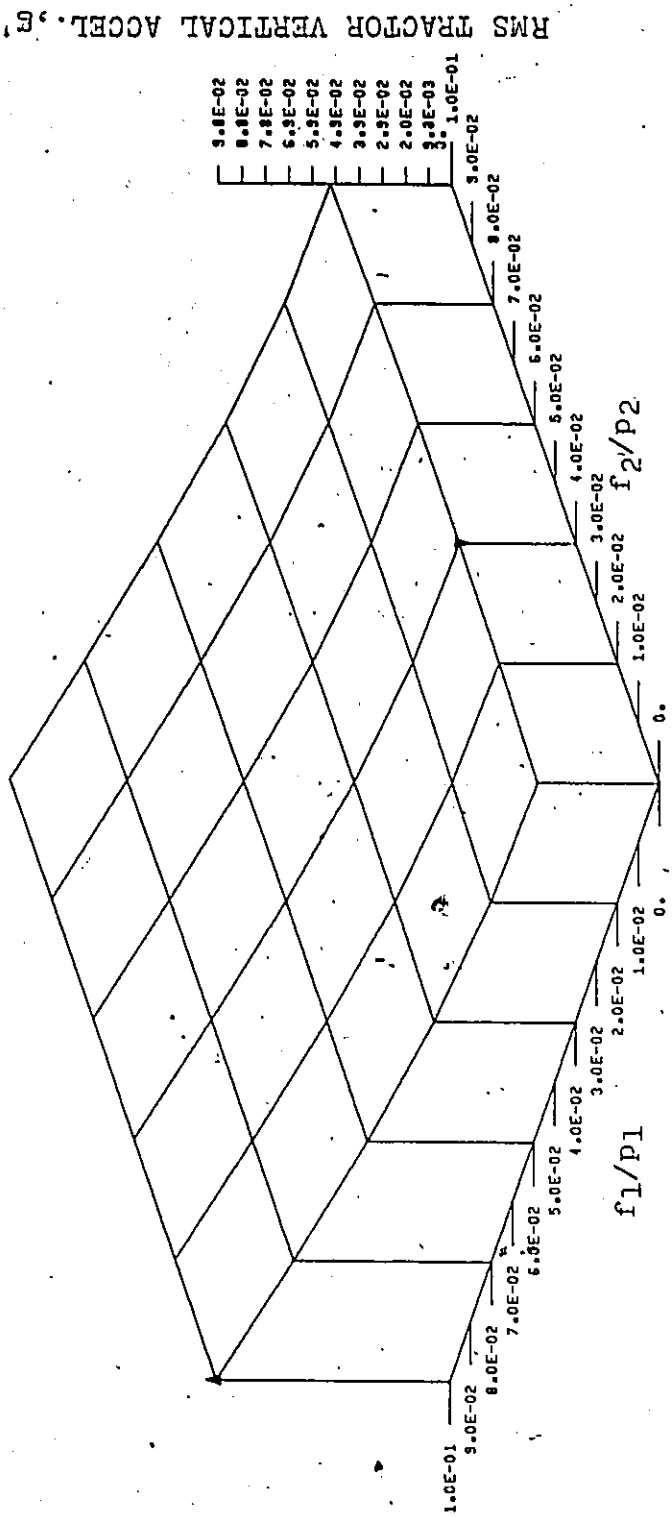

Figure 5.20 Effect of tractor front and rear dry friction dampings on rms tractor vertical acceleration - loaded vehicle, smooth road.

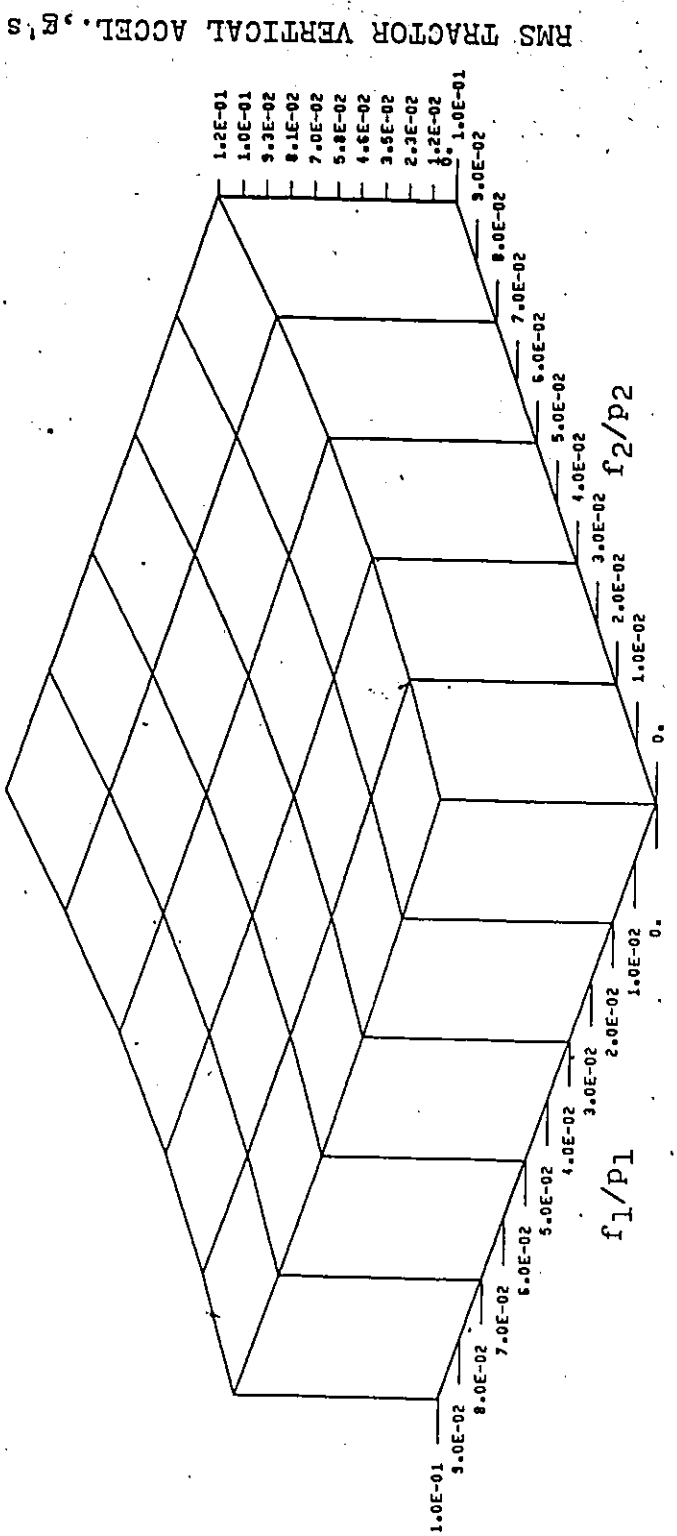

Figure 5.21 Effect of tractor front and rear dry friction dampings on rms tractor vertical acceleration - loaded vehicle, rough road.

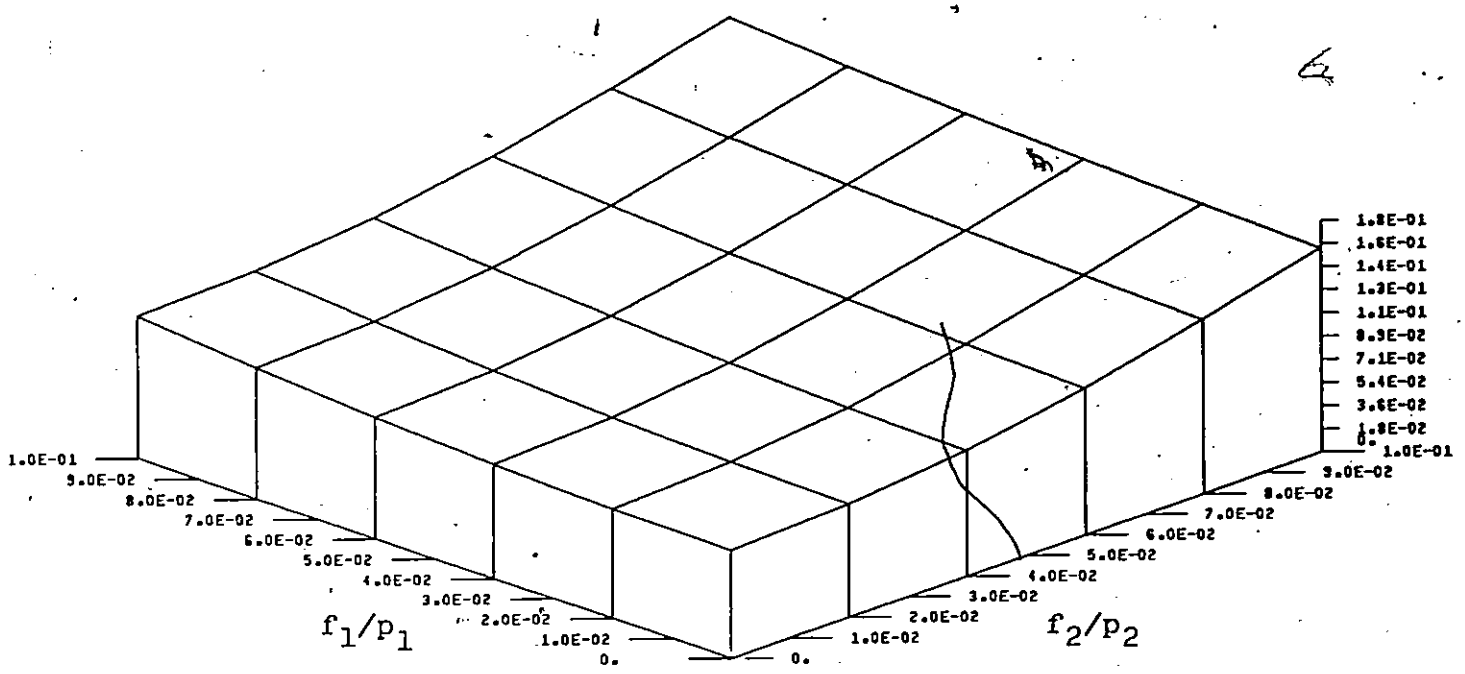

Figure 5.22 Effect of tractor front and rear dry friction dampings on rms driver vertical acceleration - loaded vehicle, smooth road.

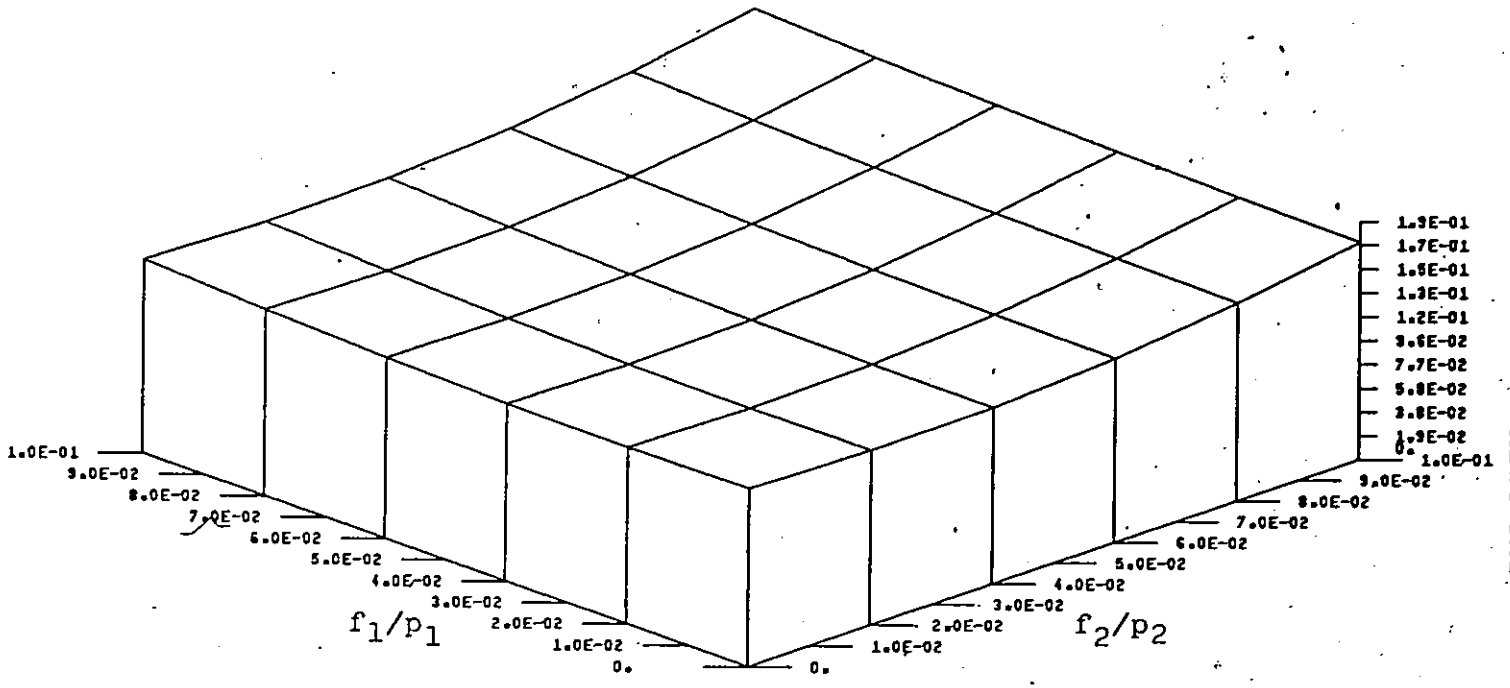

Figure 5.23 Effect of tractor front and rear dry friction dampings on rms driver vertical acceleration - loaded vehicle, rough road.

the ratio of the dry frictional forces of each axle to the corresponding axle static loads. From a study of the plots it may be concluded that the dry friction damping in vehicle suspension is not unidirectional. The dry friction damping improves the ride comfort expressed in rms acceleration up to a certain extent. The optimum friction damping is different for different roads and different locations in the vehicle structure. In the case of a smooth road, the optimum values of dry friction are zero at the tractor's front axle and 4% of the static load at the tractor's rear axle for the rms acceleration at the tractor's centre of gravity. The corresponding values for the vehicle operating on the rough road are 4% of the static load at the front axle and 2% of the static load at the rear axle. The rms driver vertical acceleration are minimum for frictional forces of zero values at the front and rear axles for the smooth road, and 2% of the static loads at the front and rear axles for rough road.

The difference in the optimum values of the frictional forces that provide minimum values of the rms accelerations at the tractor's centre of gravity and at the driver's position is due to the tractor's pitching acceleration which is increased with increasing the dry friction dampings independently of the road quality, Figures 5.24 and 5.25. Beyond the optimum values of the frictional forces, increasing frictional forces will increase the rms accelerations and consequently decrease the comfort level.

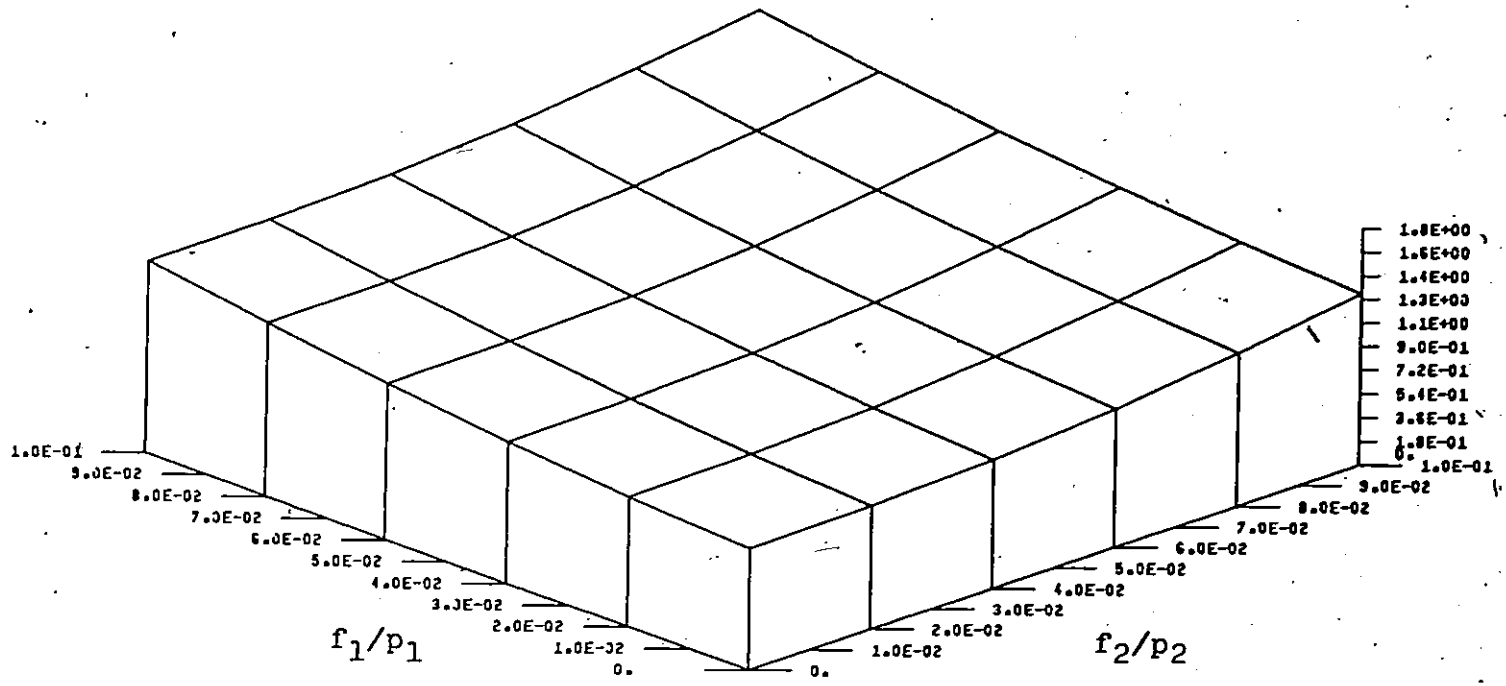

Figure 5.24 Effect of tractor front and rear dry friction dampings on rms tractor pitch acceleration - loaded vehicle, smooth road.

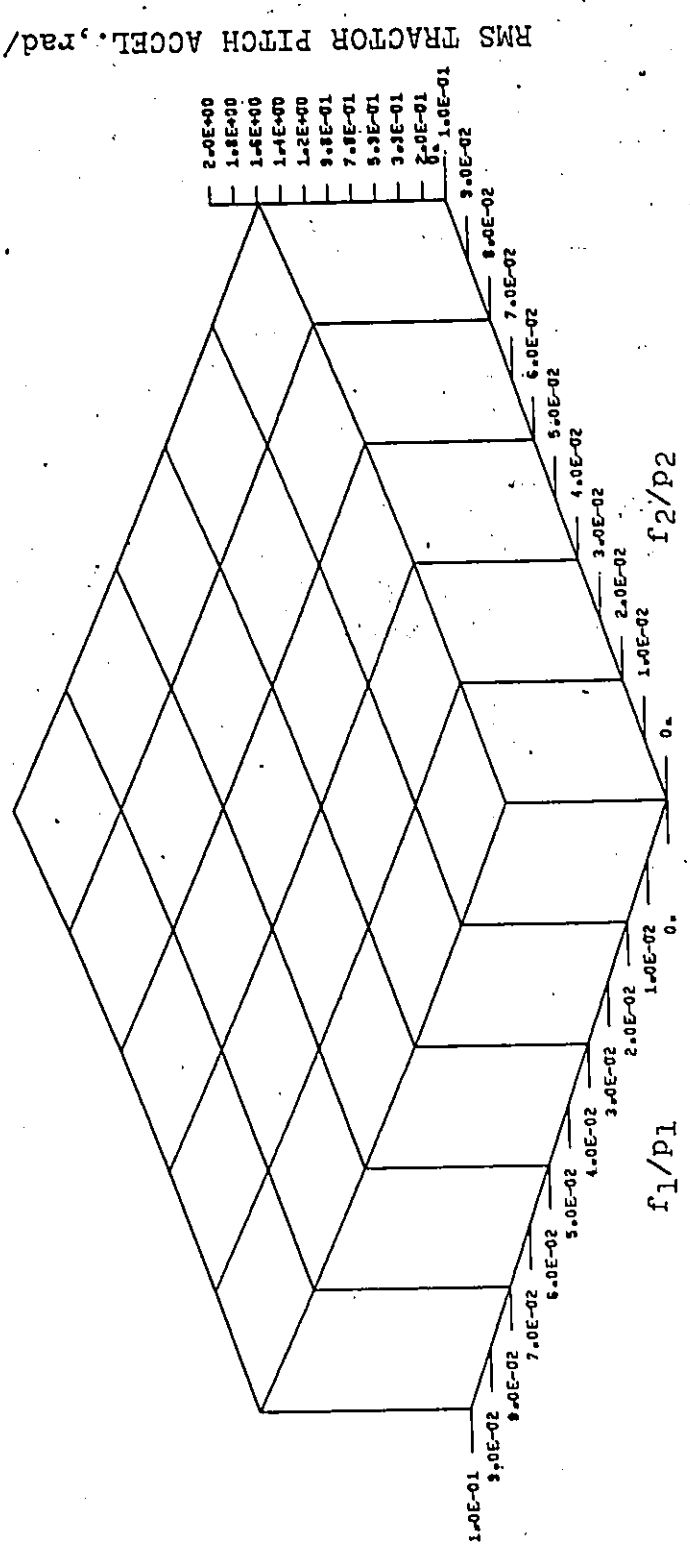

Figure 5.25 Effect of tractor front and rear dry friction dampings on rms tractor pitch acceleration - loaded vehicle, rough road.

Figures 5.26 and 5.27 present three-dimensional plots of the rms tractor and driver vertical accelerations, respectively, for the unloaded vehicle operating on route A at 80 km/h, in terms of the frictional forces at the front and rear suspension. By comparing Figures 5.26 and 5.27 with Figures 5.20 and 5.22, respectively, it can be stated that the optimum frictional forces are different for varying loading conditions.

The optimum values of the frictional forces are also different for various vehicle velocities, as can be seen from Figure 5.28 which gives the rms tractor acceleration for the loaded vehicle running on route B at 120 km/h. The optimum values of dry friction are 6% of the static load at the tractor's front axle and 8% of the static load at the tractor's rear axle. It can also be seen that the rms accelerations increase with increasing the vehicle's forward velocity regardless of the amounts of dry friction.

Axle Dynamic Excursion: Axle dynamic excursion or dynamic spring deflection is the relative motion between the sprung and unsprung masses. This dynamic excursion plays an important role in determining the clearance space between the sprung and unsprung masses. It is desirable to make the clearance space as small as possible from a volume economy point of view and to minimize rolling and pitching movements arising from vehicle manoeuvers. On the other hand, it is necessary to provide enough clearance for static deflections due to vehicle loading variations and for dynamic spring deflections arising from vehicle motion on an uneven road.

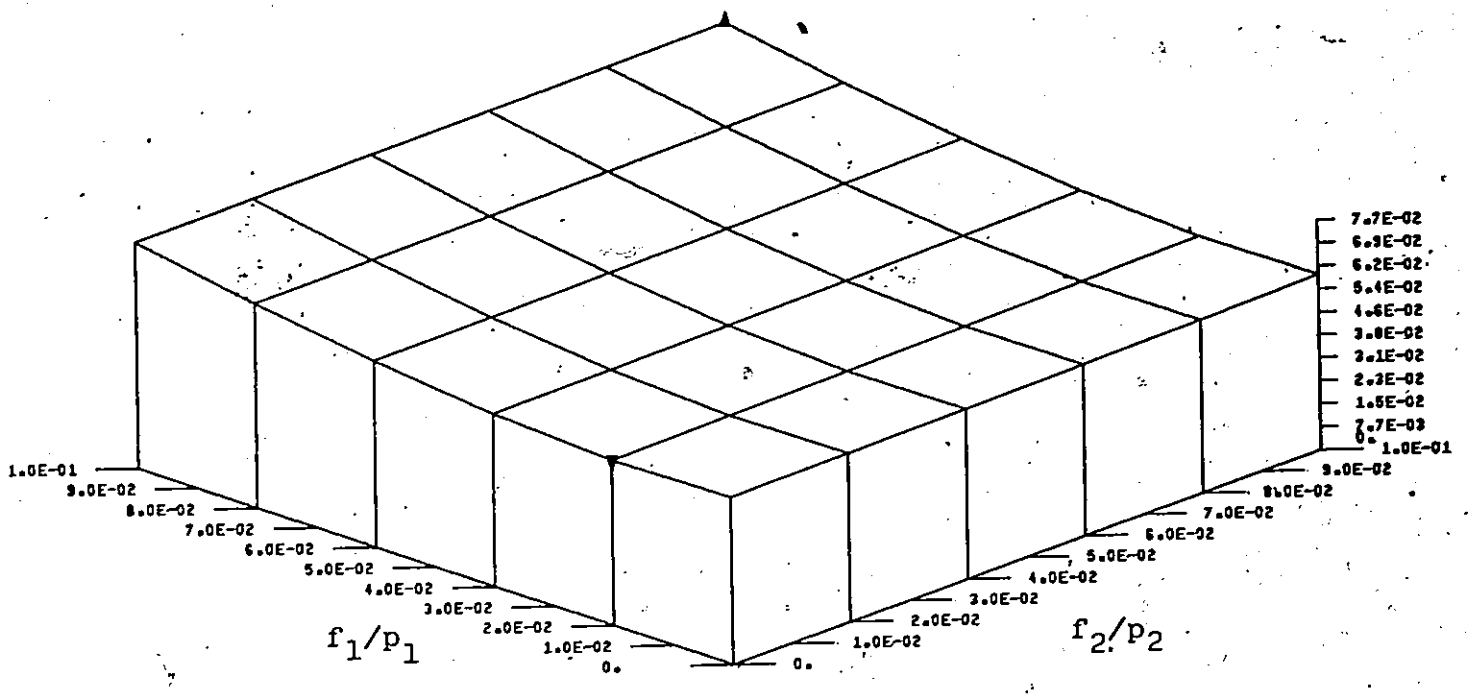

Figure 5.26 Effect of tractor front and rear dry friction dampings on rms tractor vertical acceleration - unloaded vehicle, smooth road.

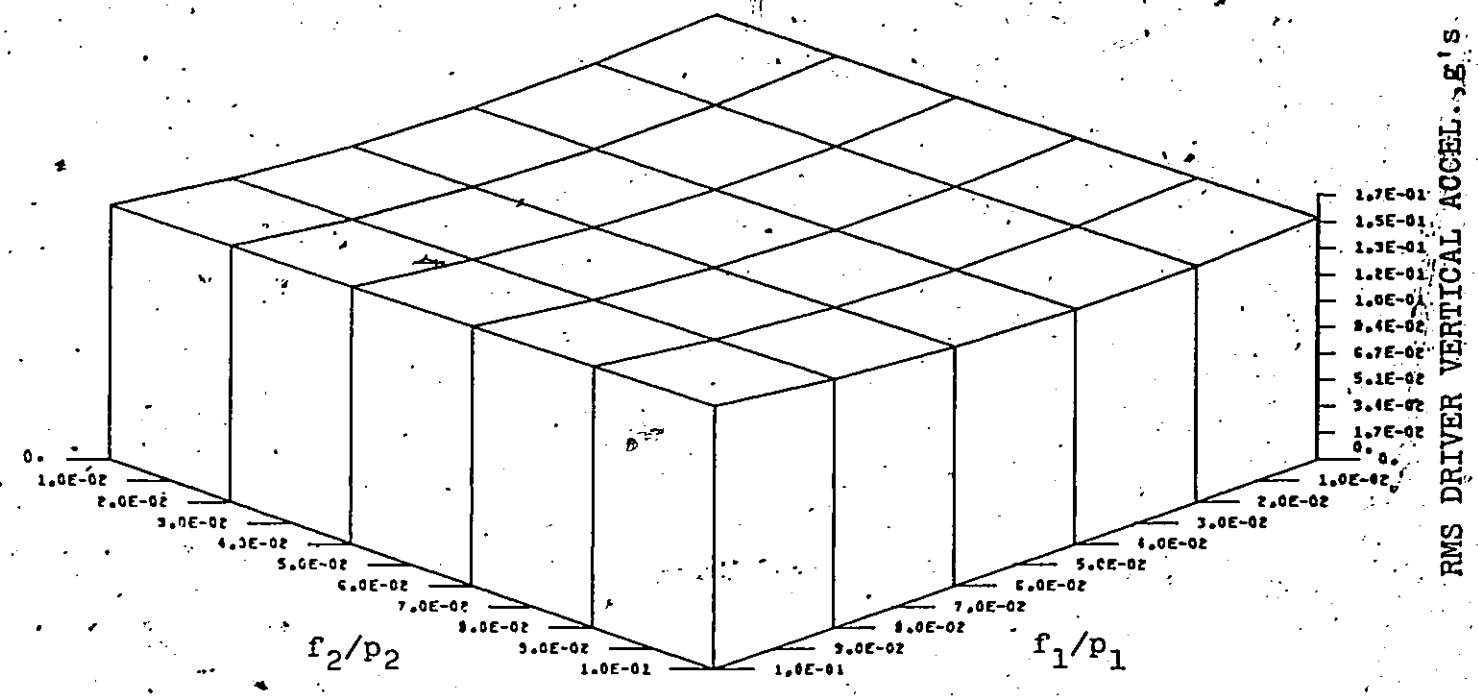

Figure 5.27 Effect of tractor front and rear dry friction dampings on rms driver vertical acceleration - unloaded vehicle, rough road.

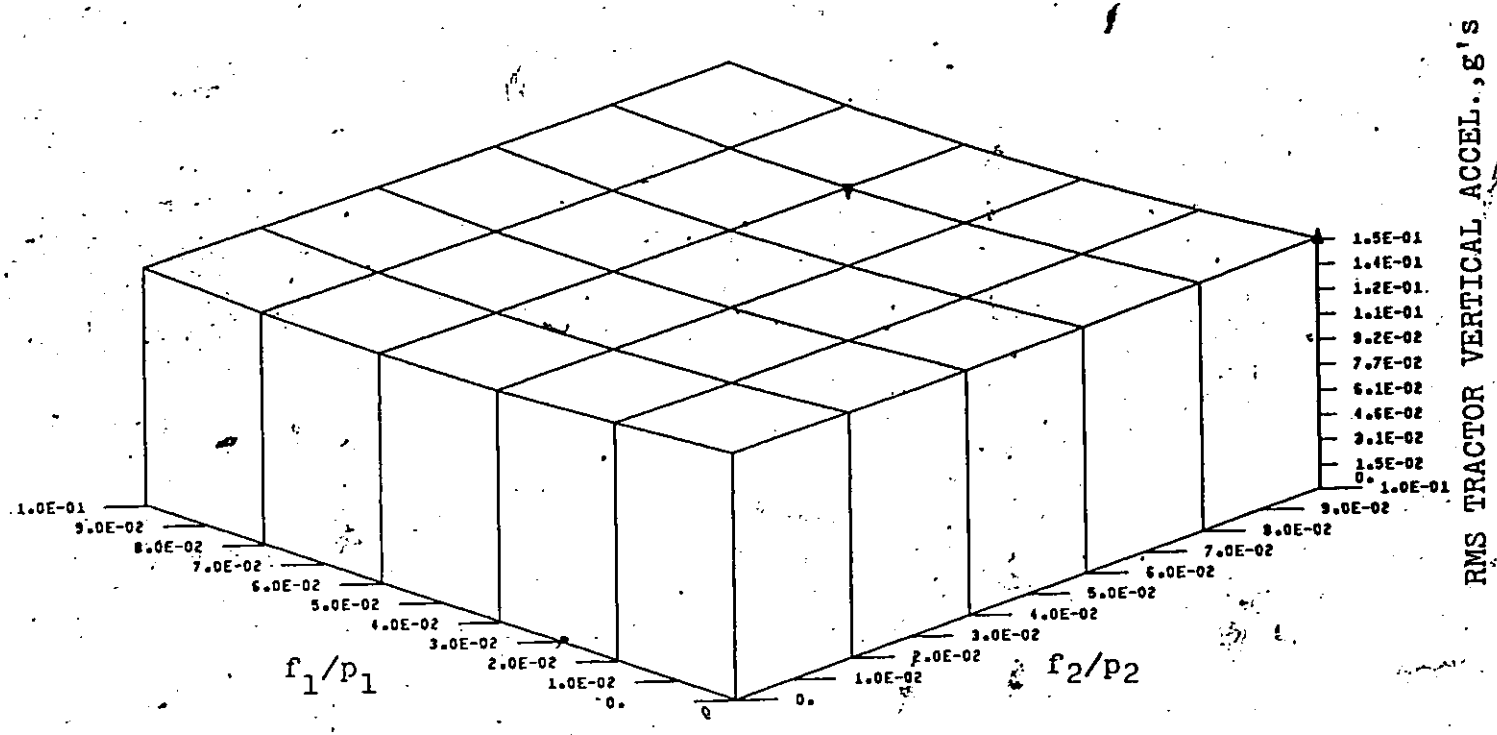

Figure 5.28 Effect of tractor front and rear dry friction dampings on rms tractor vertical acceleration - loaded vehicle, rough road and vehicle speed of 120 km/h.

The power spectral densities of the dynamic excursions for the front and rear axles of the tractor are given in Figures 5.29 - 5.31. These spectra are obtained for loaded and unloaded vehicle running on route A, Figures 5.29 and 5.30, respectively, and for loaded vehicle running on route B, Figure 5.31, with different values of friction forces. The results indicate that as the friction is increased axle dynamic excursion will be decreased in the whole frequency range. The results also indicate that some amount of friction in the suspension is effective in reducing the probability of bottoming between the sprung mass and the unsprung mass.

The rms values of the dynamic excursion have been calculated for loaded and unloaded vehicle running on smooth road at 80 km/h. The results for the tractor front axle are plotted in Figures 5.32 and 5.33 in terms of the frictional forces at the front and rear suspensions. It can be inferred from the figures that the rms dynamic excursion is decreased with increasing the frictional forces. It can also be inferred that the dynamic excursion at the front axle is not sensitive to changes in the frictional forces at the tractor rear suspensions.

Dynamic Wheel Loads: The power spectral densities of the ratio of the dynamic wheel loads to the static wheel loads are plotted in Figures 5.34 - 5.36. These plots represent both front and rear wheels of the tractor at various amounts of dry friction for loaded and unloaded vehicle operating on route A, and for loaded vehicle operating on route B. The effect of including the friction forces in the dynamic

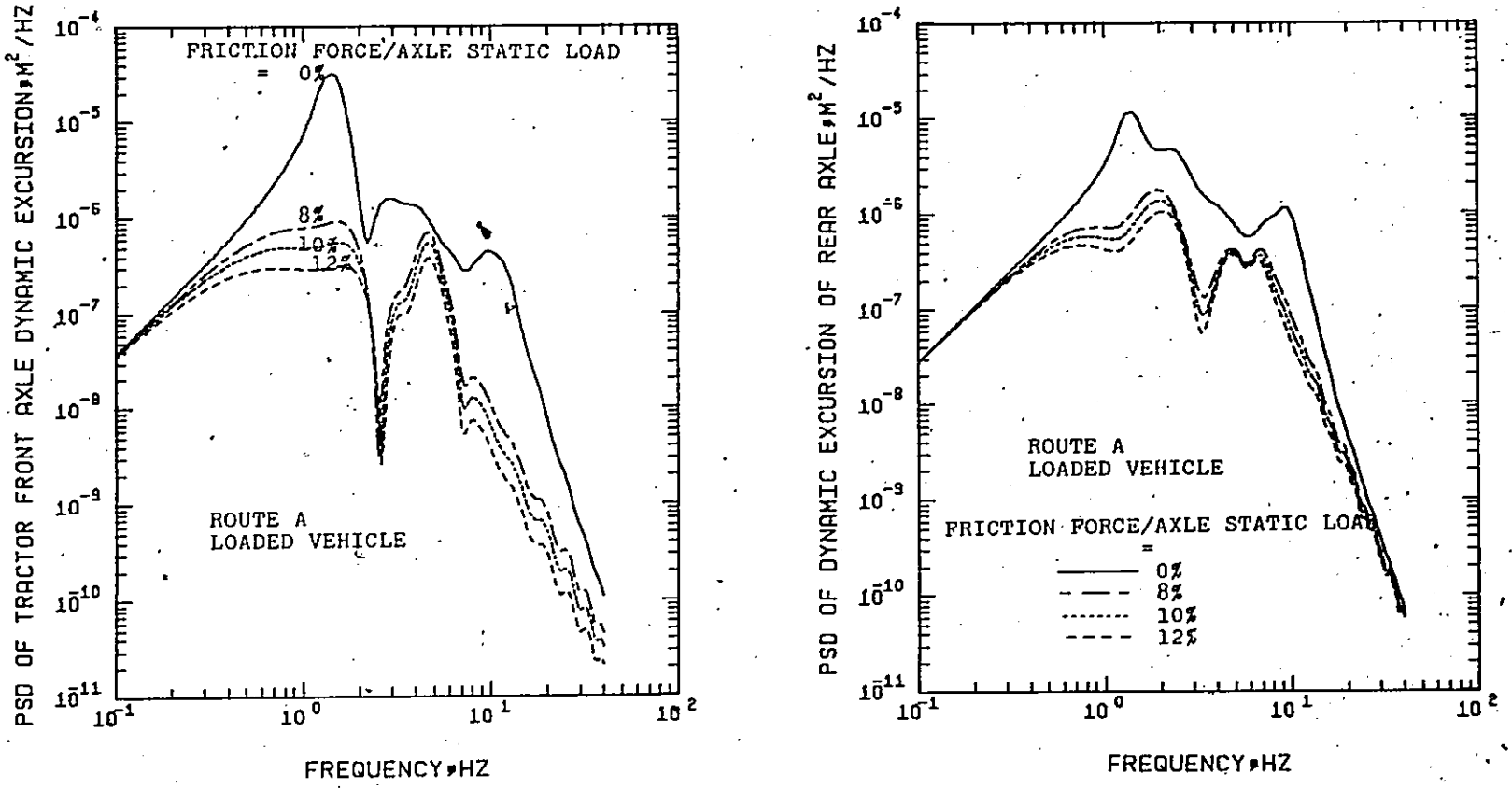

Figure 5.29 Effect of directly coupled friction damping on tractor front and rear axle dynamic excursion spectra - loaded vehicle, smooth road.

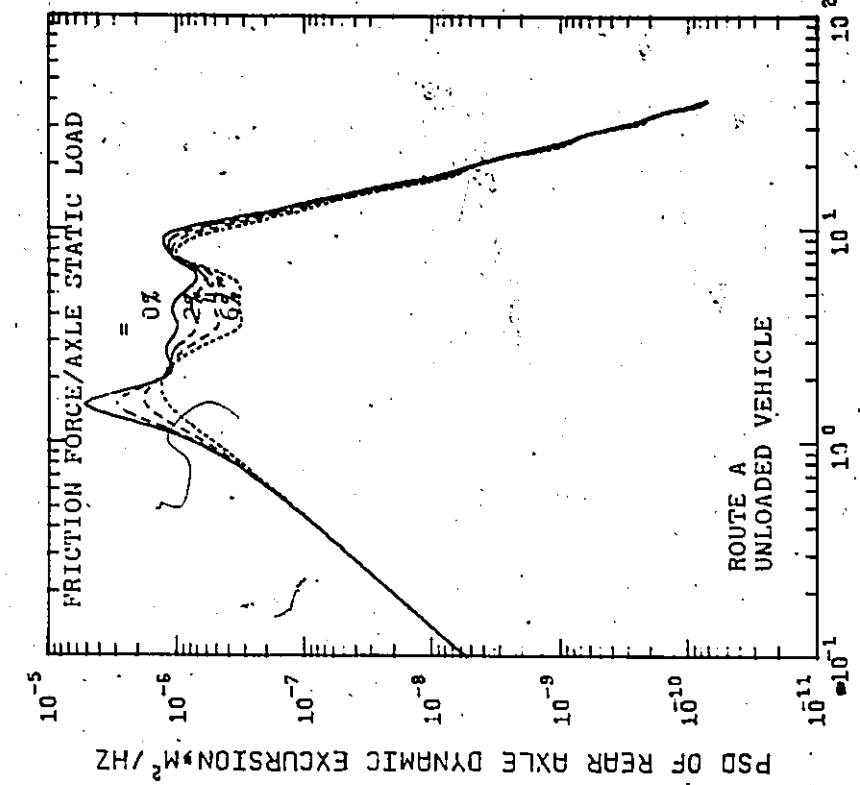

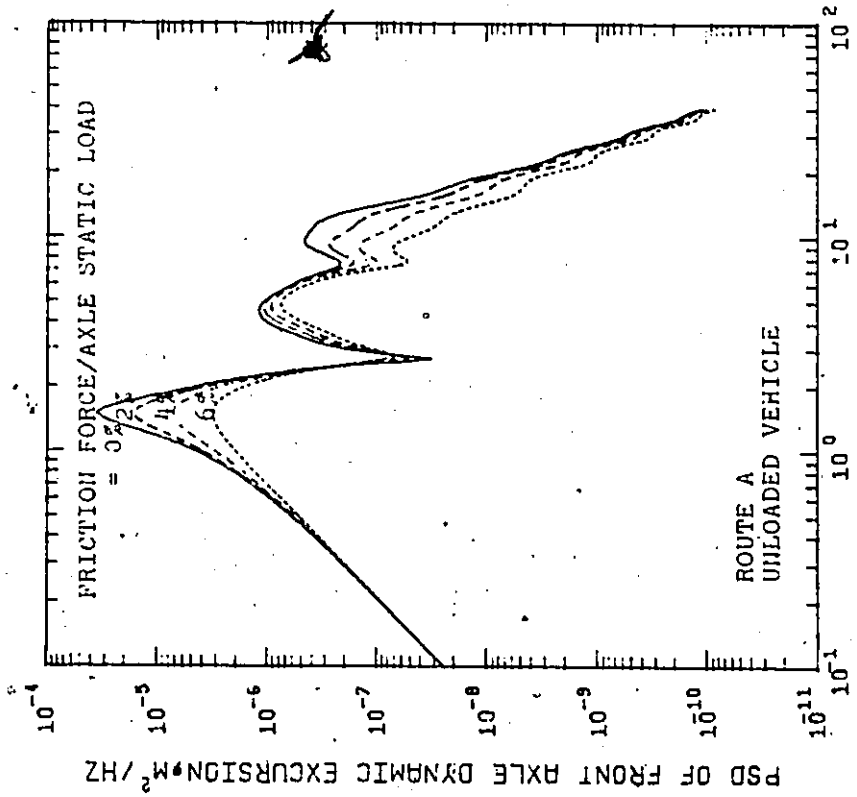

Figure 5.30 Effect of directly coupled friction damping on tractor front and rear axle excursion spectra - unloaded vehicle, smooth road.

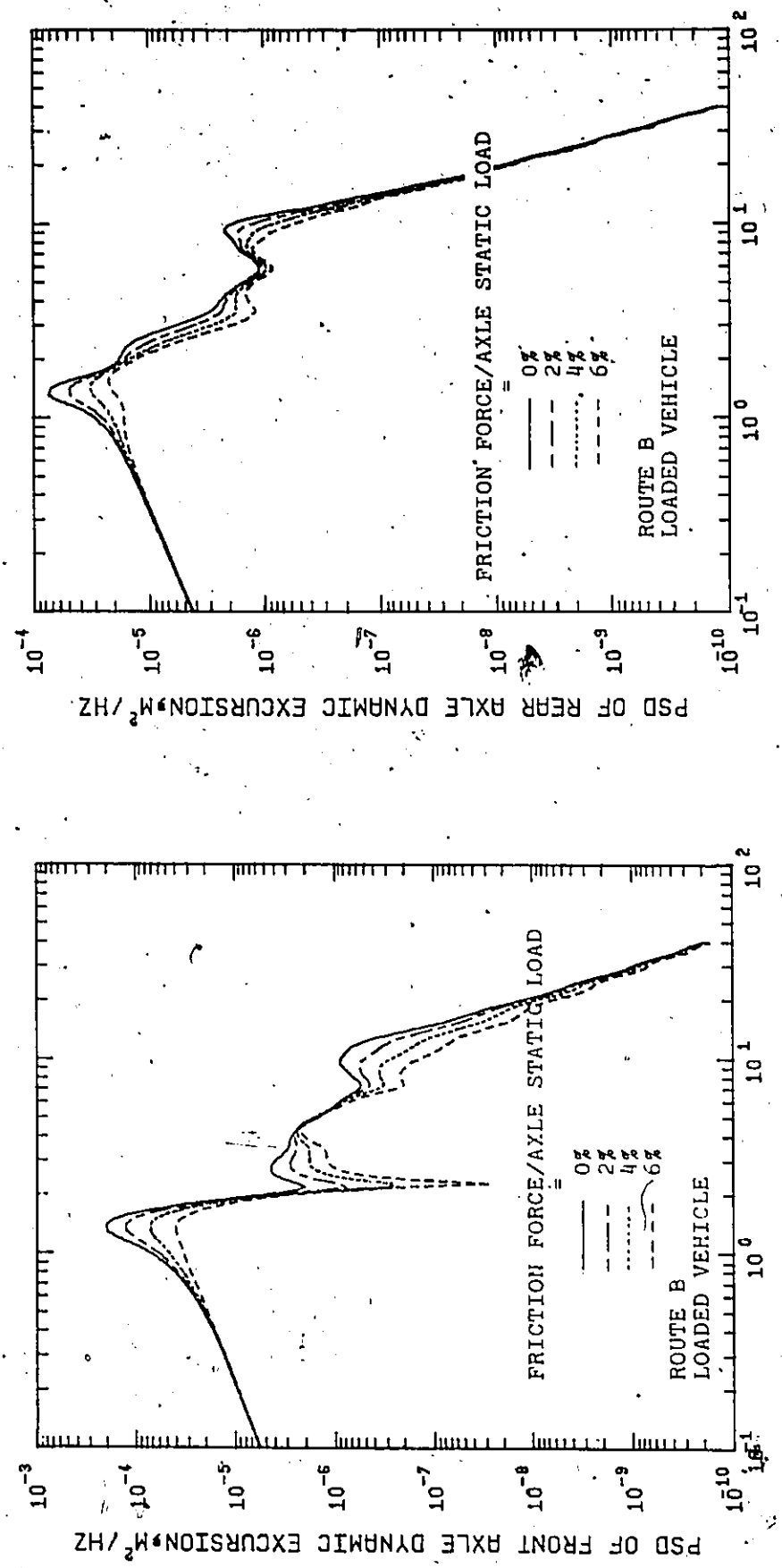

Figure 5.31 Effect of directly coupled friction damping on tractor front and rear axle excursion spectra - loaded vehicle, rough road.

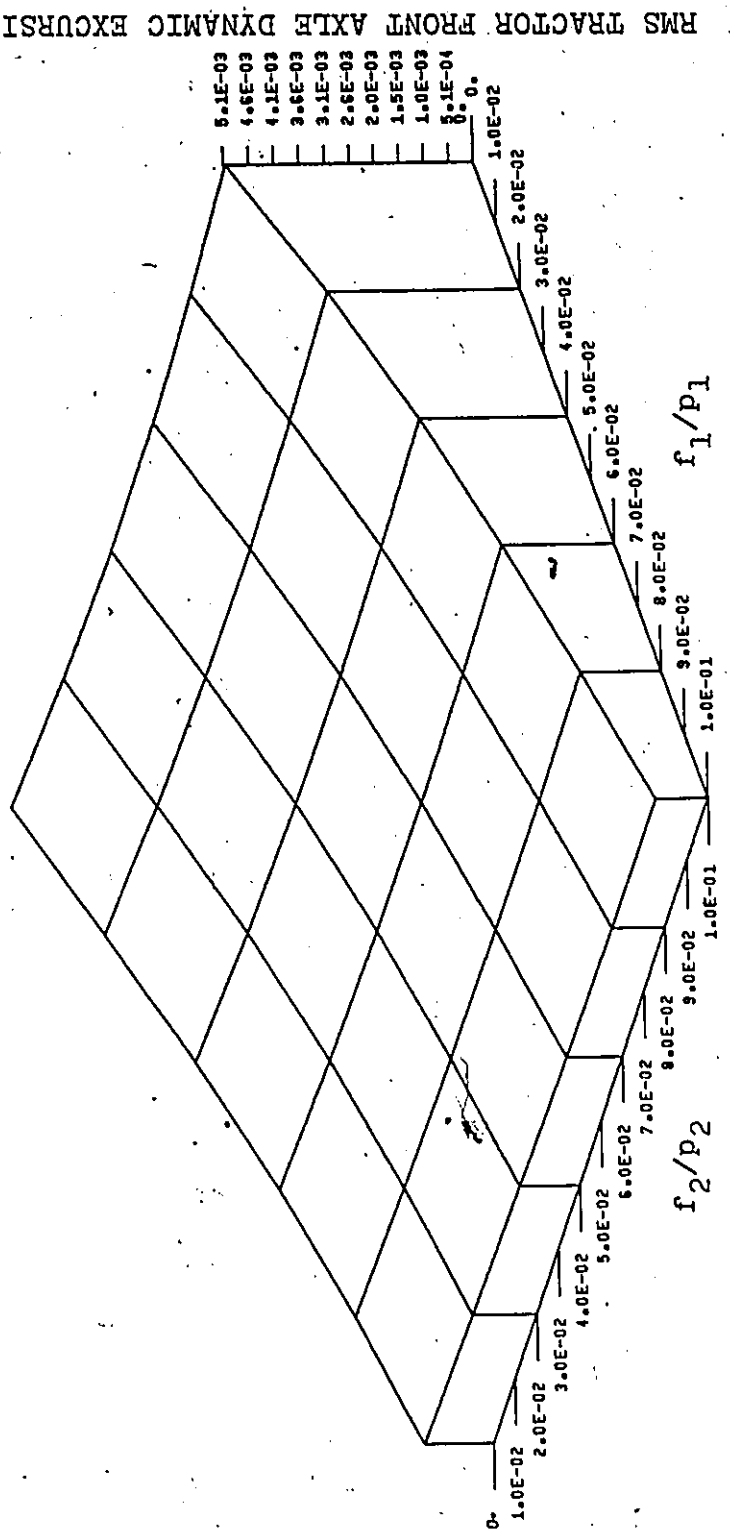

Figure 5.32 Effect of tractor front and rear dry friction dampings on rms tractor front axle dynamic excursion - loaded vehicle, smooth road.

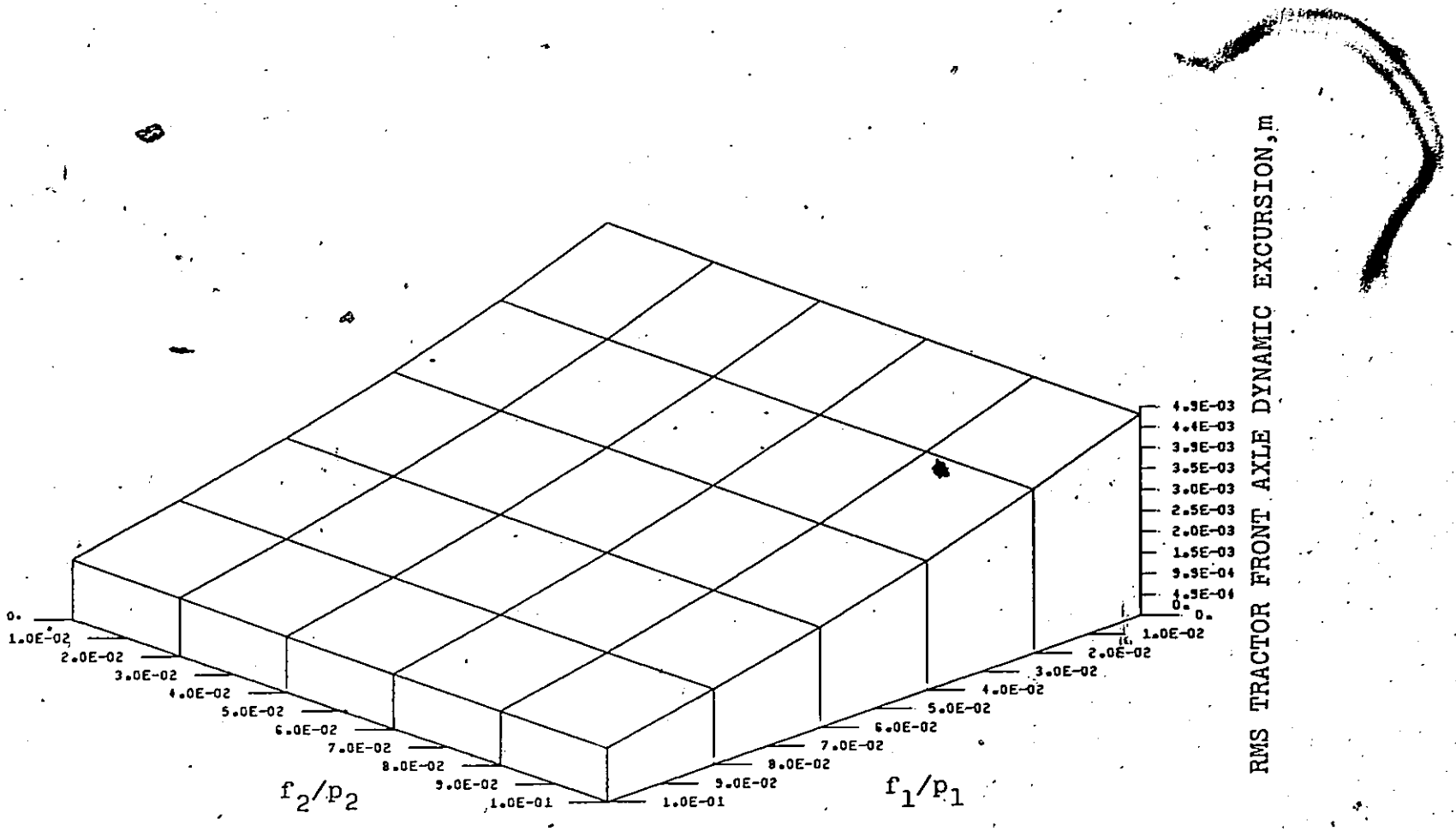

Figure 5.33 Effect of tractor front and rear dry friction dampings on rms tractor front axle dynamic excursion - unloaded vehicle, smooth road.

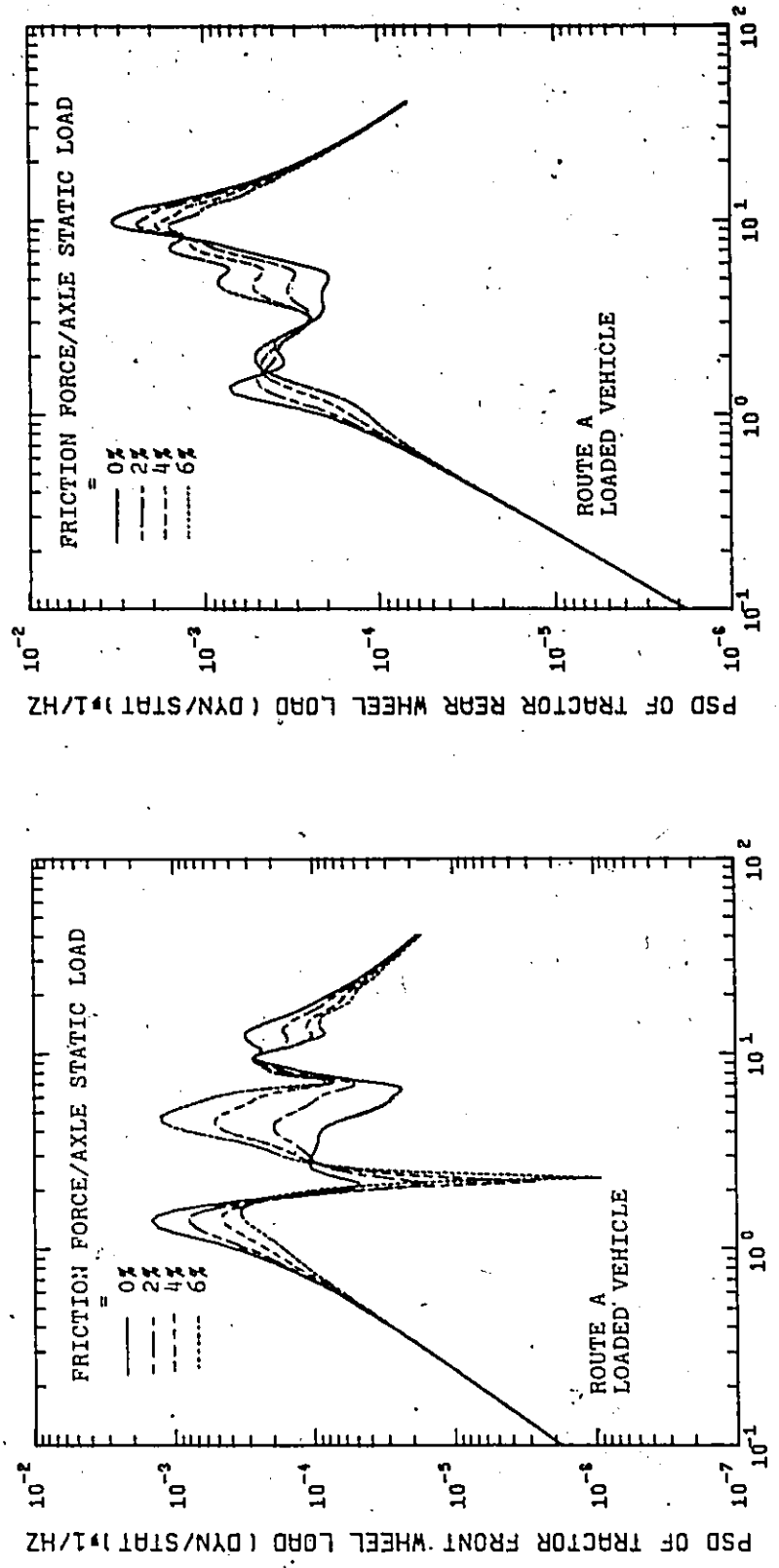

Figure 5.34 Effect of directly coupled friction damping on tractor front and rear wheel load spectra - loaded vehicle, smooth road.

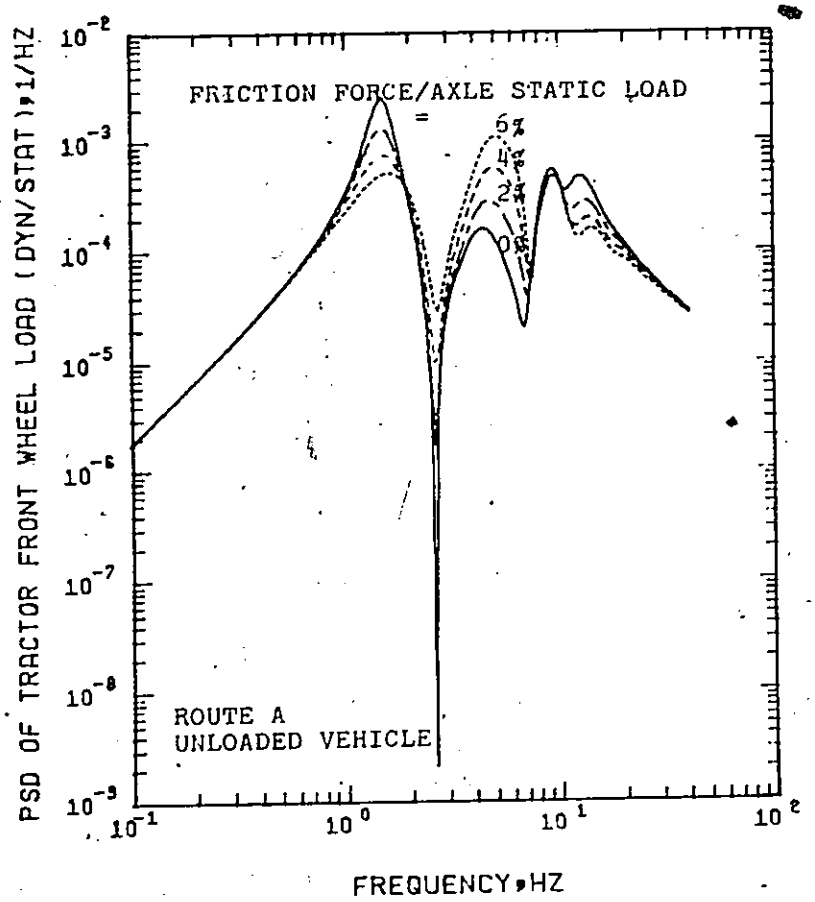

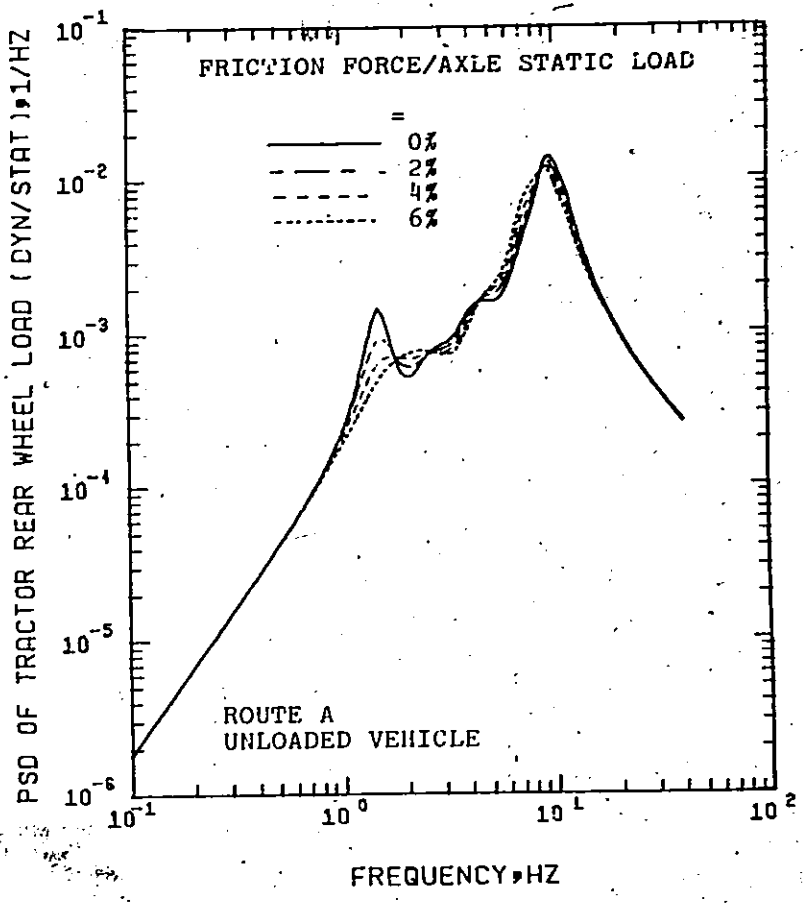

Figure 5.35 Effect of directly coupled friction damping on tractor front and rear wheel load spectra - unloaded vehicle, smooth road.

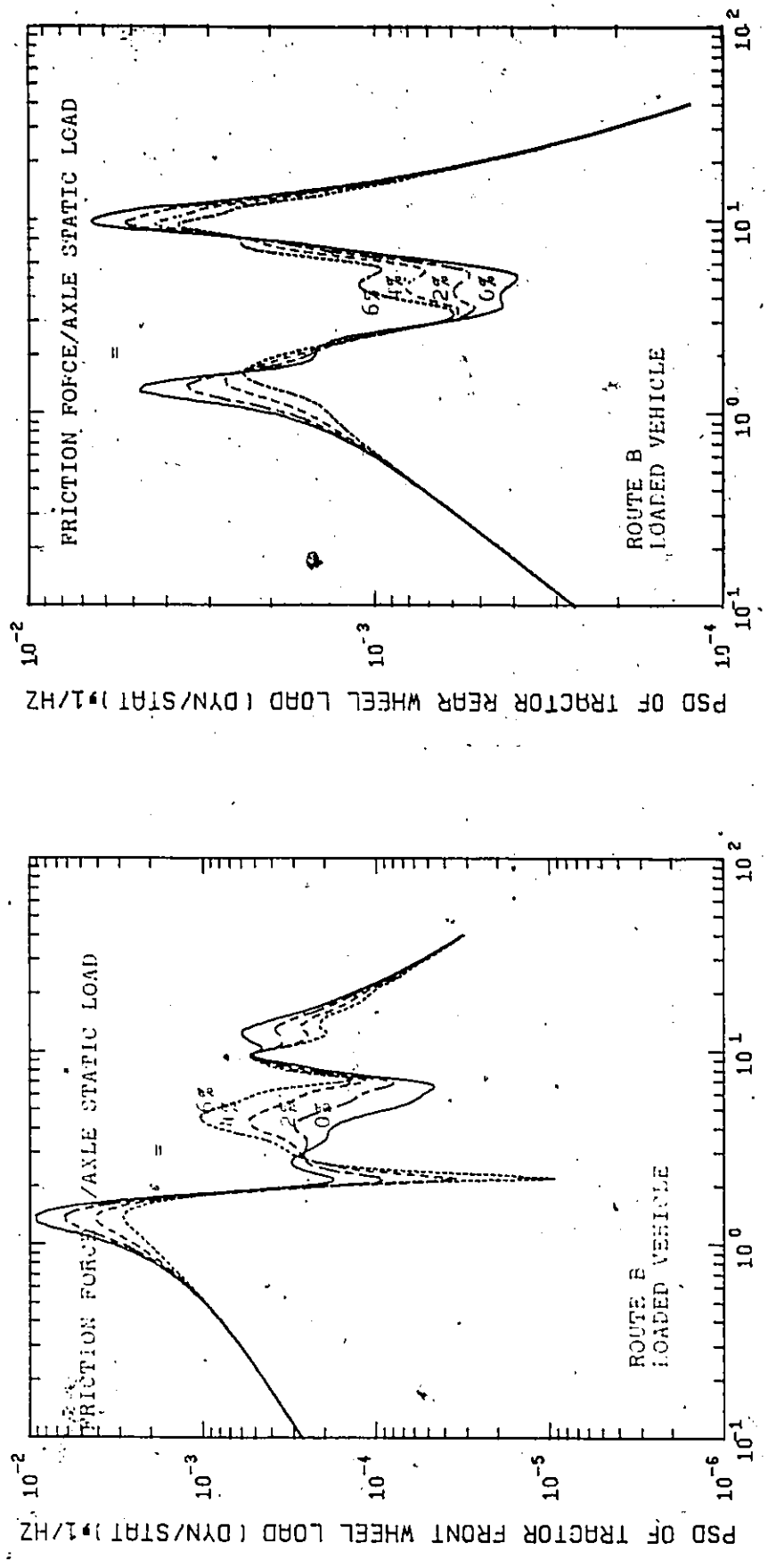

Figure 5.36 Effect of directly coupled friction damping on tractor front and rear wheel load spectra - loaded vehicle, rough road.

analysis reduces the peak dynamic loads in the low and high frequency ranges. In the medium frequency range 2 - 8 Hz the dynamic loads are increased as the friction forces are increased. This is due to the effect of the pitching modes. The values of the spectra for the unloaded vehicle are higher than the corresponding values for the loaded vehicle. It is apparent from these results that the unloaded vehicle has a greater tendency to lift its wheel off the road than does the loaded vehicle.

To provide a better insight into the effect of dry friction damping on the dynamic wheel loads, the ratio of the rms dynamic front and rear wheel loads to their static loads is computed and plotted by varying the frictional forces at the tractor's front end rear suspension. This ratio can be used as a criterion for the contact between the wheel and the road. Low values of this ratio mean that the wheel load fluctuation is not important. However, as the ratio increases then the wheel begins to lose its contact with the road.

Figures 5.37 and 5.38 give the front wheel load ratio for loaded and unloaded vehicles, respectively, operating on a smooth road at 80 km/h. Figures 5.39 and 5.40 give the rear wheel load ratio for loaded and unloaded vehicles, respectively, operating on a rough road at 80 km/h. From the plots shown in Figures 5.37 - 5.40, it may be concluded that for the unloaded vehicle the danger of departure of the wheel from the road is higher than with the loaded vehicle. The increased safety of the loaded vehicle is principally due to the increase in static load.

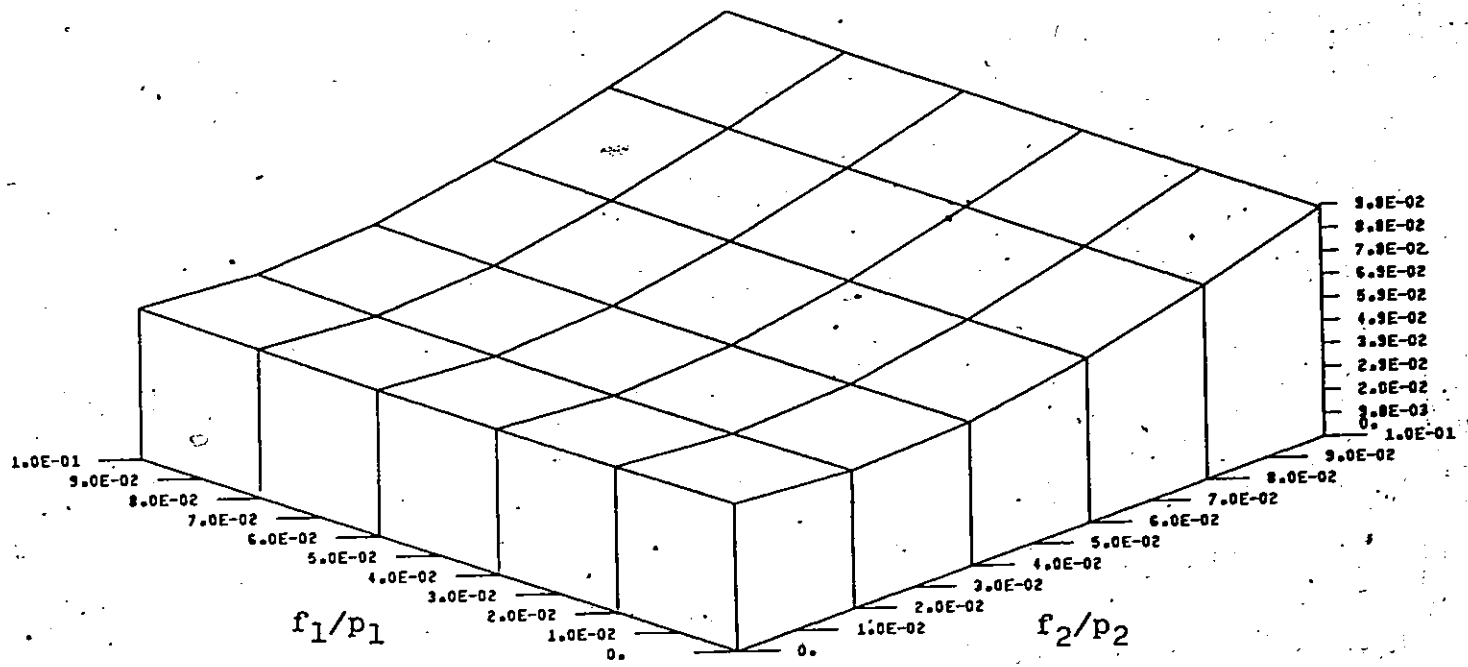

Figure 5.37 Effect of tractor front and rear dry friction dampings on rms tractor front wheel load - loaded vehicle, smooth road.

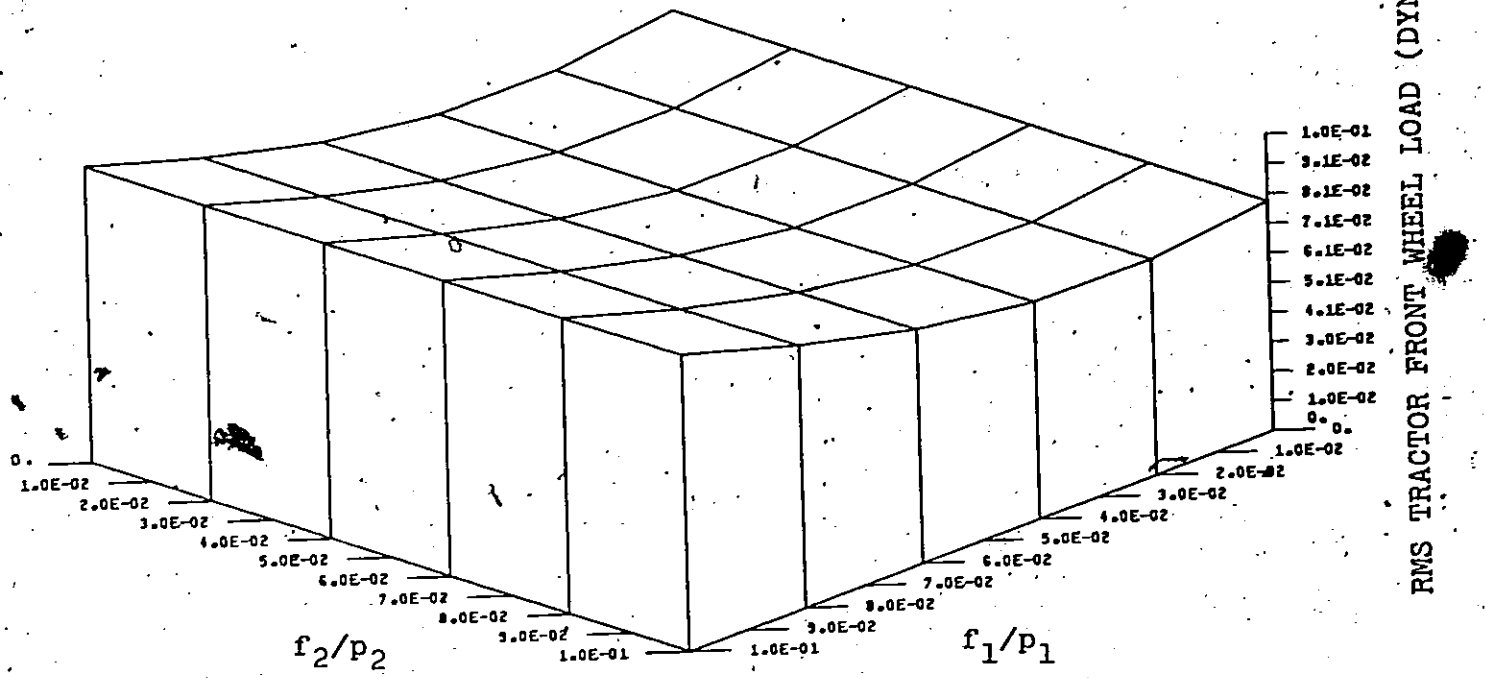

Figure 5.38 Effect of tractor front and rear dry friction dampings on rms tractor front wheel load - unloaded vehicle, smooth road.

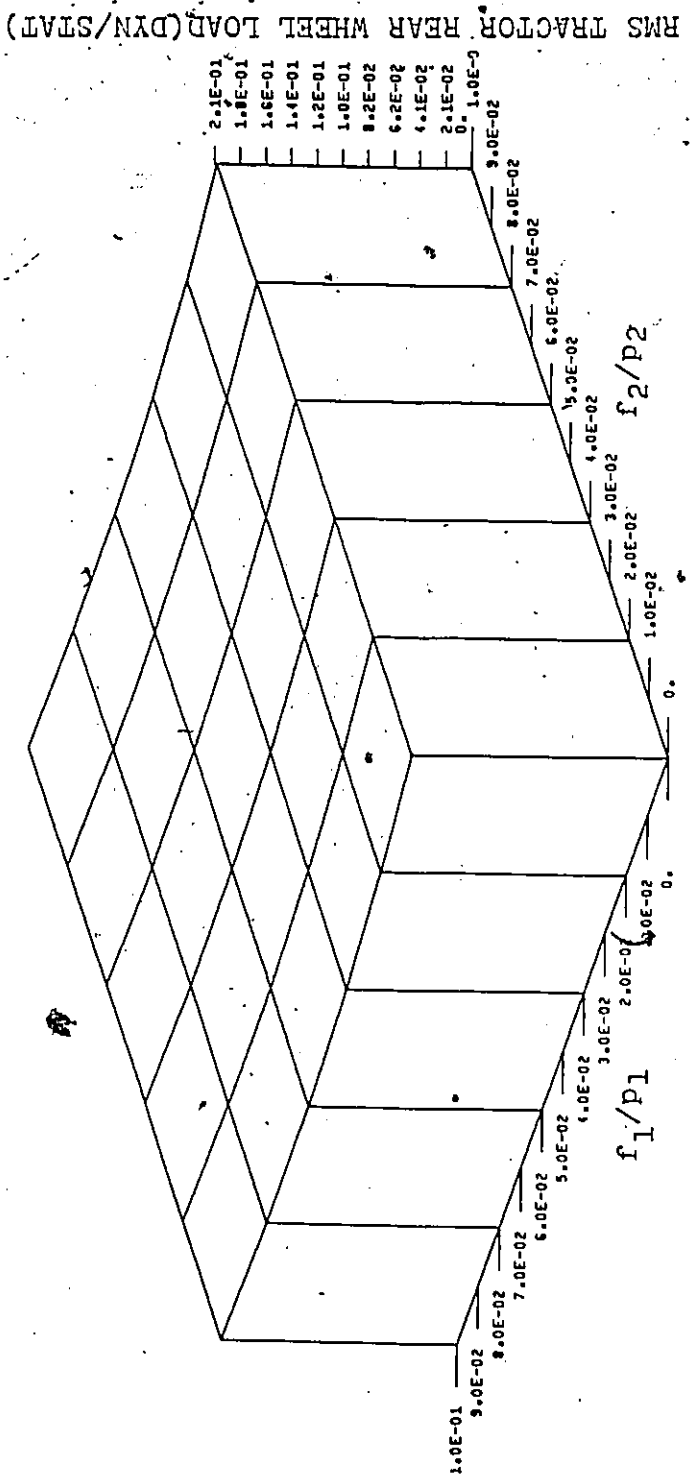

Figure 5.39 Effect of tractor front and rear dry friction dampings on rms tractor rear wheel load - loaded vehicle, rough road.

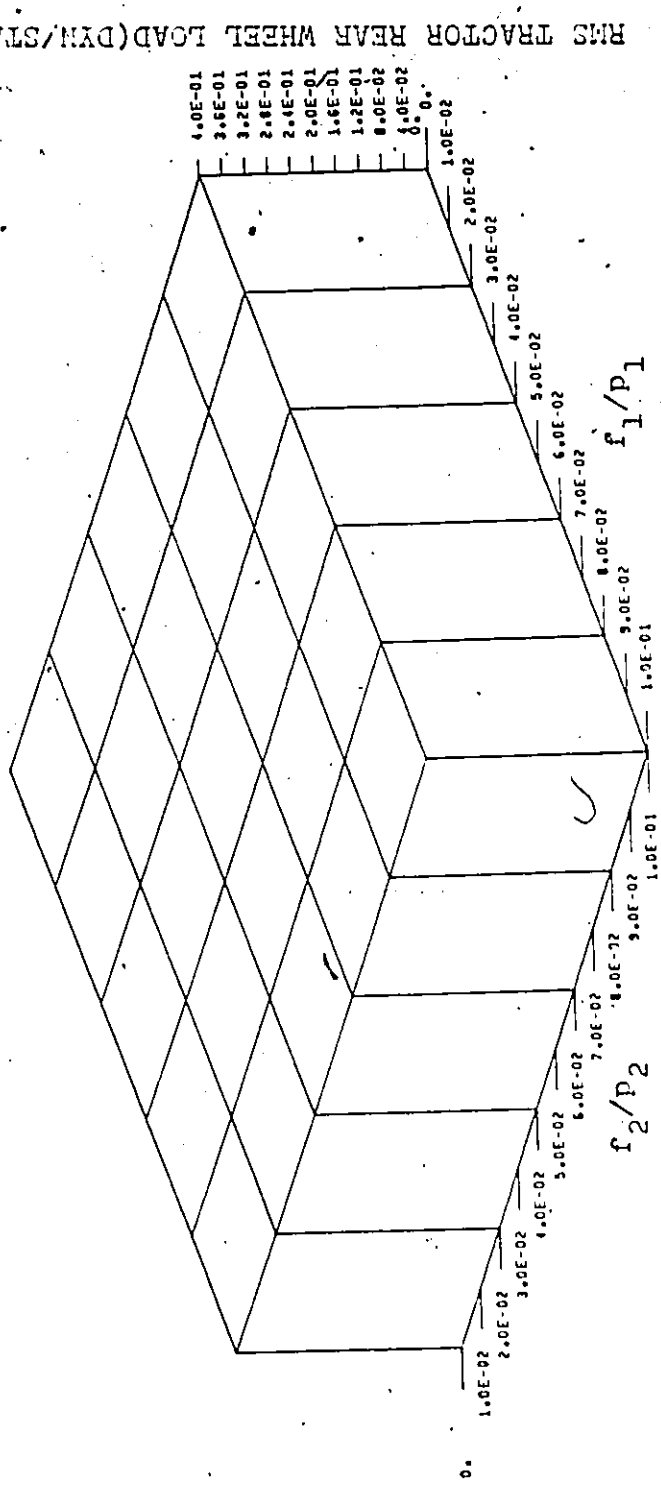

Figure 5.40 Effect of tractor front and rear dry friction dampings on rms tractor rear wheel load - unloaded vehicle, rough road.

The unloaded vehicle is the least satisfactory. Some amount of frictional forces at both the tractor front and rear suspensions are necessary to reduce the dynamic wheel load fluctuations for both the loaded and unloaded vehicles. However, the optimum values of the frictional forces are different for the two loading conditions.

5.7.1.2 Elastically Coupled Friction Damping

The suspension model consists of two elements in parallel. One element is a stiffness that represents the suspension springs. The other element consists of a stiffness in series with a dry friction. The results are obtained for a loaded vehicle operating on route A at 80 km/h and for the ratio of the series spring to the suspension spring of one.

Figure 5.41 illustrates the effect of the dry friction on the vertical acceleration spectra at the tractor's centre of gravity and at the driver's position. Figure 5.42 shows the effect of the dry friction on the fore and aft acceleration spectra at the tractor's centre of gravity and at the driver's neck level.

The results indicate that the comfort of the loaded vehicle is considerably worsened due to the effect of the dry frictional forces. With high friction damping the vertical acceleration spectra reach the ISO 1-hour standard in the first resonant region. From the figures, it can be observed that the resonant frequencies increase in the first peak region and decrease in the second peak region with increasing the friction damping. The results show that the high-frequency attenuation

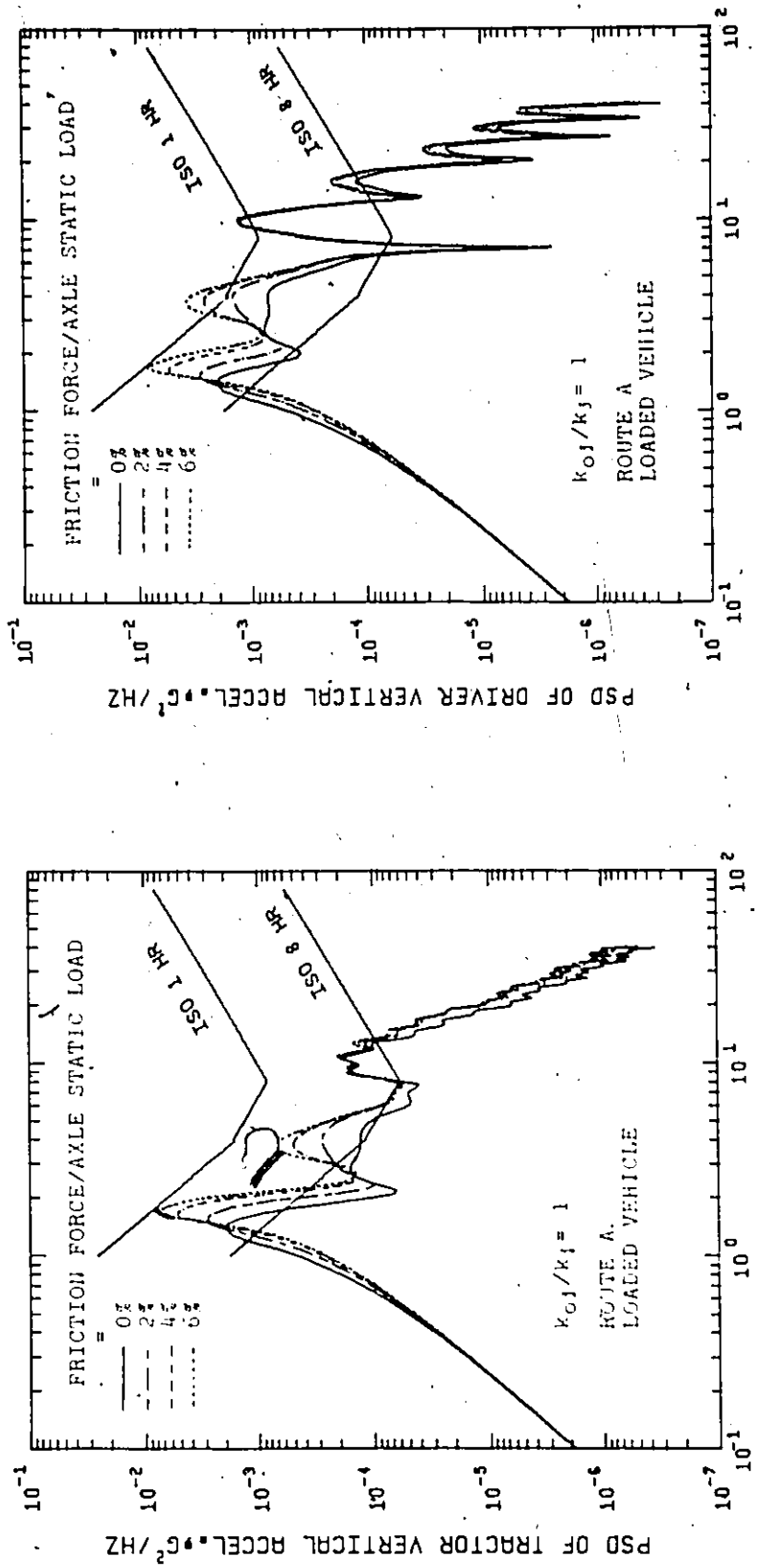

Figure 5.41 Effect of elastically coupled friction damping on tractor and driver vertical acceleration spectra - smooth road.

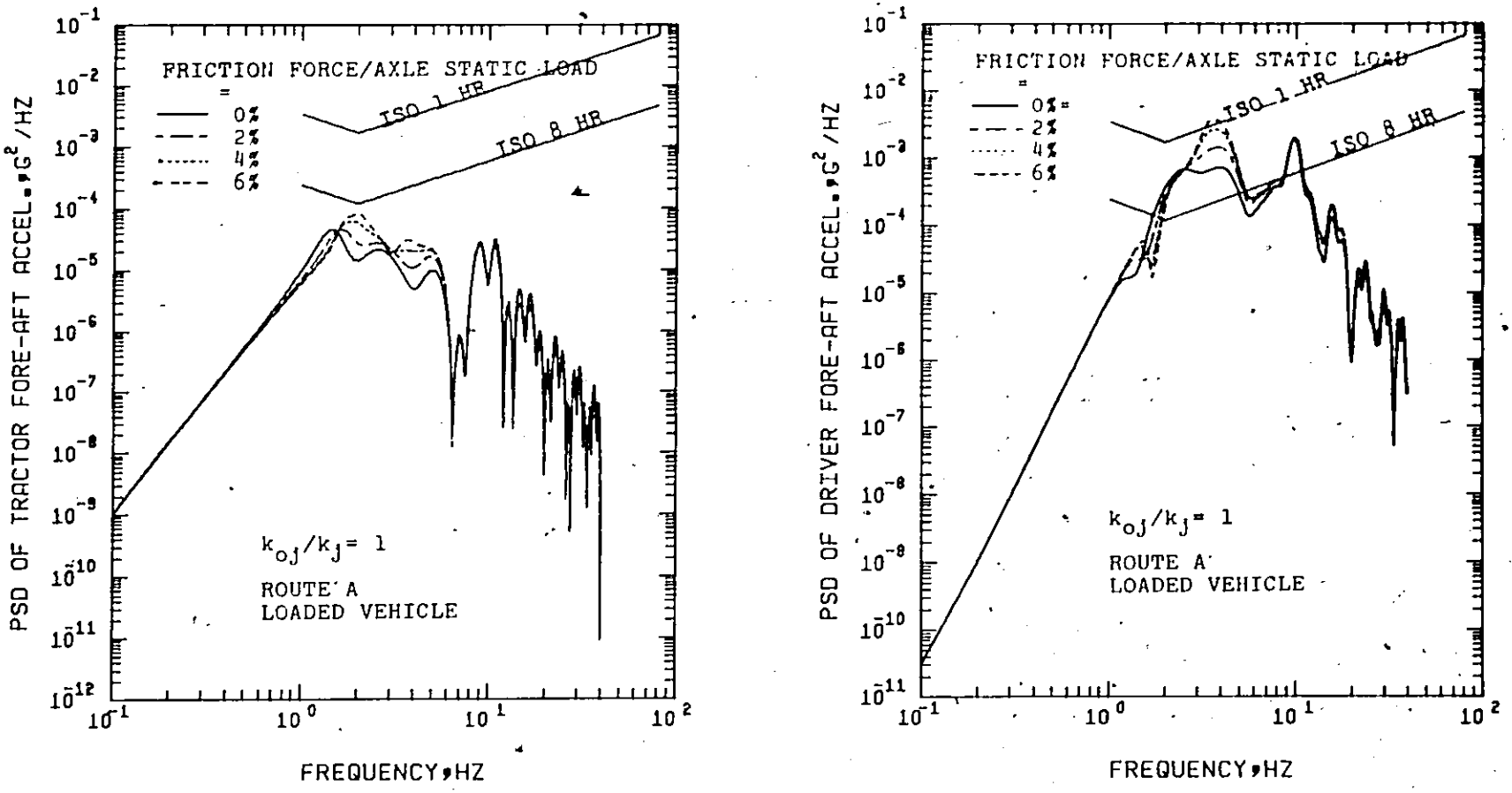

Figure 5.42 Effect of elastically coupled friction damping on tractor and driver fore and aft acceleration spectra - smooth road.

rate is generally constant regardless of the degree of friction damping.

Comparing the power spectra for directly coupled friction damping, Figures 5.10 and 5.11, with the power spectra for elastically coupled friction damping, Figure 5.41, it is clear that with increasing the damping the peak acceleration is considerably reduced for the directly coupled friction while it is greatly increased for elastically coupled friction in the low frequency region. However, the reverse occurs in the case of medium and high frequency regions.

A greater insight into the effect of the dry friction on the behaviour of the vehicle system can be obtained by calculating the rms values of vehicle response for different values of spring ratio. The frictional forces are varied from 0% to 15% of the static load on each axle of the vehicle. The results are plotted for spring ratios equal to 1, 2, 5, 25 and ∞ (directly coupled friction damping). The loaded vehicle is operating on a smooth road at 80 km/h speed.

Figure 5.43 gives the rms vertical accelerations at the tractor's centre of gravity and at the driver's position, while Figure 5.44 gives the rms tractor and semitrailer pitch accelerations. The figures show that these rms acceleration values grow rapidly with increasing the dry friction forces, particularly at low values of spring ratio. The figures also show that the rms acceleration values increase in a nonlinear fashion with increasing friction up to certain values which depend on the spring ratio. With an increase of the frictional forces beyond these particular values, the rms values will increase linearly. In the case of spring ratio equals infinity, directly coupled friction

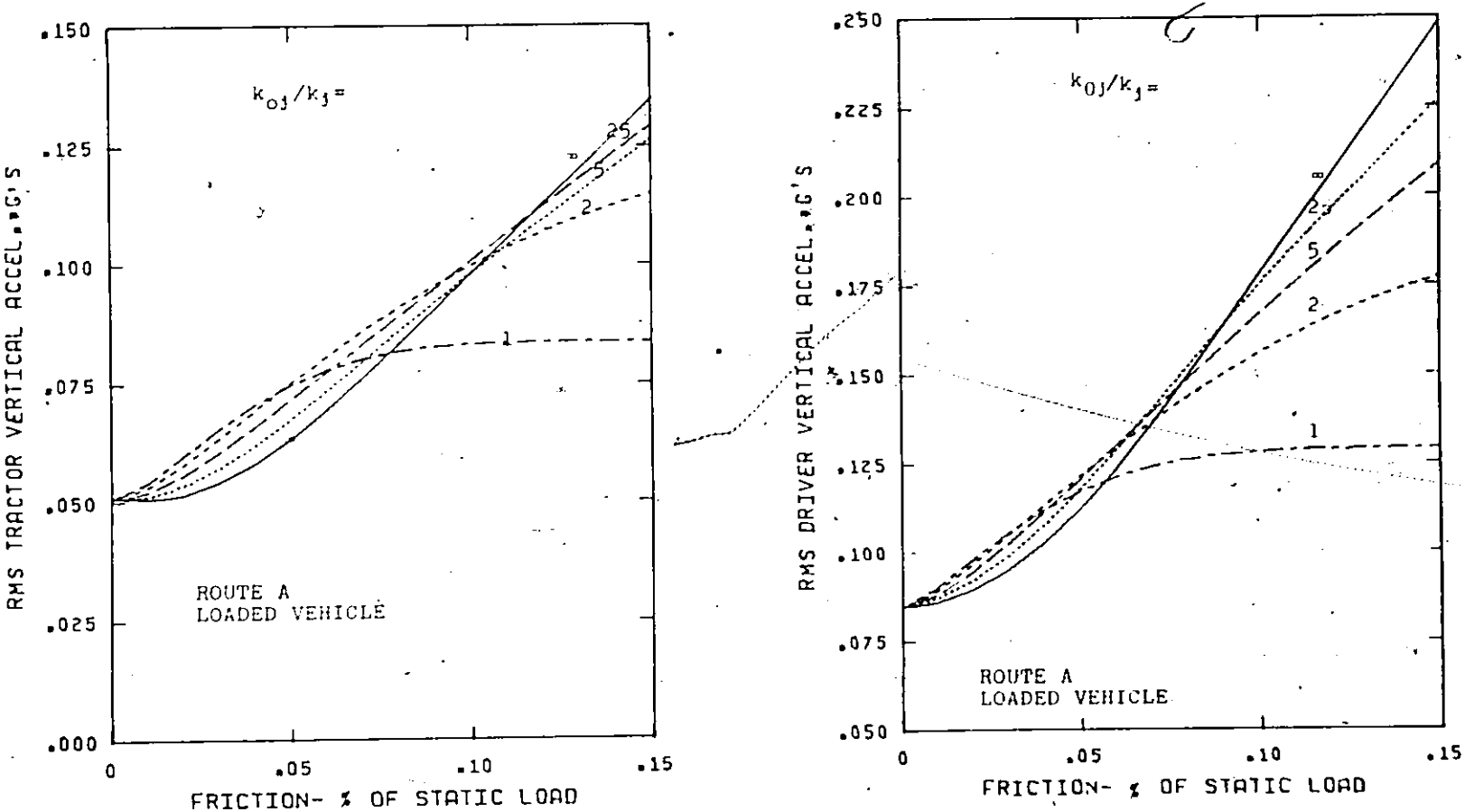

Figure 5.43 Effect of frictional forces on rms tractor and driver vertical acceleration, varying spring ratios.

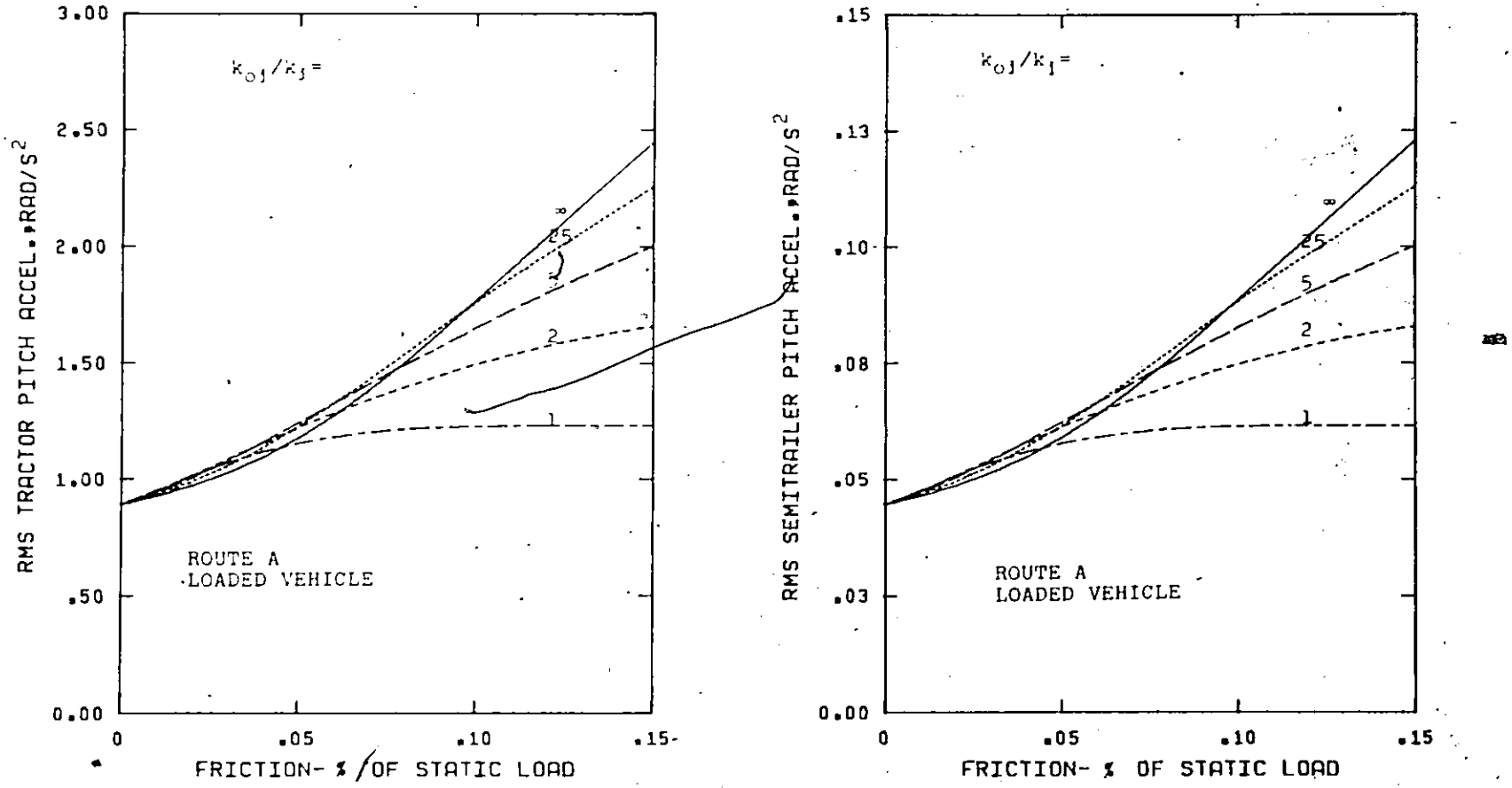

Figure 5.44 Effect of frictional forces on rms tractor and semitrailer pitch accelerations - varying spring ratios.

damping, the tractor rms acceleration decreases slightly as the frictional forces increase from 0% to 2% of the static load and increases very rapidly when the frictional forces become greater than 5% of the static load.

In Figure 5.45, the plots of axle dynamic excursions versus the frictional force ratio are shown for the various spring ratios. It may be observed from the figure that the dynamic excursions due to the road input are influenced by the choice of spring ratio. For small spring ratio there is a minimum value of the axle dynamic excursion at some values of the dry friction. However, increasing the dry friction forces beyond these values will increase the axle dynamic excursions. It is interesting to observe that the front suspension is locked at frictional forces equal to 14% of the axle static loads.

The ratio of the dynamic wheel loads to the static wheel loads for the three axles of the vehicle versus the frictional force ratio for different values of the spring ratio is shown in Figure 5.46. A study of this figure reveals that the variations in the wheel loads are largest for spring ratio 5 to ∞. For spring ratio between 1 and 2, the dynamic wheel loads decrease first slightly as the frictional forces in the suspension increase and then increase with increasing the frictional forces. It is evident that the effect of the dry frictional forces on the wheel dynamic loads is more pronounced in the case of large spring ratios. It may be seen from Figure 5.46 that there are optimum values for the frictional forces which are different for different spring ratios.

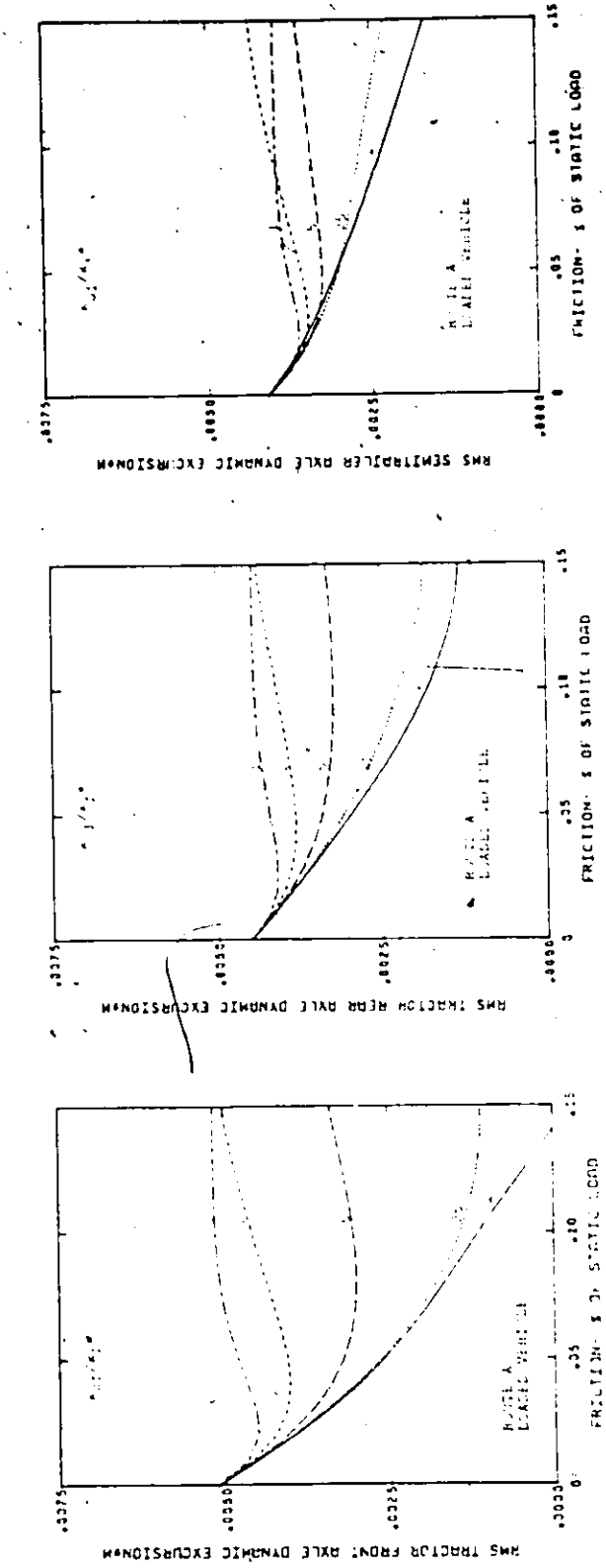

Figure 5.45 Effect of frictional forces on rms axle dynamic excursions - varying spring ratios.

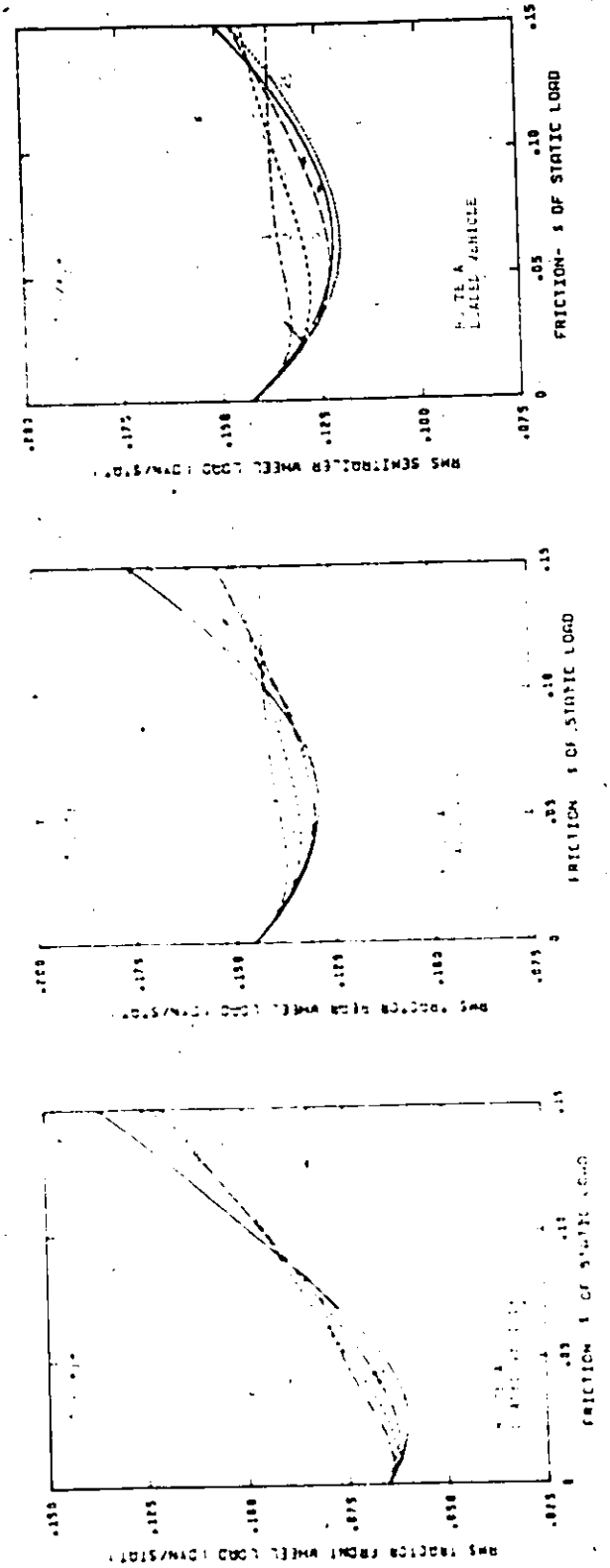

Figure 5.46 Effect of frictional forces on rms wheel loads - varying spring ratio.

5.7.2 Effect of Speed on Articulated Vehicle Motion with Dry Friction in the Suspension

Variations with vehicle speed of the rms responses; vertical and fore and aft accelerations at the centre of gravity of the tractor and at the driver's position, pitch accelerations, stroking displacements and wheel dynamic loads are obtained by the analytical techniques described previously. Computations are carried out for the laden vehicle running on route A and route B, and for the unladen vehicle running on route B. The effect of the vehicle's forward speed is investigated to determine if a critical speed exists within the operating range of the vehicle. The dry frictional forces in the laminated suspension modeled as a constant friction in parallel with the main spring, are also included in the study.

Figure 5.47 shows the rms vertical accelerations at the centre of gravity of the tractor and at the driver position for a loaded vehicle. In general, the rms acceleratons are increased with increasing the vehicle speed. However, for the linear system, at the tractor's centre of gravity, the effect at 32 km/h is minimal. It can be inferred from the figure that the rate of increase of the rms vertical accelerations at the tractor's centre of gravity at different values of dry friction is the same. It can also be inferred from the figure that there is a possibility of resonant condition at about 100 km/h for the vertical acceleration at the driver's position for the linear system. For a small amount of dry friction, 0-2% of the axle static load, the linear system gives reasonable results; however, for higher dry friction, the

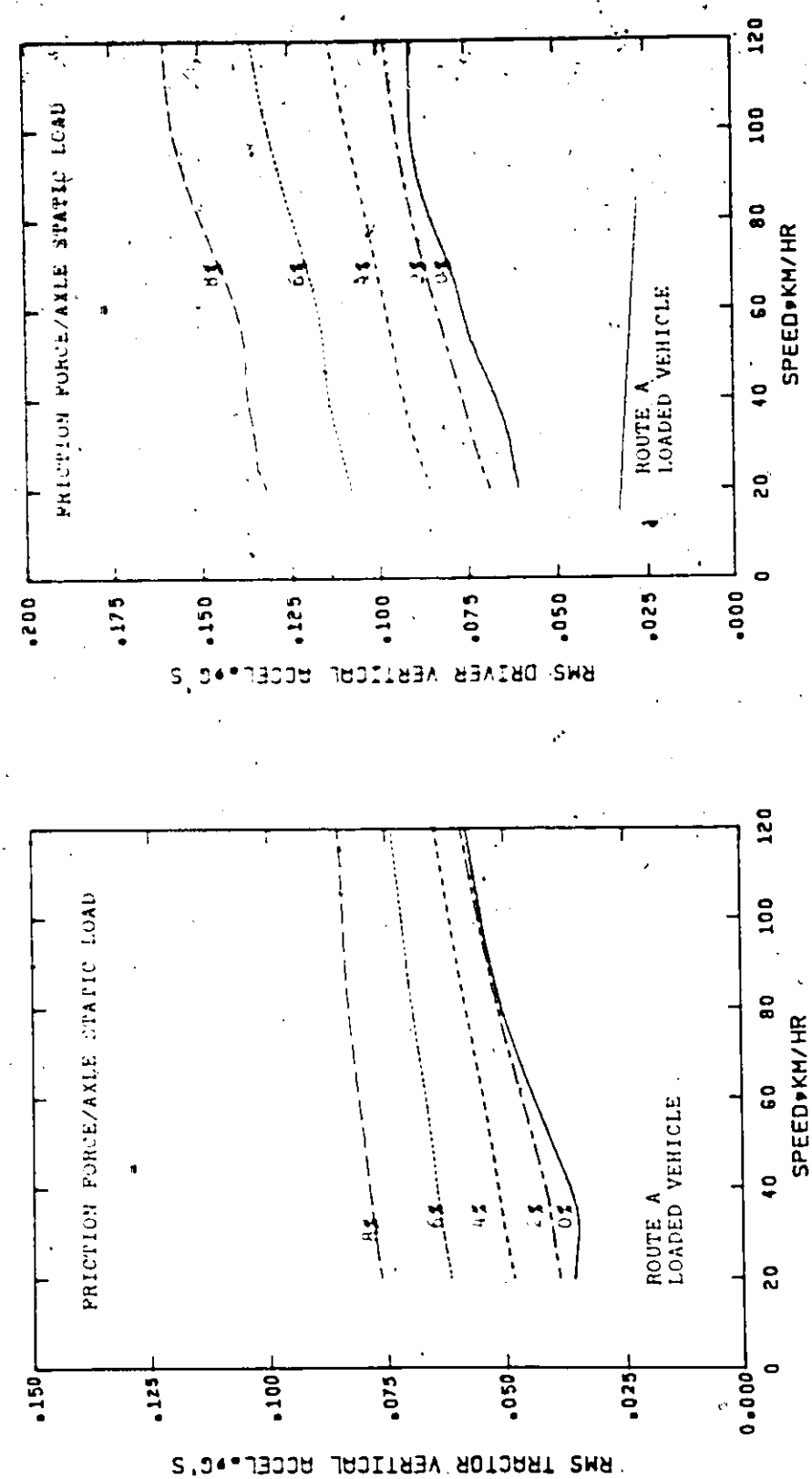

Figure 5.47 Effect of speed on rms tractor and driver vertical accelerations - varying frictional forces, loaded vehicle, smooth road.

effect of friction should be considered in obtaining the response and the linear system is not adequate for the analysis.

Figures 5.48 and 5.49 show the rms vertical accelerations at the tractor centre of gravity and at the driver's position for loaded and unloaded vehicles, respectively, running on route B. As can be seen from the figures, the interleaf friction in the vehicle suspension drastically changes the detailed features of the rms response curves. The high rms response found for high dry friciton at low speeds is caused by the articulated vehicle acting more as a rigid body, because the interleaf forces are relatively large. At higher speeds the initial breakaway friction force is easily overcome, and the vehicle acts more as a system of separate elements between which a large amount of relative motion is possible.

The results shown in Figures 5.48 and 5.49 indicate that the presence of dry friction in the suspension is detrimental to the ride motion at low speeds; however, at high speeds a small amount of friction might be effective in reducing the vibration. The rms accelerations for the unloaded vehicle are higher than the corresponding values for the loaded vehicle.

The rms fore and aft accelerations at the tractor's centre of gravity and at the driver's neck level for a loaded vehicle operating on a smooth road are shown in Figure 5.50. The rms fore and aft accelerations at the driver's neck level for loaded and unloaded vehicles operating on a rough road are shown in Figure 5.51. The rms tractor pitch and semitrailer pitch accelerations are shown in Figures

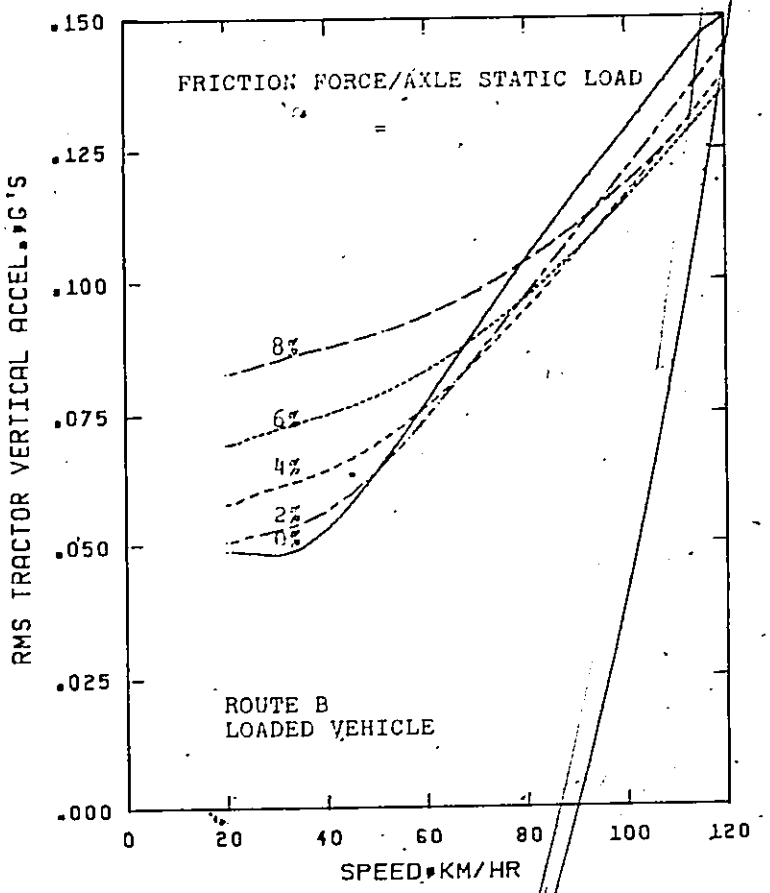

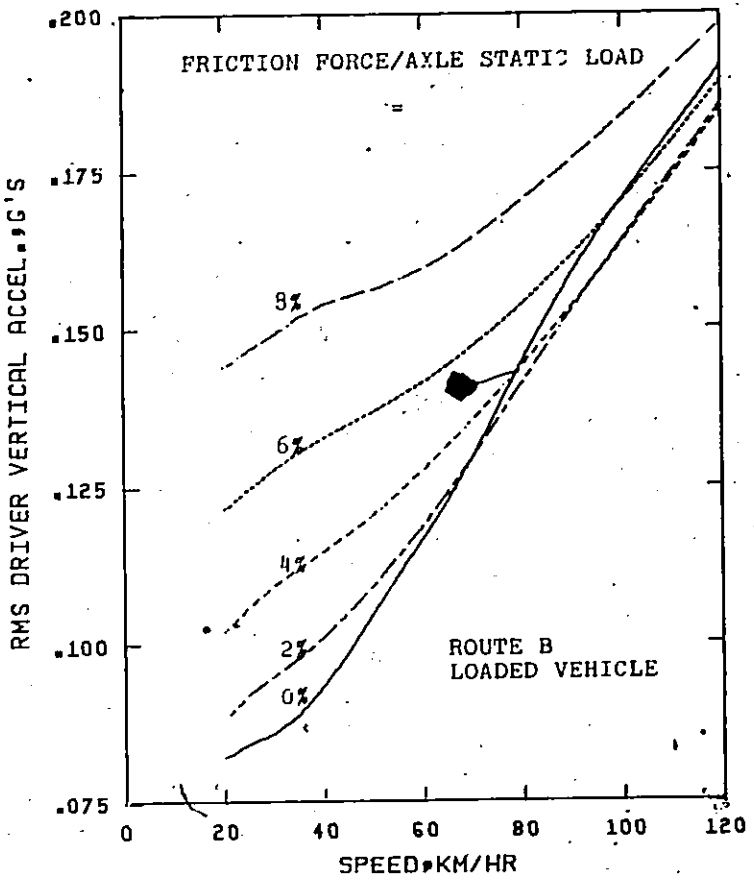

Figure 5.48 Effect of speed on rms tractor and driver vertical accelerations - varying frictional forces, loaded vehicle, rough road.

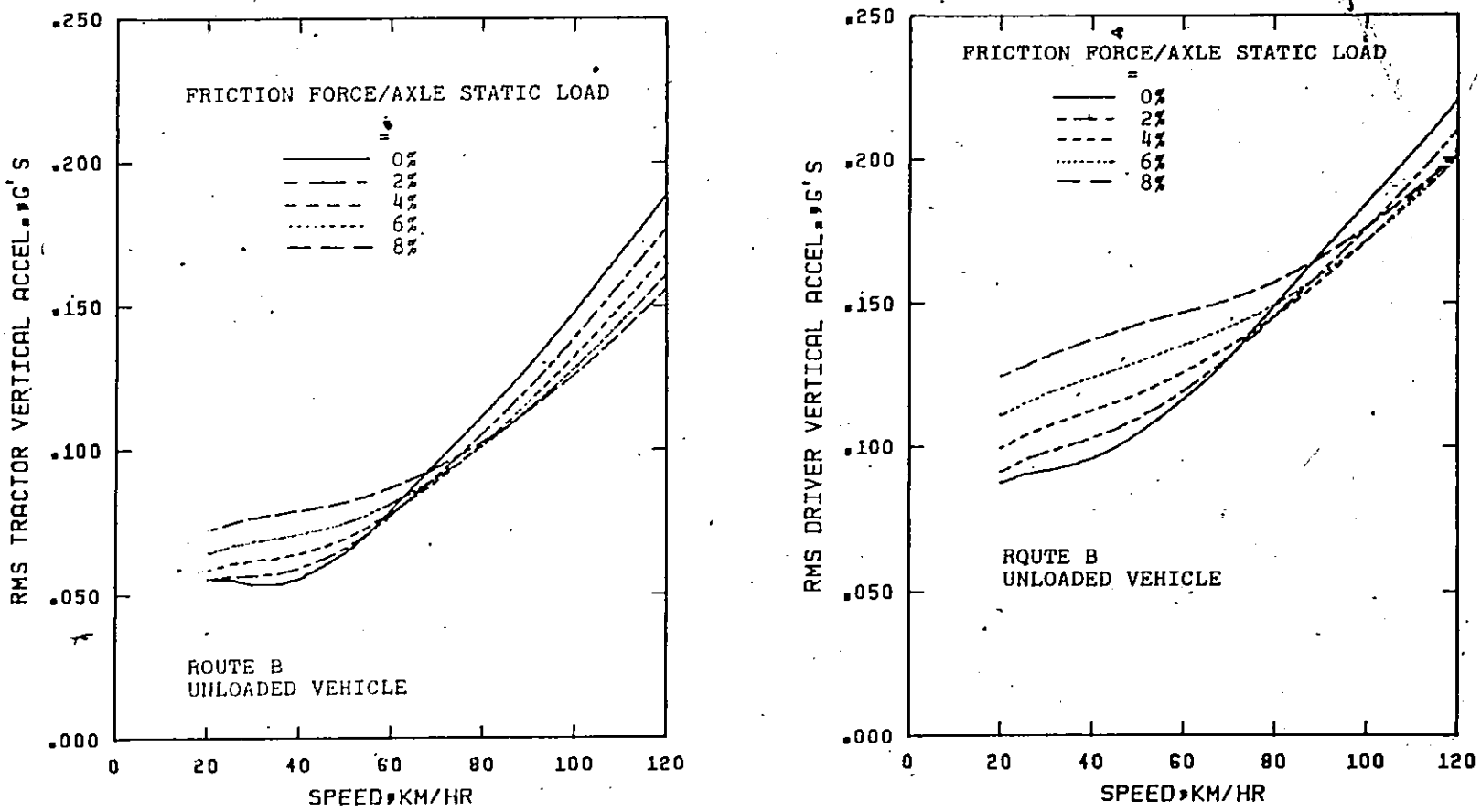

Figure 5.49 Effect of speed on rms tractor and driver vertical accelerations - varying frictional forces, unloaded vehicle, rough road.

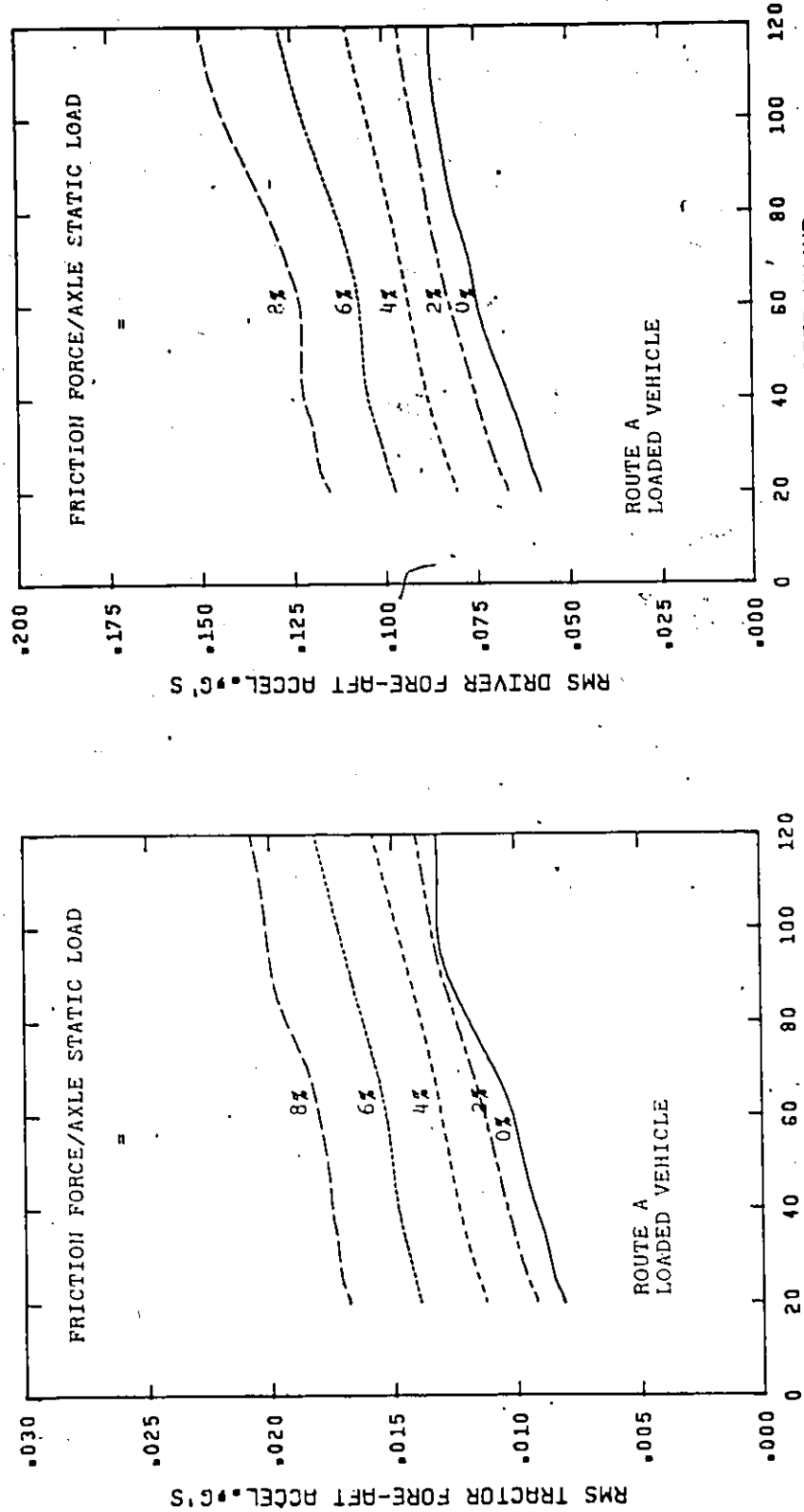

Figure 5.50 Effect of speed on rms tractor and driver fore and aft accelerations - varying frictional forces, loaded vehicle, smooth road.

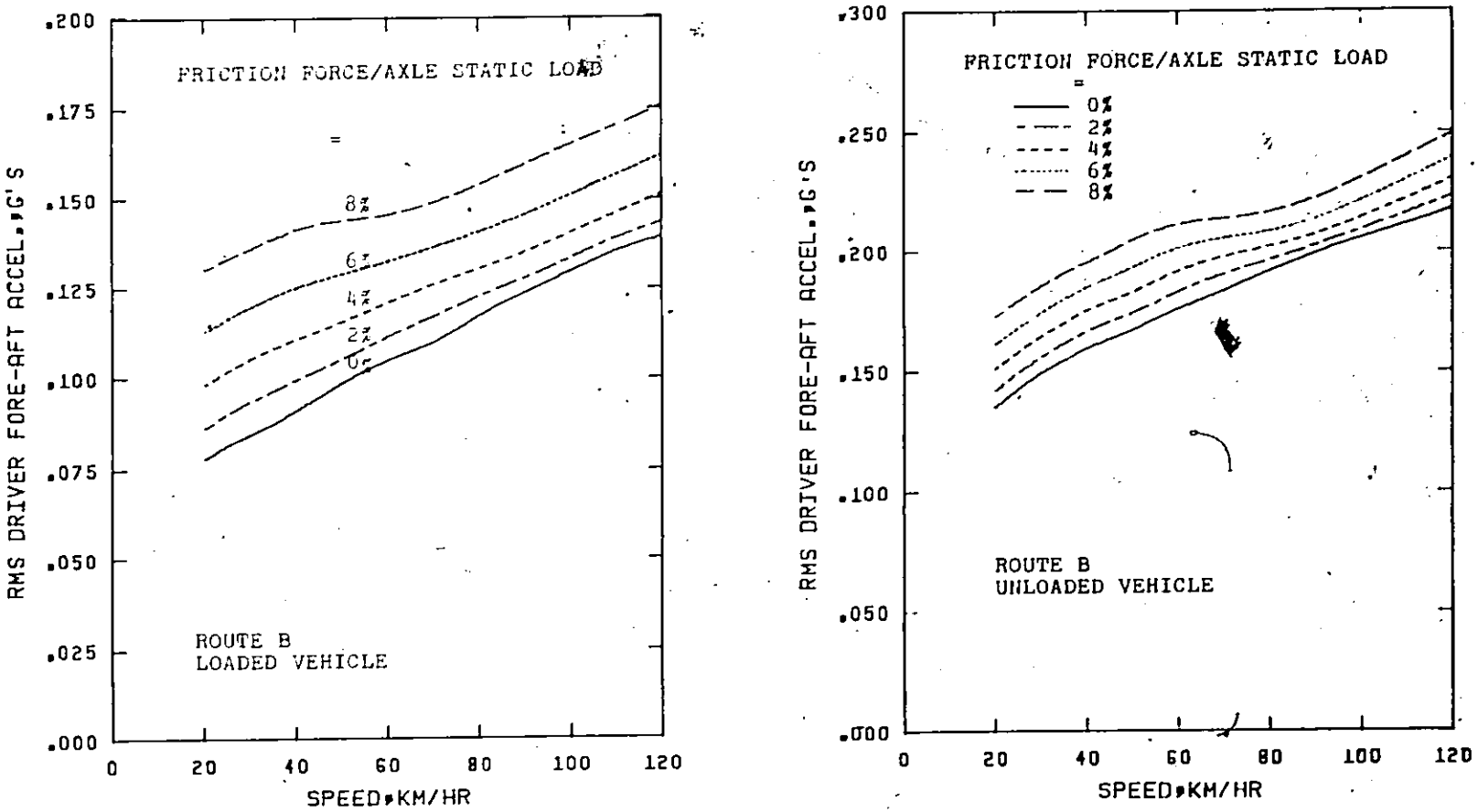

Figure 5.51 Effect of speed on rms driver fore and aft accelerations - varying frictional forces, rough road.

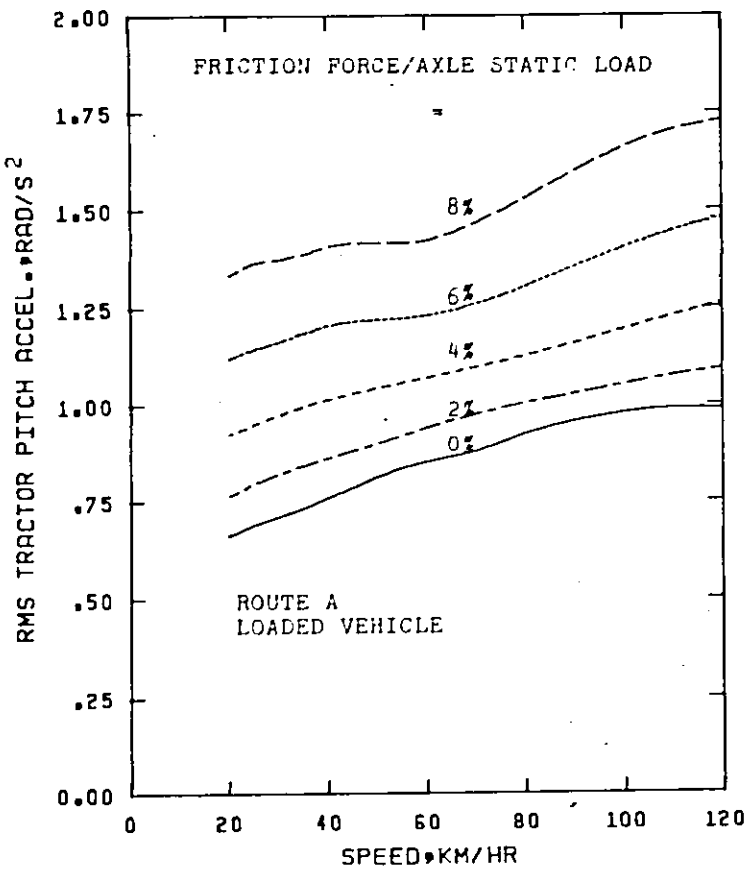

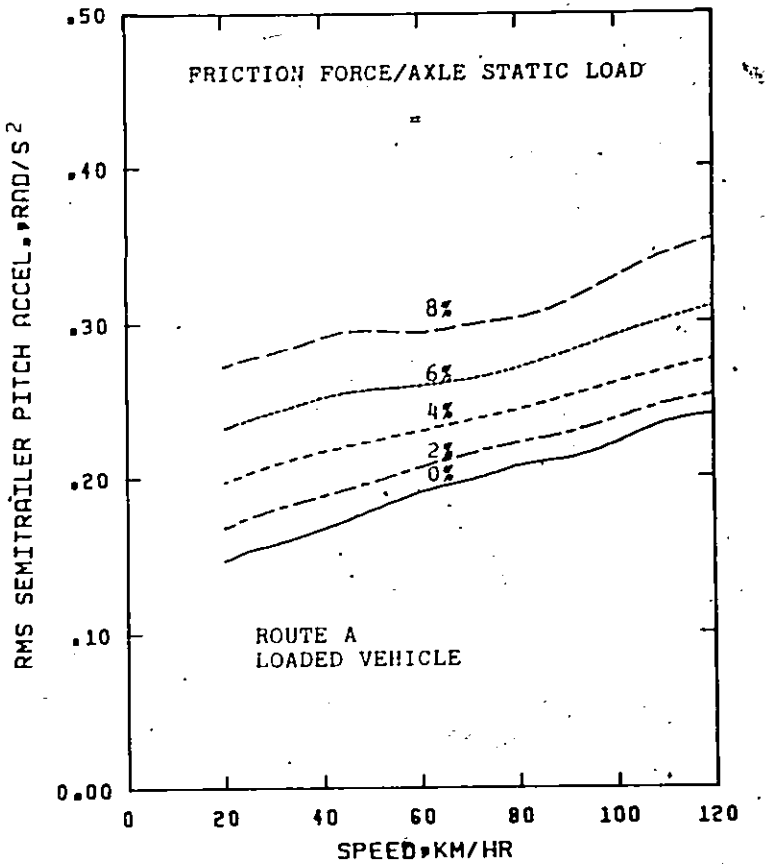

Figure 5.52 Effect of speed on rms tractor and semitrailer pitch accelerations - varying frictional forces, loaded vehicle, smooth road.

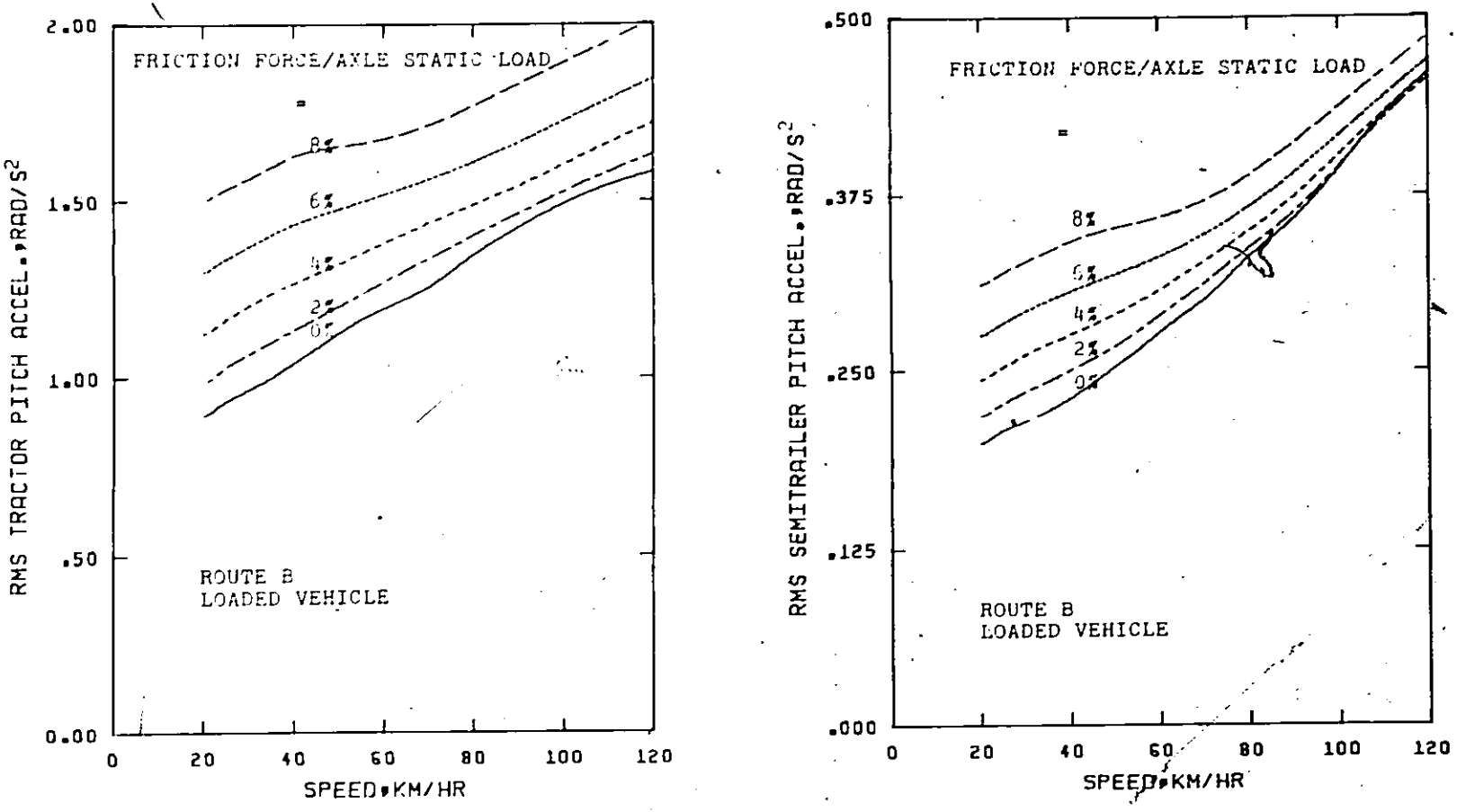

Figure 5.53 Effect of speed on rms tractor and semitrailer pitch accelerations - varying frictional forces, loaded vehicle, rough road.

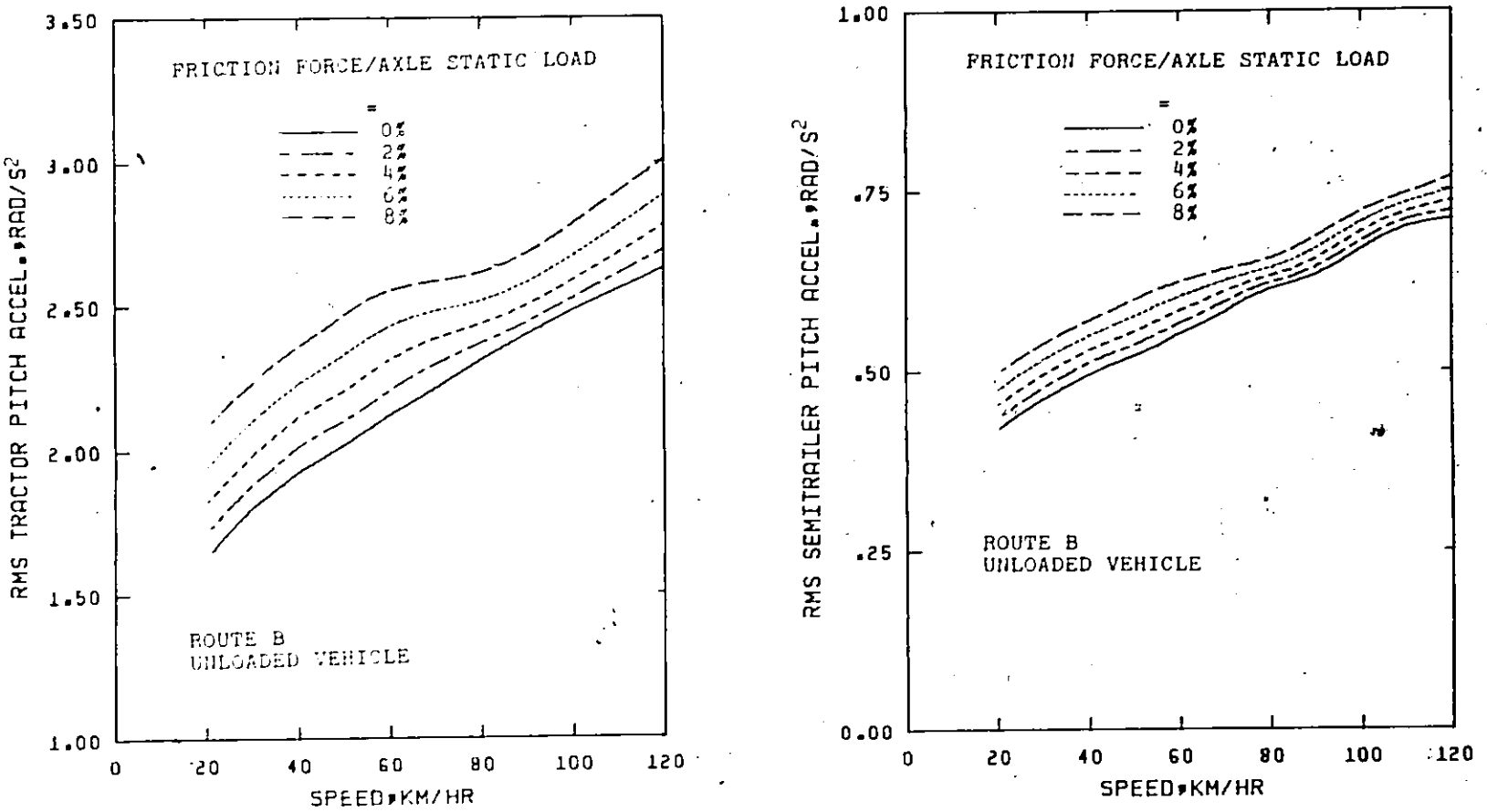

Figure 5.54 Effect of speed on rms tractor and semitrailer pitch accelerations - varying frictional forces, unloaded vehicle, rough road.

5.52 - 5.54. It can be seen from the figures that the rms accelerations increase quite rapidly at speeds above 60 km/h for high dry friction. It can also be seen that the tractor exhibits very high pitch accelerations which contribute to considerable fore and aft accelerations at the driver's neck level. The dry friction has a significant effect on the rms responses and as can be seen from the figures the rms values at friction force of 8% of the static load are from 1.7 - 2 times the rms values for the linear system.

Figures 5.55 - 5.57 illustrate the effect of speed on the different axle dynamic excursion for different values of the dry friction. For the linear system and for low values of dry friction the curves representing the dynamic excursion exhibit some undulations. At higher values of dry friction the response increases more uniformly with vehicle speed. Referring to the curves representing the tractor's front axle dynamic excursion, it can be seen that the rms values decrease quite rapidly at vehicle speeds up to about 32 km/h. At higher speeds, however, the response curves show a high rate of increase. For the semitrailer axle dynamic excursion, a peak occurs at about 45 km/h. Above this speed the response decreases to a minimum value at about 70 km/h and then increases with increasing the speed.

Figure 5.58 gives the ratio of the rms dynamic load to the static load for the tractor rear wheel and semitrailer wheel for different values of dry friction as a function of the vehicle speed. As can be seen from the figure some dry friction in the suspension is beneficial

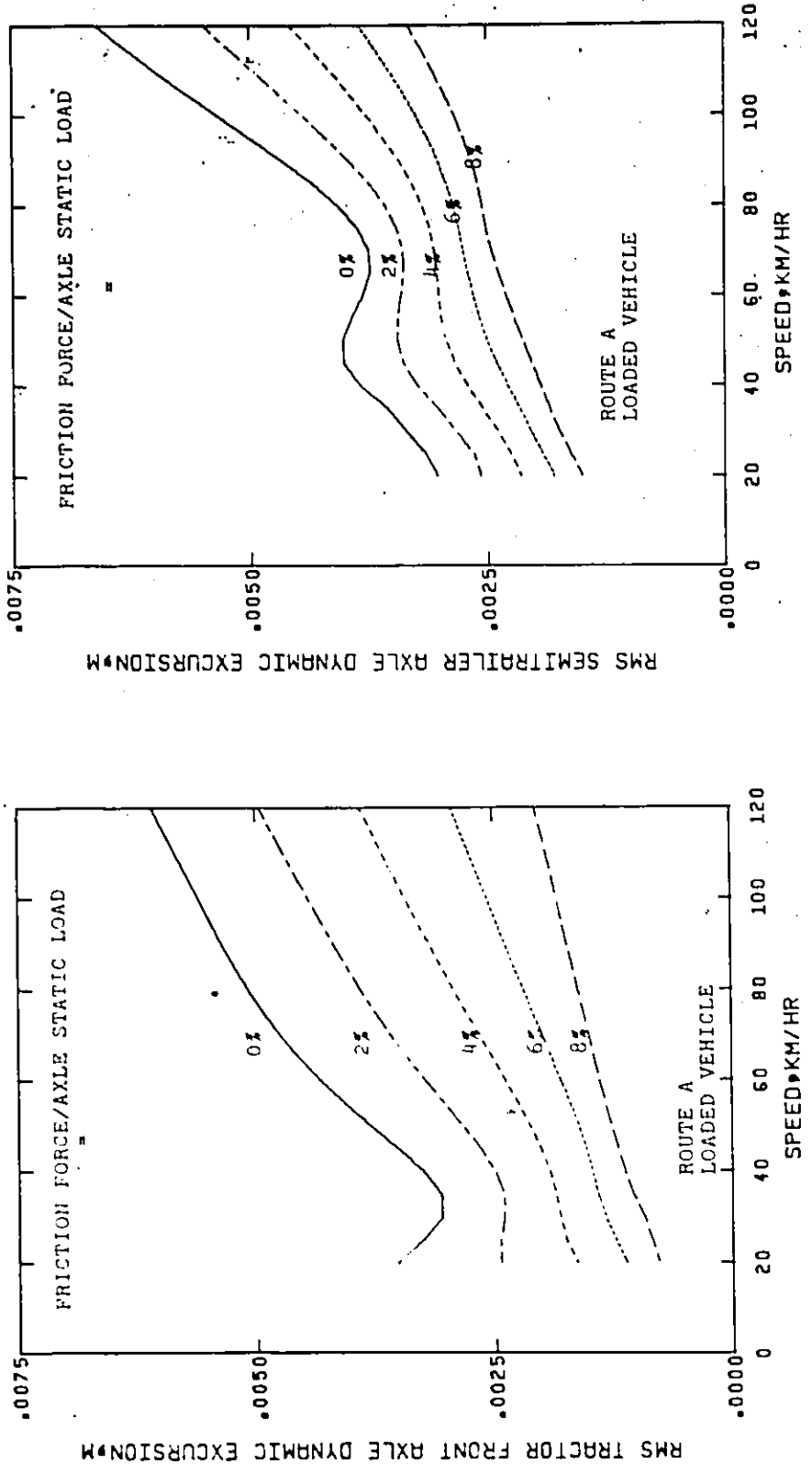

Figure 5.55 Effect of speed on rms vehicle axle dynamic excursions - varying frictional forces, loaded vehicle, smooth road.

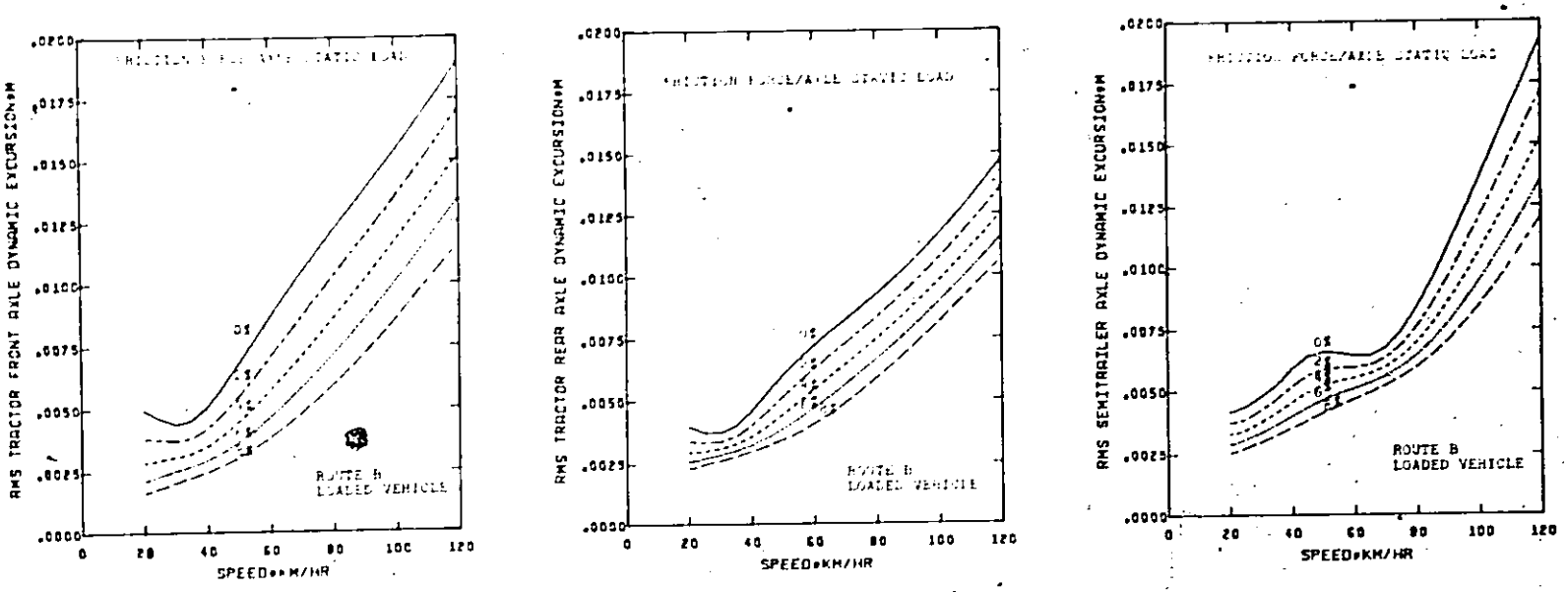

Figure 5.56 Effect of speed on rms vehicle axle dynamic excursions - varying frictional forces, loaded vehicle, rough road.

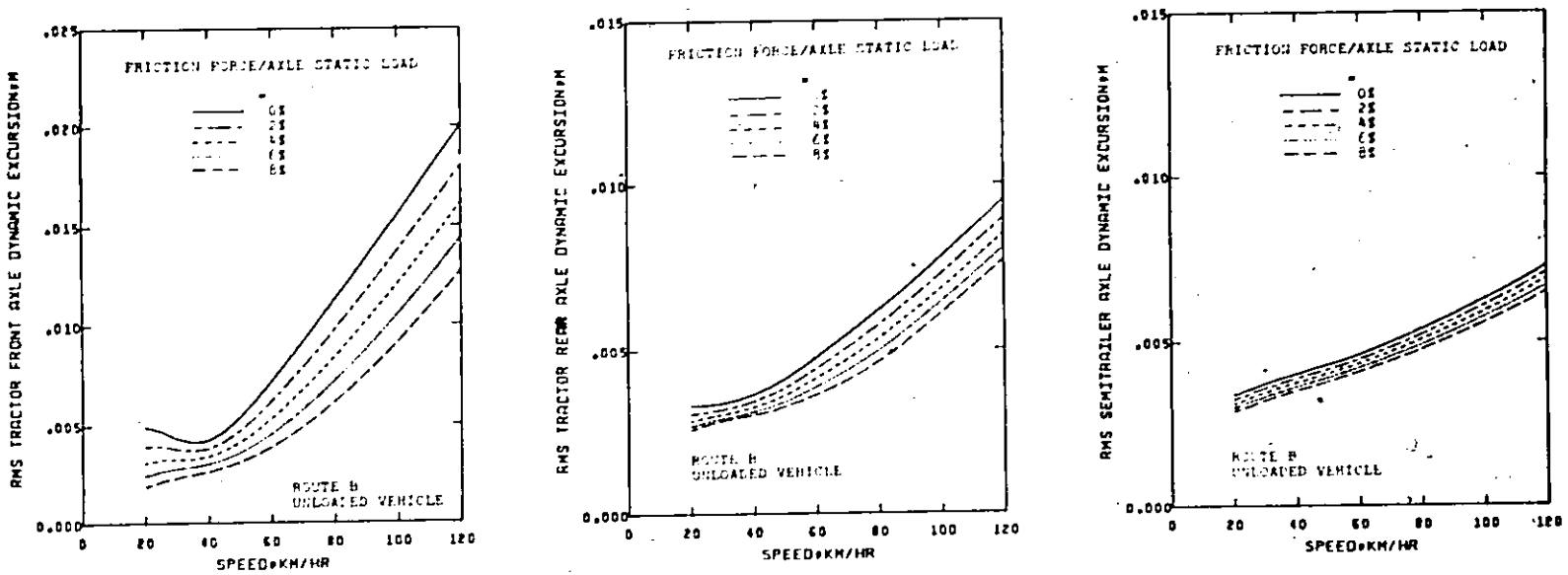

Figure 5.57 Effect of speed on rms vehicle axle dynamic excursions - varying frictional forces, unloaded vehicle, rough road.

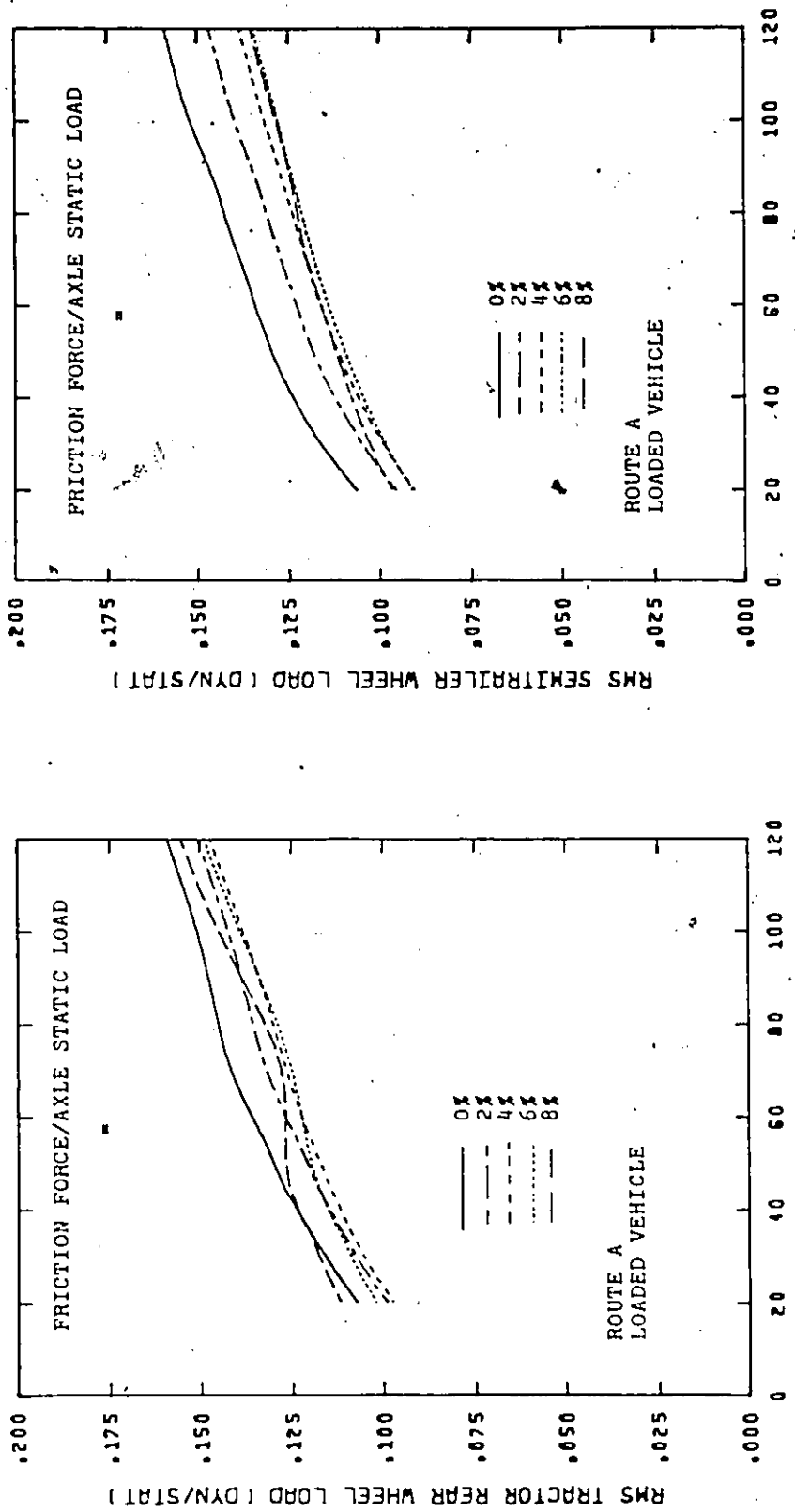

Figure 5.58 Effect of speed on rms vehicle wheel loads - varying frictional forces, loaded vehicle, smooth road.

in reducing the fluctuation of the dynamic load; however, at a higher value of dry friction, 8% of the axle static load, the response gives an irregular curve and exhibits an irrational shape. The difference in the results of the linear and nonlinear models emphasizes the effects of the nonlinearities on the behavior of the system, Figures 5.58 - 5.60.

The probability of the wheel's departure from the road is given in Figure 5.61 for an unloaded vehicle operating on route B. From the curves shown in Figures 5.58 - 5.61 it may be concluded that with a loaded vehicle the danger of the wheel's departure is less than that with an unloaded one. The wheels of a loaded vehicle running on route B practically do not depart from the road. For an unloaded vehicle running on a rough road the probability of departure of the semitrailer wheel is high; some frictional forces may be beneficial in reducing the fluctuations of the wheel dynamic loads and consequently in reducing the probability of departure of the wheel from the road. Specifically, some amounts of frictional forces are required for the tractor front and rear suspension at high speeds, while the frictional forces are required for the semitractor wheel at all speeds.

The suspension equivalent dampings for a loaded vehicle operating on route A, and for loaded and unloaded vehicles operating on route B are given in Figures 5.62 - 5.64, respectively. In each figure the suspension equivalent dampings are given as a function of vehicle speed for different values of dry frictional forces. The curves show that the equivalent dampings are consistently higher for a loaded vehicle

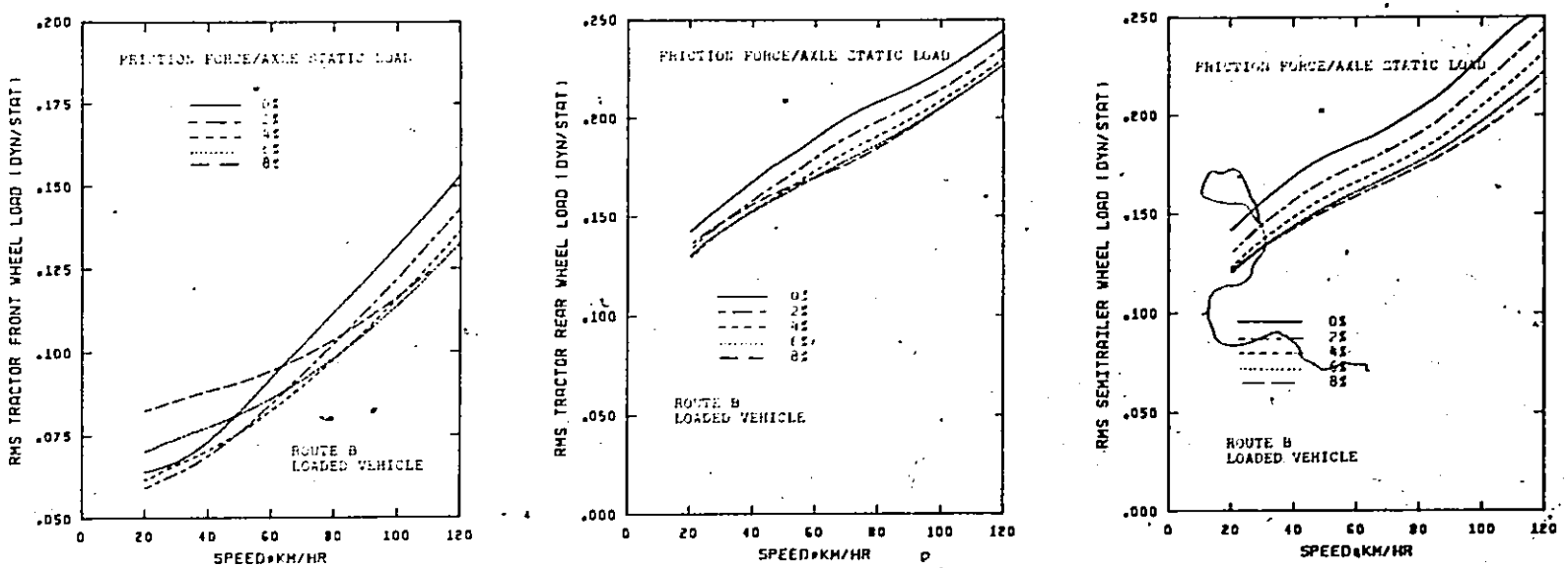

Figure 5.59 Effect of speed on rms vehicle wheel loads - varying frictional forces, loaded vehicle, rough road.

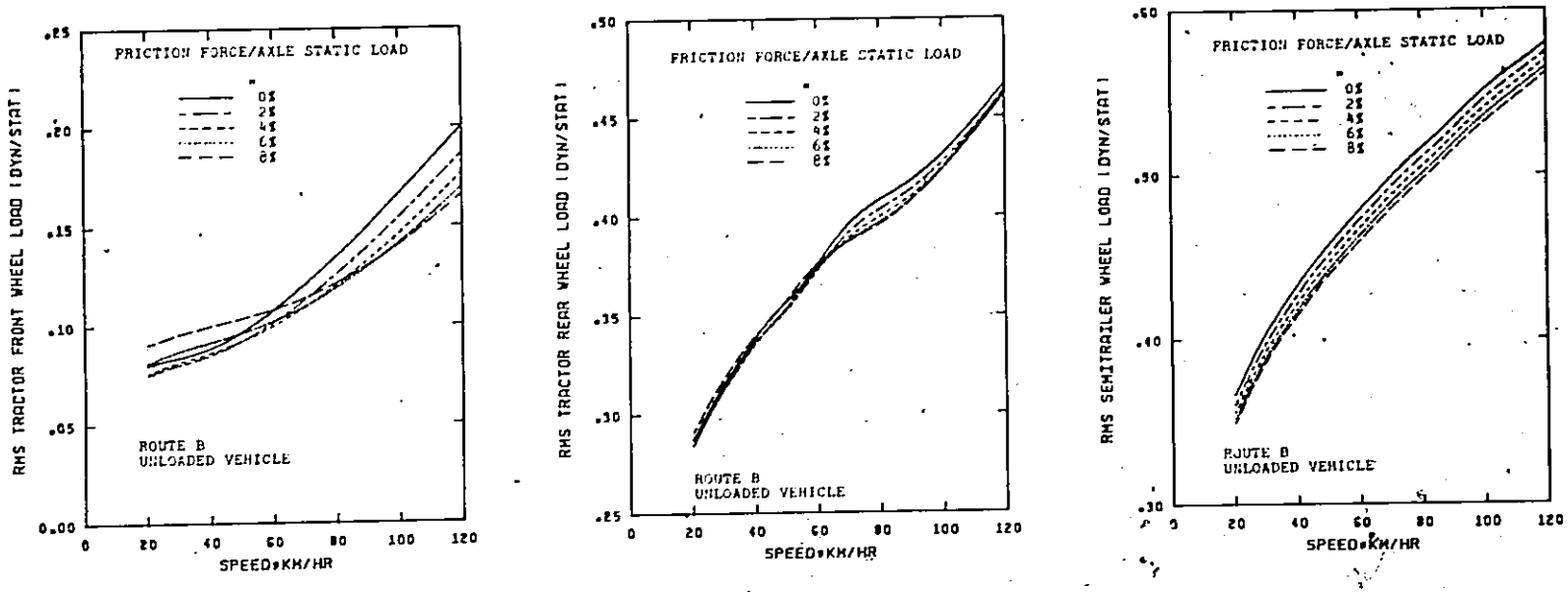

Figure 5.60 Effect of speed on rms vehicle wheel loads - varying frictional forces, unloaded vehicle, rough road.

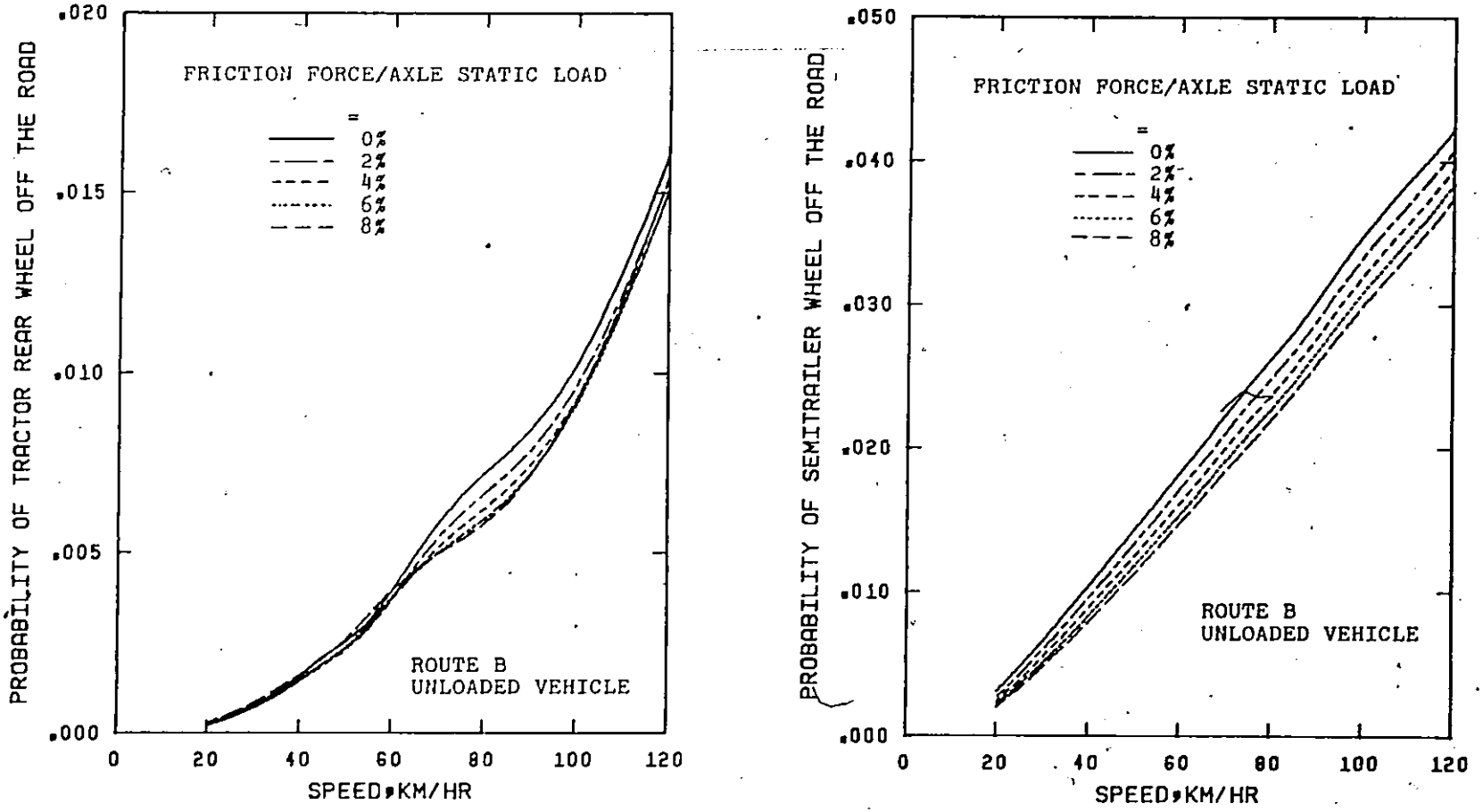

Figure 5.61 Effect of speed on probability of vehicle wheels off the road - varying frictional forces, unloaded vehicle, rough road.

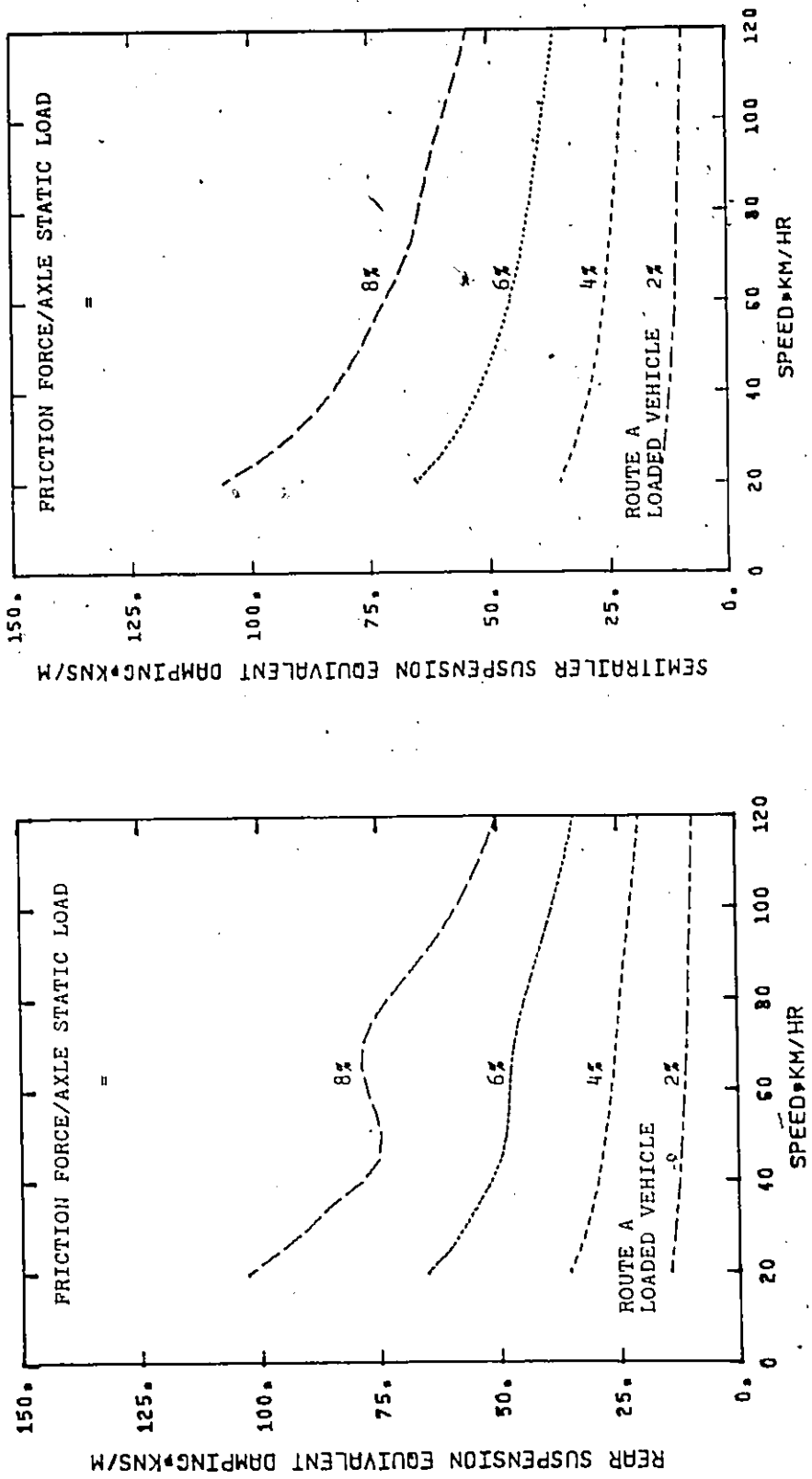

Figure 5.62 Effect of speed on vehicle suspension equivalent dampings - varying frictional forces, loaded vehicle, smooth road.

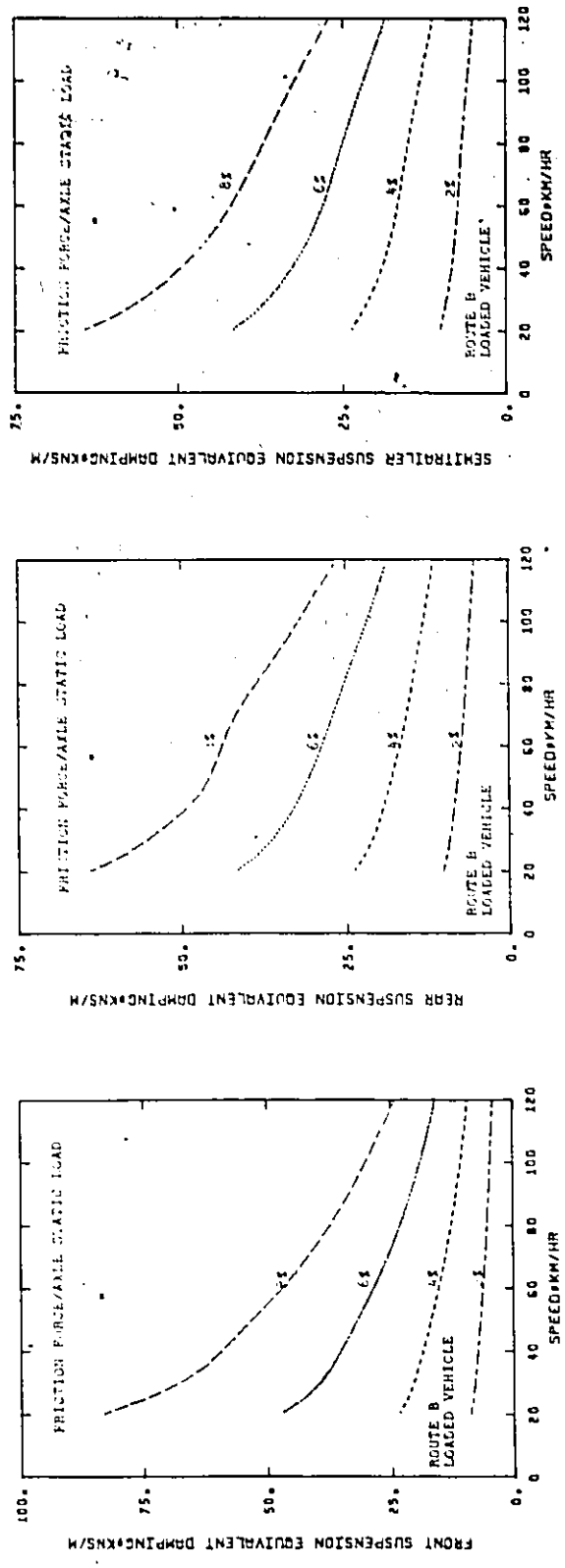

Figure 5.63 Effect of speed on vehicle suspension equivalent dampings - varying frictional forces, loaded vehicle, rough road.

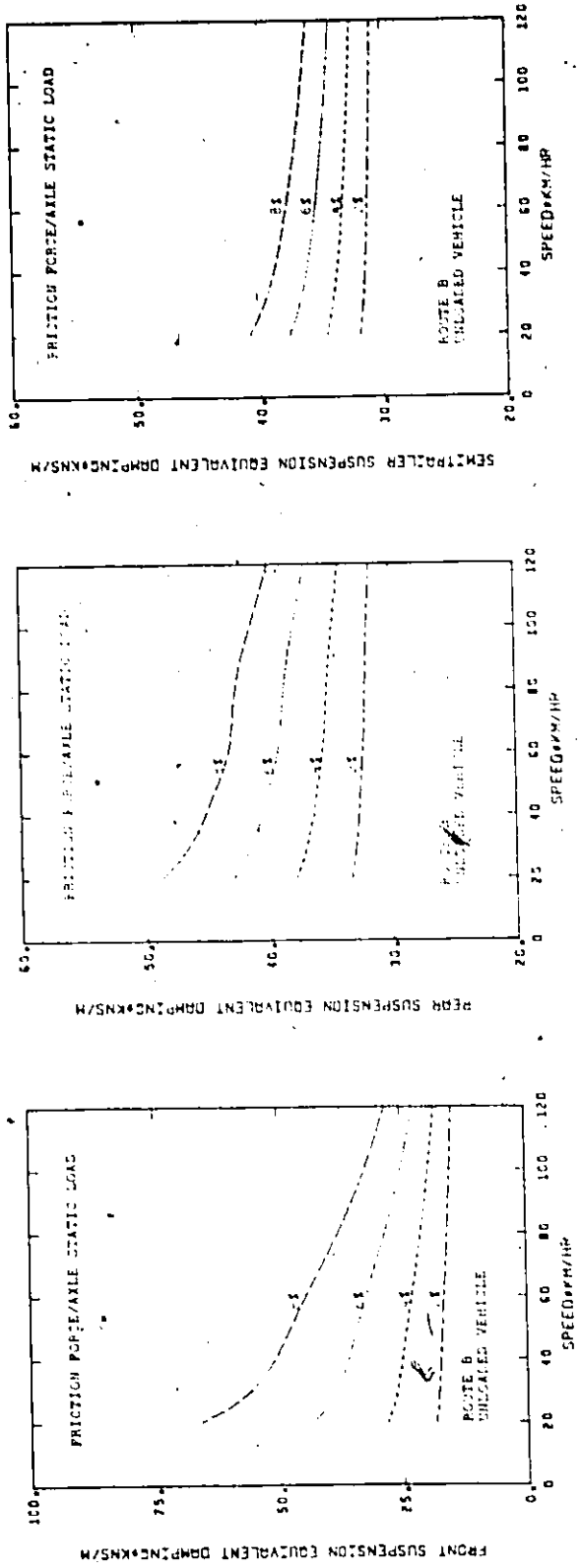

Figure 5.64 Effect of speed on vehicle suspension equivalent dampings - varying frictional forces, unloaded vehicle, rough road.

operating on a smooth road than for one operating on a rough road. In other words, for a loaded vehicle operating on a smooth road, the suspension would seem to be very stiff and the vibrations of the unsprung masses would significantly transfer to the vehicle body without considerable damping. It may be observed from Figures 5.62 - 5.64 that the equivalent damping of higher dry friction forces are significantly reduced at high speeds. Obviously, a vehicle with large frictional forces does exhibit poor ride comfort at low speeds. In this case, the vehicle would vibrate on the tires as can be seen from Figure 5.55.

5.7.3 Effect of Bump-Stop Clearance

The suspension bump-stop clearance is defined as the suspension deflection which can take place before the bump stops come into contact. The effect of bump-stop clearance on the ride motion of the vehicle is investigated for the loaded vehicle operating on the rough road, B, and moving at 80 km/h. Figures 5.65 and 5.66 show the response spectra of the acceleration at the centre of gravity of the tractor and at the driver's position for vertical and fore and aft motions, respectively. These spectra are obtained for various values of the bump-stop clearance with bump-stop spring rate, k^{*}_{oj}, equal to ten times the main suspension spring rate, k_j. A study of Figures 5.65 and 5.66 reveals that the acceleration values are strongly affected by the presence of the bump-stops. Decreasing the bump-stop clearance will impair the ride comfort, particularly at the low and medium frequency ranges. A large

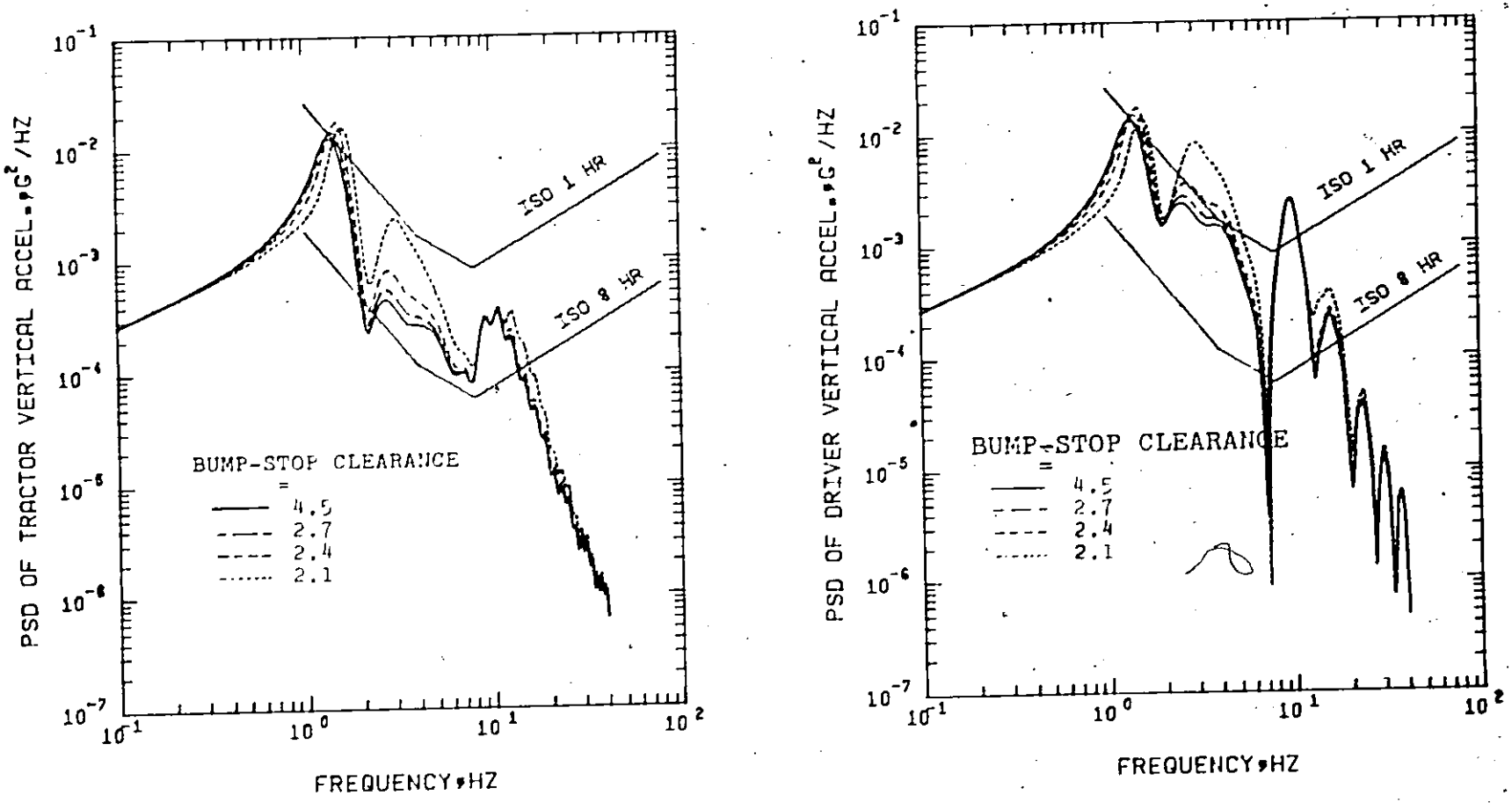

Figure 5.65 Effect of bump-stop clearance on tractor and driver vertical acceleration spectra - loaded vehicle, rough road.

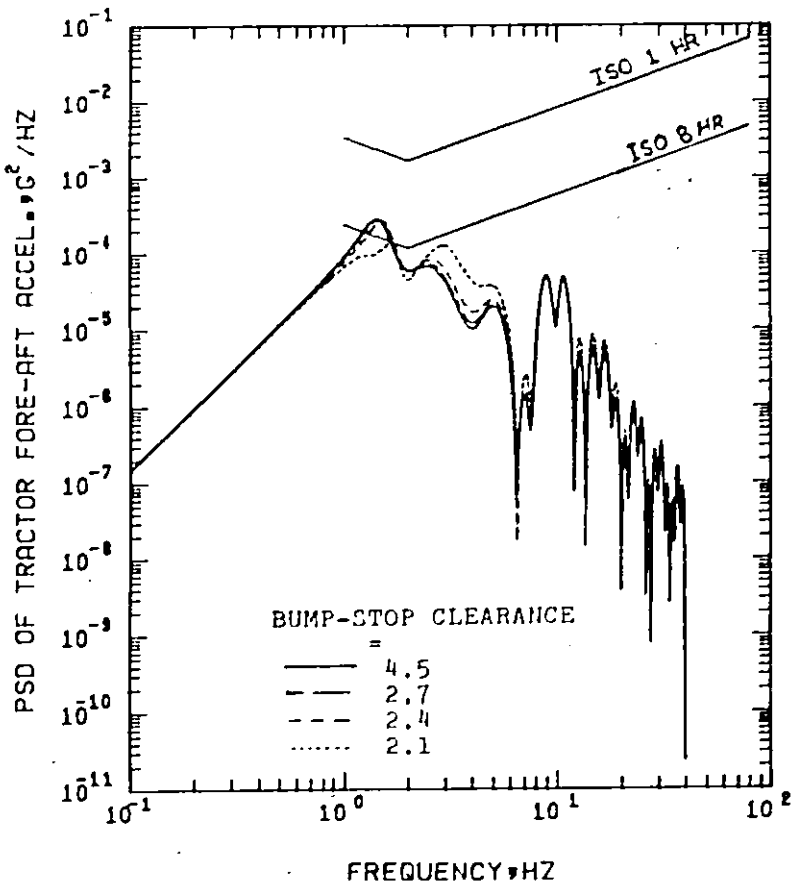

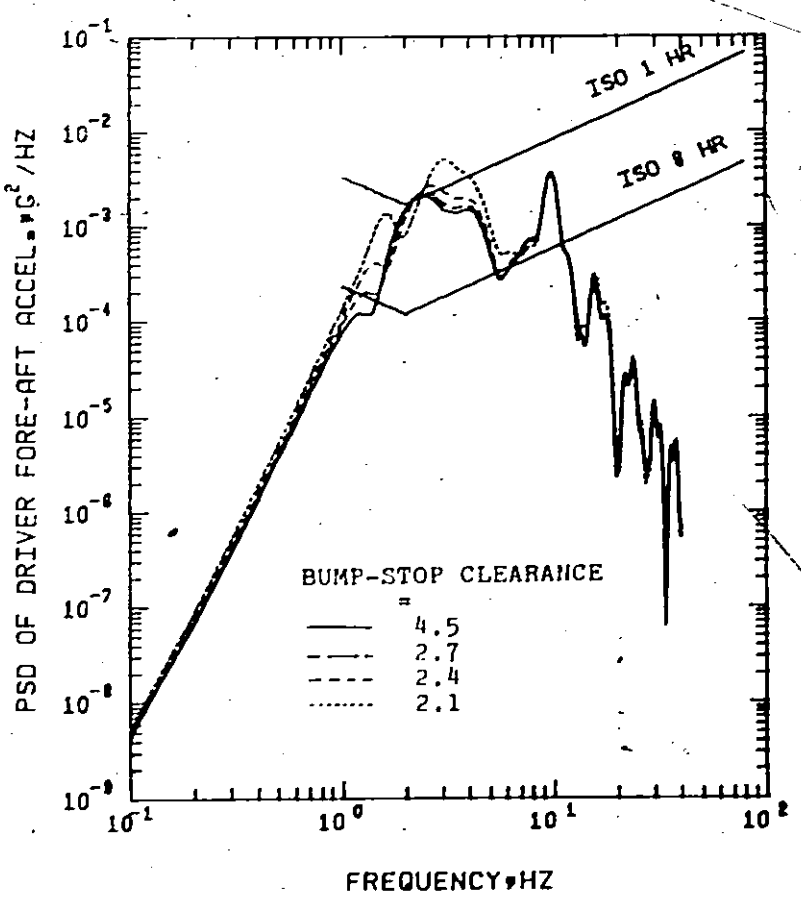

Figure 5.66 Effect of bump-stop clearance on tractor and driver fore and aft acceleration spectra - loaded vehicle, rough road.

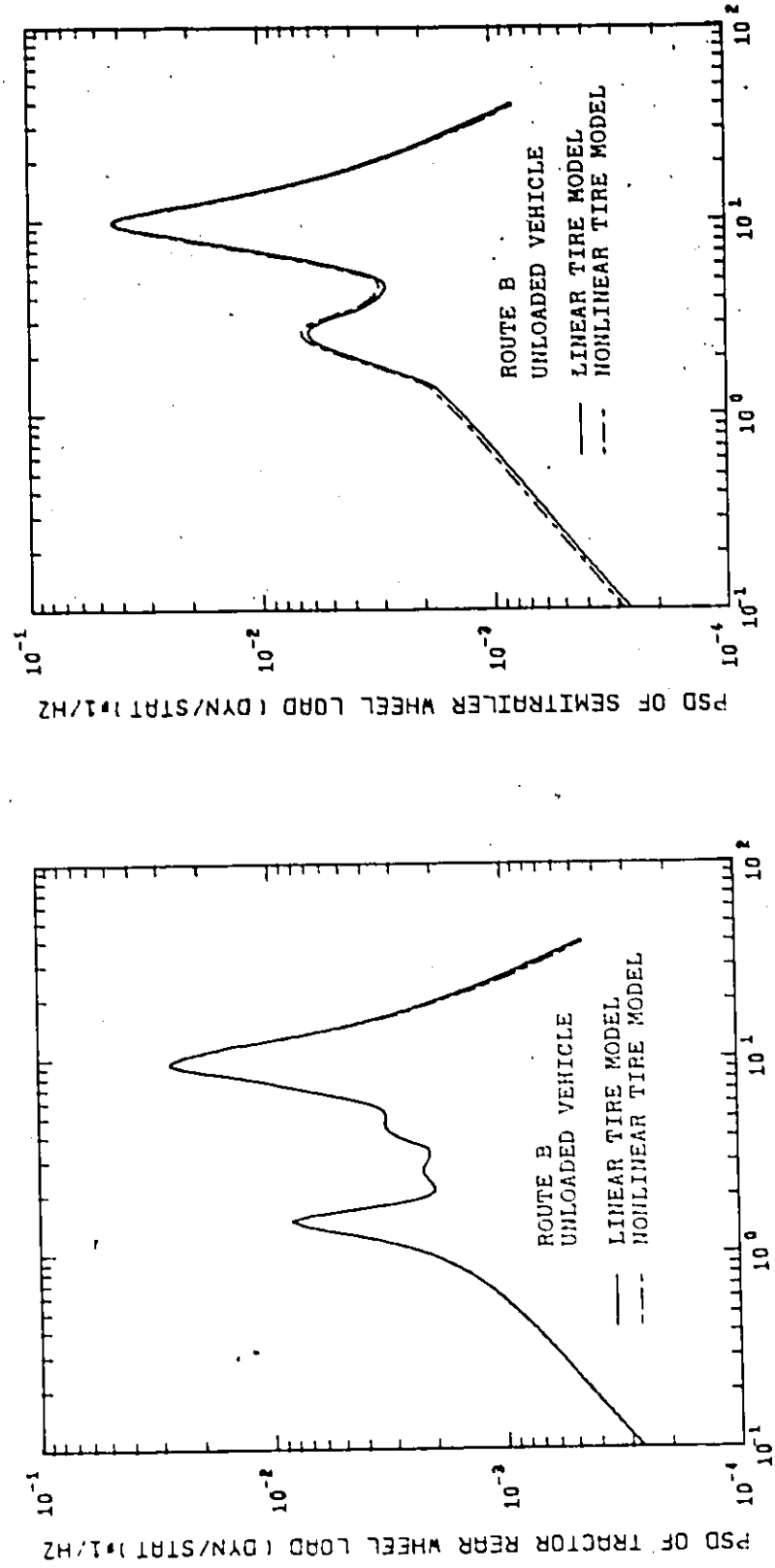

Figure 5.67 Effect of wheel hop nonlinearity on tractor rear and semitrailer wheel loads - unloaded vehicle, rough road.

peak is formed in the frequency range of 2 - 6 Hz. Because of this peak, the acceleration spectra will exceed the ISO 1-hour reduced comfort boundaries. The acceleration spectra are almost identical in the high frequency range. Obviously, when the clearance space is reduced, the bottoming between the sprung and unsprung masses tends to occur more frequently, and the vehicle ride is impaired. The conclusion is that the bump-stop clearance should be increased to minimize the bottoming of the suspension, without introducing undesirable dynamic characteristics of the suspension, such as the high values of the rms axle dynamic excursions.

5.7.4 Effect of Wheel Hop

The effect of wheel hop nonlinearity on the ride motion of the articulated vehicle is examined for the unloaded vehicle operating on the rough road, B, and moving at 80 km/h.

Figure 5.67 presents the tractor rear and semitrailer wheel loads for both the linear and nonlinear tire models. On the basis of data exhibited in Figure 5.67, it is noted that the linear and nonlinear tire models yield very similar results in the whole frequency region. The probability of tractor rear wheel departure from the road is 0.72%, and the corresponding value for semitrailer wheel is 2.6%. It is evident, therefore, that the linear analysis provides a good approximation to the nonlinear analysis of the tire model.

5.8 Summary

The problem of the dynamic interaction between the articulated vehicle and the road surface undulations is investigated in depth by means of nonlinear analyses. The effects of the frictional forces generated in the laminated springs, bump stops and wheel hop on the ride comfort and road safety are discussed and evaluated.

The equivalent linearization technique is adopted and further developed to give a technique applicable to this problem. The principle of the method is to replace the nonlinear system with an equivalent linear system in such a way that the mean square error between the two systems is minimized. Next the solution of the nonlinear system is approximated by the solution of the equivalent linear system. The technique can deal with nonsymmetrical nonlinear functions.

CHAPTER-6

CONCLUSIONS

The intent of this thesis has been to analytically examine the interaction of the articulated vehicle with the road, relating road surface undulations to the vehicle ride performance. The dynamic characteristics of the vehicle have been investigated in depth, both qualitatively and quantitatively, seeking to understand the basic physical mechanics underlying the ride quality of the articulated vehicles. The fundamental data necessary for preliminary design of complex articulated vehicle structures travelling on random road surface has been presented in this thesis. This data will be useful for the articulated vehicle designers, who have been dependent mainly on their experience, as a course of design being established on the theoretical base.

The linear and nonlinear random analyses show that the analytical techniques could be exceptionally effective tools in the hands of the engineering designers. Using the analytical techniques would allow the design of particular components to be checked in terms of their effect on the vibrational response of the overall vehicle structure. These analytical techniques may also serve as aids in designing the tests and in interpreting the test results.

The linear random analysis is necessary to determine the general effects on ride quality due to generic changes in vehicle suspension parameters, vehicle speed, and road characteristics. While such linear analysis places some restrictions on the applicability and the validity of the conclusions it does provide an attractive and convenient solution that will yield a good deal of insight into the vehicle behaviour.

For bump stop and wheel hop nonlinearities, it is possible to determine the probability of suspension bottoming and the probability of the wheel leaving the road surface. These probabilities indicate the percentage of total time in which the vehicle system follows the linear analysis. When this time percentage is nearly 100% then it may be stated that the linear analysis provides a good approximation of the vehicle riding behaviour. In studying the effect of dry friction dampings, however, the nonlinear analysis should be used.

The vibratory motions of the articulated vehicles are characterized by the presence of some factors that affect its ride quality, and make them considerably lower than that of typical passenger vehicles. The higher natural frequency of the semitrailer pitching mode, combined with the greater tractor pitch excitation and the high location of the operator produce large acceleration levels in both the vertical and longitudinal directions. The tractor bounce and pitch and semitrailer pitch natural frequencies are higher for the unloaded cases, and these frequencies are in the range of human body resonances. This could be very uncomfortable if not deleterious. Thus an unloaded vehicle has poorer ride quality than a loaded vehicle.

The analyses of the ride motion of the articulated vehicles show that vehicle parameters must be studied, both individually as well as in combination with one another, in order to understand their effect on the vehicle ride performance. The ride comfort of the articulated vehicles can be greatly improved by using low spring stiffnesses. However, lowering the spring stiffnesses below certain values will increase the dynamic wheel loads, allow excessive dynamic suspension deflections, and consequently increase the probability of suspension bottoming. The choice of suspension spring stiffnesses, therefore, is a compromise between riding comfort and road safety. Adequate suspension dampings are essential to control resonances, reduce dynamic suspension strokes, and to ensure continuous contact between wheels and road.

Rough road surface influences vehicle ride behaviour in a highly negative way. A rather strongly disturbed riding behaviour may result.

The dry friction dampings are detrimental to the ride comfort according to the ISO criteria. Excessive friction dampings increase the transmitted force and hence lead to an increase in shock wave transmission to the vehicle body. However, small values of friction in the suspension are beneficial, as auxiliary damping devices, in reducing the fluctuation of the wheel loads and consequently reducing the probability of wheel departure from the road.

Using the rms values of accelerations as comfort criteria, the results show that the dry friction dampings improve the riding comfort to a certain extent. The optimum frictional forces depend significantly on load conditions, the statistical properties of the road, vehicle

forward speed, and the response location on the vehicle body.

By increasing bump-stop clearance, the bottoming between the sprung and unsprung masses tends to occur less frequently, thus eliminating the large acceleration peaks. The wheel hop nonlinearity does not affect the ride behaviour of the vehicle for the cases considered.

It is recommended that future work be directed to extend the analysis to investigate the effects of frame beaming, cab mounting and roll mode upon the, dynamic characteristics of articulated vehicles. Effort is also needed to integrate this analysis with other design considerations such as wheelbase length, fifth wheel location, etc., and to develop integrated design procedures.

The pronounced effects of dry friction damping representation on vehicle motion have been demonstrated in this study. Future dynamic studies of articulated vehicles must emphasize realistic suspension representation in both spring rate and damping rate.

In order to verify the analytical result by the equivalent linearization technique and to examine the articulated vehicle behaviour every moment, digital simulations may be carried out by making up the artificial random road roughness with statistical properties which are similar to those assumed in the analysis, and then comparing their results with the analytical ones.

An optimization technique could be developed to evaluate the optimum values of vehicle parameters for which the optimum ride quality could be achieved.

Experiments on actual articulated vehicles should be performed in order to verify the theoretical studies which have been performed.

BIBLIOGRAPHY

[1] Allen, R.E., "Limits of Ride Quality Through Cab Isolation", SAE, Paper No. 750165, February 1975.

[2] "An Analysis of the Literature on Tire-road Skid Resistance", ASTM Special Technical Publication 541, July 1973.

[3] Andronov, A., Pontryagin, L. and Witt, A., "On Statistical Investigation of Dynamical Systems", Zh. Eksp. Teor. Fiz, 3, 1933, pp. 165-180.

[4] Anon., "Performance Specifications and Engineering Design Requirements for the UTACV", DOT Specification, 1972.

[5] Anon., "Proposal for Generalized Road Inputs to Vehicles", International Standard Organization Document No. ISO/TC108/WG9 (Secretariat-2) 5, June 1972.

[6] Anon., "Guide for the Evaluation of Human Exposure to Whole Body Vibration", International Standard ISO 2631-1974(E), International Organization for Standardization, New York.

[7] Ariaratnam, S.T., "Random Vibrations of Nonlinear Suspensions", Journal of Mechanical Engineering Science, Vol. 2, No. 3, 1960, pp. 195-201.

[8] Atalik, T.S. and Utku, T., "Stochastic Linearization of Multi-Degree-of-Freedom Nonlinear Systems", Earthquake Engineering and Structural Dynamics, Vol. 4, 1976, pp. 411-420.

[9] Bekker, M.G., Introduction to Terrain-Vehicle Systems, Ann Arbor, The University of Michigan Press, 1969.

[10] Bendat, J.S., and Piersol, A.G., Random Data: Analysis and Measurement Procedures, Wiley-Interscience, 1971, New York.

[11] Bender, B.K., "Optimization of the Random Vibration Characteristics of Vehicle Suspensions", D.Sc. Thesis, M.I.T., 1967.

[12] Bidwell, J.B., Nordeen, D.L., and Rasmussen, R.E., "Tire Properties Affecting Vehicle Ride and Handling", Automotive Safety Seminar, July 1970, General Motors Corp.

[13] Bieniek, M.P., "Suspension Dynamics", Automobile Engineer, 1960, pp. 143-147.

[14] Bobbert, B., "Evaluation of Vibration Design Data by Statistical Means", Advances in Automobile Engineering III, New York, Pergamon Press, 1965, pp. 59-75.

[15] Bogdanoff, J.L., Cote, L.J., and Kozin, F., "Introduction to a Statistical Theory of Land Locomotion ... II Ground Roughness", Journal of Terramechanics, 1965, 2(3), pp. 17-27.

[16] Booton, R.C., Jr., "Nonlinear Control Systems with Random Inputs", IRE Transactions Circuitry Theory, CT-1, 1954, pp. 9-18.

[17] Brust, J.M., "Determination of Fragility to Meet Random and Sinusoidal Vibration Environments", SAE-430A, National Aeronautic, Space Engineering, Manufacturing Meeting, Los Angeles, Calif., October 9-13, 1961.

[18] Burns, R.N., and Sachs, H.K., "Investigation on Vehicle Suspensions having Asymmetric Damping Characteristics", Proceedings of the First International Conference on Vehicle Mechanics, Detroit, Michigan, July 16-18, 1968, pp. 323-336.

[19] Butkunas, A.A., "Power Spectral Density and Ride Evaluation", SAE, Paper No. 660138, 1966.

[20] Caldwell, W.N., "Ride and Tracking Vibration Problems of TOFC-COFC Cars in High Speed Service", presented at the Association of American Railroads Conference on Track/Train Dynamics Interaction, December 15, 1971, Chicago, pp. 154-199.

[21] Carstens, J.P., and Kresge, M.D., "Literature Survey of Passenger Comfort Limitations of High Speed Ground Transports", United Aircraft Corporation Research Lab. Report D-910353-1, July 1965.

[22] Caughey, T.K., "Response of a Nonlinear Spring to Random Loading", Journal of Applied Mechanics, Vol. 26, 1959, pp. 341-344.

[23] Caughey, T.K., "Random Excitation of a System with Bilinear Hysteresis", Journal of Applied Mechanics, Vol. 27, 1960, pp. 649-652.

[24] Caughey, T.K., "Derivation and Application of the Fokker-Planck Equation to Discrete Nonlinear Dynamical Systems Subjected to White Random Excitation", Journal of the Acoustical Society of America, Vol. 35, No. 11, 1963, pp. 1683-1692.

[25] Caughey, T.K., "Equivalent Linearization Techniques", Journal of the Acoustical Society of America, Vol. 35, 1963, pp. 1706-1711.

[26] Caughey, T.K., "Nonlinear Theory of Random Vibrations", Advances in Applied Mechanics, Vol. 11, 1971, pp. 209-253.

[27] Chace, M.A., and Smith, D.A., "DAMN: Digital Computer Program for the Dynamic Analysis of Generalized Mechanical Systems", SAE, Paper No. 710244, 1971.

[28] Chalmers, W.G., "A New Concept in Commerical Vehicle Suspension", SAE, Paper No. 730656, June 1973.

[29] Clark, D.C., "A Preliminary Investigation into the Dynamical Behaviour of Vehicles and Highways", SAE, 1962, 70, pp. 447-453.

[30] "Commercial Vehicles - Engineering and Operation", I. Mech. E., London, 1967.

[31] Cote, L.J., Kozin, F., and Bogdanoff, J.L., "Introduction to a Statistical Theory of Land Locomotion ... I", Journal of Terramechanics, 1965, 2(2), pp. 17-23.

[32] Cote, L.J. Kozin, F., and Bogdanoff, J.L., "Introduction to a Statistical Theory of Land Locomotion ... IV Effect of Vibration on the Contents of Vehicle and Conclusions", Journal of Terramechanics, 1966, 3(4), pp. 47-51.

[33] Craggs, A., "The Assessment of Road Test Track Loads Using Random Vibration Analysis", Advances in Automobile Engineering, Vol. 7, Part 3, ed. by G.H. Tidbury, Pergamon Press, London, 1965.

[34] Crandall, S.H., Random Vibration - Volume 1, Technology Press/ Wiley, 1958.

[35] Crandall, S.H., Random Vibration - Volume 2, M.I.T. Press, 1963.

[36] Crandall, S.H., "Random Vibrations of a Nonlinear System with a Set-up Spring", Journal of Applied Mechanics, Vol. 29, 1962, pp. 306-314.

[37] Crandall, S.H., "Perturbation Techniques for Random Vibration of Nonlinear Systems", Journal of the Acoustical Society of America, Vol. 35, 1963, pp. 1700-1705.

[38] Crandall, S.H., and Mark, W.D., Random Vibrations in Mechanical Systems, Academic Press, New York, 1963.

[39] Crosby, M.J., and Allen, R.E., "Cab Isolation and Ride Quality", SAE, Paper No. 740294, 1974.

[40] Dailey, G., Caywood, W.C., and O'Connor, J.C., "A General Purpose Computer Program for the Dynamic Simulation of Vehicle-Guideway Interactions", AIAA Journal, Vol. 11, No. 3, 1973, pp. 278-288.

[41] Davis, J.C., "Modal Modelling Techniques for Vehicle Shake Analysis", SAE, Paper No. 720045, 1972.

[42] dePater, A.E., "Nonlinear Vibration in Vehicle Engineering", WTHD No. 4, Afdeling Der Werktuigbouwkunde, Technische Hogeschool, Delft, The Netherlands, presented at the Fourth Conference on Nonlinear Oscillations at Prague, Czechoslovakia, September 1967.

[43] Dodds, C.J., "The Laboratory Simulation of Vehicle Service Stress", Journal of Engineering for Industry, May 1974, pp. 391-398.

[44] Dodds, C.J., and Robson, J.D., "The Response of Vehicle Components to Random Road Surface Undulations", Proc. 13, F.I.S.I.T.A. Congress, Paper 17-2D, Brussels, 1970.

[45] Dodds, C.J., and Robson, J.D., "The Description of Road Surface Roughness", Journal of Sound and Vibration, 1973, 31(2), pp. 175-184.

[46] Dokainish, M.A., and ElMadany, M.M., "Dynamic Response of Tractor-Semitrailer Vehicle to Random Inputs", Proceedings of the 5th VSD 2nd IUTAM Symposium on Dynamics of Vehicles on Roads and Tracks, September 1977, pp. 237-255.

[47] Dokainish, M.A., and ElMadany, M.M., "Random Response of Tractor-Semitrailer System", accepted for publication in the Journal of Vehicle System Dynamics.

[48] Donati, F., Genesio, R., Laurentini, A., Mauro, V., Menga, G., and Milanese, M., "Dynasim 3: A Computer Program for Simulation of Vehicle Riding Motions", VSD, 3, 1974, pp. 141-161.

[49] Ellis, J.R., "Experimental Confirmation of Ride Theory", Advances in Automobile Engineering, New York, The Macmillan Co., 1963, pp. 123-144.

[50] Ellis, J.R., "The Ride and Handling of Semitrailer Articulated Vehicle", Automobile Engineering, Vol. 26, 1966, pp. 523-529.

[51] Ellis, J.R., Vehicle Dynamics, Business Books, 1969.

[52] Ellis, J.R., and Goldwyn, N.A.H., "Wheel Hop ... A Study in Simulation Techniques", Auto. Engg., 1963, 53, pp. 106-108.

[53] ElMadany, M.M., "On the Dynamic Analysis of Standard and Self-Steering Semitrailers", M.Eng. Thesis, McMaster University, Hamilton, Ontario, June 1975.

[54] ElMadany, M.M., and Dokainish, M.A., "On the Steady-state Response of Tractor-Semitrailer", Proceedings of the Third Symposium on Engineering Applications of Solid Mechanics, June 7-8, 1976, Vol. 1, pp. 267-285.

[55] ElMadany, M.M., and Dokainish, M.A., "Optimum Suspension of Tractor-Semitrailer Vehicle", accepted for publication in Society of Automotive Engineers.

[56] ElMadany, M.M., Dokainish, M.A., and Siddall, J.N., "On the Optimum Design of Tractor-Semitrailer Suspension", Sixth CANCAM, Vancouver, 1977.

[57] ElMadany, M.M., Dokainish, M.A., and Allan, A.B., "Ride Dynamics of Articulated Vehicles - A Literature Survey", submitted for publication in the Journal of Vehicle System Dynamics, 1978.

[58] Foster, A.W., "A Heavy Truck Cab Suspension for Improved Ride", SAE, Paper No. 780408, 1978.

[59] Foster, E.T., "Semilinear Random Vibrations in Discrete Systems", Journal of Applied Mechanics, Vol. 35, No. 3, pp. 560-564.

[60] Genesio, R., Laurentini, A., Mauro, V., and Milanese, M., "A Comprehensive Analysis of Methods for Vehicle Dynamics Simulation", Proceedings of IUTAM Symposium on the Dynamics of Vehicles on Roads and on Railway Tracks, August 18-22, 1975.

[61] Goldman, D.E., "A Review of Subjective Responses to Vibratory Motion of the Human Body in the Frequency Range 1 to 70 C.P.S.", Project N.M. 004001, Naval Medical Research Institute, March 16, 1948.

[62] Goldman, D.E., and von Gierke, H.E., "The Effects of Shock and Vibration on Man", Naval Medical Research Institute, Lecture and Review Series No. 60-3, January 1960.

[63] Hales, F.D., "The Rigid Body Dynamics of Road Vehicle Trains", Proceedings of IUTAM Symposium, August 1975, pp. 131-151.

[64] Hales, F.D., et al., "The Assessment of Vehicle Ride and Handling", Proc. Auto. Div. I. Mech. Eng., 182(38), 1967/8.

[65] Hanamoto, B., "Vehicle Ride Characteristics", Land Locomotion Laboratory, Report No. 6, USATAC, Warren, Michigan, November 1966.

[66] Hanes, R.M., "Human Sensitivity to Whole-body Vibration in Urban Transportation Systems: A Literature Review", Applied Physical Laboratory for DOT, No. APL/JHU-TPR 004, May 1970.

[67] Healey, A.J., "Passenger Response to Random Vibration in Transportation Vehicles - A Literature Review, Report RR30, Council for Advanced Transportation Studies, The University of Texas at Austin, June 1975.

[68] Helling, J., "Beitrag zur Abstimmung Schwingungsfahiger Systeme in Lastkraftwagen", (Optimization of Vibratory System in Trucks), ATZ, No. 1, 1962.

[69] Helling, J., "Elektrisches Modellverfahren zur Untersuchung des Federungsverhaltens von Sattelkraftwagen", (Electronic Modelling of Springing of Semitrailers), Deutsche Kraftfahrforschung und Strassenverkehrstechnik, Heft 171, Dusseldorf, 1964.

[70] Howell, L.J., "Power Spectral Density Analysis of Vehicle Vibration using the NASTRAN Computer Program", SAE, Paper No. 740328, 1974, pp. 124-133.

[71] Ilosvai, L. and Szues, B., "Random Vehicle Vibrations as Effected by Dry Friction in Wheel Suspensions", VSD 1, 1972, pp. 197-209.

[72] Inok, T., et al., "Tuning Techniques for Controlling Heavy-duty Truck Shake - Vertical, Torsional and Lateral", SAE, Paper No. 730650, 1973.

[73] Iwan, W.D., "A Distributed-Element Model for Hystresis and its Steady-State Dynamic Response", Journal of Applied Mechanics, Vol. 33, No. 4, 1966, pp. 893-900.

[74] Iwan, W.D., "A Generalization of the Methods of Equivalent Linearization", International Journal of Non-linear Mechanics, Vol. 8, 1973, pp. 279-287.

[75] Iwan, W.D. and Lutes, L.D., "Response of the Bilinear Hysteretic System to Stationary Random Excitation", Journal of the Acoustical Society of America, Vol. 43, 1968, pp. 545-552.

[76] Iwan, W.D. and Yang, J., "Application of Statistical Linearization Techniques to Non-linear Multi-Degree-of-Freedom Systems", Journal of Applied Mechanics, Vol. 39, 1972, pp. 545-550.

[77] Janeway, R.N., "Passenger Vibration Limits", SAE Journal, August 1948.

[78] Janeway, R.N., "A Better Truck Ride for Driver and Cargo: Problems and Practical Solutions", SAE, Special Publication, No. 154.

[79] Janeway, R.N., "Improving Truck Ride", SAE Journal, Vol. 66, June 1958, pp. 66-72.

[80] Janeway, R.N., "A Practical Approach to Truck Ride Instrumentation and Evaluation - A Summary", SAE, Paper No. 660140, 1966.

[81] Janeway, R.N., "Which Spring? Where?", SAE, Paper No. 736689, June 1973.

[82] Janeway, R.N., "Human Vibration Tolerance Criteria and Application to Ride Evaluation", SAE, Paper No. 750166, February 1975.

[83] Kamash, K.M.A., and Robson, J.D., "Implications of Isotropy in Random Surfaces", Journal of Sound and Vibration, 1977, 54(1), pp. 131-145.

[84] Kamash, K.M.A., and Robson, J.D., The Application of Isotropy in Road Surface Modelling", Journal of Sound and Vibration, 1978, 57(1), pp. 89-100.

[85] Kaneshige, I., "Application of the Probability Theory to the Design of an Endurance Test Track Surface", SAE, Paper No. 69011, 1969.

[86] Kemper, J.D., and Ayre, R.S., "Optimum Damping and Stiffness in a Nonlinear Four-Degree-of-Freedom System Subjected to Shock Load", Journal of Applied Mechanics, 1971, pp. 135-142.

[87] Klein, G.H., "Random Excitation of a Nonlinear System with Tangent Elasticity Characteristics", Journal of the Acoustical Society of America, Vol. 36, 1964, pp. 2095-2105.

[88] Klosterman, A.L., "A Combined Experimental and Analytical Procedure for Improving Automotive System Dynamics", SAE, Paper No. 720093, 1972.

[89] Kozin, F., Bogdanoff, J.L., and Cote, L.J., "Introduction to a Statistical Theory of Land Locomotion ... III Vehicle Dynamics", Journal of Terramechanics, 1966, 3(3), pp. 69-81.

[90] Krylov, N., and Bogoliubov, N., Introduction to Nonlinear Mechanics, Kiev, Translation by Princeton University Press, Princeton, New Jersey, 1943.

[91] La Barre, R.P., Forbes, R.T., and Andrew, S., "The Measurement and Analysis of Road Surface Roughness", MIRA Report No. 1970/5, 1969.

[92] Lee, R.A., and Pradko, F., "Analytical Analysis of Human Vibration", SAE Transactions, Vol. 77, Paper No. 680091, January 1968.

[93] LeFevre, W.F., "Truck Ride Guide", Rockwell-Standard Corporation, Automotive Division, Detroit, Michigan, 1967.

[94] Leppert, E.L., Lee, S.H., Day, F.D., Champman, P.C., and Wada, B.K., "Comparison of Modal Test Results: Multiple Sine Versus Single-Point Random", SAE, Paper No. 760879, 1976.

[95] Lins, W.F., "Vehicle Vibration Analysis using Frequency Domain Techniques", ASME, Journal of Engineering for Industry, November 1969, pp. 1075-1079.

[96] Lin, Y.K., Probabilistic Theory of Structural Dynamics, McGraw-Hill, 1967.

[97] Lutes, L.D., "Approximate Technique for Treating Random Vibration of Hysteretic Systems", Journal of the Acoustical Society of America, Vol. 48, 1970, pp. 299-306.

[98] Lyon, R., "On the Vibration Statistics of a Randomly Excited Hard-Spring Oscillator", Journal of the Acoustical Society of America, Vol. 32, 1960, pp. 716-719.

[99] Lyon, R., "On the Vibration Statistics of a Randomly Excited Hard-Spring Oscillator II", Journal of the Acoustical Society of America, Vol. 33, 1961, pp. 1395-1403.

[100] Macaulay, M.A., "Measurement of Road Surfaces", Advances in Automobile Engineering, Cranfield International Symposium, Series 4, 1963, pp. 93-112.

[101] Metcalf, W.W., "The Ride Behaviour of a Multi-Element Vehicle Traversing Cross-Country Terrain", Cornell Aeronautical Laboratory, Cornell University, Buffalo, New York, 1961.

[102] Mitschke, E.M., "Influence of Road and Vehicle Dimensions on the Amplitude of Body Motions and Dynamic Wheel Loads (Theoretical and Experimental Vibration Investigations)", SAE, 1962, vol. 70, pp. 434-496.

[103] Mustin, R.W., "Survey of Modal Vibration Test/Analysis Techniques", SAE, Paper No. 760870, 1976.

[104] Noon, W.D., "The Application of an Analog Computer to the Study of a Tractor-Trailer Suspension System", General Motors Engineering Journal, 1960 April-May-June, pp. 27-31.

[105] Parkhilovskiy, I.G., "Investigations of the Probability Characteristics of the Surfaces of Distributed Types of Roads", Avtom, 1968, Prom. 8, pp. 18-22.

[106] Parkhilouskiy, I.G., and Zaitseva, N.R., "A Statistical Investigation of Automotive Vibrations on an Analogue Computer", Journal of Terramechanics, 1965, 2(1), pp. 9-23.

[107] Potts, G.R., "Interim Report of a Vibration Analysis of a 3-Axle, Fully Articulated Highway Vehicle," A Master's Report, Kansas, State University, 1969.

[108] Potts, G.R., and Walker, H.S., "Nonlinear Truck Ride Analysis", ASME Transaction, Journal of Engineering for Industry, May 1974, pp. 597-602.

[109] Pradko, F., Orr, T.R., and Lee, R.A., "Human Vibration Analysis", System Simulation Lab. U.S. Army Tank Automotive Command Rep. No. 14, Warren, Michigan.

[110] Pradko, F., "Human Response to Random Vibrations", The Shock and Vibration Bulletin, No. 34, Part 4, February 1965, U.S. Naval Res. Lab., Washington, D.C.

[111] Pradko, F., and Lee, R.A., "Vibration Comfort Criteria", SAE, Paper No. 660139, 1966.

[112] Pradko, F., Lee, R.A., and Kaluza, V., "Theory of Human Vibration Response", ASME, Paper No. 66-WA/BHF-15, Novemeber 1966.

[113] Quinn, B.E., and De Vries, T.W., "Highway Characteristics as Related to Vehicle Performance", Pavement Performance Concept, Highway Research Board, Bulletin No. 250, 1960.

[114] Quinn, B.E., and Hildebrand, S.E., "Effect of Road Roughness on Vehicle Steering", Highway Research Record 471, 1973, pp. 62-75.

[115] Quinn, B.E., and Thompson, D.R., "Effect of Pavement Conditions upon Dynamic Vehicle Reactions", Purdue University, Dept. of Maths., Report BPR-611004.

[116] Ribarits, J.I., Aurell, J., and Andersers, E., "Ride Comfort Aspects of Heavy Truck Design", SAE, Paper No. 781067, 1978.

[117] Richardson, M., and Kniskern, T., "Identifying Modes of Large Structures from Multiple Input and Response Measurements", SAE, Paper No. 760875, 1976.

[118] Robson, J.D., An Introduction to Random Vibration, Edinburgh, Edinburgh University Press, 1964.

[119] Robson, J.D., and Dodds, C.J., "Stochastic Road Inputs and Vehicle Response", VSD 5 (1975/76), pp. 1-13.

[120] Robson, J.D., and Kamash, K.M.A., "Road Surface Description in Relation to Vehicle Response", Proceedings of 5th VSD-2nd IUTAM Symposium, September 1977, pp. 222-228.

[121] Rossini, L.R., "Applicazione di Criteri Statistici allo Studio delle Vibrazioni Verticali delle Sospensioni", A.T.A., 1967.

[122] Ryba, D., "Improvements in Dynamic Characteristics of Automobile Suspension Systems: Part I - Two-Mass Systems", VSD 3 (1974), pp. 17-46.

[123] Ryba, D., "Improvement in Dynamic Characteristics of Automobile Suspension Systems: Part II - Three-Mass Systems", VSD 3 (1974), pp. 55-98.

[124] Sattaripour, A., "The Effect of Road Roughness on Vehicle Behaviour", Proceedings of 5th VSD - 2nd IUTAM Symposium, September 19-23, 1977, pp. 229-235.

[125] Shimogo, T., "Isolation of Random Vibration by Laminated Spring", Journal of the Society of Automotive Engineers of Japan, Vol. 26, No. 3, 1972, pp. 251-261.

[126] Shyrock, R.A., et al., "System Modeling Techniques to Improve the Ride and Vibration Isolation Characteristics of Heavy Equipment", SAE, Paper No. 770594, 1977.

[127] Smith, C.C., "On Using the ISO Standard to Evaluate the Ride Quality of Broad-band Vibration Spectra in Transportation Vehicles", ASME, Journal of Dynamic Systems, Measurement and Control, December 1976, pp. 440-443.

[128] Smith, P.W., "Response of Nonlinear Structures to Random Excitation", Journal of the Acoustical Society of America, Vol. 34, 1962.

[129] Smith, R.E., "Optimum Vehicle Suspension Designs by Computer Simulation", Journal of Terramechanics, Vol. 2, No. 4, 1965, pp. 17-30.

[130] Spanos, P-T.D., "Linearization Techniques for Non-linear Dynamical Systems", Ph.D. Thesis, California Institute of Technology, 1977.

[131] "Tandem Truck Ride and Vibration Problems", SAE, Special Publication, No. 260.

[132] Thompson, A.G., "Optimum Damping in a Randomly Excited Nonlinear Suspension", Proc. Instn. Mech. Engrs., 1969-70, Vol. 184 (Pt 2A), pp. 169-184.

[133] Thompson, W.E., "Measurements and Power Spectra of Runway Roughness at Airport in Countries and the North Atlantic Treaty Organization", NACA TN 4304, July 1958.

[134] Tidbury, G.H., "An Introduction to Random Process Theory", Advances in Automobile Engineering III, New York, Pergamon Press, 1965, pp. 3-30.

[135] Tung, C.C., Penzien, J. and Horonjeff, R., "The Effects of Runway Unevenness on the Dynamic Responses of Supersonic Transports", NASA CR-119, University of California, Berkeley, 1964.

[136] Tung, C.C., "The Effects of Runway Roughness on the Dynamic Response of Airplanes", Journal of Sound and Vibration, 1967, 5(1), pp. 164-172.

[137] Van Deusen, B.D., "Analytical Techniques for Designing Riding Quality into Automotive Vehicles", SAE Transactions, Vol. 76, 1967, pp. 155-165.

[138] Van Deusen, B.D., "A Statistical Technique for Dynamic Analysis of Vehicles Traversing Rough Yielding and Non-yielding Surfaces", NASA CR-659, March 1967.

[139] Van Deusen, B.D., "Human Response to Vehicle Vibration", SAE Transactions, Vol. 77, 1968, pp. 328-345.

[140] Van Deusen, B.D., "Truck Suspension System Optimization", SAE, Paper No. 710222.

[141] Van Deusen, B.D., "Truck Suspension System Optimization", Journal of Terramechanics, 1973, Vol. 9, No. 2, pp. 83-100.

[142] Van Eldik Thieme, H.C.A., "Passenger Riding Comfort Criteria and Methods of Analyzing Ride and Vibration Data", SAE - Paper 295 A, presented at the 1961 SAE International Congress and Exposition of Automotive Engineering, Cobo Hall, Detroit, Michigan, January 7-13, 1961.

[143] Vanmarche, E.H., "Properties of Spectral Moments with Applications to Random Vibration", ASCE, Journal of the Engineering Mechanics Division, 1972, pp. 425-446.

[144] Varterasian, J.H., and Thompson, R.R., "The Dynamic Characteristics of Automobile Seats with Human Occupants", SAE, Paper No. 770249, 1977.

[145] Von Gierke, H.E., "The ISO Standard Guide for the Evaluation of Human Exposure to Whole-Body Vibrations", SAE, Paper No. 751009, November 1975.

[146] Walker, H.S., and Potts, G.R., "Truck Vibrations ... An Old Problem with a Modern Solution via Computer", Proceedings of the National Meeting of the American Astronautical Society on Space Technology Applied to Earth Problems, Las Cruces, New Mexico, October 23-25, 1969.

[147] Walls, J.H., and et al., "Some Measurements and Power Spectra of Runway Roughness", NACA, T.N. 3305.

[148] Walther, W.D., Gossard, D., and Fensel, P., "Truck Ride - A Mathematical and Empirical Study", SAE, Paper No. 690099, January 13-17, 1969.

[149] Wambold, J.C., Breckman, A.D., Park, W.H., and Igram, J., "Effect of Road Roughness on Vehicle Braking", Highway Research Record 471, 1973, pp. 76-82.

[150] Wendeborn, J.O., "Description of Road Profile by Means of the Spectral Density of the Irregularities", A.T.Z. 69 No. 5 (1967).

[151] Whitehead, G.D., "The Application of Statistics to the Motor Vehicle Ride Comfort Problem", Advances in Automotive Engineering III, New York, Pergamon Press, 1965, pp. 147-183.

[152] Whittemore, A.P., "A Technique for Measuring Effective Road Profile", SAE, Paper No. 720094, January 1972.

[153] Winkler, C.B., "Measurements of Inertial Properties and Suspension Parameters of Heavy Highway Vehicles", SAE, Paper No. 730182, 1973.

[154] Yang, I., "Stationary Random Response of Multidegree-of-Freedom Systems", Ph.D. Thesis, California Institute of Technology, 1970.

APPENDIX I

EQUATIONS OF MOTION

The equations of motion for the articulated vehicle model shown in Figure 5.1 and subject to the forces described in Chapter 5 are given below. Deduction of the linear equations from the nonlinear equations is also given. Details of the derivation of the linear part of these equations may be found in references [53, 107].

Due to the articulation between the tractor and semitrailer units, there are two equations of kinematic constraints,

$$Y_s = Y_t + b_5\,\theta_t + b_4\,\theta_s \tag{I.1}$$

and

$$X_s = X_t + a_1\,\theta_t - a_2\,\theta_s. \tag{I.2}$$

One dynamical equation revealed an ignorable coordinate which provided the integrated equation,

$$X_t = -\frac{M_5}{M_4+M_5}\,(a_1\,\theta_t - a_2\,\theta_s) \tag{I.3}$$

Therefore, there are six independent coordinates. They are Y_t, θ_t, θ_s, Y_1, Y_2 and Y_3.

Tractor Body Vertical

$$(M_t + M_s)\ddot{Y}_t + M_s\,b_5\,\ddot{\theta}_t + M_s\,b_4\,\ddot{\theta}_s + (c_1 + c_2 + c_3)\,\dot{Y}_t$$
$$+ (-b_1\,c_1 + b_2\,c_2 + b_5\,c_3)\,\dot{\theta}_t + (b_3 + b_4)\,\dot{\theta}_s - c_1\,\dot{Y}_1$$

$$- c_2 \dot{Y}_2 - c_3 \dot{Y}_3 + (k_1 + k_2 + k_3) Y_t + (-b_1 k_1 + b_2 k_2 + b_5 k_3)\theta_t$$
$$- k_1 Y_1 - k_2 y_2 - k_3 Y_3 + F_{11} + F_{12} + F_{13} + B_{11} + B_{12} + B_{13} = 0 \qquad (I.4)$$

Tractor Body Pitch

$$(I_t + b_5^2 M_s + \frac{M_4 M_5}{M_4+M_5} a_1^2) \ddot{\theta}_t + b_5 M_s \ddot{Y}_t + (b_4 b_5 M_s$$
$$- \frac{M_4 M_5}{M_4+M_5} a_1 a_2) \ddot{\theta}_s + (-b_1 c_1 + b_2 c_2 + b_5 c_3) \dot{Y}_t$$
$$+ (b_1^2 c_1 + b_2^2 c_2 + b_5^2 c_3) \dot{\theta}_t + (b_3 + b_4) b_5 c_3 \dot{\theta}_s$$
$$+ b_1 c_1 \dot{Y}_1 - b_2 c_2 \dot{Y}_2 - b_5 c_3 \dot{Y}_3 + (-b_1 k_1 + b_2 k_2 + b_5 k_3) Y_t$$
$$+ (b_1^2 k_1 + b_2^2 k_2 + b_5^2 k_3) \theta_t + (b_3 + b_4) b_5 k_3 \theta_s + b_1 k_1 Y_1 - b_2 k_2 Y_2$$
$$- b_5 k_3 Y_3 - b_1 F_{21} + b_2 F_{22} + b_5 F_{23} - b_1 B_{21} + b_2 B_{22} + b_5 B_{23} = 0 \qquad (I.5)$$

Semitrailer Body Pitch

$$(I_s + b_4^2 M_s + \frac{M_4 M_5}{M_4+M_5} a_1^2) \ddot{\theta}_s + b_4 M_s \ddot{Y}_t + (b_4 b_5 M_s - \frac{M_4 M_5}{M_4+M_5} a_1 a_2) \ddot{\theta}_t$$
$$+ (b_3 + b_4) c_3 \dot{Y}_t + b_5 (b_3 + b_4) c_3 \dot{\theta}_t + (b_3 + b_4)^2 c_3 \dot{\theta}_s$$
$$- (b_3 + b_4) c_3 \dot{Y}_3 + (b_3 + b_4) k_3 Y_t + b_5 (b_3 + b_4) k_3 \theta_t$$
$$+ (b_3 + b_4)^2 k_3 \theta_s - (b_3 + b_4) k_3 Y_3 + (b_3 + b_4) F_{33} + (b_3 + b_4) B_{33}$$
$$= 0 \qquad (I.6)$$

Tractor Front Unsprung Mass Vertical

$$M_1\ddot{Y}_1 - c_1\dot{Y}_t + b_1c_1\dot{\theta}_t + c_1\dot{Y}_1 - k_1Y_t + b_1k_1\theta_t + k_1Y_1 - F_{41} - B_{41} + T_{44} = 0 \qquad (I.7)$$

Tractor Rear Unsprung Mass Vertical

$$M_2\ddot{Y}_2 - c_2\dot{Y}_t - b_2c_2\dot{\theta}_t + c_2\dot{Y}_2 - k_2Y_t - b_2k_2\theta_t + k_2Y_2 - F_{52} - B_{52} + T_{55} = 0 \qquad (I.8)$$

Semitrailer Unsprung Mass Vertical

$$M_3\ddot{Y}_3 - c_3\dot{Y}_t - b_5c_3\dot{\theta}_t - (b_3 + b_4)c_3\dot{\theta}_s + c_3\dot{Y}_3 - k_3Y_t - b_5k_3\theta_t - (b_3 + b_4)k_3\theta_s + k_3Y_3 - F_{63} - B_{63} + T_{66} = 0 \qquad (I.9)$$

where

$$M_4 = M_t + M_1 + M_2,$$

$$M_5 = M_s + M_3,$$

$$F_{11} = F_{21} = F_{41},\ F_{12} = F_{22} = F_{52},\ F_{13} = F_{33} = F_{63},$$

$$B_{11} = B_{21} = B_{41},\ B_{12} = B_{22} = B_{52},\ B_{13} = B_{33} = B_{63}$$

The linear equations of motion for the vehicle model shown in Figure 3.1 can be deduced from equations (I.4) - (I.9) by letting $F_{ij} = 0$, $B_{ij} = 0$ and

$$T_{44} = c_{t4}(\dot{Y}_1 - \dot{w}_1) + k_{t4}(Y_1 - w_1), \qquad (I.10.a)$$

$$T_{55} = c_{t5}(\dot{Y}_2 - \dot{w}_2) + k_{t5}(Y_2 - w_2), \tag{I.10.b}$$

$$T_{66} = c_{t6}(\dot{Y}_3 - \dot{w}_3) + k_{t6}(Y_3 - w_3). \tag{I.10.c}$$

Let $\bar{x}(Y_t, \theta_t, \theta_s, Y_1, Y_2, Y_3)$ represent the vector of the generalized coordinates, and $\bar{y}$ represent the vector of the relative displacements across the nonlinear elements, i.e.

$$y_1 = Y_t - b_1\theta_t - Y_1 \tag{I.11}$$

$$y_2 = Y_t + b_2\theta_t - Y_2 \tag{I.12}$$

$$y_3 = Y_t + b_5\theta_t + (b_3 + b_4)\theta_s - Y_3 \tag{I.13}$$

$$y_4 = Y_1 - w_1 \tag{I.14}$$

$$y_5 = Y_2 - w_2 \tag{I.15}$$

$$y_6 = Y_3 - w_3 \tag{I.16}$$

Therefore, the relation between $\bar{x}$ and $\bar{y}$ is given by

$$\bar{y} = A\bar{x} + \bar{u}, \tag{I.17}$$

where

$$A = \begin{bmatrix} 1 & -b_1 & 0 & -1 & 0 & 0 \\ 1 & b_2 & 0 & 0 & -1 & 0 \\ 1 & b_5 & b_3+b_4 & 0 & 0 & -1 \\ 0 & 0 & 0 & 1 & 0 & 0 \\ 0 & 0 & 0 & 0 & 1 & 0 \\ 0 & 0 & 0 & 0 & 0 & 1 \end{bmatrix} \tag{I.18}$$

and $\bar{u}' = [0, 0, 0, w_1, w_2, w_3]$ (I.19)